November, 1982

LIDS-TH-1254

Research Supported By:

NASA Ames and Langley Research Centers
Grant NGL-22-009-124

Air Force Office of Scientific Research (AFSC)
Grant AFOSR-77-3281

E.I. DuPont de Nemours and Co., Inc.

ADAPTIVE CONTROL IN THE PRESENCE OF UNMODELED DYNAMICS

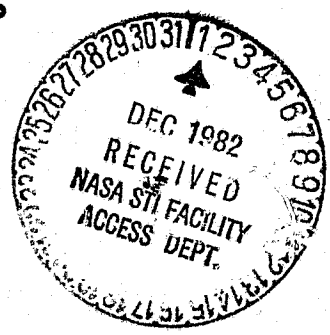

Charles Edward Rohrs

Laboratory for Information and Decision Systems
MASSACHUSETTS INSTITUTE OF TECHNOLOGY, CAMBRIDGE, MASSACHUSETTS 02139

November, 1982 LIDS-TH-1254

ADAPTIVE CONTROL IN THE PRESENCE OF UNMODELED DYNAMICS

by

Charles Edward Rohrs

This report is based on the unaltered thesis of Charles Edward Rohrs, submitted in partial fulfillment of the requirements for the degree of Doctor of Philosophy at the Massachusetts Institute of Technology in August, 1982. The research was conducted at the M.I.T. Laboratory for Information and Decision Systems, with support provided in part by the NASA Ames and Langley Research Centers under Grant NGL-22-009-124, Air Force Office of Scientific Research (AFSC) under Grant AFOSR-77-3281, and E.I. DuPont de Nemours and Co., Inc.

Laboratory for Information and Decision Systems
Massachusetts Institute of Technology
Cambridge, MA 02139

ADAPTIVE CONTROL IN THE PRESENCE OF UNMODELED DYNAMICS

by

Charles Edward Rohrs

B.S.E.E., University of Notre Dame du Lac
(1976)

S.M., Massachusetts Institute of Technology
(1978)

E.E., Massachusetts Institute of Technology
(1979)

SUBMITTED IN PARTIAL FULFILLMENT OF
THE REQUIREMENTS FOR THE
DEGREE OF

DOCTOR OF PHILOSOPHY

at the

MASSACHUSETTS INSTITUTE OF TECHNOLOGY

August 1982

Signature of Author .....Charles E. Rohrs.....
Department of Electrical Engineering
and Computer Science, August 13, 1982

Certified by .....Michael Athans.....
Michael Athans
Thesis Co-Supervisor

Certified by ...Lena Valavani.....
Lena Valavani
Thesis Co-Supervisor

Accepted by .....
Arthur C. Smith
Chairman, Department Graduate Committee

ABSTRACT

This thesis contains an exhaustive analytical and numerical investigation of stability and robustness properties of a wide class of adaptive control algorithms in the presence of unmodeled dynamics and output disturbances. The class of adaptive algorithms considered are those commonly referred to as model reference adaptive control algorithms, self-tuning controllers, and dead beat adaptive controllers; they have been developed for both continuous-time systems and discrete-time systems. The existing adaptive control algorithms have been proven to be globally asymptotically stable under certain assumptions, the key ones being (a) that the number of poles and zeroes of the unknown plant are known, and (b) that the primary performance criterion is related to good command following. These theoretical assumptions are too restrictive from an engineering point of view. Real plants always contain unmodelled high-frequency dynamics and small delays, and hence no upper bound on the number of the plant poles and zeroes exists. Also real plants are always subject to unmeasurable output additive disturbances, although these may be small. Hence, it is important to critically examine the stability robustness properties of the existing adaptive algorithms when some of the theoretical assumptions are removed, in particular, their stability and performance properties in the presence of unmodeled dynamics and output disturbances.

A unified analytical approach has been developed that can be used to examine the class of existing adaptive algorithms. It was discovered that all existing algorithms contain an infinite-gain operator in the dynamic system that defines command reference errors and parameter errors; it is argued that such an infinite gain operator appears to be generic to all adaptive algorithms, whether they exhibit explicit or implicit parameter identification. The practical engineering consequences of the existence of the infinite-gain operator are disasterous. Analytical and simulation results demonstrate that sinusoidal reference inputs at specific frequencies and/or sinusoidal output disturbances at any frequency including d.c. cause the loop gain of the adaptive control system to increase without bound, thereby exciting the (unmodeled) plant dynamics, and yielding an unstable control system. Hence, it is concluded that none of the adaptive algorithms considered can be used with confidence in a practical control system design, because instability will set in with a high probability.

Thesis Co-Supervisor: Dr. Michael Athans
Title: Professor of Systems Science and Engineering

Thesis Co-Supervisor: Dr. Lena Valavani
Title: Research Scientist, Laboratory for Information and Decision Systems

ACKNOWLEDGEMENTS

A Ph.D. thesis represents more than the body of research reported upon in this document. It represents a culmination of the first phase of one's professional life. Thus I take this time to acknowledge and thank not only those who aided with the research itself and those who aided me personally through the years of research, but also those who brought me to the point where I was prepared to undertake the task of earning a doctorate.

Among the technical contributors, I thank Prof. Michael Athans my thesis co-supervisor, for providing the initial motivation for my researching the topic of this thesis, for guiding my progress throughout the research and for his painstaking review of the drafts of this thesis. I thank Dr. Lena Valavani, my thesis co-supervisor, for her enthusiam about the subject, for her patience while I was learning the literature, for her time and effort in the many thought provoking discussions we had especially those leading to the initial results of the research, and for her thoughful review of the drafts of this thesis. I thank Prof. Gunter Stein, a reader of this thesis, for sharing his tremendous insights in interpreting the results attained in this research and for his willingness to teach any time a question arose. I thank Prof. Shankar Sastry for his encouragement and suggestions while acting as a reader. I thank my officemates Dr. Marcel Coderch, Dr. Peter Thompson, and Dr. Howard Chizeck for their valuable time in discussing any topic of interest, including many details of this thesis. I received a great part of my M.I.T. education from them.

I thank Fifa Monserrate for typing the manuscript, Art Giordani for drafting the figures, and Marilyn Pierce for cutting a great deal of red tape for me during my stay at MIT.

First and foremost among those who helped keep me not only sane but happy during my stay at MIT is my wife, Cathy. Her support was total, her commitment unshakable, her laughter contagious, and her love immeasurable. With all my love, I thank her.

I thank the ubiquitous Prof. Paul Lagace and his season Red Sox tickets, Frank Field and the men of MIE, my brother Tom and his wife Marion, the Rileys, the MacRaes, the Lauers, the Thompsons, the Cooks, the students of MacGregor and Next House and all who have touched my life in Boston and helped to make it good.

Foremost among those who brought me to the point where a Ph.D. was in the realm of possibility are my parents, Charles and Florence Rohrs. The knowledge attained in the study for a Ph.D. is significant compared to that which they imparted through the loving attention I received in their "old-fashioned" home. I only hope that I have the patience and devotion to teach my children as they taught me.

I thank all the teachers I have had through these twenty-three years of formal education, especially Prof. James Massey and Prof. David Cohn, who went out of their way to offer me advice and assistance. Finally, I thank Prof. Jim Melsa, a professor who befriended a student, and his wife, Cathy, for their advice and concern especially during the hard times.

The research of this thesis was carried out at the M.I.T. Laboratory for Information and Decision Systems with support provided by the NASA Ames and Langley Research Centers under grant NASA/NGL-22-009-124 by the U.S. Air Force Office of Scientific Research under grant AFOSR 77-3281, and by a grant from the E.I. duPont de Nemours and Co., Inc.

TO CATHY AND KELLY

TABLE OF CONTENTS

LIST OF FIGURES

LIST OF TABLES

CHAPTER 1

INTRODUCTION

1.1 Introduction

The development of a systematic design methodology for the synthesis of practical self-adjusting control systems which can maintain first stability and second performance improvement, in the presence of rapid and large variations in the open-loop dynamics, represents a very important generic goal in control systems engineering, in view of its wide applicability to industrial and defense applications. The so-called "adaptive control problem" has received attention by theoreticians and practitioners alike for the past 25 years. About a dozen books and hundreds of articles have been devoted to the subject; different philosophies have been developed (model reference adaptive control, self-tuning regulators, dual-control methods, multiple-model adaptive control, etc.) and a variety of (mostly academic) examples have been simulated.

If classes of practical adaptive control algorithms were available, then numerous application areas would benefit in both the military and commercial sectors. Advances in microprocessor technology allow the engineer to implement in real-time the nonlinear, time-varying algorithms necessary to implement the adaptive dynamic compensator necessary to stabilize and improve the performance of a plant with poorly understood characteristics.

We present below a typical, but non-exhaustive, list of problems of practical importance that will benefit from the development of practical adaptive control algorithms. It should be noted that in these typical application areas the common characteristic is that the physical system to be controlled is characterized by rapidly changing dynamics; also, the application requires a consistent improvement in performance.

(a) Design of stability augmentation systems of highly maneuverable aircraft. In this class of problems rapid changes in dynamic pressure and operation in high angle of attack and high sideslip environments result in very variable effectiveness of aerodynamic surfaces; the aircraft stability augmentation system must rapidly adapt to such dynamic pressure variations.

(b) High performance surface-to-air and air-to-air missiles. Similar problems as in (a) arise in the design of the autopilot of highly maneuverable interceptor missiles capable of non-nuclear kill (NNK) of highly maneuverable and evasive targets; rapid changes in the aerodynamic characteristics can be expected in the end-game portion of the engagement as the target

undergoes last-ditch evasive maneuvers. The missile autopilot must maintain a high bandwidth to cope with the rapid changes in the commanded signals, and to compensate for changes in the low frequency missile dynamics.

We remark that the issues presented in (a) and (b) above are also present in problems involving the control of submarines and of torpedos. High speed submarine maneuvers can stress the stability of a fixed (non-adaptive) control system . Highly maneuverable torpedos present similar problems as missiles.

Different adaptive control problems are present in the process control area. It is widely recognized that more sophisticated control systems than the traditional Proportional-Integral-Derivative (PID) controller can increase the productivity and improve the energy efficiency of many processes. The stumbling block is that even reasonable finite dimensional dynamic models for such processes are extremely difficult to obtain, due to the complexity of the thermodynamic relations and the inevitable transport delay phenomena.

The above examples are representative and they are not meant to be exhaustive. For most control systems, some need for adaptation exists; the design of high-energy laser systems, active control flexible structures (space structures, towed arrays etc.), the

control of advanced turbofan engines, and emergency control of power systems represent additional major prospects for good adaptive control.

By the end of the 1970's considerable progress had been made in the theory of adaptive control systems. Specifically, model reference adaptive control algorithms were proposed in the literature which, under certain assumptions, achieved global asymptotic stability; that is, no matter what initial values and reference inputs were used, the output of the controlled plant would asymptotically match the output of the reference model [3-12]. In addition, unification work was performed to enable other algorithms, such as certain types of self-tuning regulator designs to be viewed as special cases of model reference adaptive control [13,14].

Unfortunately, the stability proofs of all these algorithms have in common a very restrictive assumption. For continuous-time implementations this assumption is that the relative degree of the plant, i.e., its number of poles minus its number of zeroes, is known. This implies that the phase of the system is known for high frequencies. On the other hand, it is a well known fact that models of physical systems become very inaccurate in describing high frequency phase characteristics. Indeed,

relative degree is not even a well-defined quantity for infinite dimensional systems. Finally, for practical reasons, most controller designs need to be based on models which do not contain all of the plant's dynamics in order to keep the complexity of the compensator within bounds. Consequently, it is imperative to explore the behavior of adaptive control algorithms when the unrealistic, from an engineering viewpoint, relative degree assumption is violated.

The counterpart of the relative degree assumption for discrete-time adaptive control algorithms is that the pure delay in the plant is exactly an integer number of sampling periods and that this integer is known. In addition, it is assumed that the degree of the model of the plant is at least equal to the degree of the plant itself. Again, these are mathematical assumptions that are violated in any practical control design. The delay of a plant is rarely known precisely and is often a variable quantity. Even more importantly the actual order of a system is often prohibitively high or even infinite.

Another problem with the published algorithms is that there has been no statement as to how the algorithms will react when presented with general disturbances, especially additive output

disturbances. Indeed only one algorithm includes any disturbance consideration at all and that consists of a disturbance of a very particular structure. [12].

This thesis deals with a problem that, until the initiation of the research reported upon here, had not been dealt with in the adaptive control literature.* A simple statement of the problem is as follows:

How will the published adaptive control algorithms behave if they are designed assuming that the nominal system has a certain order and are implemented on a system consisting of the assumed nominal system in series with another system? The second system will represent the unmodeled dynamics of the plant. Such unmodeled dynamics will be thought of as affecting only the high-frequency behavior of the system.

It will be seen in the sequel that in order to design an adaptive control system which behaves well, even in the disturbance free case, in the presence of such high-frequency unmodeled dynamics requires great care and insight.

---

*In 1976 a visiting postdoctoral fellow at MIT, Dr. Martin-Sanchez, under the supervision of Professor Athans, conducted some (unpublished) simulations of the Model Reference Adaptive Control algorithm for the F-8 Aircraft longitudinal dynamics. In the absence of any sensor noise simulations of the adaptive algorithm performed extremely well over a very wide range of operating conditions. However, even in the presence of very small additive sensor noise, the algorithm performed very poorly even in the absence of unmodeled dynamics.

However, it will also be seen that even carefully designed systems encounter grave instability problems if, in addition to the high frequency unmodeled dynamics, they encounter even small sinusoidal output disturbances at any frequency. Since the deisgner cannot control the disturbance environment in which a control system operates, and since physical systems always have unmodeled dynamics at sufficiently high frequencies, one cannot use any of the adaptive control algorithms examined in this thesis with confidence in engineering applications, because they will lead to unstable systems with high probability.

1.2 A Survey of the More Recent Adaptive Control Literature

The adaptive control algorithms studied in this dissertation have their roots in the solutions to the "adaptive observer" problem. An "adaptive observer" is a system which simultaneously estimates the states and parameters of an unknown linear system.

The "adaptive observer" problem for single-input single-output linear time-invariant systems was well understood by the mid 1970's. Many different versions of globally asymptotically stable adaptive observers - of minimal and nonminimal orders - appeared in the literature [15-22] and their stability and convergence properties were analyzed [23-25]. The results reported in [15-25] were obtained with the additional assumptions of exact process modelling and the absence of process and/or measurement noise.

At about the same time, attention was then shifted to what could be considered the logical continuation of the adaptive observer problem; namely, the design of an adaptive controller for the same class of systems and under the same assumptions mentioned above. However, contrary to the expectations of research workers, its solution did not follow directly from the solutions obtained for the adaptive observer, except in the case where the entire state vector of the plant was assumed accessible [18].

The complications arose in the control problem, on the one hand, when it was attempted to design a controller for an unknown plant using its input-output data alone and with no accessibility to any other point; on the other hand, due to noise considerations, explicit use of differentiators was to be excluded. The difficulty was enhanced further by the feedback configuration used in the case of control, which gave rise to nonlinear time-varying differential equations for the adaptive loop unlike the linear dynamics which pertained in the open-loop adaptive observer problem.

An important contribution in the design of an adaptive controller was made by Monopoli [26] who suggested an ingenious scheme for control that removed the need for differentiators by use of an augmented error signal.

In 1978, motivated by Monopoli's idea of using an augmented error signal two advances came about. Feuer and Morse [4] created an

adaptive control algorithm which also claimed asymptotic stability of the adaptive loop, although it was clearly too complex to be of any practical value except in very simple cases. Narendra and Valavani [3] succeeded in designing a simple controller structure whose stability was proven for the cases when the relative degree of the plant (the number of poles minus the number of zeroes) was less than three. The stability of the algorithm was conjectured for the cases of relative degree greater than three. This conjecture remains unresolved. We note that all the above algorithms were designed for continuous-time systems.

Based upon this framework, the stable adaptive control problem broke open by 1980. At the same time, papers were published in which Narendra, Lin, and Valavani [5] proved a modified version of the original conjecture of [3], Morse [6] simplified his algorithm, while Narendra and Lin [7] had proved asymptotic stability for the discrete-time version of the algorithm of [5] and Goodwin, Ramadge, and Caines [10] had developed a series of their own globally asymptotically stable discrete-time adaptive control algorithms, which were motivated from entirely different considerations than the algorithms mentioned so far. Shortly thereafter, Landau [9] extended a stability theorem of Landau and Silveira [8] which, when applied to the formulation of [7], created another algorithm.

Elliott [27] has recently created a hybrid algorithm. Egardt [11,12] has created algorithms for both continuous-time and discrete-time.

The algorithms mentioned in the foregoing have been proven globally asymptotically stable under appropriate assumptions on the controlled plant. The required assumptions are that the plant be a minimum phase SISO linear time-invariant system, whose relative degree and the sign of the high frequency gain are known, along with an upper bound on the plant order and on the magnitude of the high frequency gain. Under the above assumptions, these algorithms produce systems whose output asymptotically matches the output of a given reference model when presented with the same reference input. In addition, the parameter errors and state variables of these systems remain bounded. All of the algorithms mentioned above, except for one of the three algorithms presented in [10], are of the direct control type. Furthermore, the results obtained hold only in the purely deterministic case and their stability analysis does not account for the effects of unmodeled dynamics at high frequencies.

At the same time, or even earlier, progress was being made in the area of indirect adaptive control. In this approach, an adaptive observer is used to identify the plant parameters and estimate the plant state. This information is then used to synthesize an appropriate

control signal. Åström and his co-workers [28-31], Kreisselmeier [32-33], and Elliott and Wolovich [34] have created indirect algorithms which, while requiring fewer assumptions on the plant, do require instead "sufficiently rich" signals (in the adaptive loop) for general stability. In [33], Kreisselmeir also proves stability under zero reference input without any "richness" assumptions. The work of Egardt did much to increase the understanding of the similarities in the various approaches to adaptive control by creating new general algorithms [11,12] which contained algorithms such as those of [5]-[10] and [28-31] as special cases as shown in [13,14].

Another trend during the 1970's was the examination of stochastic adaptive control problems including process and measurement noise. The adaptive control problem was posed as a stochastic optimal control problem and several algorithms - mostly iterative in nature - were developed by approximating the dynamic programming solution. This led to the development of the so-called dual control methdology, surveyed by Athans and Varaiya [35] and in a more recent paper by Bar-Shalom in [36].

As mentioned earlier, after the first designs of adaptive observers appeared in the literature, considerable research effort was directed in the more detailed analysis of the (uniform) asymptotic stability properties of these newly designed algorithms. Such studies were carried out by Anderson [23], Yuan and Wonham [25], and Morgan and

Narendra [24], who obtained sufficient conditions for asymptotic stability in terms of different aspects of a "persistently spanning" property for the combined state and input vector of the adaptive process. The problem of accurately estimating plant parameters was also addressed from an optimization point of view, in terms of an optimal choice of inputs, by many researchers, among whom are Aoki and Staley [37], Goodwin, et.al. [38], Reid [39], Nahi and Napjus [40], Keviczky [41], Lopez-Toledo and Athans [42], Chen [43], and Mehra [44]. Unfortunately, the "persistent excitation" requirement which is invariably present, in some form or another in the literature cited above, cannot be guaranteed to hold globally in a closed loop system, although Kreisselmeier showed that it can be preserved locally [32].

The presence of observation noise, in the earlier literature, was dealt with by adopting time-decreasing adaptation gains [45], in the already existing algorithms, along the lines suggested by stochastic approximation methods, and without any formal proofs. The most significant research in the rigorous study of such adaptive systems was carried out by Ljung [46,47] who introduced his ordinary-differential equations (ODE) approach, to study the convergence properties of discrete-time stochastic adaptive algorithms in terms of the properties of an ordinary differential equation associated with each one of them.

The approach is asymptotic and the results valid only locally, in certain domains in parameter space, within which the "adjusted" system is stable. The developed theory, however, cannot define in a precise manner what these domains are, or guarantee that the adaptive system is actually evolving within one of them. More recently, Goodwin, et.al., [48,49] obtained mean-square boundedness of the output error for the stochastic adaptive algorithm which was a modified version of [10], in which positive realness of the noise transfer function was required. Again, all the above results were obtained under the assumption of perfect modeling.

Due to the fact that little theoretical work has been done to analyze the behavior of adaptive control algorithms under conditions which are anything less than ideal, there is a limited experience regarding their use in practical applications. The collection [50] provides a reasonable sampling of the present practical applications of adaptive control theory.

Only very recently some progress has been made in theoretical studies of adaptive algorithms, based on more practically realistic and relaxed assumptions. Preliminary results of the research presented in this dissertation have appeared in the literature. In Rohrs, et.al., [1], simulation studies which displayed the dangerous effects of unmodeled dynamics on one adaptive control algorithm were reported. In Rohrs, et.al. [2], the effects seen in [1] were displayed analytically

for first order systems and a number of algorithms. Chapter 3 and Section 5.1 of this thesis are expansions of the work reported in [2].

Ioannou and Kokotovic [51] used singular perturbation methods to study the properties of adaptive observers in the presence of unmodeled dynamics. Although this paper does not deal with closed loop adaptive control, the results demonstrate that significant errors can occur when the high frequency dynamics get excited. Furthermore, they showed that the parameter errors can remain bounded and that their bound becomes tighter as the unmodeled dynamics become faster and the input used becomes smoother. Ioannou [52] and Ioannou and Kokotovic [53] have recently extended their singular perturbation approach to include the adaptive control algorithm of [3]. They show that this algorithm will remain locally stable in the presence of very high frequency unmodeled dynamics and zero reference input. They also show that a modified version of the algorithm will remain locally stable in the presence of very high frequency unmodeled dynamics with low frequency reference inputs. There is no study of the effects of disturbances in these papers.

Anderson and Johnson [54-55] and Anderson and Johnstone [56] have shown that, with a "sufficient excitation" condition, discrete-time adaptive observers and the adaptive control scheme of [10] become not only asymptotically stable but also exponentially stable and thus should retain stability in the presence of disturbances. Since exact parameter convergence, however, was a key factor in obtaining the above results,

they cannot apply in the control scheme of e.g. [5], when unmodeled dynamics are present; it is not clear in such a case what parameter convergence to the "true" values really means. Notwithstanding, it is shown in Section 5.1.1 of this thesis that the algorithm of [10] is of a particular form that, despite relatively good performance under exact modeling asssumptions, is extremely sensitive to unmodeled dynamics and is therefore of limited practical use. Despite their theoretical importance, the results in [54-56] do not provide an estimate of the order of the exponential stability; hence the amount of modeling error that can be tolerated is not predictable even under the assumptions of perfect modeling. Besides, one should also be cautious of the adverse effects that such "sufficient excitations" can have on the stability properties of the overall system under imperfect modeling.

Finally, Narendra and Peterson [57] and Kreisselmeier and Narendra [58] produced some ad hoc and highly restrictive modifications of known algorithms to insure bounded errors in the presence of disturbances.

1.3 Contributions of this Thesis

In this thesis, the behavior of adaptive control algorithms is analyzed when such algorithms are implemented on systems which contain dynamics that are not modeled as part of the adaptive control design process. Such dynamics will be referred to as unmodeled dynamics. The behavior of adaptive control algorithms operated in the presence of constant and sinusoidal output disturbances is also examined.

The contributions to the theory of adaptive control are as follows:

- the demonstration of an analysis method for evaluating the behavior of adaptive control algorithms when such algorithms are implemented in the presence of unmodeled dynamics and used with constant inputs in a disturbance-free environment. The analysis method proves to be insightful and constructive despite the fact that it is applicable under rather restrictive assumptions.

- The isolation of an infinite gain operator inherently present in the design of adaptive control algorithms and the demonstration that in the presence of unmodeled dynamics such infinite gain operators lead to unstable responses to certain classes of reference inputs.
- The demonstration of two mechanisms by which adaptive control algorithms react poorly to any sinusoidal or constant disturbance which, in turn, leads to unstable behavior, if unmodeled dynamics are also present.

In the process of developing the above points, it is shown that, if the assumption on the degree or relative degree of the plant is violated, the asymptotic stability properties of the adaptive control algorithms are lost.

The first mechanism of instability involves the so-called error system loop. If the gain of this loop is too large, the loop bandwidth will also be large so that any unmodeled dynamics which are present will become excited, thus causing instability. The high loop gain may be attributed to the fact that, unless intentionally normalized, the error loop gain will be proportional to the square of the size of the signals in the nominal control system. Even when a normalization of the adaptation gains is used

to create an error system whose gain is independent of the size of the signals in the nominal control system, these gains must still be carefully chosen in order to limit the bandwidth of the error loop and not to excite unmodeled dynamics.

A high gain error system may also result from the fact that for certain sinusoidal input signals, the gain of the error system itself increases with time. This is a nonlinear effect and causes instability for high frequency sinusoidal inputs in the presence of high frequency unmodeled dynamics.

The second mechanism for instability involves the primary control loop. A deterministic additive output disturbance at any frequency, including constant disturbances, which is not measured will create a situation in which the output error can not be driven to zero. The parameters in the control system will drift in certain directions, resulting in a large gain, high bandwidth nominal control system. Such a controller will excite unmodeled dynamics in the plant causing instability. This second mechanism can also occur if the algorithm cannot attain zero error for reasons other than disturbances. It is conceivable for example, that the controller does not provide enough flexibility for the controlled plant complete with unmodeled dynamics to match the reference model for the inputs given. This will also cause a steady non-zero error driving the nominal controller to high bandwidth and eventual instability.

To summarize, in this dissertation, adaptive control in the presence of unmodeled dynamics is examined and grave stability problems are found. Some of these problems can be alleviated by the use of tools developed in this thesis that enable the designer to choose the parameters of the adaptive control system and the reference inputs wisely. However, there still remains the debilitating problem demonstrated in this dissertation that, if an adaptive controller is implemented in the presence of unmodeled dynamics and a persistent unmeasurable output disturbance, the system is likely to become unstable.

1.4 Outline of the Thesis

Chapter 2 contains a few mathematical preliminaries and introduces seven adaptive algorithms which will be studied, using a common notation. Section 2.1 provides the necessary notation while Section 2.1.1 provides a primer on positive real systems and their role in stability proofs of feedback systems. Positive realness is an important concept in the stability proofs of adaptive control algorithms and its introduction allows outlines of the stability proofs associated with some of the algorithms. From these stability proof outlines it becomes apparent that the assumptions made on the relative degree are very fundamental to the global stability proof. This argument is presented in Section 2.2.1.5

for the algorithm of Narendra and Valavani [3] and Feuer and Morse [4], referred to as CA1. The remarks concerning the proof of CA1 are directly applicable to the stability proofs of the other algorithms studied, namely the algorithm of Narendra, Lin, and Valavani [5] and the first algorithm of Morse [6], both referred to as CA2, the second algorithm of Morse [6], referred to as CA3, the algorithm of Egardt [11] referred to as CA4, the algorithm of Narendra and Lin [7], referred to as DA1, the algorithm of Goodwin, Ramadge, and Caines [10], referred to as DA2, and the algorithm of Egardt [12], referred to as DA3.

In Section 2.2 the continuous-time algorithms, CA1 to CA4, are introduced and in Section 2.3 the discrete-time algorithms DA1 to DA3 are introduced. The algorithms are presented with a common, consistent notation and the error system for each algorithm is developed. The equations for each algorithm are summarized in tabular form within each subsection.

In Chapter 3, the analysis technique is developed for continuous-time algorithms with constant inputs and no disturbances. The technique involves linearizing the error system around a nominal control system. The resulting analysis proves useful in guiding the selection of certain important parameters that impact the design of adaptive control systems for a variety of conditions.

In Section 3.2 the concepts of the linearization analysis that is used throughout Chapter 3 and Section 5.1 are introduced and discussed.

In Section 3.3 it is shown that the gain of the error system of CA1, the simplest adaptive system, is proportional to the square of the magnitude of the signals present in the controller. In Subsection 3.3.2 it is shown that too large a reference input signal will produce a high frequency control signal even when the assumptions on the plant degree are correct. In Subsection 3.3.4 it is shown that in the presence of unmodeled dynamics, high frequency control signals will excite the unmodeled dynamics and cause instability. The analysis provides a measure as to how large an input is necessary to produce instability given a certain configuration of the real plant with unmodeled dynamics. In addition, it is shown in Subsection 3.3.5 that, at values of the error loop gain which are considerably lower than those which ultimately cause instability the system parameters will be forced to move away from the values that provide good model matching in order to maintain stability. The analysis in Section 3.3 suggests that the stability problem exposed in Section 3.3.4 can be remedied by normalizing the gain of the adaptation equations, making this gain inversely proportional to the square of the signals in the loop. The gain of the error system can then be designed independently of the size of the input.

This normalization is an integral part of algorithms CA3 and CA4. The analysis for these algorithms is contained in Section 3.5 and 3.6. The importance of the proper selection of the adaptation gains is reiterated during the analysis. Section 3.4 deals with the algorithms CA2 which limits the gain of the error loop not by a direct normalization but by adding an inner loop to the error system. The function of this inner feedback is to place zeroes in the error transfer function and therefore to limit the bandwidth of the error loop.

The analysis of all the continuous-time algorithms is demonstrated throughout Chapter 3 by use of a numerical example where the adaptive control system is designed using a first order model but the actual plant consists of an unmodeled pole pair in series with the nominal first order system. Digital computer simulations of the non-linear adaptive control system provide verification of the analysis.

The message of the analysis of Chapter 3 can be summarized as follows:

- Keep the gains of the adaptation mechanism low so that the bandwidth of the error system will remain small.

The method of analysis developed in Chapter 3 provides for a given plant with unmodeled dynamics, a way to determine what gain will allow satisfactory response to constant inputs in the absence of disturbances.

Chapter 4 provides insight into the response of the continuous-time algorithms in situations not covered by the analysis of Chapter 3. Particular attention is paid to the response to sinusoidal inputs and constant or sinusoidal disturbances.

In Section 4.2, it is shown that present in each of the algorithms studied is an operator with unbounded gain. Such an operator will produce unbounded output signals in response to certain bounded input signals. Indeed, when the operator is presented with a sinusoidal input of constant amplitude, a component of the output will be a sinusoid of the same frequency whose amplitude linearly increases with time.

It is also argued in Section 4.2 that not only is this infinite gain operator present in all seven algorithms considered in this work, but that such an operator is generic to all approaches to the adaptive control problem involving explicit or implicit identification.

In Section 4.3 a heuristic argument is presented that the infinite gain operator can cause instability by two mechanisms.

The first mechanism of instability is connected to the fact that, since the infinite gain operator is in a feedback loop, the increasing amplitude sinusoid at the output can be fed back to the input, thus compounding the problem. The result is a sinusoidal error signal which increases slowly in amplitude until the gain of the error system loop is increased beyond unity, at which point gross instability develops.

The first mechanism will cause instability, only if a sinusoidal signal develops at a frequency where the phase characteristics of the feedback loop defining the output and parameter errors cause reinforcement of the sinusoide at the input to the infinite gain operator.

The second mechanism for instability is associated with a nonzero steady-state output error. A steady-state output error at any frequency, including constant errors, will, through the action of the infinite gain operator, cause the parameters to increase without bound. The parameters will eventually reach values for which the overall system with unmodeled dynamics is unstable.

In Section 4.4, the following statement, conjectured to be true by the analytical argument of Section 4.3 is demonstrated to be true by digital simulations:

- In the presence of unmodeled dynamics, certain frequency reference inputs will cause the adaptive algorithms CA1-CA4 to become unstable.

In Section 4.5, it is shown that the instability problems explained in Section 4.3 cannot be eliminated by such "fixes" as filters on the plant output or output error.

In Section 4.6 the following statement, also conjectured to be true in Section 4.3, is verified as true by digital simulation:

- A sinusoidal output disturbance at any frequency or a constant output disturbance will cause the adaptive systems CA1-CA4 to become unstable in the presence of unmodeled dynamics.

Chapter 5 provides the same analysis for discrete-time algorithms, DA1 to DA3, as Chapters3 and 4 provide for continuous-time algorithms. Indeed, the analysis is an exact parallel with all the principles learned in the continuous-time case carrying over to the discrete-time case.

Section 5.1 provides the analysis of discrete-time algorithms under the conditions of constant reference input and no disturbances.

The analysis proceeds as in the continuous-time case and proves just as insightful for design purposes. Indeed, two more design "rules of thumb" become aparent in the analysis of Section 5.1.

The analysis of Section 5.1.2 shows that the structure of the algorithm DA2 requires that there be a high feedback gain in the nominal control system. This leaves the algorithm unable to match the model and maintain stability in the presence of unmodeled dynamics. The algorithm DA3 is similar to DA2 except that it provides for extra filtering which makes it possible for the algorithm to match the model with feedback gains of any size. Therefore, this algorithm has ability to match the model in the presence of unmodeled dynamics.

One must realize that situations such as those described in the preceding paragraph arise because all of the algorithm considered are designed on the basis of satisfying a single criterion, namely, to follow asymptotically a specified response to a reference input. It is up to the designer to assure that, if the algorithm converges, the nominal control system will be an adequate one with respect to rejecting disturbances and sensor noise and being able to function in the presence of unmodeled dynamics. Thus, the analysis has pointed out the following design rule:

- design a good nominal control loop.

Finally, the analysis of Section 5.1.2.3 shows that many of the problems connected with unmodeled dynamics are alleviated when the system is sampled slowly enough so that the poles and zeroes of the unmodeled dynamics essentially cancel. Of course, it is well known that sampling systems too slowly results in jerky step response and poor disturbance rejection. Thus, the last rule of thumb shown by the analysis on constant input systems is particular to discrete-time algorithms:

- For good response in the presence of unmodeled dynamics, sample the system as slowly as other considerations will allow.

Section 5.2 demonstrates that there is a discrete-time equivalent to the infinite gain operator of continuous-time systems. That the operator leads to instabilities with certain high frequency inputs is demonstrated with simulations in Section 5.2.4. It is also shown, in Section 5.3, that this is another problem intimately connected with unmodeled dynamics and can be greatly alleviated by slow sampling.

However, it is shown in Section 5.3 that a problem not alleviated by slow sampling is the instability caused by a sinusoidal output disturbances. The residual error still drives the parameters to such a high bandwidth nominal control system, that any modeling errors will cause instability. This is shown in the analysis and simulations of Section 5.2.5.

Chapter 6 provides the conclusions and possible direction for future research in the area.

CHAPTER 2

INTRODUCTION TO ADAPTIVE CONTROL ALGORITHMS

2.1 Introduction

The purpose of this chapter is to provide an exposition of a number of algorithms which represent the state of the art in adaptive control and to set up the machinery necessary to analyze the performance of these algorithms in the presence of unmodeled dynamics. All of the algorithms considered have been proven to be globally asymptotically stable when the proper assumptions are realized. Each algorithm that is presented has been chosen because it displays particular characteristics when certain assumptions are relaxed. The various algorithms will be compared and contrasted in the sequel. The introduction of the algorithms will be divided into two parts; the first will deal with continuous-time algorithms and the second will deal with discrete-time algorithms.

The following notation will be used:

Capital letters will represent system polynomials and lower case letters will represent time functions or constant gains. In particular,

$$y(t) = \frac{kB}{A}\,[x(t)]$$

will be used to indicate that $y(t)$ is the output of a linear time-invariant system whose input is $x(t)$ and whose transfer function is $\frac{kB(\cdot)}{A(\cdot)}$ where A and B are polynomials in the Laplace transform variable s or the backward shift operator q^{-1}. An underlined lower case letter will represent a vector of time functions or gains and an underlined capital letter will represent a matrix.

A superscript in parenthesis will be used to indicate the degree of a polynomial, e.g., $A^{(n)}$ indicates that the polynomial A(s) has degree n. This notation will be used only when knowledge of the degree is important for the understanding of the point being made.

The relative degree of the transfer function $\frac{B^{(m)}}{A^{(n)}}$ is the number of poles minus the number of zeroes, in this case, n-m. The relative degree will usually be denoted as n*.

Discrete-time linear time-invariant systems will be represented in terms of the backwards shift operator q^{-1}, e.g.,

$$y(t) = \frac{kq^{-d}\, B^{(m)}}{A^{(n)}} [x(t)]$$

where $B^{(m)} = 1+b_1q^{-1} + b_2q^{-2} +\ldots+ b_mq^{-m}$

$$A^{(n)} = 1+a_1q^{-1} + a_2q^{-2} +\ldots+ a_nq^{-n}$$

and d is the delay of the system.

2.1.1 A Positive Real Primer

Due to the importance of positive real systems in the adaptive control literature, this section summarizes pertinent results. The results for continuous-time systems are paralleled by the results for discrete-time systems.

Definition 1-1 [59] A linear time-invariant system with transfer function H(s) is positive real, if H(s) has no poles with positive real parts, the poles of H(s) with zero real parts are simple and have positive real residues and $\mathrm{Re}[H(j\omega)] \geq 0$ holds for all ω. The system is strictly positive real, if H(s-ϵ) represents a positive real system for some real scalar $\epsilon > 0$.

A less formal statement of this definition can be given as follows:

> a positive real system is a stable system whose Nyquist diagram lies in the closed right half plane.

The relative simplicity of maintaining stability in a feedback configuration, such as that shown in Figure 2-1, with a positive real system in the forward path and a linear time-invariant system in the feedback path is seen by considering the Nyquist criterion. The Nyquist criterion shows that such a feedback connection will be stable if the feedback path is itself positive real. Such a system would be stabilized by its phase properties independent of the size of the gain of the system.

Note also that in order for a continuous system to be positive real it must necessarily be of relative degree 0, 1, or -1.

The phase properties of positive real systems can be exploited further when the feedback system is time-varying by use of the following two lemmas.

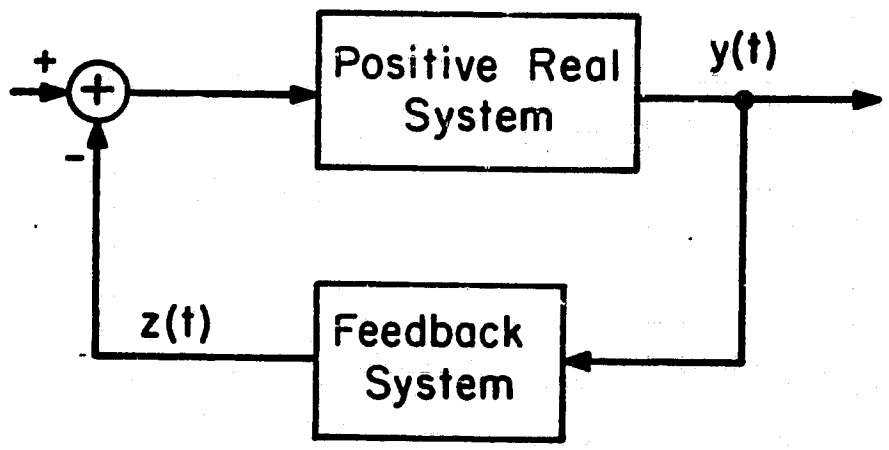

Figure 2-1. Feedback configuration with a positive real system

Lemma 1.1: Popov's Hyperstability Condition [60]

The negative feedback interconnection, such as that of Figure 2-1, of a strictly positive real linear time-invariant system and a system whose input is y(t) and output is z(t) is asymptotically stable if y(t) and z(t) satisfy, for all t,

$$\int_0^t y(\tau)z(\tau)d\tau \geq -\ell^2$$

where ℓ is a constant independent of t. Such feedback operators are called positive or passive.

Note again that there is no upper bound limitation for the gain of the feedback operator if the passivity requirement is satisfied.

Lemma 1.2: Kalman-Yacubovich Lemma [61]

If $[\underline{A},\underline{b},\underline{c}]$ is a minimal realization of a strictly positive real transfer function, i.e., $\dot{\underline{x}}(t) = \underline{A}\underline{x}(t) + \underline{b}u(t)$, $y(t) = \underline{c}^T\underline{x}(t)$, then there exist matrices $\underline{P}=\underline{P}^T > \underline{0}$, $\underline{Q}=\underline{Q}^T > \underline{0}$ such that

$$\underline{A}^T\underline{P} + \underline{P}\,\underline{A} = -\underline{Q} \tag{2-1}$$

and

$$\underline{P}\,\underline{b} = \underline{c} \tag{2-2}$$

Lemma 1.2 is used to obtain Lyapunov functions for feedback configurations involving positive real operators. There is a generalization of this lemma to include positive real systems with relative degree zero but this generalization will not be needed in the sequel. [61]

The corresponding lemmas for discrete-time systems are exact parallels of the results for continuous time systems but are not needed in the sequel [62].

Note, however, that, in order for a discrete-time system $H(q^{-1}) = \frac{q^{-d} B^{(m)}(q^{-1})}{A^{(n)}(q^{-1})}$ to be positive real, it must be stable and its discrete Nyquist plot, i.e., the image of $H(q^{-1})$, $q=e^{j\theta}$, $0 \leq \theta \leq 2\pi$, must remain in the closed right half plane. Since the magnitude of this plot does not go to zero except at zeroes of $B(z^{-1})$, $H(z^{-1})$ must have the same number of poles as zeroes. This implies that the delay d must be zero.

The above definitions and lemmas play vital roles in the published stability proofs of adaptive control algorithms. They will be used in Section 2.2.1.5 to provide a sketch of one such stability proof. This sketch will demonstrate the importance of the assumption that the relative degree of the plant is known in the stability proof.

2.2 Continuous Time Algorithms

In this section, four continuous-time algorithms for adaptive control are introduced. The assumptions which are sufficient to prove global asymptotic stability are presented. The error system for each of the algorithms is developed. The error system provides a point of departure for the analysis of the various algorithms.

In subsections 2.2.1.5 and 2.2.2.4 sketches of the key steps in the stability proofs of two of the algorithms are presented. These sketches serve the purpose of establishing the importance of the positive real condition in the stability proof. Since the satisfaction of a positive real condition is brought about by the assumption that the relative degree of the plant is known, a relaxation of the known relative degree assumption must make the retention of global asymptotic stability suspect.

2.2.1 Continuous-Time Algorithm No.1 (CA1)

2.2.1.1 Introduction

The first algorithm, CA1, is the prototype model reference adaptive control algorithm. Its origins go back at least to Monopoli [26]. This algorithm has been proven asymptotically stable only for the case when the relative degree of the plant is unity. Hence, the algorithm will be considered only when a unity relative degree plant is nominally assumed. The algorithms published by Narendra and Valavani [3] and Feuer and Morse [4] reduce to CA1 for the pertinent case.

2.2.1.2 Assumptions

Assume the plant is linear and time-invariant and is described by:

$$y_p(t) = \frac{g_p B^{(m)}}{A^{(n)}} \quad [u(t)] \qquad (2\text{-}3)$$

where A and B are unknown polynomials which satisfy the following assumptions:

A1) Gain Sign Assumption:

The sign of g_p is known and, without loss of generality, is assumed positive.

A2) Minimum Phase Assumption:

B is monic and Hurwitz, i.e. its leading coefficient is unity and all zeroes of B(s) have negative real parts.

A3) Relative Degree Assumption:

$A^{(n)}$ is of degree n and $B^{(m)}$ is of degree m so that the relative degree $n^*=n-m$ is known.

Assumption A3 can be relaxed to an assumption that an upper bound on the degree of A is known and that the relative degree of the plant is known exactly. However, in the present work, Assumption A3 will be used as is since the fundamental problems connected with the known relative degree assumption remain basically unaltered while the development is simpler with the more restrictive form of the assumption. We

also remark that much of the material of this dissertation is concerned with the behavior of adaptive control systems which are designed assuming that Assumption A3 holds when, in the presence of unmodeled dynamics, it does not.

2.2.1.3 Controller Structure

The structure for the adaptive controller CA1 appears in Figure 2-2. The controller generates auxiliary signals $\underline{w}_u(t)$ from $u(t)$ and $\underline{w}_y(t)$ from $y(t)$ in the following manner: the i^{th} component of the vector $\underline{w}_u$ is

$$w_{ui}(t) = \frac{s^{i-1}}{P^{(n-1)}} [u(t)]; \quad i=1,2,\ldots n-1 \tag{2-4}$$

where $P^{(n-1)}(s)$ is an $(n-1)^{th}$ degree monic Hurwitz polynomial and s is the Laplace transform variable. Similarly,

$$w_{yi}(t) = \frac{s^{i-1}}{P^{(n-1)}} [y(t)]; \quad i=1,2,\ldots,n \tag{2-5}$$

The input to the plant, $u(t)$, is

$$u(t) = k_r(t)r(t) + \underline{k}_u^T(t)\underline{w}_u(t) + \underline{k}_y^T(t)\underline{w}_y(t) \tag{2-6}$$

where $k_r(t)$ is a time-varying gain, $\underline{k}_u(t)$ is an $(n-1)$ vector of time-varying gains, $\underline{k}_y(t)$ is an n vector of time-varying gains, and $r(t)$ is the scalar reference input.

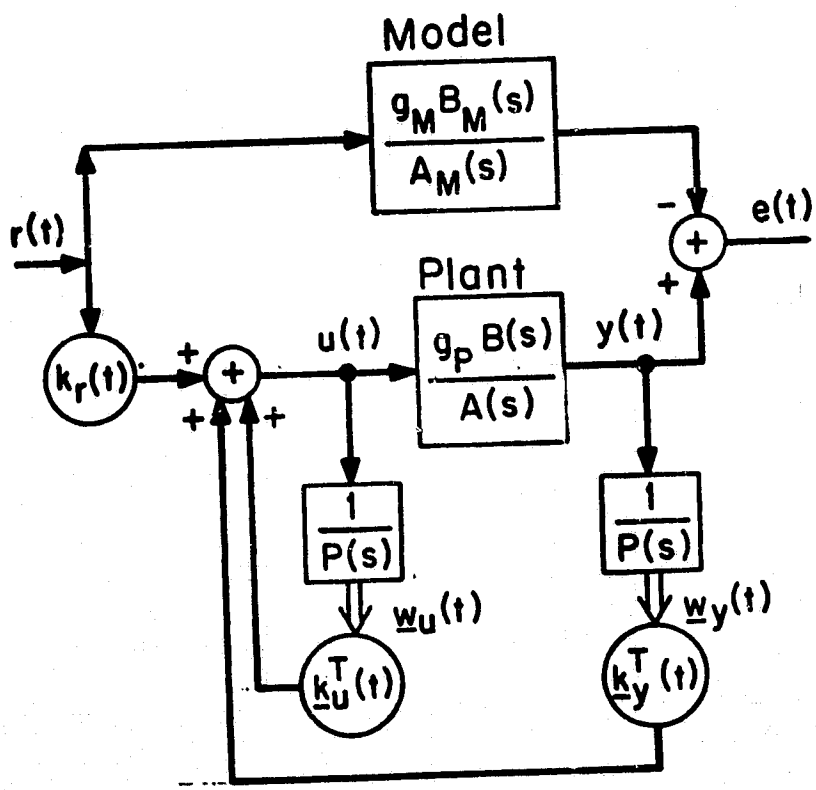

Figure 2-2. Controller structure for CA1

The object of the adaptive control algorithm is to adjust the time-varying control gains in such a manner as to make the actual plant output, $y(t)$, match the output, $y_M(t)$, of a model driven by the reference input, $r(t)$.

$$y_M(t) = \frac{g_M B_M^{(m)}}{A_M^{(n)}} [r(t)] \tag{2-7}$$

where $B_M^{(m)}$ is an m^{th} order monic Hurwitz polynomial $A_M^{(n)}$ is an n^{th} order monic Hurwitz polynomial, and g_M is a constant gain.

Furthermore, a joint requirement on $B_M^{(m)}$ and $P^{(n-1)}$ has to be satisfied, i.e., that

$$B_M^{(m)} \text{ divides } P^{(n-1)} \tag{2-8}$$

In the unity relative degree case, $m=n-1$ and, therefore,

$$B_M = P \tag{2-9}$$

The reference model is chosen by the designer. It should be chosen in such a manner so that, if the controlled plant matches the model, the resulting controller has a large loop gain at low frequencies and a reasonable bandwidth. The choice of the model is a main element in the design of a control system which performs well at least asymptotically.

Two composite vectors are now defined.

$$\underline{w}(t) = \begin{bmatrix} r(t) \\ \underline{w}_u(t) \\ \underline{w}_y(t) \end{bmatrix} \qquad \underline{k}(t) = \begin{bmatrix} k_r(t) \\ \underline{k}_u(t) \\ \underline{k}_y(t) \end{bmatrix}$$

In this notation

$$u(t) = \underline{k}^T(t)\underline{w}(t) \tag{2-10}$$

So,
$$y(t) = \frac{g_p B}{A} [\underline{k}^T(t)\underline{w}(t)] \tag{2-11}$$

The description of the algorithm is completed by specifying the control gain adjustment mechanism.

$$\dot{\underline{k}}(t) = -\underline{\Gamma}\, \underline{w}(t) e(t) \tag{2-12}$$

where

$\underline{\Gamma} = \underline{\Gamma} > 0$ is called the adaptation gain matrix, and

$$e(t) = y(t) - y_M(t) \tag{2-13}$$

is the output error.

2.2.1.4 Error Equations

It is often desirable to analyze the behavior of an algorithm with respect to a particular set of constant gains. In this subsection equations will be developed which relate the output error of eqn. (2-13)

to the difference between the actual parameters and a nominal set of parameters. Let

$$\underline{k}(t) = \underline{k}^* + \tilde{\underline{k}}(t) \tag{2-14}$$

where $\underline{k}^*$ is a constant n vector. Substituting eqn. (2-14) in eqn. (2-11), we obtain

$$y(t) = \frac{g_p B}{A} [\underline{k}^{*T}\underline{w}(t)+\tilde{\underline{k}}^T(t)\underline{w}(t)]= \frac{g_p B}{A} [\underline{k}^{*T}\underline{w}(t)]+ \frac{g_p B}{A} [\tilde{\underline{k}}^T(t)\underline{w}(t)] \tag{2-15}$$

From the definitions of $\underline{k}$ and $\underline{w}$, it follows that

$$\underline{k}^{*T}\underline{w}(t) = k_r^* r(t) + \underline{k}_u^{*T}\underline{w}_u(t) + \underline{k}_y^{*T}\underline{w}_y(t) \tag{2-16}$$

with the obvious correspondences.

Define the polynomials

$$K_u^{*(n-2)}(s) = k_{u(n-1)}^* s^{n-2} + k_{u(n-2)}^* s^{n-3} +\ldots+ k_{u1}^* \tag{2-17}$$

where k_{ui}^* is the i^{th} component of $\underline{k}_u^*$, and

$$K_y^{*(n-1)}(s) = k_{yn}^* s^{n-1} + k_{y(n-1)}^* s^{n-2} +\ldots+ k_{y1}^* \tag{2-18}$$

where k_{yi}^* is the i^{th} component of $\underline{k}_y^*$.

Then, from eqn. (2-4) and eqn. (2-17)

$$\underline{k}_u^{*T}\,\underline{w}(t) = \frac{K_u^*(s)}{P(s)}\,[u(t)] \tag{2-19}$$

and from eqn. (2-5) and eqn. (2-18)

$$\underline{k}_y^{*T}\,\underline{w}_y(t) = \frac{K_y^*(s)}{P(s)}\,[y(t)] \tag{2-20}$$

Equation (2-15) can now be written as

$$y(t) = \frac{g_p B}{A}\left[k_r^*\, r(t) + \frac{K_u^*}{P}\, u(t) + \frac{K_y^*}{P}\, y(t)\right] + \frac{g_p B}{A}\left[\tilde{\underline{k}}^T(t)\underline{w}(t)\right]$$

or

$$y(t) = \frac{K_u^*}{P}\,[y(t)] + \frac{g_p B K_y^*}{AP}\,[y(t)] + \frac{g_p B}{A}\left[k_r^*\, r(t) + \tilde{\underline{k}}^T(t)\underline{w}(t)\right]$$

or

$$y(t) = \frac{\dfrac{g_p B}{A}}{1 - \dfrac{K_u^*}{P} - \dfrac{g_p B K_y^*}{AP}}\left[k_r^*\, r(t) + \tilde{\underline{k}}^T(t)\underline{w}(t)\right]$$

or

$$y(t) = \frac{k_r^* g_p B P}{AP - AK_u^* - g_p B K_y^*}\left[r(t) + \frac{\tilde{\underline{k}}^T(t)\underline{w}(t)}{k_r^*}\right] \tag{2-21}$$

$$= \frac{g^* B^*}{A^*}\left[r(t) + \frac{\tilde{\underline{k}}^T(t)\underline{w}(t)}{k_r^*}\right] \tag{2-22}$$

where B* and A* are defined to be coprime with B* monic.

Remark 1: $\frac{g^*B^*}{A^*}$ is the closed-loop transfer function that would result if $\tilde{k}$ were identically zero, i.e., if a constant control law $k = k^*$ were used.

Remark 2: If the Assumption A3 holds and B_M divides P (eqn. 2-8), then k^* can be chosen, i.e., k_r^*, k_u^*, k_y^* can be chosen, so that

$$\frac{g^*B^*}{A^*} \triangleq \frac{k_r^* g_p B^{(n)} P^{(n-1)}}{\left(P^{(n-1)} - K_u^{*(n-2)}\right) A^{(n)} - g_p K_y^{*(n-1)} B^{(m)}}$$

$$= \frac{g_M P^{(n-1)}}{\left(\frac{P^{(n-1)}}{B_M^{(m)}}\right) A_M^{(n)}} = \frac{g_M B_M^{(m)}}{A_M^{(n)}} \qquad (2\text{-}23)$$

Equation (2-23) is derived using the facts that, given the freedom of choice in k^*, $(P^{(n-1)} - K_u^{*(n-2)})$ is an arbitrary monic $(n-1)^{th}$ order polynomial, $K_y^{*(n-1)}$ is an arbitrary $(n-1)^{th}$ order polynomial, $A^{(n)}$ and $B^{(m)}$ are coprime so that $K_y^{*(n-1)}$ and $K_u^{*(n-2)}$ provide 2n-1 degrees of freedom and hence the denominator is an arbitrary $(2n-1)^{th}$ polynomial. By setting the denominator equal to $B^{(m)} A_M^{(n)} \left(\frac{P}{B_M}\right)^{(n-m-1)}$ (remember, B_M divides P), eqn. (2-23) follows.

Remark 3: If the Relative Degree Assumption (A3) is violated, $\frac{g^*B^*}{A^*}$ can only get as close to $\frac{g_M B_M}{A_M}$ as the feedback structure of the controller allows.

The system error equations can now be derived in a particularly convenient form. Subtracting eqn. (2-7) from eqn. (2-22) yields:

$$e(t) = y(t) - y^*(t) = \left(\frac{g^*B^*}{A^*} - \frac{g_M B_M}{A_M}\right)\left[r(t)\right] + \frac{g^*B^*}{A^*}\left[\frac{\tilde{\underline{k}}^T(t)\underline{w}(t)}{k_r^*}\right] \qquad (2\text{-}24)$$

Combining eqn. (2-12) with eqn. (2-14) gives

$$\dot{\underline{k}}(t) = \dot{\underline{k}}^* + \dot{\tilde{\underline{k}}}(t) = \dot{\tilde{\underline{k}}}(t) = -\underline{\Gamma}\,\underline{w}(t)\underline{e}(t) \qquad (2\text{-}25)$$

In operator notation, one can write

$$\tilde{\underline{k}}(t) = \frac{1}{s}\,\underline{I}[-\underline{\Gamma}\,\underline{w}(t)e(t)] \qquad (2\text{-}26)$$

where $\frac{1}{s}\underline{I}$ denotes a diagonal transfer function matrix with each diagonal element equal to $\frac{1}{s}$.

The error system defined by eqns. (2-24) and (2-26) is represented in Figure 2-3.

Table 2-1 summarizes the equations for CAl.

2.2.1.5 Stability Analysis

The feedback system of Figure 2-3 will be the object of much attention. Due to the dependence of $\underline{w}(t)$ on $e(t)$, it is, in essence, a non-linear system. However, it can and will be viewed more simply as a linear time-varying feedback system as represented in Figure 2-3.

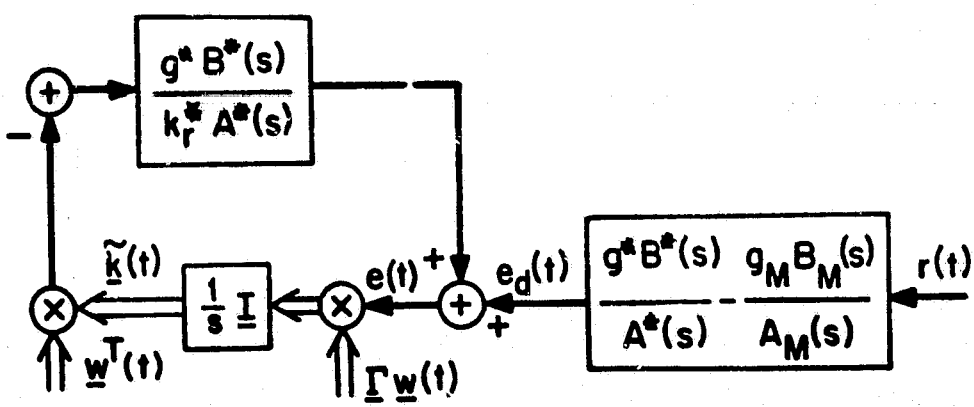

Figure 2-3. Error system for CA1

TABLE 2-1

EQUATIONS FOR CAl

Plant

$$y(t) = \frac{g_p B}{A}\,[u(t)] \qquad (2\text{-}3)$$

Auxiliary Variables

$$w_{ui}(t) = \frac{s^{i-1}}{P}\,[u(t)];\ i=1,2,\ldots,n-1 \qquad (2\text{-}4)$$

$$w_{yi}(t) = \frac{s^{i-1}}{P}\,[y(t)];\ i=1,2,\ldots,n \qquad (2\text{-}5)$$

$$\underline{w}(t) = \begin{bmatrix} r(t) \\ \underline{w}_u(t) \\ \underline{w}_y(t) \end{bmatrix}; \quad \underline{k}(t) = \begin{bmatrix} k_r(t) \\ \underline{k}_u(t) \\ \underline{k}_y(t) \end{bmatrix}$$

Model

$$y_M(t) = \frac{g_M B_M}{A_M}\,[r(t)] \qquad (2\text{-}7)$$

Input

$$u(t) = \underline{k}^T(t)\underline{w}(t) \qquad (2\text{-}10)$$

Output Error

$$e(t) = y(t) - y_M(t) \qquad (2\text{-}13)$$

Parameter Adjustment Law

$$\dot{\underline{k}}(t) = -\underline{\Gamma}\,\underline{w}(t)e(t) \qquad (2\text{-}12)$$

Nominal Controlled Plant

$$\frac{g^* B^*}{A^*} = \frac{k_r^* g_p B\, P}{AP - AK_u^* - g_p B K_y^*} \qquad (2\text{-}22)$$

Error Equation

$$e(t) = \left(\frac{g^* B^*}{A^*} - \frac{g_M B_M}{A_M}\right)[r(t)] + \frac{g^* B^*}{A^*}\left[\frac{\tilde{\underline{k}}^T(t)\underline{w}(t)}{k_r^*}\right] \qquad (2\text{-}24)$$

If the plant order is properly modeled, i.e., assumption A3 holds, and $\underline{k}^*$ is chosen so that eqn. (2-23) holds, the following simplification occurs in Fig. 2-3: the driving term, $e_d(t)$ in Figure 2-3, is removed and the operator in the forward path becomes

$$\frac{g_M B_M}{k_r^* A_M} .$$

When the relative degree is unity (m=n-1), this simplification can be exploited to produce a stability proof, if the new forward path operator (equivalently, the model) is chosen to be strictly positive real.

The resulting, simplified system is shown in Figure 2-4. This system can be proven stable by hyperstability (Lemma 1.1) because the feedback operator is positive [60]. Note, however, that hyperstability arguments offer no "degree of stability" information and are not useful even if the Nyquist diagram forward path crosses into the left half plane only a small distance at very high frequencies.

To further demonstrate the fragility of the proofs of stability with respect to the positive realness of the forward operator, the proof of stability of CAl is presented next using the Kalman-Yakubovich Lemma (Lemma 1.2). Proofs of this type for adaptive control systems were first provided by Parks [63]. This is the method also used by Monopoli [26], Narendra and Valavani [3], and Feuer and Morse [4] for this algorithm.

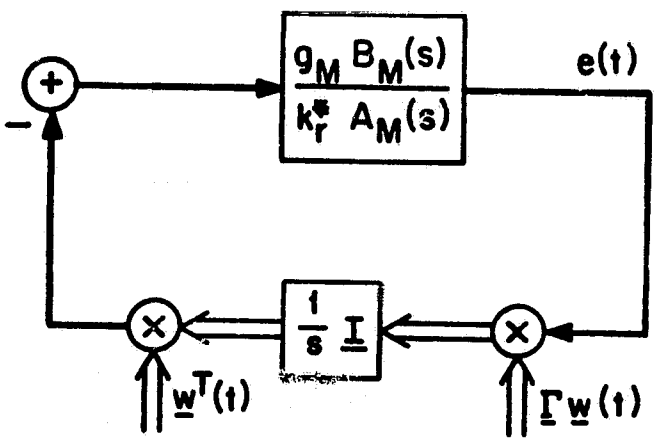

Figure 2-4. Error system of CA1 when Assumption 3 holds.

Let (A,b,c) be a minimal state space representation of the strictly positive real transfer function $\frac{g_M B_M}{k_r^* \Delta_M}$ with input u, state $\underline{x}$ and output e. Let $\underline{P}$, $\underline{Q}$ be as in Lemma 1.2 for this system. Then

$$V(\underline{x},\tilde{\underline{k}}) = \underline{x}^T \underline{P}\, \underline{x} + \tilde{\underline{k}}^T \underline{\Gamma}^{-1} \tilde{\underline{k}} \tag{2-27}$$

is a Lyapunov function with

$$\dot{V}(\underline{x},\tilde{\underline{k}}) = \underline{x}^T (\underline{A}^T \underline{P} + \underline{P}\, \underline{A}) \underline{x} + 2\underline{x}^T \underline{P}\, \underline{b}\, \tilde{\underline{k}}^T \underline{w} - 2\tilde{\underline{k}}^T \underline{w}\, e \tag{2-28}$$

$$= -\underline{x}^T \underline{Q}\, \underline{x} + 2\underline{x}^T \underline{c}\, \tilde{\underline{k}}^T \underline{w} - 2\tilde{\underline{k}}^T \underline{w}\, e \tag{2-29}$$

$$= -\underline{x}^T \underline{Q}\, \underline{x} \leq 0 \tag{2-30}$$

where the second equality makes use of eqns. (2-1) and (2-2) and the third equality uses $\underline{c}^T \underline{x} = e$. This Lyapunov analysis proves that e and $\underline{k}$ are bounded. With some additional analysis in this case it has been shown that $\lim_{t\to\infty} e(t)=0$.

The point to note here is that eqn. (1-2) is used to exactly cancel two terms of unknown size and sign in the Lyapunov function derivative. Therefore, no notion of "almost" positive real such as if eqn. (2-1) were replaced by

$$\underline{P}\, \underline{b} = \underline{c} + \underline{\epsilon} \tag{2-31}$$

where ϵ is small would be of any use. Such use of a property with such dubious physical realizability as positive realness must at least make one suspect the practicality of the results.

In Chapter 3, the properties of CA1 and other algorithms, when assumption A3 and, therefore, positive realness of the error equation are violated, will be investigated more directly.

2.2.2 Continuous-Time Algorithm No.2 (CA2)

2.2.2.1 Introduction

The algorithm CA2 maintains the same basic structure as CA1 but uses a different adjustment mechanism in order to prove stability when the relative degree of the plant is greater than one. This algorithm was published concurrently by Narendra, Lin, and Valavani [5] and Morse [6]. In [6] this algorithm represents the first of the two algorithms considered. The second algorithm in [6] will be analyzed as CA3.

There are two differences between CA1 and CA2. First, in order to achieve a positive real error operator when the relative degree of the plant is greater than one, auxiliary signals are added to the error signal used in the adjustment mechanism. Second, another term is added to the error signal in all cases. At first glance, the purpose of this term appears to be the satisfaction of a technical condition for proof of stability; however, it will be shown in Section 3.4 that this term does actually improve stability characteristics.

2.2.2.2 Controller Structure

The structure for the controller in CA2 is shown in Figure 2-5. Much of the structure is inherited from CA1. In particular, eqns. (2-2)-(2-24) apply with the exception of eqn. (2-12) which defines the adjustment mechanism. Assumptions A1-A3 of Section 2.2.1.2 are also needed for the stability proof of CA2.

In order to achieve a positive real operator in the error system when the relative degree of the plant is greater than unity, auxiliary filters not present in CA1 must be defined.

Assume that the plant has relative degree

$$n^* = n-m \geq 1 \tag{2-32}$$

Then there exists integer p and polynomials $M^{(p)}$ and $L^{(p+n^*-1)}$ so that

$$\frac{L^{(p+n^*-1)}\, q_M B_M^{(m)}}{M^{(p)} A_M^{(n)}} \tag{2-33}$$

is a desired positive real transfer function. In Morse [6], the desired function is chosen as $\frac{1}{s+\lambda_o}$. Note that the degrees of the polynomials are such that $\frac{L}{M}$ is not proper but $\frac{M}{L}$ and the entire transfer function (2-33) are.

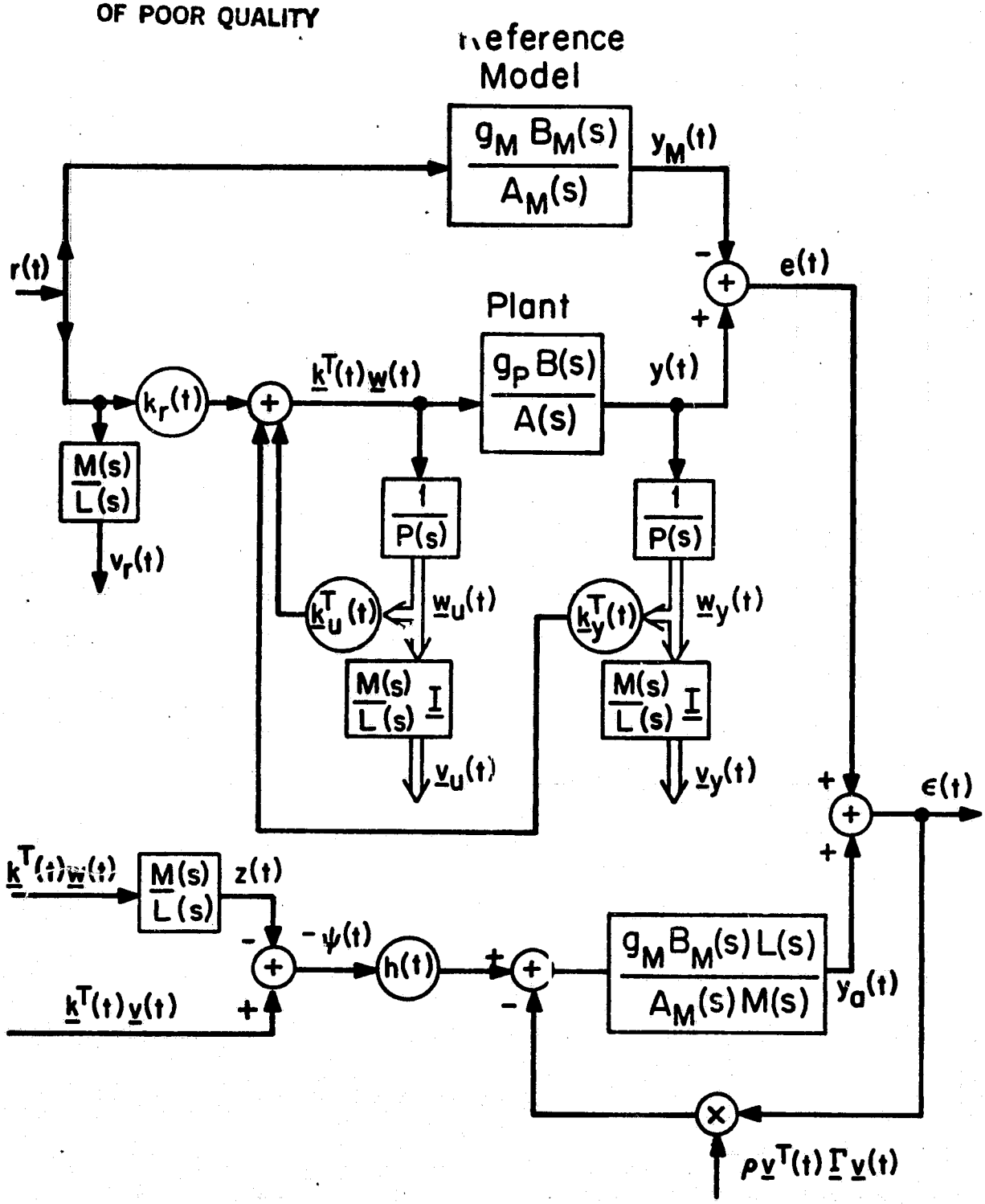

Figure 2-5. Controller structure for CA2.

To the equations (2-2)-(2-11) and (2-13)-(2-24) held over from CAl the following are appended.

$$\underline{v}(t) \triangleq \frac{M}{L}\underline{I}\,[\underline{w}(t)] \tag{2-34}$$

where $\frac{M}{L}\underline{I}$ denotes a diagonal matrix of transfer functions $\frac{M}{L}$ as in eqn. (2-26). Also define

$$z(t) \triangleq \frac{M}{L}\,[\underline{k}^T(t)\underline{w}(t)] \tag{2-35}$$

$$\psi(t) \triangleq z(t) - \underline{k}^T(t)\underline{v}(t) \tag{2-36}$$

$$y_a(t) \triangleq \frac{Lq_M B_M}{MA_M}\left[-h(t)\psi(t) - \rho\underline{v}^T(t)\underline{\Gamma}\,\underline{v}(t)\epsilon(t)\right] \tag{2-37}$$

where $$\epsilon(t) = e(t) + y_a(t) \tag{2-38}$$

$h(t)$ is a time-varying gain and ρ is a fixed positive constant. The adjustment law now is

$$\dot{\underline{k}}(t) = -\underline{\Gamma}\,\underline{v}(t)\epsilon(t) \tag{2-39}$$

$$\dot{h}(t) = \gamma\psi(t)\epsilon(t) \tag{2-40}$$

where γ is a fixed positive constant.

2.2.2.3 Error Equations

The error system for this algorithm is now developed. Use, as before,

$$\underline{k}(t) = \underline{k}^* + \tilde{\underline{k}}(t) \tag{2-14}$$

with eqns. (2-34) to (2-38) to get

$$\psi(t) = \frac{M}{L}\left[\underline{k}^T(t)\underline{w}(t)\right] - \underline{k}^T(t)\,\frac{M}{L}\,\underline{I}[\underline{w}(t)]$$

$$= \frac{M}{L}\left[\underline{k}^{*T}\underline{w}(t)\right] + \frac{M}{L}\left[\tilde{\underline{k}}^T(t)\underline{w}(t)\right] - \underline{k}^{*T}\,\frac{M}{L}\,\underline{I}[\underline{w}(t)] - \tilde{\underline{k}}^T(t)\,\frac{M}{L}\,\underline{I}[\underline{w}(t)]$$

$$= \frac{M}{L}\left[\tilde{\underline{k}}^T(t)\underline{w}(t)\right] - \tilde{\underline{k}}^T(t)\,\frac{M}{L}\,\underline{I}[\underline{w}(t)]$$

$$= \frac{M}{L}\left[\tilde{\underline{k}}^T(t)\underline{w}(t)\right] - \tilde{\underline{k}}^T(t)\underline{v}(t) \qquad (2\text{-}41)$$

The block diagram for the error system is given in Figure 2-6 where the forward operator is taken from eqn. (2-24) and the adjustment rule for h is omitted.

Let

$$h(t) = h^* + \tilde{h}(t) \qquad (2\text{-}42)$$

then

$$e(t) = y_a(t) + e(t) = \frac{Lg_MB_M}{MA_M}\left[-h^*\psi(t) - \tilde{h}(t)\psi(t) - \rho\underline{v}^T(t)\underline{\Gamma}\,\underline{v}(t)e(t)\right]$$

$$+ \frac{g^*B^*}{k_r^*A^*}\left[\tilde{\underline{k}}^T(t)\underline{w}(t)\right] + \left(\frac{g^*B^*}{A^*} - \frac{g_MB_M}{A_M}\right)[r(t)]$$

Substituting eqn. (2-41) for ψ in the first term yields

$$e(t) = \left(\frac{g^*B^*}{k_r^*A^*} - \frac{h^*g_MB_M}{A_M}\right)\left[\tilde{\underline{k}}^T(t)\underline{w}(t)\right] + \frac{h^*g_MB_ML}{A_MM}\left[\tilde{\underline{k}}^T(t)\underline{w}(t)\right]$$

$$+ \frac{g_MB_ML}{A_MM}\left[-\tilde{h}(t)\psi(t) - \rho\underline{v}^T(t)\underline{\Gamma}\underline{v}(t)e(t)\right] + \left(\frac{g^*B^*}{A^*} - \frac{g_MB_M}{A_M}\right)[r(t)] \qquad (2\text{-}43)$$

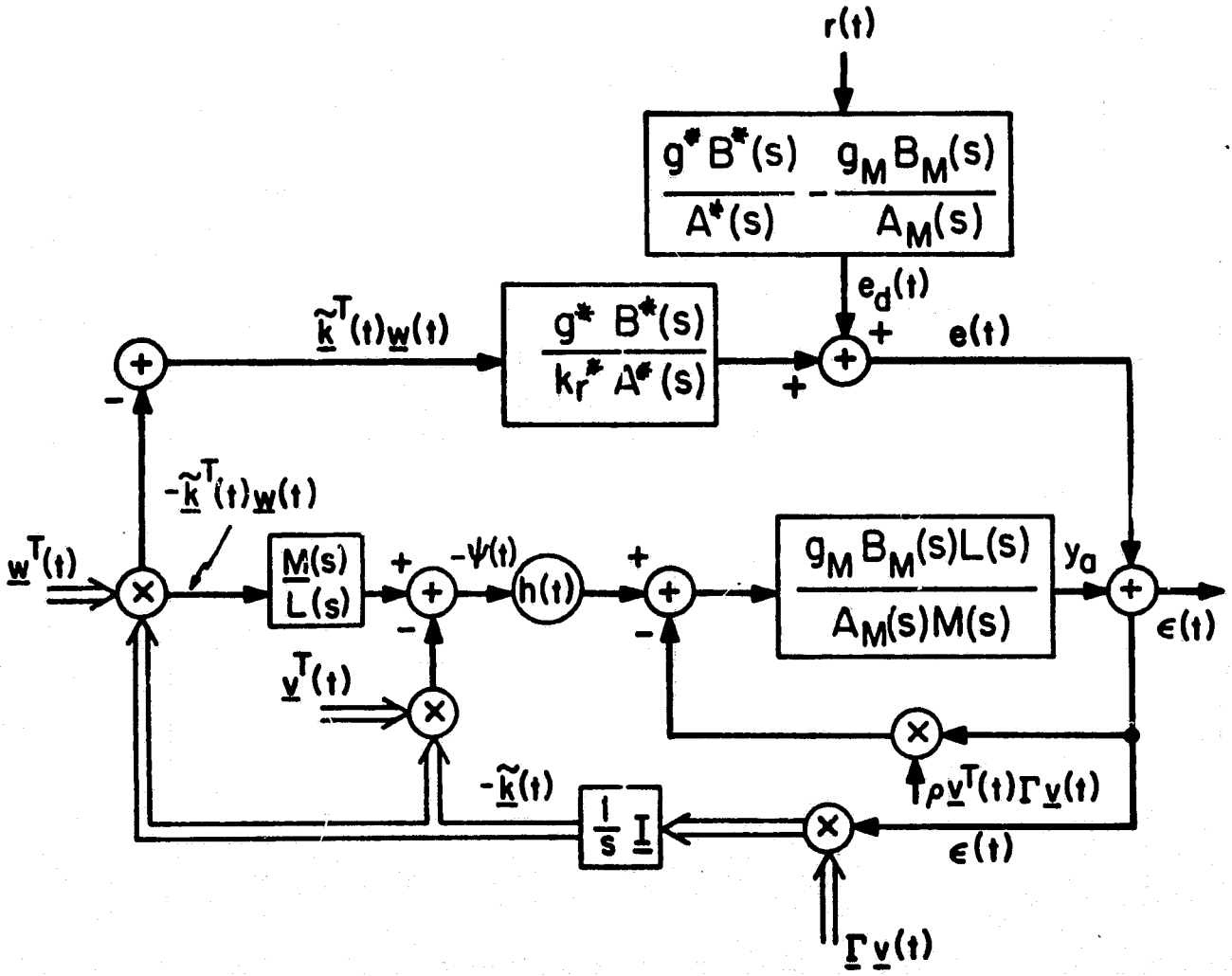

Figure 2-6. Error system for CA2.

A diagram for this way of representing the error equations is shown in Figure 2-7. Again the equation for adjusting $\tilde{h}$ is omitted as is also the generation of ψ.

The equations for CA2 are summarized in Table 2.2.

2.2.2.4 Stability Analysis

Clearly the error system of Figure 2-7 is still a very complex system. Some simplifying assumptions will be made in order to better understand how the system is behaving. Consider first the situation where the plant is modeled correctly, i.e. assumption A3 of Section 2.2.2.2 is satisfied. Pick $\underline{k}^*$ so that eqn. (2-23) is satisfied and pick $h^* = \frac{1}{k_r^*}$ so that the first term and the last term in eqn. (2-43) vanish. Then

$$e(t) = \frac{h^* g_M B_M L}{A_M M}\left[\tilde{\underline{k}}^T(t)\underline{v}(t) - \frac{\tilde{h}(t)\psi(t)}{h^*} - \frac{\rho \underline{v}^T(t)\Gamma\, \underline{v}(t)e(t)}{h^*}\right] \qquad (2\text{-}44)$$

Since $\frac{h^* g_M B_M L}{A_M M}$ is strictly positive real, the Kalman-Yakubovich Lemma can again be used in a Lyapunov analysis. Let $(\underline{A},\underline{b},\underline{c})$ be a minimal realization of $\frac{h^* g_M B_M L}{A_M M}$ with state variable x and let $\underline{P}$ and $\underline{Q}$ be as in Lemma 1.2. Then, using eqns. (2-39) and (2-40)

$$V(\underline{x},\tilde{\underline{k}}) = \underline{x}^T P\, \underline{x} + \tilde{\underline{k}}^T \Gamma^{-1} \tilde{\underline{k}} + \frac{\tilde{h}^2}{\gamma h^*} \qquad (2\text{-}45)$$

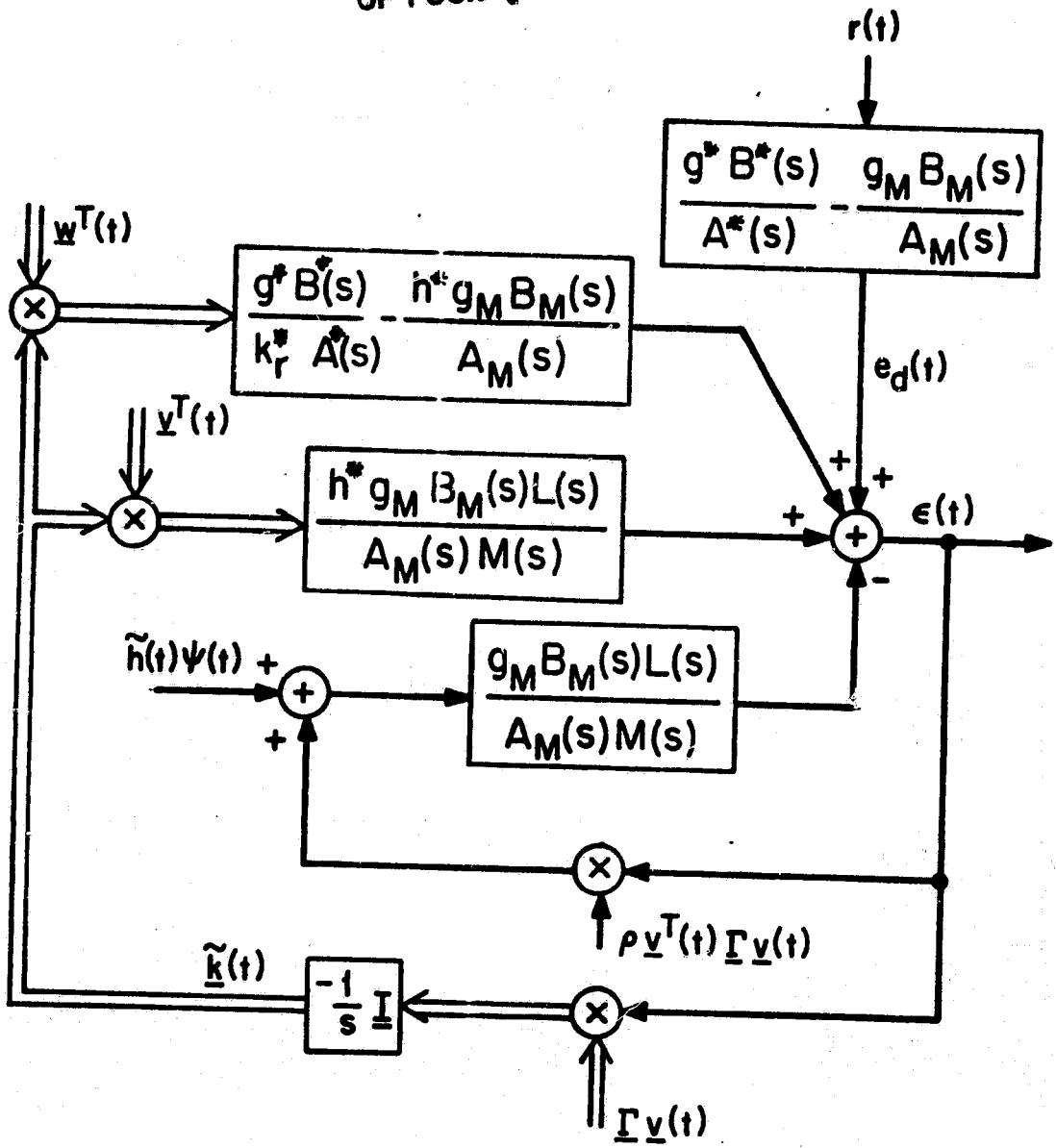

Figure 2-7. Alternate representation of the error system of CA2.

TABLE 2-2

EQUATIONS FOR CA2

Plant	$y(t) = \frac{g_p B}{A}[u(t)]$	(2-3)
Auxiliary Variables	$w_{ui}(t) = \frac{s^{i-1}}{P}[u(t)]; \; i=1,2,\ldots,n-1$	(2-4)
	$w_{yi}(t) = \frac{s^{i-1}}{P}[y(t)]; \; i=1,2,..,n$	(2-5)
	$\underline{w}(t) = \begin{bmatrix} r(t) \\ \underline{w}_u(t) \\ \underline{w}_y(t) \end{bmatrix} \quad \underline{k}(t) \begin{bmatrix} k_r(t) \\ k_u(t) \\ k_y(t) \end{bmatrix}$	
	$\underline{v}(t) = \frac{M}{L}\ \underline{I}[\underline{w}(t)]$	(2-34)
	$z(t) = \frac{M}{L}\ [\underline{w}^T(t)\underline{k}(t)]$	(2-35)
	$\psi(t) = z(t) - \underline{k}^T(t)\underline{v}(t)$	(2-36)
Model	$y_M(t) = \frac{g_M B_M}{A_M}[r(t)]$	(2-7)
Input	$u(t) = \underline{k}^T(t)\underline{w}(t)$	(2-10)
Output Error	$e(t) = y(t) - y_M(t)$	(2-13)

TABLE 2-2 CONT.

Augmented Error

$$\epsilon(t) = e(t) + y_a(t) \tag{2-38}$$

$$y_a(t) = \frac{Lg_M B_M}{MA_M}\left[-h(t)\psi(t)-\rho \underline{v}^T(t)\underline{\Gamma}\,\underline{v}(t)\epsilon(t)\right] \tag{2-37}$$

Parameter Adjustment Law

$$\dot{\underline{k}}(t) = -\underline{\Gamma}\,\underline{v}(t)\epsilon(t) \tag{2-39}$$

$$\dot{h}(t) = \gamma\psi(t)\epsilon(t) \tag{2-40}$$

Nominal Controlled Plant

$$\frac{g^*B^*}{A^*} = \frac{k_r^* g_p B\, P}{AP - AK_u^* - g_p B K_y^*} \tag{2-22}$$

Error Equation

$$\epsilon(t) = \left(\frac{g^*B^*}{k_r^*A^*} - \frac{h^* g_M B_M}{A_M}\right)\left[\tilde{\underline{k}}^T(t)\underline{w}(t)\right]$$

$$+ \frac{h^* g_M L B_M}{MA_M}\left[\tilde{\underline{k}}^T(t)\underline{v}(t)\right] + \frac{g_M B_M L}{A_M M}\left[-\tilde{h}(t)\psi(t)-\rho \underline{v}^T(t)\underline{\Gamma}\,\underline{v}(t)\epsilon(t)\right]$$

$$+ \left(\frac{g^*B^*}{A^*} - \frac{g_M B_M}{A_M}\right)[r(t)] \tag{2-43}$$

is a Lyapunov function with

$$\dot{V}(\underline{x},\tilde{\underline{k}}) = \underline{x}^T(\underline{A}^T\underline{P}+\underline{P}\underline{A})\underline{x} + \underline{x}^T\underline{P}\underline{b}\,\tilde{\underline{k}}^T\underline{y} - \frac{\tilde{h}\psi e}{h^*} - \frac{\rho \underline{v}^T\underline{\Gamma}\,\underline{v}\,e}{h^*}$$

$$- e\,\tilde{\underline{k}}^T\underline{v} + \frac{e\tilde{h}\psi}{h^*}$$

$$= -\underline{x}^T\underline{Q}\,\underline{x} - \frac{\rho}{h^*}\,e^2\,\underline{v}^T\underline{\Gamma}\,\underline{v} \leq 0 \qquad (2\text{-}46)$$

which proves that $\underline{k}(t)$ and $e(t)$ are bounded. Note, however, that now $e(t)$ being bounded does not itself ensure that $y(t)$ is bounded. The proof that y is bounded is very involved and is performed in [5] and [6], where it is also proved that $\lim_{t\to\infty} e(t)=0$.

2.2.2.5 A Special Case ($n^*=1$)

When the relative degree of the plant, n^*, equals one the algorithm CA2 simplifies greatly. In this case, let $\frac{k_M B_M}{A_M}$ be positive real and let $\frac{L}{M}$ be the identity operator, which results in $\underline{w}=\underline{v}$ and $\psi=0$. Then eqn. (2-43) becomes

$$e(t) = \frac{g^*B^*}{k_r^*A^*}\left[\tilde{\underline{k}}^T(t)\underline{w}(t)\right] - \frac{g_M B_M}{A_M}\left[\rho \underline{w}^T(t)\underline{\Gamma}\,\underline{w}(t)e(t)\right]$$

$$+ \left(\frac{g^*B^*}{A^*} - \frac{g_M B_M}{A_M}\right)\left[r(t)\right] \qquad (2\text{-}47)$$

This error system for the case $n^*=1$ is shown in Figure 2-8.

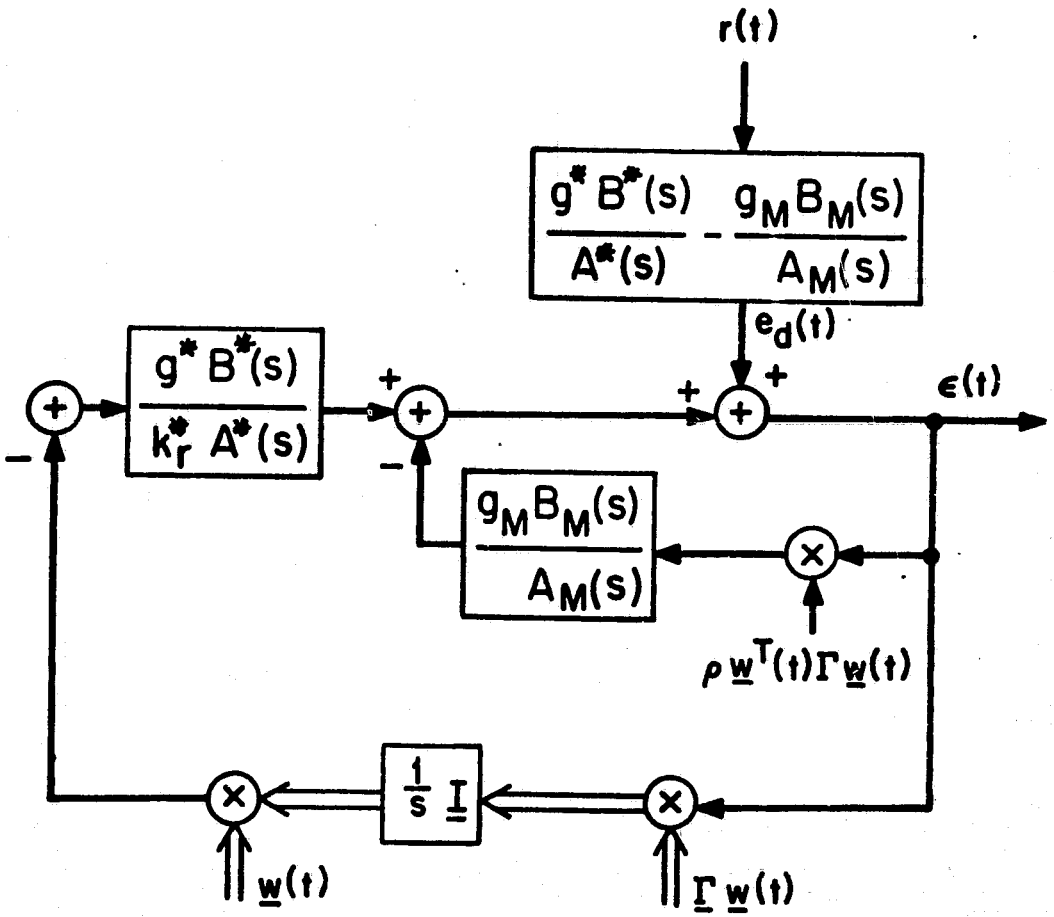

Figure 2-8. Error system for CA2 when $n^*=1$.

It can be seen from Figure 2-8 that the only difference between the error systems for CA1 (see Figure 2-3) and CA2 is the added inner feedback loop in CA2. Although this loop was added for technical reasons regarding the stability proof it will be seen in Section 3.4 that the added loop does in general improve stability properties.

The equations for CA2 in the case where the relative degree of the plant is unity are summarized in Table 2.3.

2.2.3 Continuous-Time Algorithm No. 3 (CA3)

Algorithm CA3 is very similar to algorithm CA2. The major difference is that, in CA3, $\frac{L}{M}$ is picked so that $\frac{g_M B_M L}{A_M M}$ is a memoryless system and $\frac{M}{L}$ has unity d.c. gain. If M is of order p, L must now be of order p+n* instead of p+n*-1 as it was in CA2. This change causes other small changes. The term $\rho \underline{v}^T \underline{\Gamma} \underline{v} \epsilon$ is no longer an input to the equations generating y_a so eqn. (2-37) is replaced by

$$y_a(t) = \frac{g_M B_M L}{A_M M} \left[-h(t)\psi(t)\right] = - g_o h(t)\psi(t) \qquad (2\text{-}48)$$

where g_o is the dc gain of the model.

The quadratic expression does, however, appear as a normalizing term in the parameter adjustment equations. Specifically, eqs. (2-39) and (2-40) become

TABLE 2-3

EQUATIONS FOR CA2 WITH $n^*=1$ and L=M

Plant	$y(t) = \frac{g_p B}{A}\,[u(t)]$	(2-3)
Auxiliary Variables	$w_{ui}(t) = \frac{s^{i-1}}{P}\,[u(t)];\ i=1,2,\ldots,n-1$	(2-4)
	$w_{yi}(t) = \frac{s^{i-1}}{P}\,[y(t)];\ i=1,2,\ldots,n$	(2-5)
	$\underline{w}(t) = \begin{bmatrix} r(t) \\ \underline{w}_u(t) \\ \underline{w}_y(t) \end{bmatrix}\ ;\quad \underline{k}(t) \begin{bmatrix} k_r(t) \\ \underline{k}_u(t) \\ \underline{k}_y(t) \end{bmatrix}$	
Model	$y_M(t) = \frac{g_M B_M}{A_M}\,[r(t)]$	(2-7)
Input	$u(t) = \underline{k}^T(t)\underline{w}(t)$	(2-10)
Output Error	$e(t) = y(t) - y_M(t)$	(2-13)
Augmented Error	$\epsilon(t) = e(t) + y_a(t)$	(2-38)
	$y_a(t) = \frac{g_M B_M}{A_M}\,[-\rho \underline{w}^T(t)\underline{\Gamma}\,\underline{w}(t)\epsilon(t)]$	(2-37)
Parameter Adjustment Law	$\dot{\underline{k}}(t) = -\underline{\Gamma}\,\underline{w}(t)\epsilon(t)$	(2-39)

TABLE 2-3 CONT.

Nominal Controlled Plant	$\frac{g^*B^*}{A^*} = \frac{k^*_c g_p B\ P}{AP - AK^*_u - g_p B K^*_y}$	(2-22)
Error Equations	$e(t) = \frac{g^*B^*}{k^*_r A^*}[\underline{k}^T(t)\underline{w}(t)] - \frac{g_M B_M}{A_M}[\rho \underline{w}^T(t)\underline{\Gamma}\ \underline{w}(t)e(t)]$ $+ \left(\frac{g^*B^*}{A^*} - \frac{g_M B_M}{A_M}\right)[r(t)]$	(2-47)

$$\dot{\underline{\tilde{k}}}(t) = \frac{-\underline{\Gamma}\,\underline{v}(t)e(t)}{\lambda_o + \underline{v}^T(t)\underline{\Gamma}'\underline{v}(t)} \qquad (2\text{-}49)$$

$$\dot{h} = \frac{+\gamma\psi(t)e(t)}{\lambda_o + \underline{v}^T(t)\underline{\Gamma}'\underline{v}(t)} \qquad (2\text{-}50)$$

where λ_o is a positive constant.

The proof of stability for this algorithm is given by Morse [6].* The effect on the error system of the changes made by Morse is shown in Figure 2-9 which is the parallel of Figure 2-7 for CA2. Note that no simplification occurs for the case $n^*=1$ because, in CA3, $\frac{M}{L}$ must still have relative degree one when the plant does.

It will be seen in Section 3.5 that the normalization of the error in the parameter adjustment mechanism results in an important improvement of the system's response to constant inputs in the presence of unmodeled dynamics.

The equations for CA3 are summarized in Table 2.4.

---

*In [6], Morse proves stability of this algorithm with $\underline{\Gamma}=\underline{\Gamma}'$. The version with both $\underline{\Gamma}$ and $\underline{\Gamma}'$ positive definite matrices allows more flexibility while Morse's proof holds mutatis mutandis.

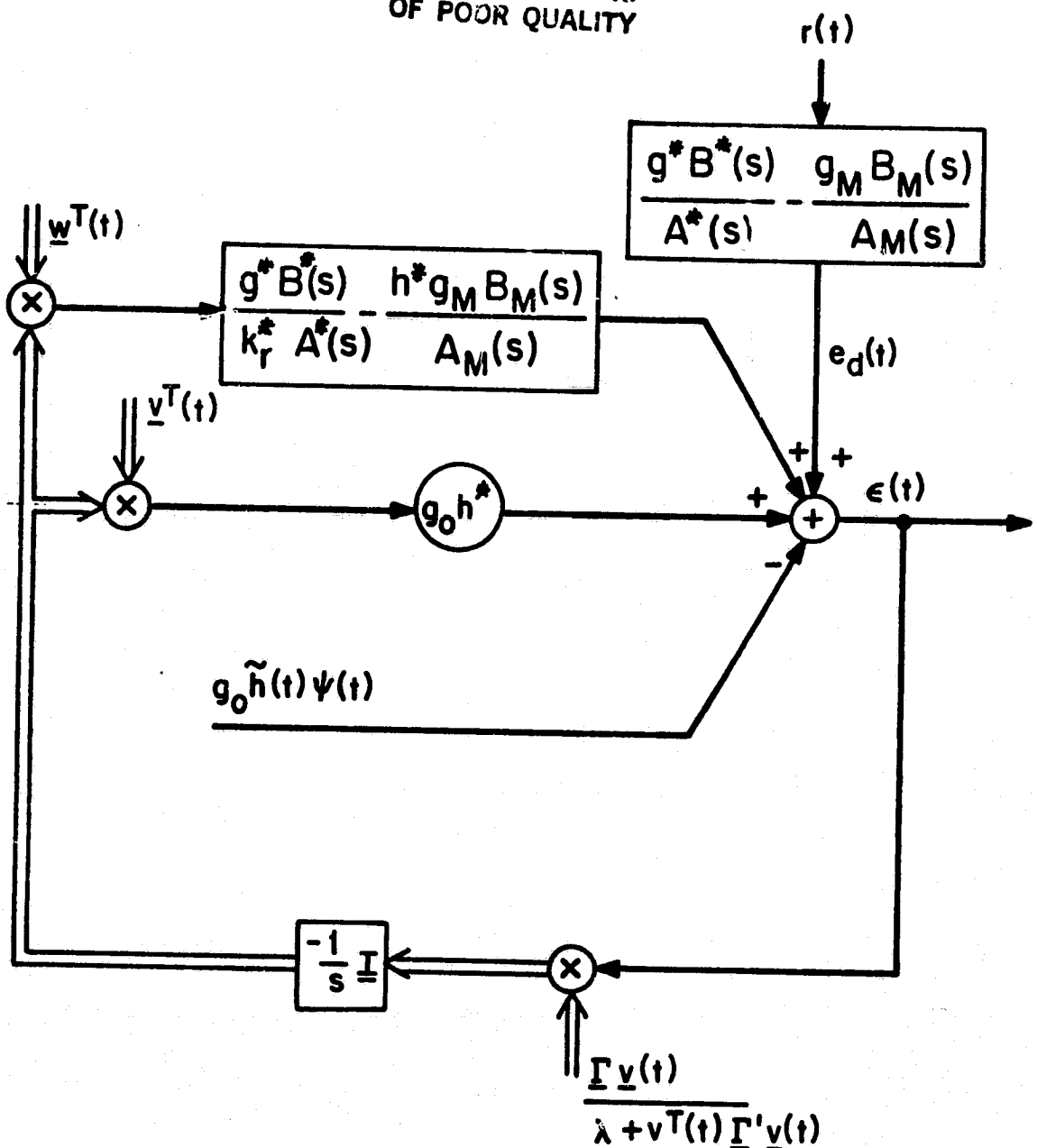

Figure 2-9. Error system for CA3.

TABLE 2-4

EQUATIONS FOR CA3

Plant

$$y(t) = \frac{g_p B}{A}\,[u(t)] \qquad (2\text{-}3)$$

Auxiliary Variables

$$w_{ui}(t) = \frac{s^{i-1}}{P}\,[u(t)];\ i=1,2,\ldots,n-1 \qquad (2\text{-}4)$$

$$w_{yi}(t) = \frac{s^{i-1}}{P}\,[y(t)];\ i=1,2,\ldots,n \qquad (2\text{-}5)$$

$$\underline{w}(t) = \begin{bmatrix} r(t) \\ \underline{w}_u(t) \\ \underline{w}_y(t) \end{bmatrix};\ \underline{k}(t) = \begin{bmatrix} k_r(t) \\ \underline{k}_u(t) \\ \underline{k}_y(t) \end{bmatrix}$$

$$\underline{v}(t) = \frac{M}{L}\,\underline{I}[\underline{w}(t)] \qquad (2\text{-}34)$$

$$z(t) = \frac{M}{L}\,[\underline{w}^T(t)\underline{k}(t)] \qquad (2\text{-}35)$$

$$\psi(t) = z(t) - \underline{k}^T(t)v(t) \qquad (2\text{-}36)$$

Model

$$y_M(t) = \frac{g_M B_M}{A_M}\,[r(t)] \qquad (2\text{-}7)$$

Input

$$u(t) = \underline{k}^T(t)\underline{w}(t) \qquad (2\text{-}10)$$

Output Error

$$e(t) = y(t) - y_M(t) \qquad (2\text{-}13)$$

Augmented Error

$$\epsilon(t) = e(t) + y_a(t) \qquad (2\text{-}38)$$

$$y_a(t) = -g_o h(t)\psi(t) \qquad (2\text{-}48)$$

$$g_o = \left.\frac{g_M B_M}{A_M}\right|_{s=0}$$

TABLE 2-4 CONT.

Parameter Adjustment Law

$$\dot{\underline{k}}(t) = \frac{-\underline{\Gamma}\,\underline{v}(t)\epsilon(t)}{\lambda_o + \underline{v}^T(t)\underline{\Gamma}\,\underline{v}(t)} \tag{2-49}$$

$$\dot{h}(t) = \frac{\gamma\psi(t)\epsilon(t)}{\lambda_o + \underline{v}^T(t)\underline{\Gamma}\,\underline{v}(t)} \tag{2-50}$$

Nominal Controlled Plant

$$\frac{g^*B^*}{A^*} = \frac{k_r^* g_p BP}{AP - AK_u^* - g_p BK_y^*} \tag{2-22}$$

Error Equation

$$\epsilon(t) = \left(\frac{g^*B^*}{k_r^*A^*} - \frac{h^* g_M B_M}{A_M}\right)[\tilde{\underline{k}}^T(t)\underline{w}(t)]$$

$$-h^*[\tilde{\underline{k}}^T(t)\underline{v}(t)] - \tilde{h}(t)\psi(t)$$

$$+\left(\frac{g^*B^*}{A^*} - \frac{g_M B_M}{A_M}\right)[r(t)] \tag{2-51}$$

2.2.4 Continuous-Time Algorithm No. 4 (CA4)

2.2.4.1 Introduction

The algorithm that will be referred to as CA4 is representative of the class of algorithms developed by Egardt [11]. It differs from the preceding algorithms in that it prefilters the reference input and then uses extra filtering in the control loop to convert the controlled plant into a memoryless system. The system is shown in Figure 2-10.

This algorithm is of interest because it provides a continuous time analogy to many popular discrete-time adaptive control algorithms. Also, this algorithm provides the designer with a simple yet flexible controller structure with which to work.

2.2.4.2 Controller Structure

The plant is the same as in the other algorithms and nominally has relative degree $n^*=n-m$. As before,

$$y(t) = \frac{g_p B^{(m)}}{A^{(n)}} \left[u(t)\right] \qquad (2\text{-}52)$$

The auxiliary signals, $\underline{v}(t)$, are generated by a method similar to the method used in the other algorithms except that the signals $y(t)$ and $u(t)$ are first filtered before entering the auxiliary signal generators and the reference input is filtered by the reference model before being used.

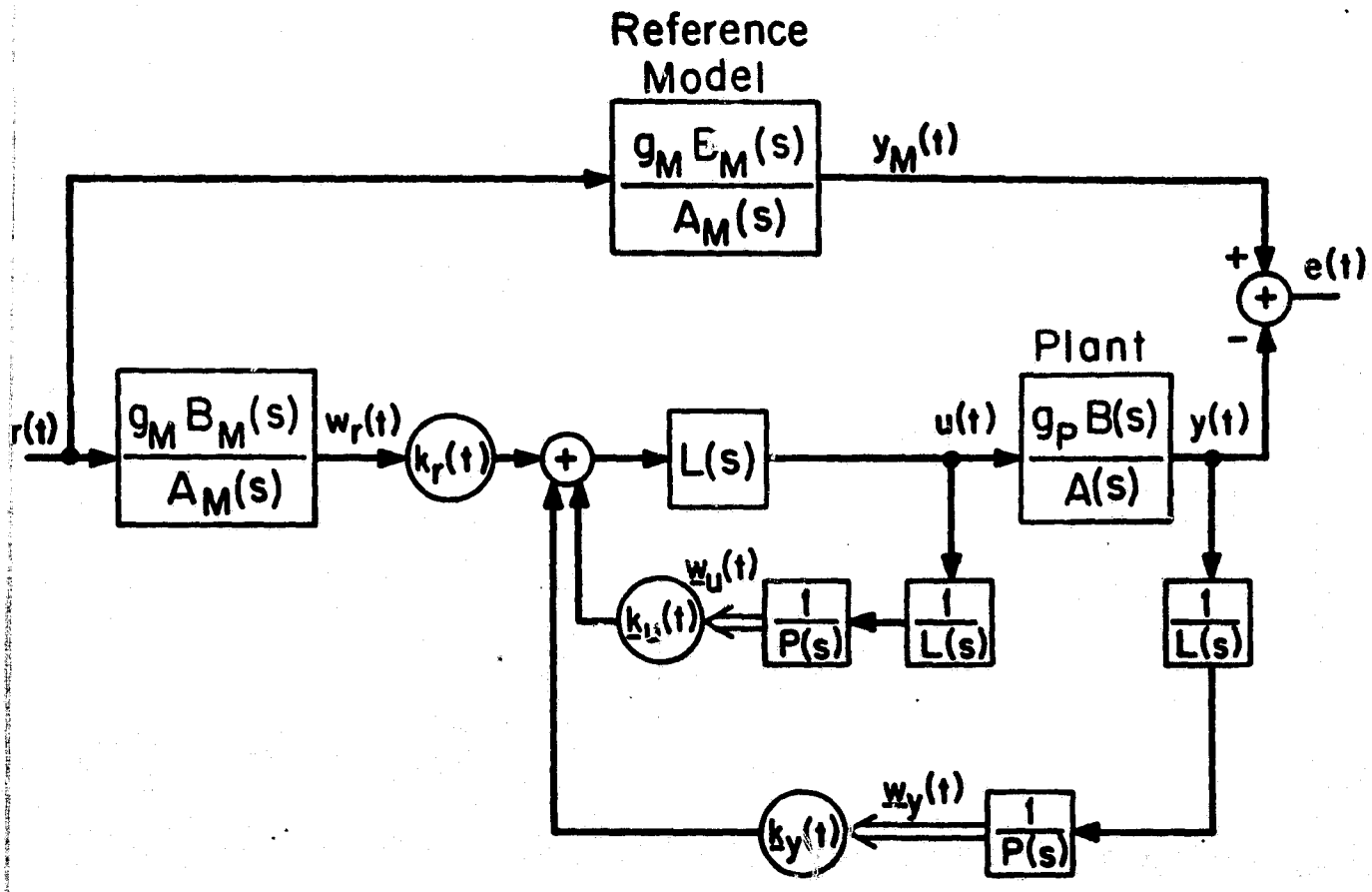

Figure 2-10. Controller structure for CA4.

The equations corresponding to eqns. (2-4) and (2-5) are:

$$w_{ui}(t) = \frac{s^{i-1}}{p^{(n-1)}_L(n^*)} \left[u(t)\right] \qquad i=1,2,\ldots,n-1 \tag{2-53}$$

$$w_{ui}(t) = \frac{s^{i-1}}{p^{(n-1)}_L(n^*)} \left[y(t)\right] \qquad i=1,2,\ldots,n \tag{2-54}$$

$$w_r(t) = y_M(t) = \frac{g_M B_M^{(m)}}{A_M^{(n)}} \left[r(t)\right] \tag{2-55}$$

The input, u(t), to the plant is formed by:

$$u(t) = L^{(n^*)}\left[\underline{k}^T(t)\underline{w}(t)\right] \tag{2-56}$$

where $\underline{k}$ is the vector of time-varying gains and $\underline{w}$ is the vector of auxiliary signals formed from w_r, $\underline{w}_u$, and $\underline{w}_y$ as was done in the other algorithms. In CA4 the gains, $\underline{k}$, are not adjusted directly but are generated from other adjustable parameters, $\underline{f}$, by

$$\underline{k}(t) = \frac{\ell_o}{\Lambda^{(n^*-1)}} \quad \underline{I}\,[\underline{f}(t)] \tag{2-57}$$

where $\Lambda(s)$ is an $(n^*-1)^{th}$ order polynomial in s and ℓ_o is chosen so that $\frac{\ell_o}{\Lambda}$ has unity d.c. gain. The parameters $\underline{f}$ are adjusted by the equation

$$\dot{\underline{f}}(t) = \frac{\underline{w}(t)\epsilon(t)}{\lambda_o + \underline{w}^T(t)\underline{w}(t)} \tag{2-58}$$

where

$$\epsilon(t) = e(t) + y_a(t) \tag{2-59}$$

and λ_o is a positive constant. The auxiliary output in this algorithm is simply

$$y_a(t) = h(t)\left(\underline{k}^T(t)-\underline{f}^T(t)\right)\underline{w}(t) = h(t)\left(\tilde{\underline{k}}^T(t)-\tilde{\underline{f}}^T(t)\right)\underline{w}(t) \tag{2-60}$$

where h(t) is a time-varying gain which is adjusted according to the following mechanism

$$\dot{h}(t) = \frac{(\underline{k}^T(t)-\underline{f}^T(t))\underline{w}(t)\epsilon(t)}{\lambda_o+\underline{w}^T(t)\underline{w}(t)} \tag{2-61}$$

2.2.4.3 Realization Issues

A few words must be said about the realizability of eqn. (2-56). This equation cannot be realized directly since it requires n* differentiations. Note, however, that an indirect realization is possible since one has available n* derivatives of $\underline{w}(t)$ through its generation (eqns. (2-53)-(2-55)) and n* derivatives of $\underline{k}(t)$ through its generation (eqns. (2-57) and (2-58)). In fact, this realizability constraint is the raison d'etre for eqn. (2-57) and the generation of $y_a(t)$.

2.2.4.4 Error Equations

By following the same procedure as in Section 2.2.1.4, K_u^* and K_y^* are again defined as in eqns. (2-17) and (2-18) and the following equations corresponding to eqns. (2-21) and (2-22) are hence developed:

$$y(t) = \left(\frac{k_r g_p B L P}{(P-K_u^*)A - g_p B K_y^*} - \frac{g_M B_M}{A_M}\right)\left[r(t)\right] + \frac{1}{k_r^*}\,\tilde{\underline{k}}^T(t)\underline{w}(t) \qquad (2\text{-}62)$$

$$= \left(\frac{g^* B^*}{A^*} - \frac{g_M B_M}{A_M}\right)\left[r(t)\right] + \frac{1}{k_r^*}\,\tilde{\underline{k}}^T(t)\underline{w}(t) \qquad (2\text{-}63)$$

For this algorithm, the objective is to make $\frac{g^*B^*}{A^*}$, the nominal closed loop system equal to a constant gain rather than equal to $\frac{g_M B_M}{A_M}$. It can be seen from the polynomial orders in eqn. (2-62) repeated below

$$\frac{k_r^* g_p B^{(m)} L^{(n-m)} P^{(n-1)}}{(P^{(n-1)} - K_u^{*(n-2)})A^{(n)} - g_p B^{(m)} K_y^{*(n-1)}}$$

that the extra filtering of L(s) makes this possible. When the system is properly modeled the error equations can be represented as:

$$e(t) = \frac{1}{k_r^*}\,\tilde{\underline{k}}^T(t)\underline{w}(t) \qquad (2\text{-}64)$$

The stability analysis uses the same assumptions as the other algorithms (A1-A3) from Section 2.2.1.2 and the proof of global asymptotic stability follows from the use of the Lyapunov function

$$V(\underline{f},h) = \underline{f}^T\underline{f} + h^2 \qquad (2\text{-}65)$$

The analysis required, after the initial Lyapunov analysis establishes bounded feedback gains, is more involved than the other algorithms but the proof outline follows some more intuitive concepts. In [11], Egardt shows that a large output error leads to large inputs which improves identification. With improved identification, the controlled plant will converge to the desired reference model.

The error system when the Relative Degree Assumption (A3) is violated is displayed in Figure 2-11.

Notice that when $n^*=1$ and $\Lambda=\ell_o$, the error system reduces to that of Figure 2-12. The equations for CA4 are summarized in Table 2-5, and, for the case where the relative degree of the plant is unity, in Table 2-6.

2.2.4.5 Comments on Problem Formulation

The controller structure of CA4 graphically demonstrates possible shortcoming of all the algorithms of adaptive control theory which aim only at achieving certain closed-loop response characteristics for

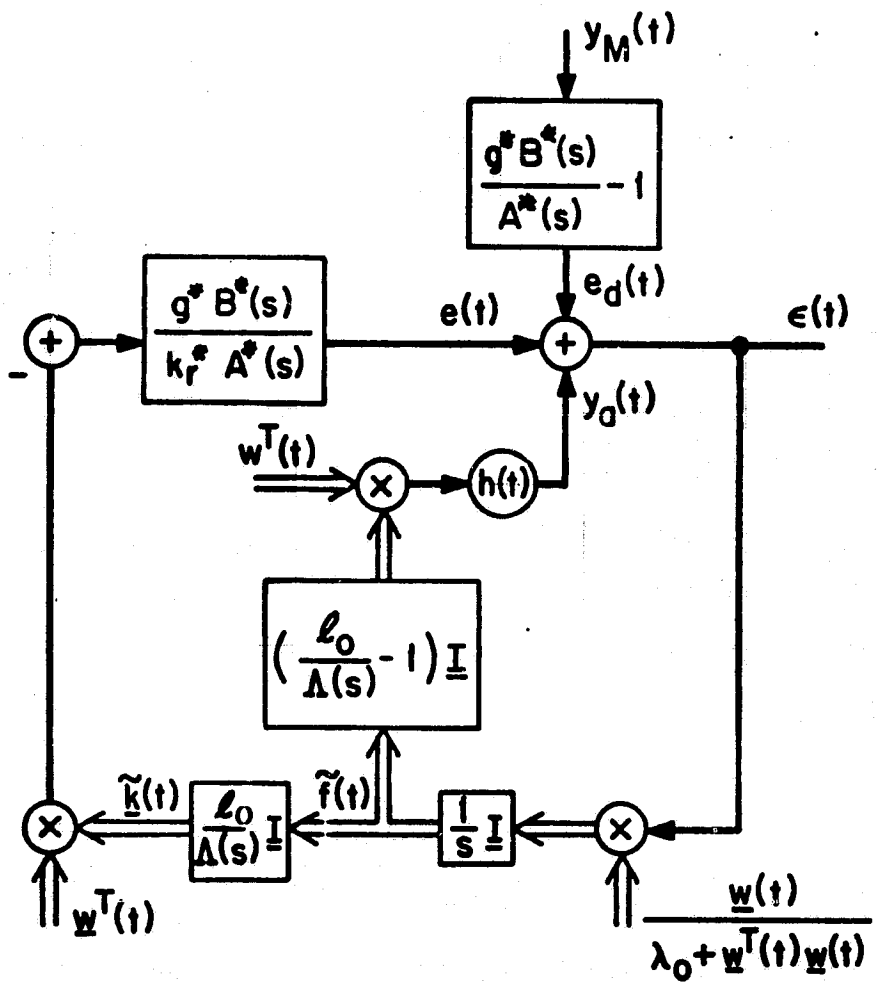

Figure 2-11. Error system for CA4.

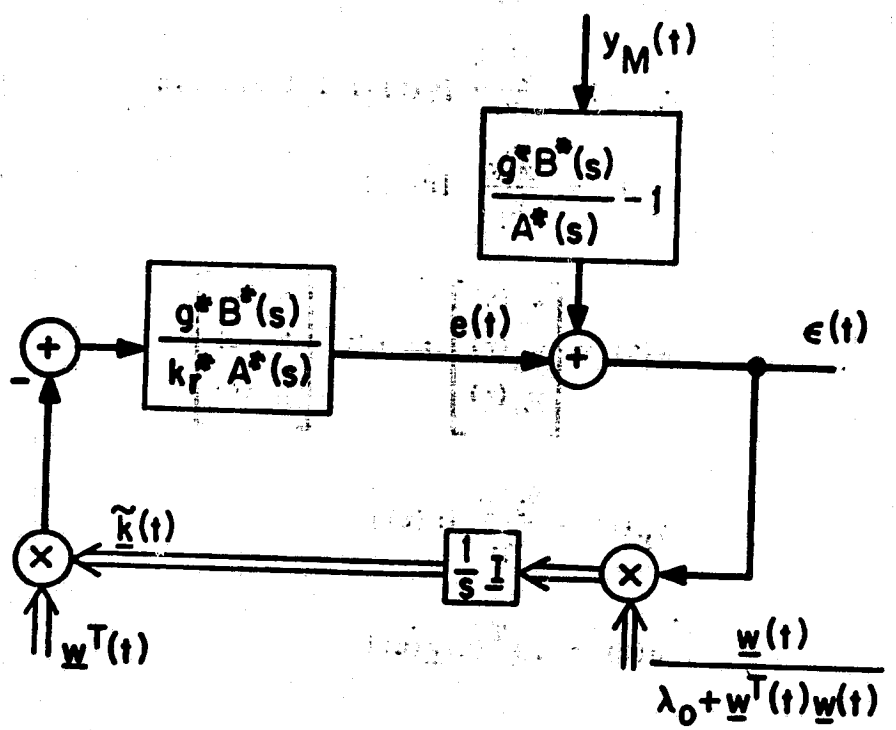

Figure 2-12. Error system for CA4 when $n^*=1$.

TABLE 2-5

EQUATIONS FOR CA4

Plant

$$y(t) = \frac{g_p B}{A}\,[u(t)] \qquad (2\text{-}3)$$

Auxiliary Variables

$$w_{ui}(t) = \frac{s^{i-1}}{PL}\,[u(t)];\ i=1,2,\ldots,n-1 \qquad (2\text{-}53)$$

$$w_{yi}(t) = \frac{s^{i-1}}{PL}\,[y(t)];\ i=1,2,\ldots,n \qquad (2\text{-}54)$$

$$w_r(t) = \frac{g_M B_M}{A_M}\,[r(t)] \qquad (2\text{-}55)$$

$$\underline{w}(t) = \begin{bmatrix} w_r(t) \\ \underline{w}_u(t) \\ \underline{w}_y(t) \end{bmatrix}; \quad \underline{k}(t) \begin{bmatrix} k_r(t) \\ \underline{k}_u(t) \\ \underline{k}_y(t) \end{bmatrix}$$

Model

$$y_M(t) = \frac{g_M B_M}{A_M}\,[r(t)] \qquad (2\text{-}7)$$

Input

$$u(t) = L[\underline{k}^T(t)\underline{w}(t)] \qquad (2\text{-}56)$$

Output Error

$$e(t) = y(t) - y_M(t) \qquad (2\text{-}13)$$

Augmented Error

$$e(t) = e(t) + y_a(t) \qquad (2\text{-}59)$$

$$y_a(t) = h(t)(\underline{k}^T(t) - \underline{f}^T(t))\underline{w}(t) \qquad (2\text{-}60)$$

$$= h(t)(\tilde{\underline{k}}^T(t) - \underline{f}^T(t))\underline{w}(t)$$

C-2

TABLE 2-5 CONT.

Parameter Adjustment Law

$$\dot{\underline{f}}(t) = \frac{\underline{w}(t)e(t)}{\lambda_o + \underline{w}^T(t)\underline{w}(t)} \qquad (2\text{-}58)^{**}$$

$$\underline{k}(t) = \frac{\ell_o}{\Lambda}\, \underline{I}[\underline{f}(t)];\ \ell_o = \Lambda(s)\Big|_{s=0} \qquad (2\text{-}57)$$

$$\dot{h}(t) = \frac{\left(\underline{k}^T(t) - \underline{f}^T(t)\right)\underline{w}(t)e(t)}{\lambda_o + \underline{w}^T(t)\underline{w}(t)} \qquad (2\text{-}61)$$

Nominal Controlled Plant

$$\frac{g^*B^*}{A^*} = \frac{k_r^* g_p B_{LP}}{(P - K_u^*)A - g_p B K_y^*} \qquad (2\text{-}63)$$

Error Equations

$$e(t) = \frac{g^*B^*}{k_r^* A^*}\left[\tilde{\underline{k}}^T(t)\underline{w}(t)\right] + h(t)\left(\tilde{\underline{k}}^T(t) - \underline{\tilde{f}}^T(t)\right)\underline{w}(t) + \left(\frac{g^*B^*}{A^*} - 1\right)\left[y_M(t)\right] \qquad (2\text{-}66)$$

TABLE 2-6

EQUATIONS FOR CAI with $n^*=1$

Plant	$y(t) = \frac{g_p B}{A}[u(t)]$	(2-3)
Auxiliary Variables	$w_{ui}(t) = \frac{s^{i-1}}{PL}[u(t)]$; $i=1,\ldots,n-1$	(2-53)
	$w_{yi}(t) = \frac{s^{i-1}}{PL}[y(t)]$; $i=1,2,\ldots,n$	(2-54)
	$w_r(t) = \frac{g_M B_M}{A_M}[r(t)]$	(2-55)
	$\underline{w}(t) = \begin{bmatrix} w_r(t) \\ \underline{w}_u(t) \\ \underline{w}_y(t) \end{bmatrix}$; $\underline{k}(t) \begin{bmatrix} k_r(t) \\ \underline{k}_u(t) \\ \underline{k}_y(t) \end{bmatrix}$	
Model	$y_M(t) = \frac{g_M B_M}{A_M}[r(t)]$	(2-7)
Input	$u(t) = L[\underline{k}^T(t)\underline{w}(t)]$	(2-56)
Output Error	$e(t) = y(t) - y_M(t)$	(2-13)
Parameter Adjustment Law	$\dot{\underline{k}}(t) = \frac{-\underline{w}(t)e(t)}{\lambda_o + \underline{w}^T(t)\underline{w}(t)}$	(2-57), (2-58)
Nominal Controlled Plant	$\frac{g^* B^*}{A^*} = \frac{k_r^* g_p BLP}{(P-K_u^*)A - g_p B K_y^*}$	(2-63)
Error Equation	$\frac{g^* B^*}{k_r^* A^*}[\underline{k}^{*T}(t)\underline{w}(t)] + \left(\frac{g^* B^*}{A^*} - 1\right)[y_M(t)]$	(2-67)

tracking reference inputs. Input tracking is a problem which can be solved without feedback if the plant is known. By filtering the reference input with the desired closed-loop transfer function, the controller may be able to achieve model matching with very small feedback gain. Indeed if L of eqns. (2-53), (2-54) and (2-56) can be chosen as the inverse of the plant, the nominal control gains $\underline{k}^*$ will be zero. While a low gain controller may be desirable in an adaptive setting due to its stability robustness, it is clearly not a "good" controller in that it will not perform well the fundamental feedback control function of disturbance rejection. Since the results on adaptive control come mainly from a problem formulation involving only tracking properties much "engineering judgement" must be applied when attempting to use these systems for the usual jobs of feedback control such as disturbance and sensor noise rejection. The results of this thesis provide insight to form the basis of this engineering judgement for adaptive control systems.

2.3 Discrete-Time Algorithms

2.3.1 Introduction

In this section, three algorithms which perform adaptive control for discrete-time systems are introduced. All of the algorithms considered have been proven in the published literature to be globally asymptotically stable when the assumptions of the following subsection are satisfied. These assumptions are exactly analogous to the assumptions used in the continuous-time algorithms.

2.3.1.1 Model and Assumptions

Assume the plant is described by

$$y(t) = \frac{g_p q^{-d} B^{(m)}}{A^{(n)}} [u(t)] \qquad (2\text{-}67)$$

where

$$B^{(m)} = 1+b_1 q^{-1} +\ldots+ b_m q^{-m} \qquad (2\text{-}68)$$

$$A^{(n)} = 1+a_1 q^{-1} +\ldots+ a_n q^{-n} \qquad (2\text{-}69)$$

and q^{-1} is the backward shift operator. i.e., $q^{-1}[u(t)] = u(t-1)$. The assumptions used in the stability proofs of the adaptive control algorithms are:

A1) Known Sign of Gain Assumption

The sign of g_p is known and, without loss of generality, positive.

A2) Nonminimum Phase Assumption

All the zeroes of B have magnitude less than one.

A3) Known Pole-Zero Numbers

The delay, d, in eqn. (2-67) is known as are the degrees of B and A, m and n respectively.

The assumption on knowing m and n can be relaxed to knowing an upper bound for m and n, but the delay, d, must be known exactly. Knowing the delay is equivalent to knowing the relative degree of the discrete-time transfer function since the delay is equal to the number of poles minus the number of zeroes of the transfer function. Assumption A3 will be used as is in the sequel since, in order to take advantage of the relaxed version of the assumption, the adaptive system must be built as if m and n were equal to their upper bounds.

The conceptual idea of using a positive real condition to obtain Lyapunov stability proofs of these algorithms is the same as in the continuous-time algorithms and will not be treated here.

What will be treated in Chapter 5, however, is the behavior of the algorithms when Assumptions A3 and A2 are violated.

2.3.2 Discrete-Time Algorithm No. 1 (DA1)

The algorithm DA1 is the discrete-time counterpart of the continuous-time algorithm CA2. It was introduced by Narendra and Lin [7].

2.3.2.1 Controller Structure

The structure of the controller is exactly analogous to the structure of CA2 given in Figure 2-5. The plant is described by eqn. (2-67). The system will be designed assuming $d \geq 1$ and n are known and m=n-d. The model is given by

$$y_M(t) = \frac{g_M q^{-d} B_M^{(n-d)}}{A_M^{(n)}} [r(t)] \qquad (2\text{-}68)$$

as shown in Figure 2-13. The auxiliary variables are generated by

$$w_{ui}(t) = \frac{q^{-(i+1)}}{p^{(n-1)}} u(t); \quad i=0,1,\ldots,n-2 \qquad (2\text{-}69)$$

$$w_{yi}(t) = \frac{q^{-i}}{p^{(n-1)}} y(t) ; \quad i=0,1,\ldots n-1 \qquad (2\text{-}70)$$

where $B_M^{(n-d)}$ divides $p^{(n-1)}$ (2-71)

The scalar control input to the plant is:

$$u(t) = \underline{k}^T(t)\underline{w}(t) \qquad (2\text{-}72)$$

where $\underline{k}(t)$ is a vector of adjustable gains. The definitions of $\underline{k}(t)$ and $\underline{w}(t)$ are as usual throughout this work, repeated in eqn. (2-73).

$$\underline{k}(t) = \begin{bmatrix} k_r(t) \\ \underline{k}_u(t) \\ \underline{k}_y(t) \end{bmatrix} \quad \underline{w}(t) = \begin{bmatrix} r(t) \\ \underline{w}_u(t) \\ \underline{w}_y(t) \end{bmatrix} \qquad (2\text{-}73)$$

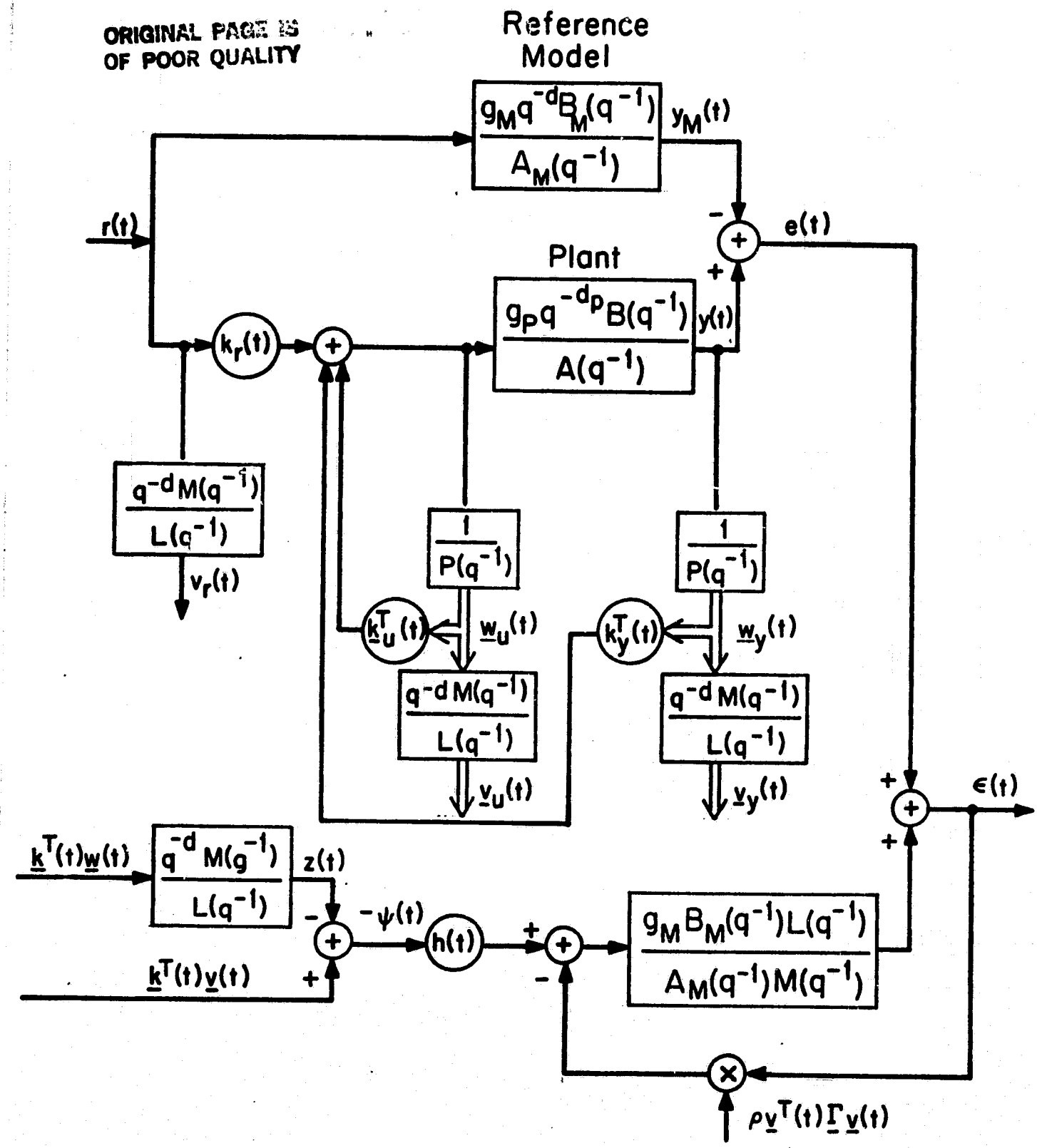

Figure 2-13. Controller structure for DA1.

The output error is

$$e(t) = y(t) - y_M(t) \tag{2-74}$$

As in CA2, auxiliary signals are fed back into the model. These signals are generatedusing the filter

$$\frac{q^{-d_M(k)}}{L^{(k+d)}} \tag{2-75}$$

which is chosen so that

$$\frac{L^{(k+d)} B_M^{(n-d)}}{M^{(k)} A_M^{(n)}} \tag{2-76}$$

is strictly positive real and that $\frac{M}{L}$ has unity d.c. gain. The auxiliary signals are generated by:

$$v(t) = \frac{q^{-d_M(k)}}{L^{(k+d)}} \underline{I}[\underline{w}(t)] \tag{2-77}$$

$$z(t) = \frac{q^{-d_M(k)}}{L^{(k+d)}} [\underline{k}^T(t)\underline{w}(t)] \tag{2-78}$$

$$\psi(t) = z(t) - \underline{k}^T(t)\underline{v}(t) \tag{2-79}$$

$$y_a(t) = \frac{q_M B_M^{(n-d)} L^{(k+d)}}{A_M^{(n)} M^{(k)}} [-h(t)\psi(t) - \underline{v}^T(t)\underline{\Gamma v}(t)e(t)] \tag{2-80}$$

where $h(t)$ is a time varying gain.

The parameter adjustment is performed by letting

$$\epsilon(t) = e(t) + y_a(t) \tag{2-81}$$

$$\underline{k}(t) = \underline{k}_o - \frac{q^{-1}}{1-q^{-1}} [\underline{\Gamma}\, \underline{v}(t)\epsilon(t)] \tag{2-82}$$

$$h(t) = h_o + \frac{q^{-1}}{1-q^{-1}} [r\psi(t)\epsilon(t)] \tag{2-83}$$

where $\underline{\Gamma}$ and γ are the constant adaptation gains.

2.3.2.2 Error Equations

As was done with CA2 the system will be analyzed with respect to a nominal parameter set $(\underline{k}^*, h^*)$ with

$$\underline{k}(t) = \underline{k}^* + \tilde{\underline{k}}(t) \tag{2-84}$$

$$h(t) = h^* + \tilde{h}(t) \tag{2-85}$$

The error equation is derived to be:

$$\begin{aligned}\epsilon(t) = &\left(\frac{g^* q^{-d_p} B^*}{k_r^* A^*} - \frac{h^* g_M q^{-d} B_M^{(n-d)}}{A_M^{(n)}}\right)\left[\tilde{\underline{k}}^T(t) w(t)\right] \\ &+ \frac{h^* g_M B_M^{(n-d)} L^{(k+d)}}{A_M^{(n)} M^{(k)}} \left[\underline{k}^T(t)\underline{v}(t)\right] \\ &+ \frac{g_M B_M^{(n-d)} L^{(k+d)}}{A_M^{(n)} M^{(k)}} \left[-\tilde{h}(t)\psi(t) - \rho \underline{v}^T(t)\underline{\Gamma}\underline{v}(t)\epsilon(t)\right] \\ &+ \left(\frac{g^* q^{-d_p} B^*}{A^*} - \frac{g_M q^{-d} B_M^{(n-d)}}{A_M^{(n)}}\right) [r(t)]\end{aligned} \tag{2-86}$$

where the nominal controlled plant is now:

$$\frac{g^* q^{-d_p} B^*}{A^*} = \frac{k_r^* g_p q^{-d_p} B P^{(n-1)}}{A(P^{(n-1)} - q^{-1} K_u^{*(n-2)}) - g_p q^{-d_p} B K_y^{*(n-1)}} \tag{2-87}$$

In the preceeding equations the following notation was adopted:

d_p is the actual delay of the plant (2-88)

$$K_y^* = k_{yo}^* + k_{y1}^* q^{-1} + \ldots + k_{y(n-1)}^* q^{-(n-1)} \tag{2-89}$$

$$K_u^* = k_{uo}^* + k_{u1}^* q^{-1} + \ldots + k_{u(n-2)}^* q^{-(n-2)} \tag{2-90}$$

A sufficient number of degrees of freedom have been left so that, if the plant is modeled correctly, the parameters can be chosen so that

$$\frac{g^* q^{-d_p} B^*}{A^*} = \frac{g_M q^{-d} B_M}{A_M} \tag{2-91}$$

i.e., there exists a set of constant feedback parameters for which the controlled plant matches the model exactly.

The stability proof proceeds using the discrete-time version of the Kalman-Yakubovich Lemma (see [7,62]). Whether the plant is properly modeled or not the error system loop is closed by the adaptation mechanism:

$$\underline{\tilde{k}}(t) = \underline{\tilde{k}}_o - \frac{q^{-1}}{1-q^{-1}} [\Gamma \underline{v}(t) e(t)] \tag{2-91}$$

$$\tilde{h}(t) = \tilde{h}_o - \frac{q^{-1}}{1-q^{-1}} [\gamma \psi(t) e(t)] \tag{2-92}$$

A diagram of the error system is shown in Figure 2-14. It is an exact counterpart of Figure 2-7. The equations for DA1 are summarized in Table 2-7.

2.3.3 Discrete-Time Algorithm No. 2 (DA2)

The algorithm introduced here as DA2 is the algorithm developed by Goodwin, Ramadge and Caines [10]. It is the simplest of all the algorithms both in structure and in the proof of stability.

2.3.3.1 Controller Structure

The structure of the controller for DA2 is given in Figure 2-15. The actual plant is represented by the equation:

$$y(t) = \frac{g_r q^{-d_p} B}{A} [u(t)]$$

and the reference model is given by:

$$y_M(t) = \frac{g_M q^{-d} B_M^{(m)}}{A_M^{(n)}} [r(t)] \qquad (2\text{-}93)$$

The system is designed assuming $d_p = d$ and the degrees of B and A are m and n respectively.

Auxiliary variables are generated simply by delayed versions of the input and output variables, as follows:

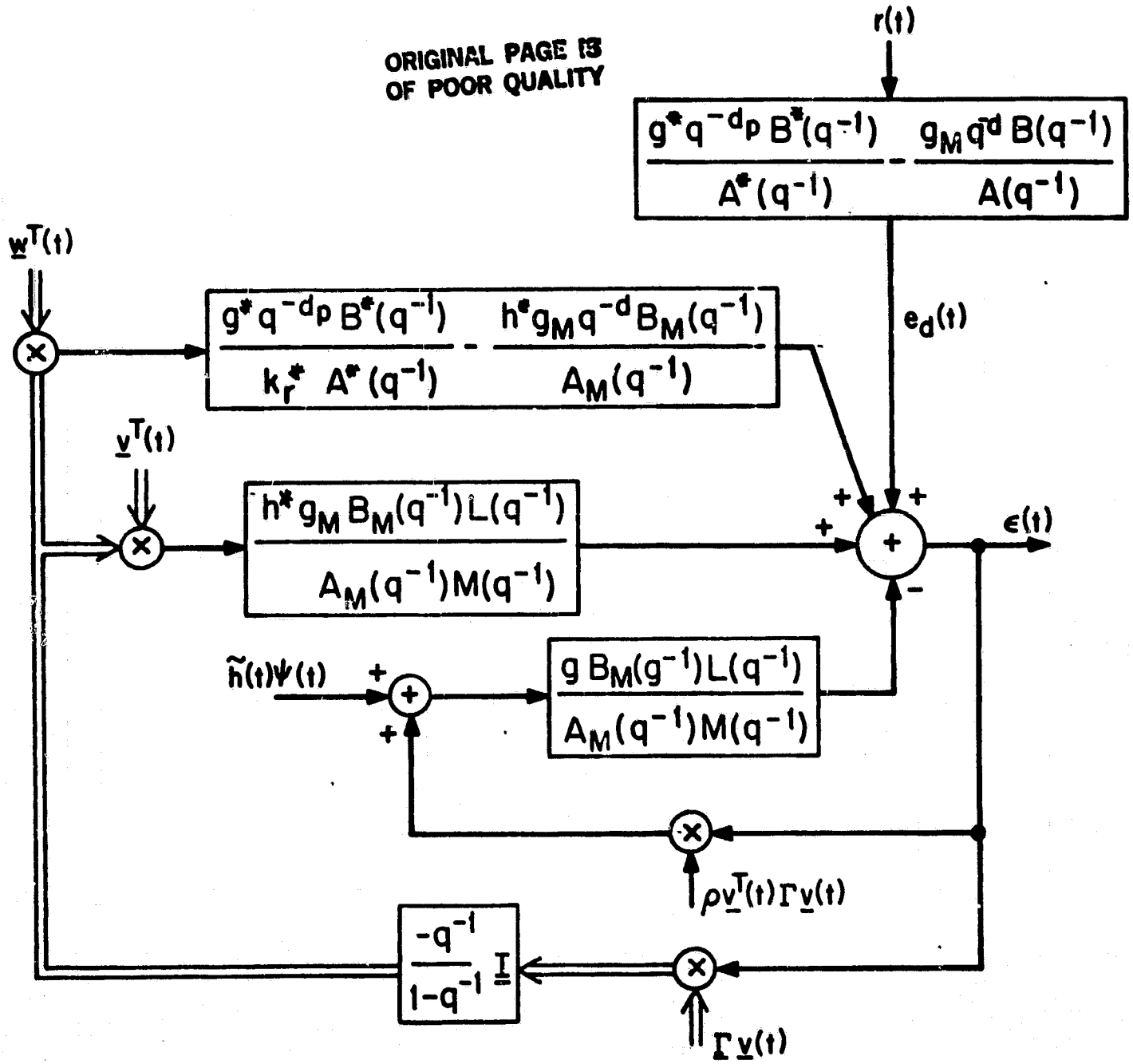

Figure 2-14. Error system for DA1.

TABLE 2-7

EQUATIONS FOR DAI

Plant

$$y(t) = \frac{g_p q^{-d_p} B}{A}[u(t)] \qquad (2\text{-}67)$$

Auxiliary Variables

$$w_{ui}(t) = \frac{q^{-(i+1)}}{p}[u(t)];\ i=0,1,\ldots,n-2 \qquad (2\text{-}69)$$

$$w_{yi}(t) = \frac{q^{-i}}{p}[y(t)];\ i=0,1,\ldots,n-1 \qquad (2\text{-}70)$$

$$\underline{w}(t) = \begin{bmatrix} r(t) \\ \underline{w}_u(t) \\ \underline{w}_y(t) \end{bmatrix}\ ,\quad \underline{k}(t) = \begin{bmatrix} k_r(t) \\ \underline{k}_u(t) \\ \underline{k}_y(t) \end{bmatrix} \qquad (2\text{-}73)$$

$$\underline{v}(t) = \frac{q^{-d_M}}{L}\underline{I}[\underline{w}(t)] \qquad (2\text{-}77)$$

$$z(t) = \frac{q^{-d_M}}{L}[\underline{k}^T(t)\underline{w}(t)] \qquad (2\text{-}78)$$

$$\psi(t) = z(t) - \underline{k}^T(t)\underline{v}(t) \qquad (2\text{-}79)$$

Model

$$y_M(t) = \frac{g_M q^{-d} B_M}{A_M}[r(t)] \qquad (2\text{-}68)$$

Input

$$u(t) = \underline{k}^T(t)\underline{w}(t) \qquad (2\text{-}72)$$

Output Error

$$e(t) = y(t) - y_M(t) \qquad (2\text{-}74)$$

TABLE 2-7 CONT.

Auxiliary Error

$$e(t) = e(t) + y_a(t) \tag{2-81}$$

$$y_a(t) = \frac{g_M B_M L}{A_M^M}[-h(t)\psi(t)-\rho v^T(t)\Gamma' v(t)e(t)] \tag{2-80}$$

Parameter Adjustment Law

$$\underline{k}(t) = \underline{k}_o - \frac{q^{-1}}{1-q^{-1}}[\Gamma \underline{v}(t)e(t)] \tag{2-82}$$

$$h(t) = h_o + \frac{q^{-1}}{1-q^{-1}}[\gamma\psi(t)e(t)] \tag{2-83}$$

Nominal Controlled Plant

$$\frac{g^* q^{-d_p} B^*}{A^*} = \frac{k_r^* g_p q^{-d_p} BP}{(P-q^{-1}K_u^*)A - g_p q^{-d_p} K_y^* B} \tag{2-87}$$

Error Equation

$$e(t) = \left(\frac{g^* q^{-d_p} B^*}{k_r^* A^*} - \frac{h^* g_M q^{-d} B_M^{(n-d)}}{A_M^{(n)}}\right)[\tilde{\underline{k}}^T(t)w(t)]$$

$$+ \frac{h^* g_M B_M^{(n-d)} L^{(k+d)}}{A_M^{(n)} M^{(k)}}[\tilde{\underline{k}}^T(t)\underline{v}(t)]$$

$$+ \frac{g_M B_M^{(n-d)} L^{(k+d)}}{A_M^{(n)} M^{(k)}}[-\tilde{h}(t)\psi(t)-\rho v^T(t)\Gamma \underline{v}(t)e(t)]$$

$$+ \left(\frac{g^* q^{-d_p} B^*}{A^*} - \frac{g_M q^{-d} B_M^{(n-d)}}{A_M^{(n)}}\right)[r(t)] . \tag{2-86}$$

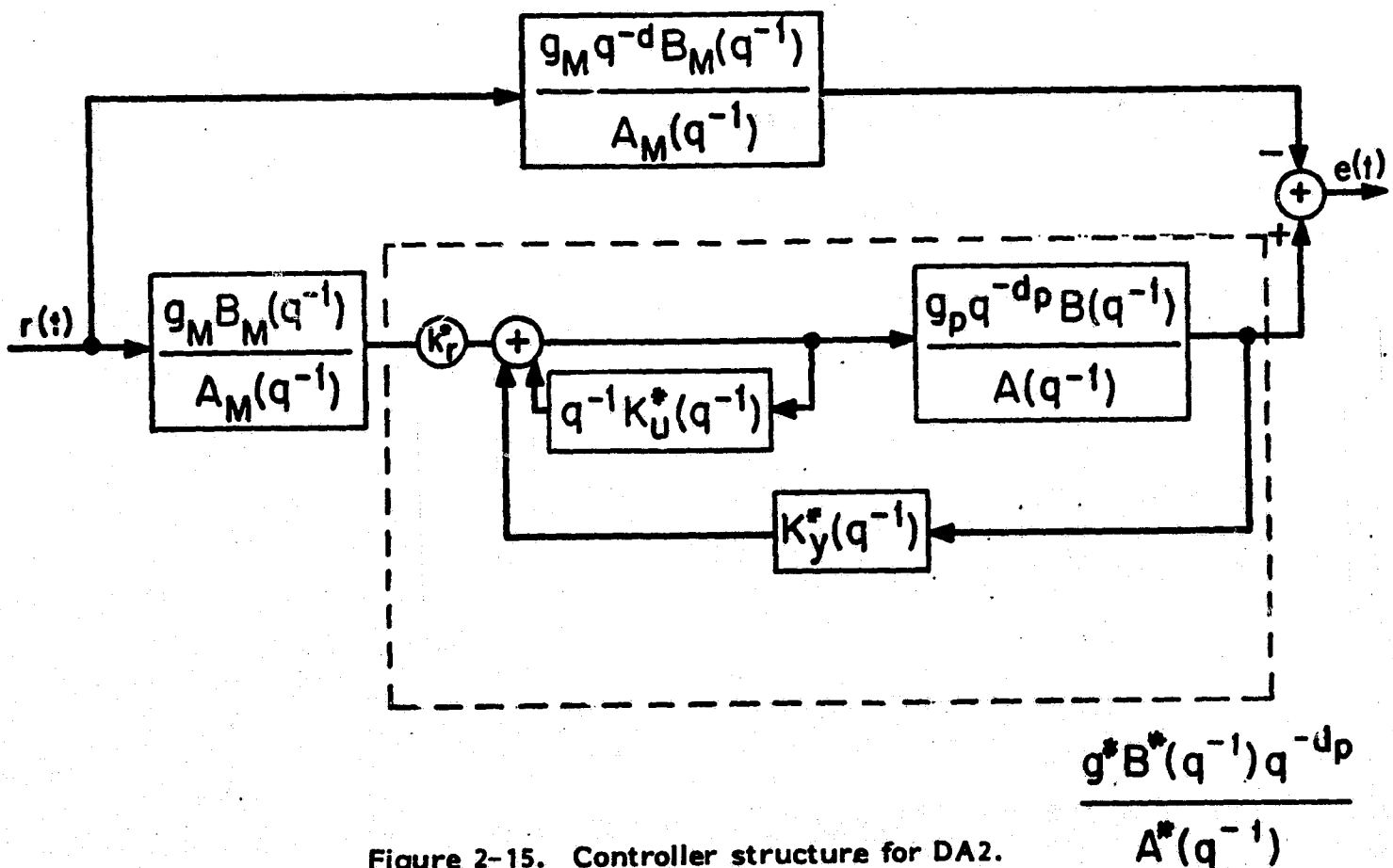

Figure 2-15. Controller structure for DA2.

$$w_{yi}(t) = q^{-i}[y(t)] \qquad i=0,1,\ldots,n-1 \tag{2-94}$$

$$w_{ui}(t) = q^{-(i+1)}[u(t)] \qquad i=0,1,\ldots,n-2 \tag{2-95}$$

$$w_r(t) = \frac{g_M B_M^{(m)}}{A_M^{(n)}}[r(t)] \tag{2-96}$$

The scalar control input to the plant is:

$$u(t) = \underline{k}^T(t)\underline{w}(t) \tag{2-97}$$

with $\underline{k}(t)$ being a vector of time-varying gains and the usual definitions for $\underline{k}(t)$ and $\underline{w}(t)$ pertaining.

$$\underline{k}(t) = \begin{bmatrix} k_r(t) \\ \underline{k}_u(t) \\ \underline{k}_y(t) \end{bmatrix} \qquad \underline{w}(t) = \begin{bmatrix} w_r(t) \\ \underline{w}_u(t) \\ \underline{w}_y(t) \end{bmatrix} \tag{2-98}$$

The specification of the algorithm is completed by the addition of the parameter adjustment mechanism:

$$\underline{k}(t) = \underline{k}_o - \frac{\gamma}{1-q^{-d}}\left[\frac{\underline{w}_d(t)e(t)}{1+\underline{w}_d^T(t)\underline{w}_d(t)}\right] \tag{2-99}$$

where

$$e(t) = y(t) - y_M(t) \tag{2-100}$$

$$\underline{w}_d(t) = q^{-d}[\underline{w}(t)] \tag{2-101}$$

and γg_p chosen so that $\gamma g_p < 2$ (2-102)

2.3.3.2 Error Equations

Since r(t) is prefiltered by $\frac{g_M B_M}{A_M}$, the goal of the control loop is to become a dead beat controller, i.e., have the closed loop transfer function $\frac{g^* B^* q^{-d_p}}{A^*}$, shown in the box in Figure 2-15, be a pure delay of d steps with a unity gain. From Figure 2-15, we obtain

$$\frac{g^* B^* q^{-d_p}}{A^*} = \frac{k_r^* g_p q^{-d_p} B}{A(1-q^{-1}K_u^*(n-2)) - g_p q^{-d_p} B K_y^*(n-1)} \qquad (2\text{-}103)$$

If the plant model is an exact representation of the plant there is enough freedom to achieve

$$\frac{g^* B^* q^{-d_p}}{A^*} = q^{-d} \qquad (2\text{-}104)$$

and the plant output will match the model output. It will be shown by an example in Section 5.1.2.2 that because this algorithm must create a deadbeat control loop to match the reference model, it requires a much higher gain in the control loop than other algorithms. It is also demonstrated in Section 5.1.2.2 that such high gains cause problems in the presence of unmodeled dynamics. The advantage of the deadbeat setup is that the stability proof for such a system is somewhat simpler than for other algorithms. However,

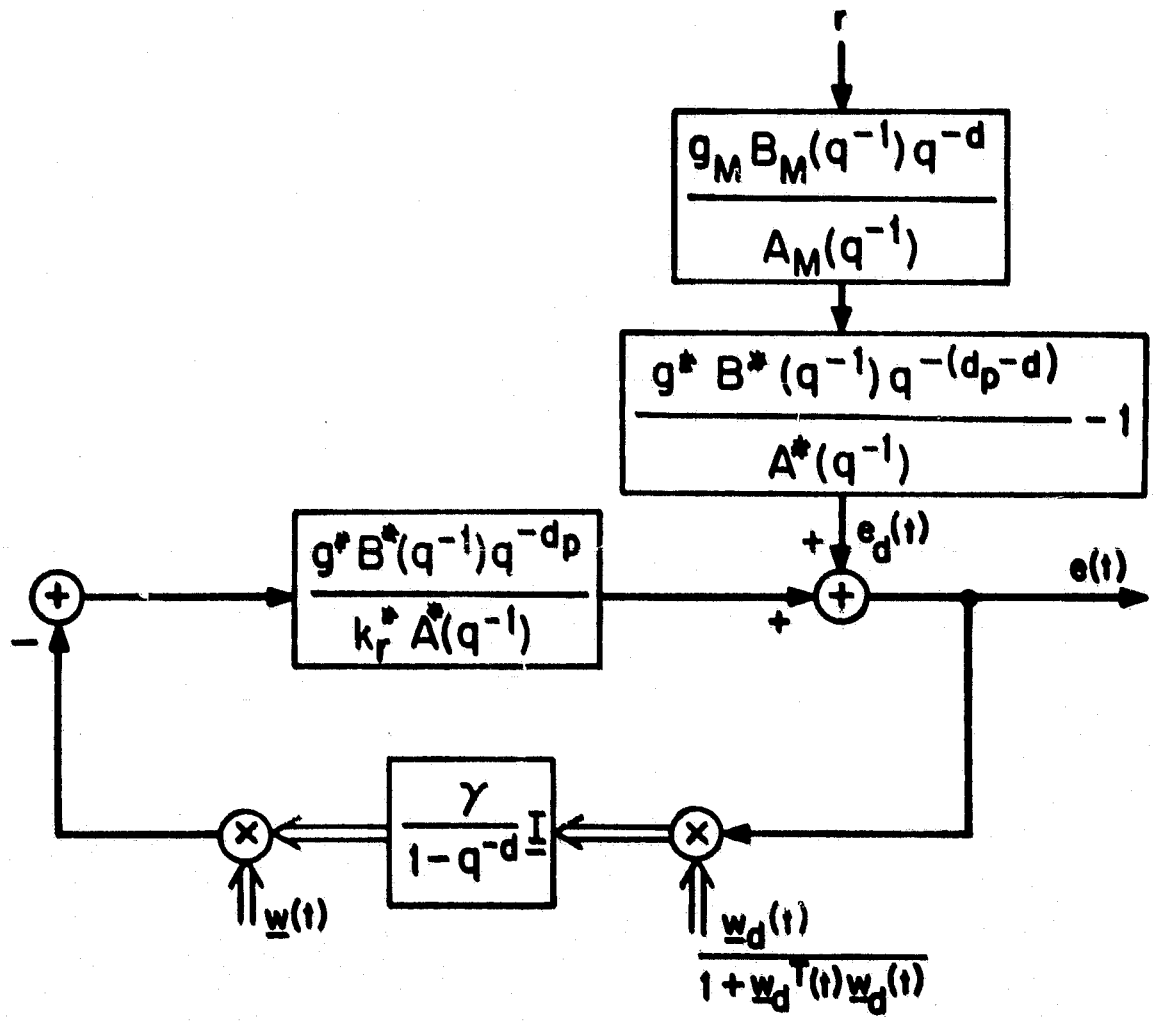

Figure 2-16. Error system for DA2.

the simplicity of the stability proof is no tradeoff for poor performance, and the problems of the DA2 algorithm will be demonstrated in Section 5.2.2.2.

The error equation for DA2 is given below:

$$e(t) = \frac{g^*B^*q^{-d_p}}{k_r^*A^*}\left[\underline{\tilde{k}}^T(t)\underline{w}(t)\right] + \left\{\frac{q_M B_M q^{-d}}{A_M} \cdot \frac{g^*B^*q^{-(d_p-d)}}{A^*} - 1\right\}\left[r(t)\right] \qquad (2\text{-}105)$$

When the plant model is an exact representation of the plant the removal of any dynamics except a pure delay in the error equation results in a stability proof which is simpler than the stability proofs of those algorithms which must account for dynamics in the error equations. The error system for the general case is represented in Figure 2-16. The equations for DA2 are summarized in Table 2-8.

It should be mentioned here that there is a version of DA2 in which certain kinds of stochastic disturbances are taken into account in the problem formulation [48]. The modifications are very similar to those that are used in the stochastic version of DA3 and, since DA3 is a more general algorithm, the effects of such modifications will be investigated in the context of DA3.

TABLE 2-8

EQUATIONS FOR DA2

Plant

$$y(t) = \frac{g_p q^{-d_p} B}{A}[u(t)] \qquad (2\text{-}67)$$

Auxiliary Variables

$$w_{yi}(t) = q^{-i}[y(t)] \quad i=0,1,\ldots,n-1 \qquad (2\text{-}94)$$

$$w_{ui}(t) = q^{-(i+1)}[u(t)] \quad i=0,1,\ldots,n-2 \qquad (2\text{-}95)$$

$$w_r(t) = \frac{g_M B_M}{A_M}[r(t)] \qquad (2\text{-}96)$$

Input

$$u(t) = \underline{k}^T(t)\underline{w}(t) \qquad (2\text{-}97)$$

Model

$$y_M(t) = \frac{g_M q^{-d} B_M}{A_M}[r(t)] \qquad (2\text{-}68)$$

Output Error

$$e(t) = y(t) - y_M(t) \qquad (2\text{-}74)$$

Parameter Adjustment Law

$$\underline{k}(t) = \underline{k}_o - \frac{\gamma}{1-q^{-d}}\left[\frac{\underline{w}_d(t)e(t)}{1+\underline{w}_d^T(t)\underline{w}_d(t)}\right] \qquad (2\text{-}99)$$

Nominal Controlled Plant

$$\frac{g^* q^{-d_p} B^*}{A^*} = \frac{k_r^* g_p q^{-d_p} B}{(1-q^{-1}K_u^*)A - g_p q^{-d_p} K_y^* B} \qquad (2\text{-}103)$$

Error System

$$e(t) = \frac{g^* q^{-d_p} B}{k_r^* A^*}[\tilde{\underline{k}}^T(t)\underline{w}(t)] + \frac{g_M B_M}{A_M} q^{-d}\left(\frac{g^* B^* q^{-(d_p-d)}}{A^*} - 1\right)[r(t)] \qquad (2\text{-}105)$$

2.3.4 Discrete-Time Algorithm No. 3 (DA3)

2.3.4.1 Introduction

The algorithm DA3 is representative of the algorithms proved asymptotically stable by Egardt [12]. Its structure is fairly general and it includes many algorithms as special cases [14].

The algorithm is especially important because one of the algorithms included is a version of the Self-Tuning Regulator of Åström et.al. [28-31]. The Self-Tuning Regulator is a heuristic scheme of combining on-line identification and control to regulate a system. Algorithm DA3 extends this concept to what may be called a Self-Tuning Controller which has the same structure as a Self-Tuning Regulator but can also follow reference inputs. Egardt's work not only enabled the unification of the Self-Tuning and the Model Reference viewpoint of adaptive control, but also provides the first global asymptotic stability proof of a Self-Tuning Algorithm.

Although the stability proofs of DA3 hold only when there are no disturbances present, the algorithm DA3 also represents an early attempt of a Model Reference scheme to handle any kind of disturbance. The disturbances considered are a very restrictive class of stochastic disturbances.

2.3.4.2 Plant and Disturbance Models

The plant and disturbance model for the algorithm DA3 is given in eqn. (2-106).

$$y(t) = \frac{g_p q^{-d_p} B}{A} [u(t)] + \frac{C}{A} [v(t)] \qquad (2\text{-}106)$$

where v(t) is a white noise sequence and the degree of C is $n_c \leq n$.

The second term in eqn. (2-106) represents a restrictive class of disturbances consisting only of those stochastic disturbances formed by white noise passing through a system with the same pole structure as the plant. Thus, if there is a frequency with considerable energy present in the disturbance due to a pole in the disturbance dynamics, the control loop will have a large gain at this frequency due to the corresponding plant pole. Thus, the control loop need only adjust to minimize the effects of the zeroes of C(s) in the noise dynamics. Indeed, if C(s) were equal to a constant, c_o, then the algorithm would be the same as it would if there were no disturbance at all.

The class of disturbances represented by the second term of eqn. (2-106) does not include such important and common disturbances as a constant output disturbance or a deterministic sinusoidal disturbance. Such deterministic disturbances may arise directly from the environment such as a disturbance at 60Hz caused by power

lines, or a disturbance caused by an oscillatory mode in an adjacent subsystem. Deterministic disturbances may also be used to capture the effects of modeling errors such as output load changes. Since the model for DA3 does not include constant or sinusoidal disturbances, there is no reason to believe that this algorithm will behave any better than any other algorithm in the presence of such disturbance. Indeed, in Section 5.2.5.3, it is shown that such disturbances will drive the bandwidth of the nominal controller of the DA3 algorithm to the point where the presence of unmodeled dynamics will cause instability.

2.3.4.3 Controller Structure

With the plant given in eqn. (2-106), the controller structure is given in Figure 2-17. The auxiliary variables are generated by

$$w_{ui}(t) = \frac{q^{-(i+1)}}{P^{(n-1)}L(d)} [u(t)] \qquad i=0,1,\ldots,m+d-2 \qquad (2\text{-}107)$$

$$w_{yi}(t) = \frac{q^{-i}}{P^{(n-1)}L(d)} [y(t)] \qquad i=0,1,\ldots,n+n_c-1 \qquad (2\text{-}108)$$

$$w_{ri}(t) = \frac{q^{-i} g_M B_M^{(m)}}{A_M^{(n)}} [r(t)] \qquad i=0,1,\ldots,n_c \leq n \qquad (2\text{-}109)$$

The usual definitions are made as follows:

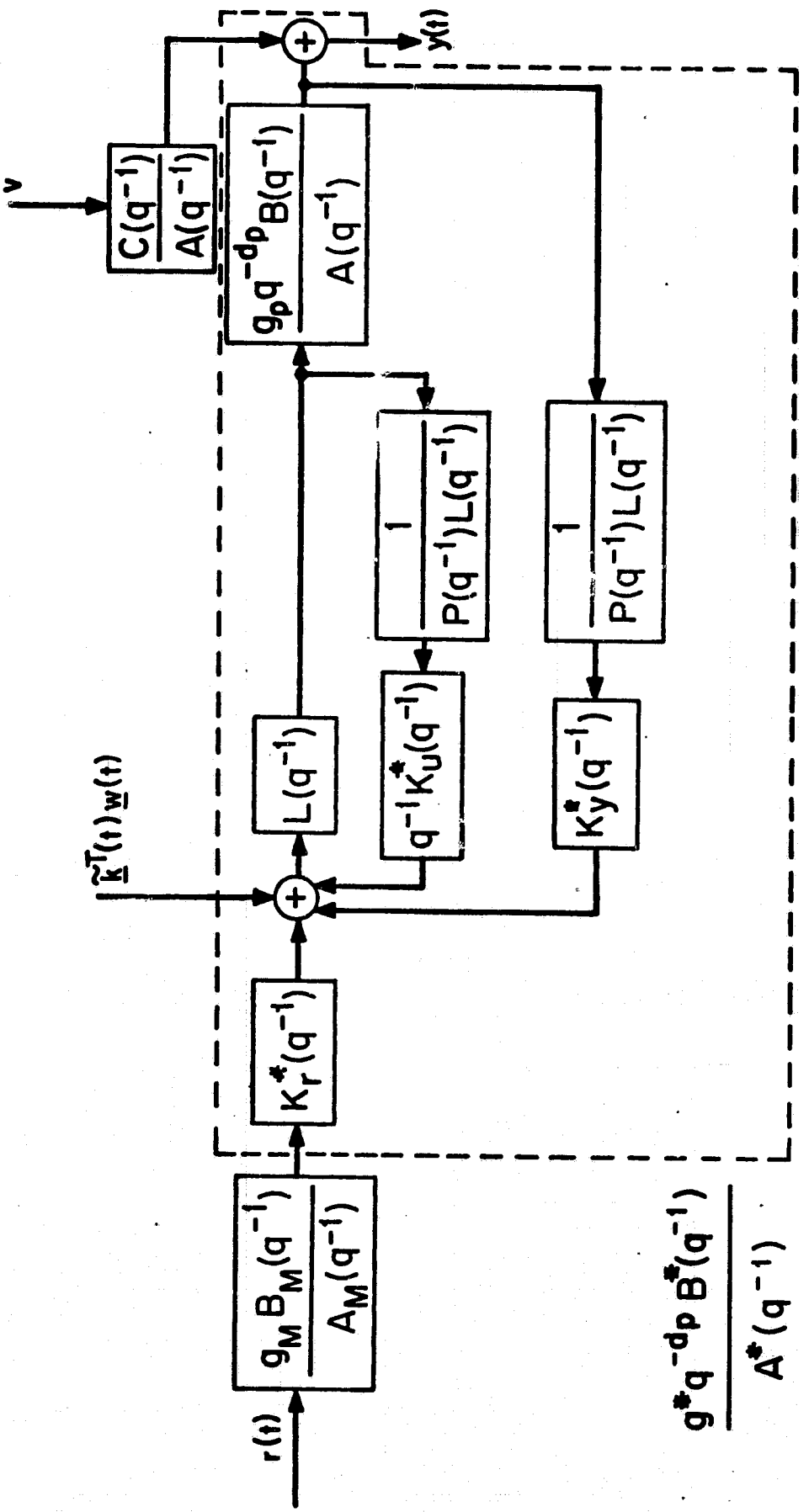

Figure 2-17. Controller structure for DA3.

$$\underline{w}(t) = \begin{bmatrix} \underline{w}_r(t) \\ \underline{w}_u(t) \\ \underline{w}_y(t) \end{bmatrix} \qquad \underline{k}(t) = \begin{bmatrix} \underline{k}_r(t) \\ \underline{k}_u(t) \\ \underline{k}_y(t) \end{bmatrix} \tag{2-110}$$

Notice that the dimension of $\underline{w}_r(t)$ and $\underline{k}_r(t)$ is n_c, the same as the order of C(s), the zero polynomial of the disturbance dynamics. These variables are added to handle the colored noise disturbance.

The scalar control input to the plant is:

$$u(t) = L^{(d)} \left[\underline{k}^T(t)\underline{w}(t)\right] \tag{2-111}$$

An auxiliary error signal is created by

$$e(t) = e(t) + y_a(t) \tag{2-112}$$

$$e(t) = y(t) - y_M(t) \tag{2-113}$$

$$y_a(t) = h(t)\left(q^{-1}\underline{I}[\underline{k}(t)] - q^{-d}\underline{I}[\underline{k}(t)]\right)^T \underline{w}_d(t) \tag{2-114}$$

with

$$\underline{w}_d(t) = q^{-d}\underline{I}[\underline{w}(t)] \tag{2-115}$$

and h(t) a time-varying gain.

The adjustment mechanism is given by

$$\underline{k}(t) = \underline{k}_o + \frac{1}{1-q^{-1}} \underline{\Gamma}\left[\frac{\underline{w}_d(t)e(t)}{\lambda_0+\underline{w}_d^T(t)\underline{w}_d(t)}\right] \tag{2-116}$$

$$h(t) = h_o + \frac{1}{1-q^{-1}} \frac{(q^{-1}\underline{I}[\underline{k}(t)]-q^{-d}\underline{I}[\underline{k}(t)])^T\underline{w}_d(t)e(t)}{\lambda + \underline{w}_d^T(t)\underline{w}_d(t)} \tag{2-117}$$

2.3.4.4 Error Equations

The system will again be analyzed around nominal parameters $\underline{k}^*$ with

$$\underline{k}(t) = \underline{k}^* + \tilde{\underline{k}}(t) \tag{2-84}$$

The nominal control system is shown by the outer box in Figure 2-17. It is given by:

$$\frac{g^*q^{-d_p}B^*}{A^*} = \frac{g_pq^{-d_p}K_r^*(n)B\,P^{(n-1)}L(d)}{(P^{(n-1)}-q^{-1}K_u^*(m+d-2))A-g_pq^{-d_p}BK_y^*(n+n_c-1)} \tag{2-118}$$

The error equation is:

$$e(t) = \frac{g^*q^{-d_p}B^*}{K_r^*A^*}[\tilde{\underline{k}}^T(t)\underline{w}(t)]+\left(\frac{g_MB_Mg^*q^{-d_p}B^*}{A_MA^*} - \frac{g_Mq^{-d_p}B_M}{A_M}\right)[r(t)]$$

$$h(t)((q^{-1}-q^{-d})\underline{I}[\underline{k}])^T\underline{w}_d(t) + \frac{B_v}{A_v}\frac{C}{A}[v(t)] \tag{2-119}$$

where

$$\frac{B_v}{A_v} = \frac{p-q^{-1}K_u^*}{(p-q^{-1}K_u^*)A-g_1q^{-d}p\,BK_y^*} \qquad (2\text{-}120)$$

The error system is completed by the addition of the parameter adjustment mechanism given by eqns. (2-116) and (2-117).

The error system is represented in Figure 2-10. The equations for DA3 are summarized in Table 3-9.

2.3.4.5 Special Cases

With certain choices of filters the algorithm DA3 can be made to be equivalent to other well known algorithms as shown by Egardt [14].

2.3.4.5.1 Reduction to DA2

If the plant to be controlled is modeled as having unity relative degree, the zero polynomial of the disturbance dynamics is modeled as a constant, the DA3 algorithm may be made identical to the DA2 algorithm by removing the additional filtering capability provided in DA3 by the input filter L and by choosing as auxiliary variables lagged versions of the input and output. That is, if

$$p=L=1;\quad n_c=1;\quad d=1 \qquad (2\text{-}121)$$

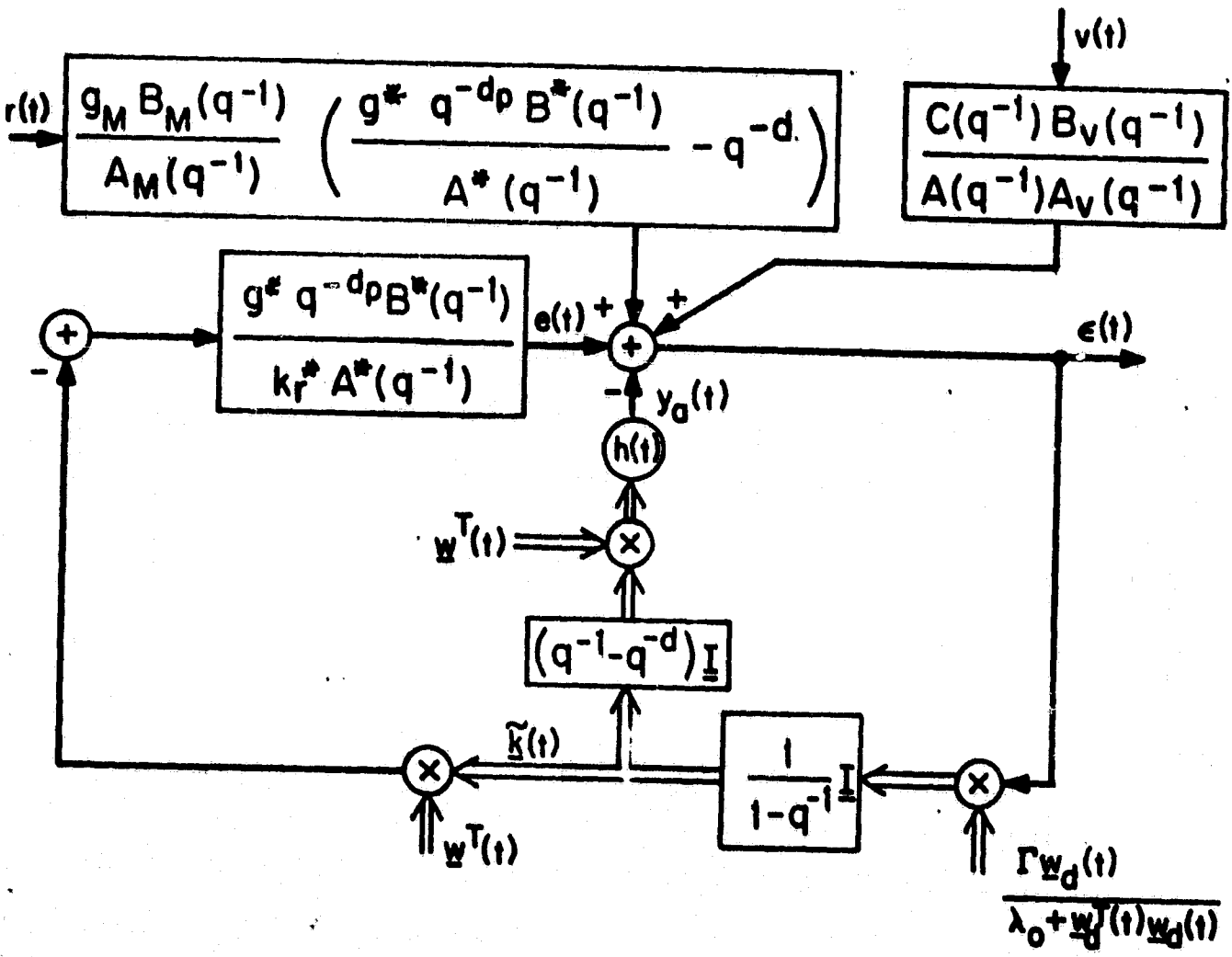

Figure 2-18. Error system for DA3.

TABLE 2-9

EQUATIONS FOR DA3

Plant

$$y(t) = \frac{g_p q^{-d_p} B}{A}[u(t)] + \frac{C}{A}[v(t)] \qquad (2\text{-}106)$$

Auxiliary Variables

$$w_{ui}(t) = \frac{q^{-(i+1)}}{PL}[u(t)];\ i=0,1,\ldots,n+d-2 \qquad (2\text{-}107)$$

$$w_{yi}(t) = \frac{q^{-i}}{PL}[y(t)];\ i=0,1,\ldots,n+n_c-1 \qquad (2\text{-}108)$$

$$w_{ri}(t) = \frac{q^{-i} g_M B_M}{A_M}[r(t)];\ i=0,1,\ldots,n_c \leq n \qquad (2\text{-}109)$$

$$\underline{w}(t) = \begin{bmatrix} \underline{w}_r(t) \\ \underline{w}_u(t) \\ \underline{w}_y(t) \end{bmatrix}; \quad \underline{k}(t) \begin{bmatrix} \underline{k}_r(t) \\ \underline{k}_u(t) \\ \underline{k}_y(t) \end{bmatrix} \qquad (2\text{-}110)$$

Input

$$u(t) = L[\underline{k}^T(t)\underline{w}(t)] \qquad (2\text{-}111)$$

Output Error

$$e(t) = y(t) - y_M(t) \qquad (2\text{-}112)$$

Auxiliary Error

$$\epsilon(t) = e(t) + y_a(t) \qquad (2\text{-}113)$$

$$y_a(t) = -h(t)((q^{-1}-q^{-d})\underline{I}[\underline{k}])^T \underline{w}_d(t) \qquad (2\text{-}114)$$

$$\underline{w}_d(t) = q^{-d}\underline{I}[\underline{w}(t)] \qquad (2\text{-}115)$$

TABLE 2-9 CONT.

Parameter Adjustment Law

$$\underline{k}(t) = \underline{k}_o + \frac{1}{1-q^{-1}} \underline{I}\left[\frac{\underline{\Gamma}\, \underline{w}_d(t)e(t)}{\lambda_o + \underline{w}_d^T(t)\underline{w}_d(t)}\right] \qquad (2\text{-}116)$$

$$h(t) = h_o + \frac{1}{1-q^{-1}}\left[\frac{((q^{-1}-q^{-d})\underline{I}[k(t)])^T \underline{w}_d(t)e(t)}{\lambda_o + \underline{w}_d^T(t)\underline{w}_d(t)}\right] \qquad (2\text{-}117)$$

Nominal Controlled Plant

$$\frac{g^* q^{-d_p} B^*}{A^*} = \frac{g_p q^{-d_p} K_x^* PLB}{(P-q^{-1}K_u^*)A - g_p q^{-d_p} K_y^* B} \qquad (2\text{-}118)$$

Error Equation

$$e(t) = \frac{g^* q^{-d_p} B^*}{K_y^* A^*}\left[\tilde{\underline{k}}^T(t)\underline{w}(t)\right] + \frac{g_M B_M}{A_M}\left(\frac{g^* q^{-d_p} B^*}{A^*} - q^{-d}\right)[r(t)]$$

$$- h(t)((q^{-1}-q^{-d})\underline{I}[\tilde{\underline{k}}(t)])^T \underline{w}_d(t) + \frac{B_v}{A_v}[v(t)] \qquad (2\text{-}120)$$

$$\frac{B_v}{A_v} = \frac{P-q^{-1}K_u^*}{(P-q^{-1}K_u^*)A - g_p q^{-d_p} K_y^* B} \qquad (2\text{-}121)$$

DA2 and DA3 are identical. If more general disturbances dynamics are allowed through more general C(s), DA3 is identical to a stochastic version of DA2 given in [48]. The two algorithms differ in the adjustment mechanisms when the relative degree of the plant is greater than unity.

It will be shown in Section 5.1.3, that the added input filter L, which is present in DA3, allows the designer an important degree of freedom not available in DA2. With the proper choice of L, the DA3 system can match the reference model with much lower loop gains than the DA2 system. It is shown in Section 5.1.3 that the added flexibility created by the filtering of L allows the designer to create a system which is better able to match the reference model and maintain stability in the presence of unmodeled dynamics.

2.3.4.5.2 A Self-Tuning Controller

The algorithm of DA3 can also be made equivalent to what is referred to as a Self-Tuning Controller. A Self-Tuning Controller which can follow reference inputs can be created from a standard Self-Tuning Regulator by feeding the reference input through the reference model to the output as suggested by Åström, et al., [28]. If the filtering of L is removed and shifted versions of the input and output are used as auxiliary variables, i.e., if

$$L=P=1 \tag{2-122}$$

in DA3, the DA3 algorithm reduces to a minimum variance Self-Tuning Controller with extended identification [28,30].

2.3.4.6 Analysis

If the model of eqn. (2-106) represents the plant and disturbances exactly, the nominal control system of eqn. (2-118) can be turned into a pure delay, i.e.

$$\frac{g^* q^{-d_p} B^*}{A^*} = q^{-d} \qquad (2\text{-}123)$$

A choice of parameters which make eqn. (2-123) true will produce perfect model matching if there is no disturbance.

The effect of a disturbance will be minimized if the parameters, $\underline{k}_r(t)$, can be adjusted so the nominal feedforward operator of the reference input

$$K_r^*(q^{-1}) = \underline{k}_{ro}^* + k_{r1}^* q^{-1} + \ldots + k_{rn_c}^* q^{-n_c} \qquad (2\text{-}124)$$

as seen in Figure 2-17 can be made to match $C(q^{-1})$ of eqn. (2-106). This will cause the identical denominator of eqn. (2-118) and eqn. (2-120) to include C(s) as a factor. The inclusion of C(s) as a factor in A_v eliminates the effect of C(s) in the disturbance dynamics and minimizesthe effect of the last term representing the disturbance in eqn. (2-119) on the error. It has been shown by Åström and Wittenmark [28] that, if this version of algorithm DA3 with the filters $L(q^{-1})$ and $P(q^{-1})$ chosen as in eqn. (1-122) converges at all, it will converge to a system which minimizes the variance of the auxiliary error, ϵ, of eqn. (2-119).

2.3.5 Normalizing Factors in the Adaptation Mechanism

In eqn. (2-99) of DA2 and eqns. (2-116) and (2-117) of DA3 there is a normalizing factor, $\lambda_o + \underline{w}_d^T(t)\underline{w}_d(t)$, in the parameter adjustment mechanism. As will be seen in Section 5.1.2 and Section 5.1.3, this normalizing factor is important if the algorithm is to maintain stability in response to constant reference inputs in the presence of unmodeled dynamics. The normalizing factor allows an upper bound on the gain of the error system loop to be set independent of the size of the reference input, if the reference input is constant. An upper bound on the gain of the error system limits the bandwidth of the error system and avoids the excitation of unmodeled dynamics and the resulting unstable behavior.

There are versions of DA2 given in [10] and DA3 given in [12] in which a stochastic approximation or a least squares identification technique is used for parameter adaptation. These techniques accumulate the normalizing factor over time so that the gains in the adaptation mechanism are time-decreasing and go to zero asymptotically.

Clearly, an algorithm whose adaptive gains go to zero can no longer satisfactorily adapt to changing parameters in the plant, if the changes in the parameters occur after the adaptation gains

have gotten very small. This problem is dealt with in practice by discounting old values of the normalizing factor so that if the signals in the system are constant, the adaptation gain will be a steady state value. An example of the use of such a "forgetting factor" follows:

Suppose eqn. (2-99) of DA2, repeated below

$$\underline{k}(t) = \underline{k}_o - \frac{\gamma}{1-q^{-1}} \frac{w_d(t)e(t)}{\lambda_o + \underline{w}_d^T(t)\underline{w}_d(t)} \qquad (2\text{-}99)$$

were

$$\underline{k}(t) = \underline{k}_o - \frac{\gamma}{1-q^{-1}} \frac{w_d(t)e(t)}{1+g(t)} \qquad (2\text{-}124)$$

with

$$g(t) = \lambda g(t-1) + w_d^T(t)w_d(t); \quad g(o)=0 \qquad (2\text{-}125)$$

The parameter λ is the forgetting factor. Setting λ=0 reduces eqns. (2-124) and (2-125) back to eqn. (2-99). Setting λ equal to one would produce a time decreasing adaptation gain. Algorithms with time decreasing gains will not be considered in the sequel since we are interested in asymptotic properties of adaptive algorithm and such algorithm are asymptotically not adaptive at all.

Algorithms with forgetting factors, $0<\lambda<1$, will not be considered separately as these algorithms will react very much like those algorithms with $\lambda=0$ for the situations considered in the sequel. Indeed, if $\underline{w}_d(t)$ is constant as it is taken to be throughout Section 5.1, we have

$$g(t) = \frac{1}{1-\lambda} \quad \underline{w}_d^T(t)\underline{w}_d(t) \tag{2-126}$$

and the effects of g can be subsumed in the parameters γ and λ_o of eqn. (2-99).

In addition, the detailed behavior of g(t) is not important to the heuristic arguments made in Section 5.2. Therefore, only the algorithms as presented throughout Section 2.3 will be considered in the sequel.

CHAPTER 3

CONTINUOUS TIME ADAPTIVE SYSTEMS WITH UNMODELED DYNAMICS AND CONSTANT INPUTS

3.1 Introduction

In this chapter the behavior of the continuous-time adaptive control algorithms which were introduced in Section 2.2 is examined for the case where the plant contains unmodeled dynamics, the reference input is constant, and there are no external disturbances.

Until the present research, little was reported in the literature dealing with the important problem of how adaptive control algorithms would behave, if they were implemented on a plant whose actual order is larger than the order assumed for the plant in the adaptive design process, i.e., if they were implemented on a plant with unmodeled dynamics.

Anderson and Johnson [52,53] and Anderson and Johstone [54] have obtained some results indirectly by showing that, with a "sufficient excitation" condition, the discrete-time algorithm DA2 is exponentially stable, implying that the system should be able to retain stability in the presence of some unmodeled dynamics or disturbances. There is, however, no estimate of the precise nature of unmodeled dynamics that are acceptable for the retention of stability. In fact, it is shown in Section 5.1.2.2 and Section 5.2.4 that the algorithm DA2 will have serious stability problems in the presence of a large class of unmodeled dynamics.

A direct examination of the effects of unmodeled dynamics in the adaptive observer problem has been published by Ioannou and Kokotovic [51,53]. Their research using singular perturbation theory displayed that high frequency unmodeled dynamics can cause significant errors even in the open-loop adaptive observer problem.

Ioannou [52] in his Ph.D. thesis* has extended the singular perturbation analysis for adaptive control algorithm CA1. For some of the situations where the plant contains very high frequency unmodeled dynamics, Ioannou has shown that, if the system is started within a certain region of initial conditions, then the output error will approach zero asymptotically in the absence of reference inputs. Thus, Ioannou has deduced the fact that the linearized error system is asymtotically stable, a fact that agrees with the analysis of this chapter; he also has derived an estimate of region of attraction of the linearized error system. However, Ioannou can obtain results for the standard CA1 algorithm for a much smaller class of unmodeled dynamics than the analysis of this chapter. In addition, his results do not predict when instability can occur as the results of this chapter do. His results were obtained only for the case of zero reference input.

Ioannou has also analyzed a modified version of CA1; his modification will be discussed in Chapter 4. Finally, Ioannou did not examine the behavior of the CA1 algorithm in the presence of disturbances as we have in Chapter 4.

---

*Ioannou's thesis became available to the author during the preparation of the final draft of his dissertation.

Preliminary results of the research presented in this dissertation have also appeared in the literature. In Rohrs, et.al., [1], simulation studies which displayed the dangerous effects of unmodeled dynamics on one adaptive control algorithm were reported. In Rohrs, et.al. [2], the effects seen in [1] were displayed analytically for first order systems and a number of algorithms. The present chapter of this dissertation is an expansion of the work reported in [2].

Thus, the contents of this chapter represent the first analytical results of the effects of unmodeled dynamics upon a wide class of adaptive control systems, using an analytical technique which is shown to be useful both in analyzing the effects of unmodeled dynamics upon a system with a constant reference input and no disturbances and, also, in providing a guide for adjusting the structure of the gains for adaptive systems to minimize the effects of unmodeled dynamics.

From this analysis, backed by simulation results, the following conclusions are made:

- The algorithm CA1 cannot be made to be stable for all reference inputs unless the forward operator in the error system of Figure 2-3 can be made to be positive real. This means that CA1 will not be even locally stable for all constant inputs in the

presence of a large class of unmodeled dynamics including all unmodeled dynamics with a pole excess of two or greater.

- With some prior information about the nature of the unmodeled dynamics, the parameters of the algorithms CA2, CA3, and CA4 may be picked, using the analysis technique of this chapter as a guide, so that these algorithms retain local stability for all constant reference inputs and no disturbances.* By local stability, we mean that the system will remain stable, if the numerical values of the parameters that describe the adaptive algorithms are close, at the initial time, to some nominal set of parameters.

The contents of the remainder of the chapter are as follows:

Section 3.2 contains a description of the analysis technique used throughout the chapter. Sections 3.3 to 3.6 contain, respectively, the analysis of algorithms CA1 to CA4 for constant reference inputs with and without unmodeled dynamics. Section 3.7 contains the conclusions of the chapter.

---

*The stability behavior of these algorithms in the presence of unmodeled dynamics with more general inputs and disturbances is not encouraging as shown in Chapter 4.

3.2 Explanation of the Analysis Technique Used for Adaptive Systems with Unmodeled Dynamics and Constant Inputs

The adaptive control systems presented in Section 2.2 are nonlinear, time-varying systems. In order to perform some analysis, in addition to the original Lyapunov-based stability analysis and to be able to analyze even local stability properties in the presence of unmodeled dynamics, a linearization technique is used. The immediate consequence is a linear, time-varying system. By assuming further that the reference input and, therefore, the model output, are constant, the system is transformed into a linear time-invariant (LTI) system. At this point, then, the well known analysis techniques for LTI systems, such as root-locus, Nyquist, Routh-Hurwitz, etc., can be brought to bear on the adaptive systems.

The assumptions used in the linearization technique correspond to the following situations:

(1) It may be assumed that, at the start of the analysis, the state and parameters of the adaptive controller are close to some desired values. Such a situation could develop when the asymptotically stable adaptive controller has already been operating for a long period of time with sufficiently rich inputs and is therefore close to final convergence.

(2) It could also arise when the plant parameters are fairly well known *a priori* and the adaptation is employed as a fine-tuning mechanism.

Clearly, any poor behavior under these relatively benign circumstances must be cause for alarm concerning the overall behavior of these algorithms.

As with any analysis based upon linearization, there is a finite subset of parameters and signals for which the linearization will give accurate predictions of the system behavior. There is, as yet, no estimate of how large that subset is for the linearizations carried out in this dissertation. At various points throughout this dissertation, the reader will encounter situations where either the parameters or the signals of the system move away from the subset of parameters and signals for which the particular linearization considered would give an accurate prediction of the system behavior.

That the linearization analysis is valid only locally, is a fact of life that one must accept. This shortcoming can be dealt with, as is done in Section 3.3.5, by performing a set of linearizations around different operating values to gain more global, albeit limited, insight. Many of the properties which have been discovered about adaptive control systems operated in the presence of unmodeled dynamics can even be

displayed with plants that are nominally first order. More specifically, systems will be studied and digital simulations will be presented where the plant is a first order system with some additional high frequency unmodeled dynamics and the adaptive controller is designed assuming that the plant is first order.

All of the analysis in this chapter assumes that the unmodeled dynamics of the plant are known exactly by the analyst. If only certain characteristics of the unmodeled dynamics are known (as is always the case), the analyst must use engineering judgement to analyze the adaptive system with sets of specific unmodeled dynamics which will capture the behavior of the entire class of unmodeled dynamics which may occur.

The simulations presented in this and the next chapter are accomplished by converting the continuous system into an equivalent discrete-time system using a sampling interval of T=.001. This sampling frequency is nearly one hundred times faster than the fastest signal present, leaving little doubt as to the closeness of the approximation of the simulation results to the actual continuous system; in other words, the instability of the closed-loop adaptive control confirmed by computer simulations is not due to poor numerical approximation of a continuous-time system by a discrete-time system.

3.3 Analysis of CA1

3.3.1 Introduction

In this section, we present the analysis of algorithm CA1 presented in Section 2.2.1. It is shown that the linearized analysis introduced in Section 3.2 is a useful tool for the study of this algorithm.

Based upon the linearized analysis and supported with computer simulations, our conclusions regarding the CA1 algorithm are as follows:

- Even in the absence of unmodeled dynamics the algorithm can generate high frequency control inputs to the plant for sufficiently large constant reference inputs.
- In the presence of unmodeled dynamics, the adaptive system will become unstable for sufficiently large constant reference inputs.

The analysis begins in Section 3.3.2 where a first order system with no unmodeled dynamics is studied, followed in Section 3.3.3 with a numerical example of such a system. In Section 3.3.4, the behavior of the CA1 algorithm is analyzed when an adaptive

controller designed for a first order system is implemented on a plant that, in addition to the nominal first order dynamics, has an unmodeled high frequency pole pair. A numerical example of the type of system analyzed in Section 3.3.4 is provided in Section 3.3.5 and much insight about the behavior of the CA1 algorithm is gained in examining this example. Section 3.3.6 provides a discussion of the analysis technique for higher order systems. Section 3.3.7 demonstrates the flexibility of the technique by analyzing a numerical example where the unmodeled dynamics are non-minimum phase. Finally, Section 3.3.8 states our conclusions concerning algorithm CA1.

3.3.2 A First Order System with No Unmodeled Dynamics

Assume initially that the plant is actually first order with no zeroes, i.e.

$$y_p(t) = \frac{g_p}{s+a}\,[u(t)]; \quad g_p > 0 \tag{3-1}$$

Assume also that the adaptive controller is designed using CA1 and assuming properly that n=1 and m=0. The equations from Table 2-1 become:

$$\underline{w}(t) = \begin{bmatrix} r(t) \\ y(t) \end{bmatrix} \quad \underline{k}(t) = \begin{bmatrix} k_r(t) \\ k_y(t) \end{bmatrix} \tag{3-2}$$

$$y_M(t) = \frac{g_M}{s+a_M}\,[r(t)] \tag{3-3}$$

$$g_M,\ a_M > 0$$

$$u(t) = k_r(t)r(t) + k_y(t)y(t) \tag{3-4}$$

$$e(t) = y(t)-y_M(t) \tag{3-5}$$

$$\dot{k}_r(t) = \dot{\tilde{k}}_r(t) = -\gamma r(t)e(t) \tag{3-6}$$

$$\dot{k}_y(t) = \dot{\tilde{k}}_y(t) = -\gamma y(t)e(t) \tag{3-7}$$

where $\underline{\Gamma}$ has been chosen as

$$\underline{\Gamma} = \gamma\,\underline{I} \tag{3-8}$$

Let

$$k_r^* = \frac{g_M}{g_p} \tag{3-9}$$

and

$$k_y^* = \frac{a-a_M}{g_p} \tag{3-10}$$

Then

$$\frac{g^*B^*}{A^*} = \frac{g_M B_M}{A_M} \tag{3-11}$$

and

$$e(t) = \frac{g_p B_M}{A_M}\,[\tilde{k}_r(t)r(t)+\tilde{k}_y(t)y(t)] \tag{3-12}$$

Using eqn. (3-3), eqn. (3-12) can be written in differential form as:

$$\dot{e}(t) = -a_M e(t) + g_p[\tilde{k}_r(t)r(t)+\tilde{k}_y(t)y(t)] \quad . \qquad (3\text{-}13)$$

The entire error system now can be derived from eqns. (3-6), (3-7) and (3-13) as follows:

$$\frac{d}{dt}\begin{bmatrix} e(t) \\ \tilde{k}_y(t) \\ \tilde{k}_r(t) \end{bmatrix} = \begin{bmatrix} -a_M & g_p y(t) & g_p r(t) \\ -\gamma y(t) & 0 & 0 \\ -\gamma r(t) & 0 & 0 \end{bmatrix} \begin{bmatrix} e(t) \\ \tilde{k}_y(t) \\ \tilde{k}_r(t) \end{bmatrix} \qquad (3\text{-}14)$$

Note that this system (3-14) is non-linear due to the fact that

$$y(t) = y_M(t) + e(t) \qquad (3\text{-}15)$$

so that there are e^2 terms on the right-hand side of eqn. (3-14). This type of system has been shown to be stable by Lyapunov analysis as explained in Section 2.2.1.5. Note that $\frac{g_p}{s+a_M}$ is strictly positive real. Further analysis has shown that $\lim_{t\to\infty} e(t)=0$. [3].

Furthermore, if the signal r(t) is "sufficiently rich" the whole error system is globally asymptotically stable with a zero equilibrium point [20].

In order to achieve some insight into the dynamic behavior of the error system (3-14), a local, as opposed to global view, will be taken. Assume that the output and parameter errors are small and linearize the system around zero error. The only change that occurs in eqn. (3-14) is that y is replaced by $y^*=y_M$. The linearized system is

$$\frac{d}{dt}\begin{bmatrix} e(t) \\ \tilde{k}_y(t) \\ \tilde{k}_r(t) \end{bmatrix} = \begin{bmatrix} -a_M & g_p y^* & g_p r \\ -\gamma y^* & 0 & 0 \\ -\gamma r & 0 & 0 \end{bmatrix} \begin{bmatrix} e(t) \\ \tilde{k}_y(t) \\ \tilde{k}_r(t) \end{bmatrix} \tag{3-15}$$

If, in addition, it is assumed that r and hence y^* are constant, eqn. (3-15) represents a linear time-invariant system. The characteristic equation for the system (3-15) is:

$$s(s^2+a_M s+g_p\gamma d^*)=0 \tag{3-16}$$

where

$$d^* = y^{*2} + r^2 \tag{3-17}$$

One pole of the error system (3-15) remains fixed at the origin while the other two can be thought of as being determined by a root locus pattern associated only with the $(s^2+a_M s+g_p\gamma d^*)$ part of eqn. (3-16) using d^* as the gain parameter; this is illustrated

in Figure 3-1. The diagram of Figure 3-1 will be referred to as the d*-root-locus of eqn. (3-16).

From Figure 3-1 and eqn. (3-17) it is seen that for large constant reference inputs, r, the algorithm produces high frequency oscillations in some subspace of $(e,\tilde{k}_1,\tilde{k}_2)$ and through eqn. (3-4), namely

$$u(t) = k_r(t)r(t) + k_y(t)y(t) \tag{3-4}$$

in the plant input u(t) as well. Thus, high frequency controls will be present for large reference input values even when this input is constant, the plant is first order, and the adaptation process is in the final approach to convergence.

The pole that is fixed at the origin is associated with the eigenvector

$$\begin{bmatrix} 0 \\ r \\ -y^* \end{bmatrix}$$

Thus, a constant input is not sufficiently rich to produce parameter convergence. Instead of approaching zero, the parameter errors approach a linear subspace defined by

$$e=0;\ \tilde{k}_y = -\frac{r}{y^*}\ \tilde{k}_r \tag{3-18}$$

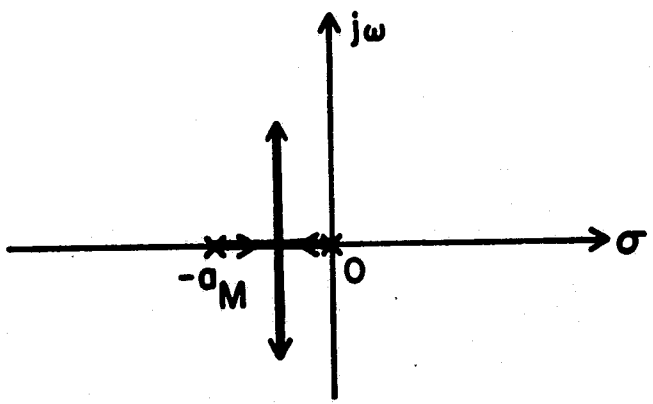

Figure 3-1. d^*-root locus of eqn. (3-16).

On this subspace, the output error remains zero so that there is no further adaptation taking place.

3.3.3 A Numerical Example of a First Order System with No Unmodeled Dynamics

An example, which will be carried throughout this and the next chapter, is presented to verify the oscillatory characteristics of the CA1 algorithm.

Assume that the plant is accurately described by the first order system

$$y(t) = \frac{2}{s+1} \quad [u(t)] \tag{3-19}$$

Suppose that the desired model behavior is given by:

$$y_M(t) = \frac{3}{s+3} \quad [r(t)] \tag{3-20}$$

Figure 3-2 shows the plant and model outputs for a digital computer simulation of the non-linear adaptive system CA1. The simulation was started with $k_u=k_y=y=y_M=0$, an adaptive gain $\gamma=1.0$ and a constant reference input of $r=2.5$. The plant output, $y(t)$, tracks the model output well after 4 seconds. Note in Figure 3-2 that there is an oscillation in the output error at a frequency approximately equal to the frequency of $\omega=4.75$ rad/sec which is predicted by the d^*-root locus of Figure 3-5. Figure 3-4 shows

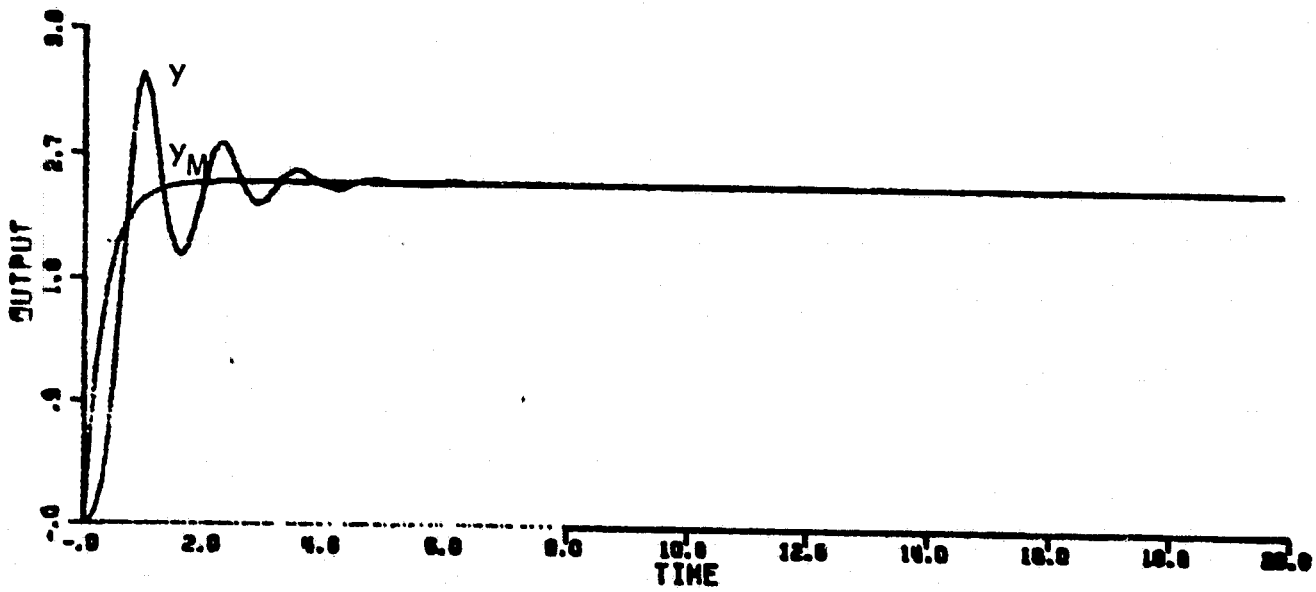

Figure 3-2. Outputs from simulation of CA1 with r=2.5.

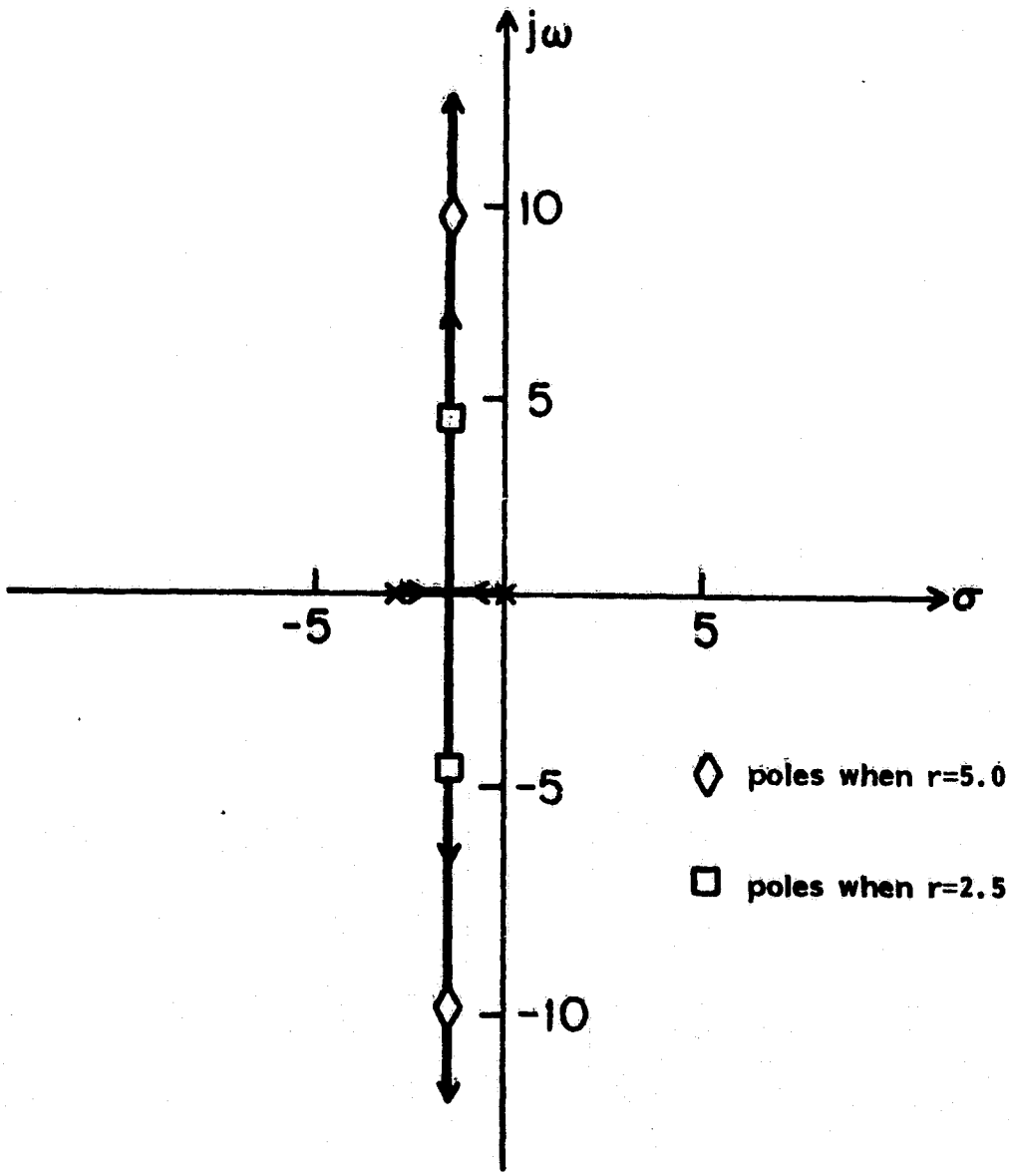

Figure 3-3. d^*-root locus of numerical example of Section 3.3.3.

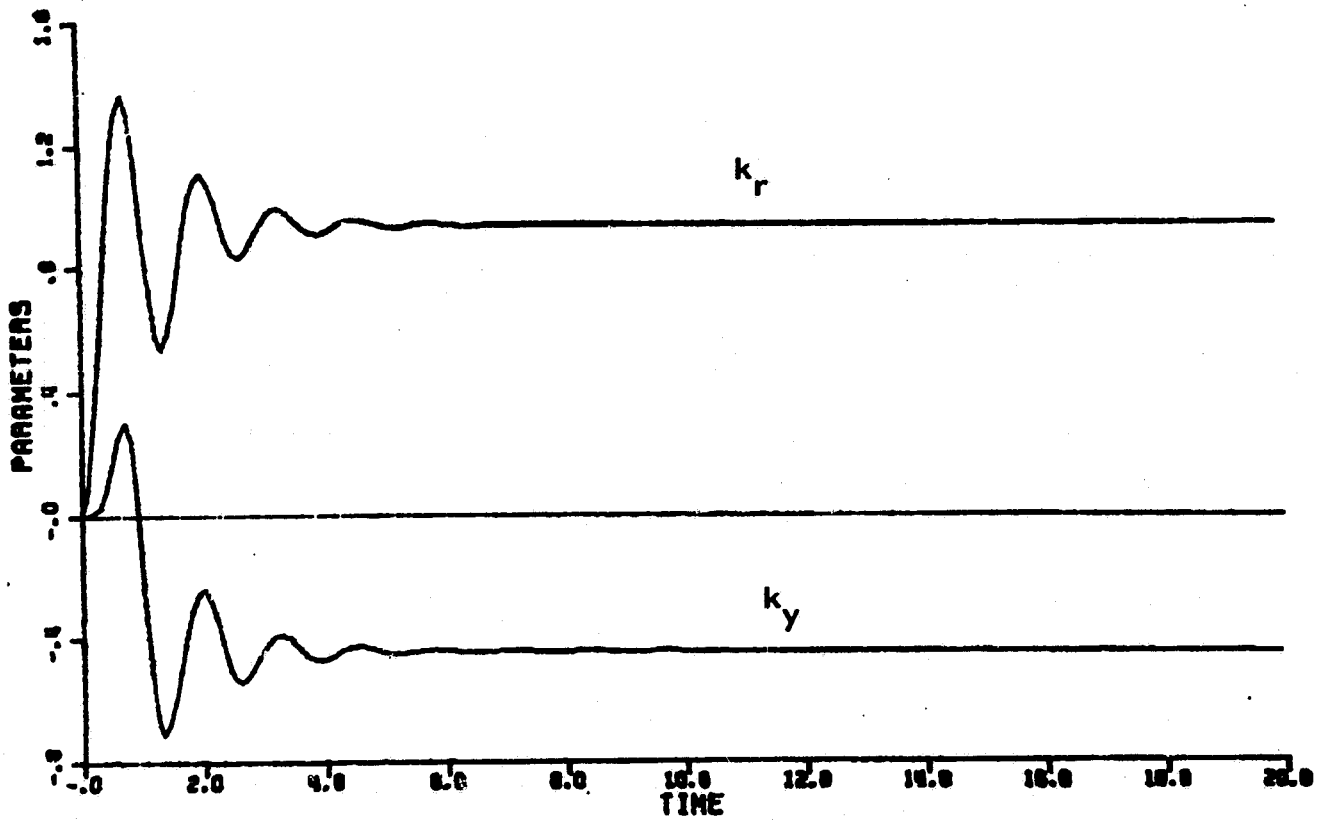

Figure 3-4. Parameters from simulation of CA1 with r=2.5.

the parameters for this simulation. The desired parameters which would make the controlled plant match the reference model exactly for this example are:

$$k_r^* = 1.5 \qquad k_y^* = -1.0$$

The parameters as seen in Figure 2-4 oscillate at the frequency of ω=4.75 rad/sec. as predicted by the previous analysis and then converge not to their desired values but to

$$k_r = 0.94 \qquad k_y = -0.44 \quad .$$

Subtracting the desired parameters from the final values of the parameters yields the final values of the parameter errors

$$-\tilde{k}_r = 0.56 = \tilde{k}_y$$

Since, for this example, y^*=r, the parameter errors have indeed converged to the subspace given by eqn. (3-18).

Finally, Figure 3-5 shows the outputs for the simulation carried out with a larger reference input r=5.0. The oscillation is now twice as fast as before. This is once more predicted by the d^*-root locus. Note from eqn. (3-16) that the frequency of oscillation of the error system would also double if the adaptation gain, γ, or the unknown plant gain, g_p, were quadrupled.

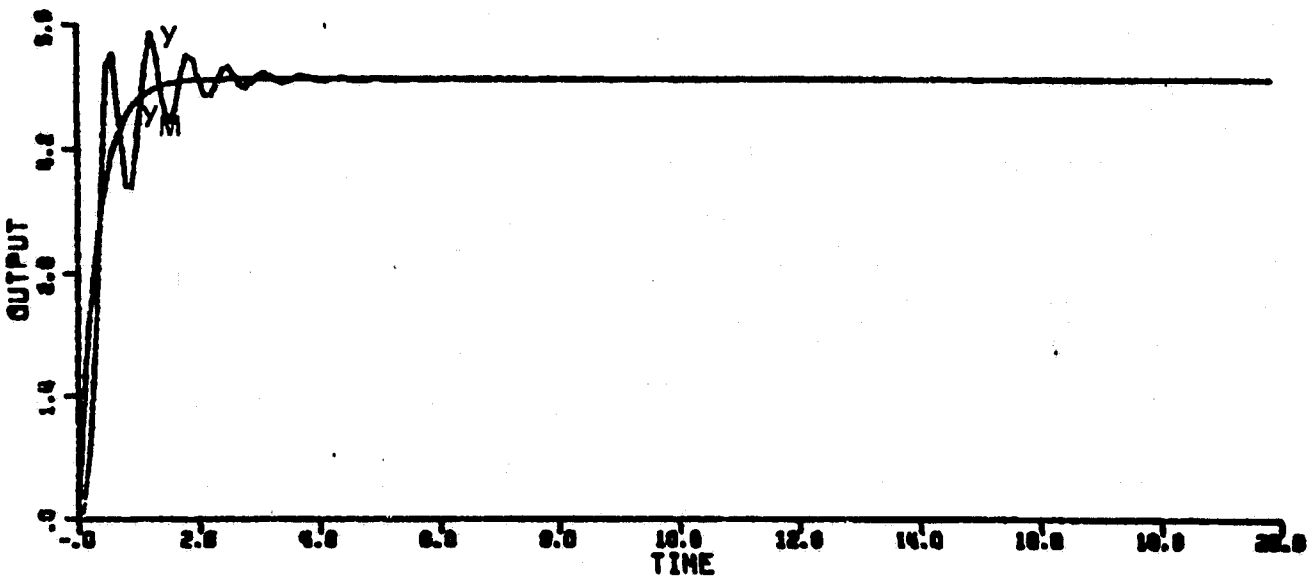

Figure 3-5. Outputs from simulation of CA1 with r=5.0.

Figure 3-6 shows the time variation of the parameters when r=5.0. Notice that they now converge to

$$k_r = 1.21 \qquad k_y = -0.71 \ ,$$

a set of values different from those to which they converged when the simulation was run with r=2.5 but still on the predicted subspace of eqn. (3-18).

Thus we have seen in Section 3.3.2 and Section 3.3.3 that even when the CAl algorithm is implemented on a first order system with no unmodeled dynamics and no disturbances, and is presented with only constant inputs, high frequency parameter oscillations which give rise to high frequency control activity will result for sufficiently large constant reference inputs.

It will be seen in the next two sections that such high frequency control activity will lead to instability in the presence of even high frequency unmodeled dynamics.

3.3.4 A First Order Nominal System with Unmodeled Dynamics

Now the effects of unmodeled dynamics will be considered. In the sequel it will be assumed that an adaptive controller is designed assuming that the plant and reference model are both first order. The behavior of the system will then be analyzed around a

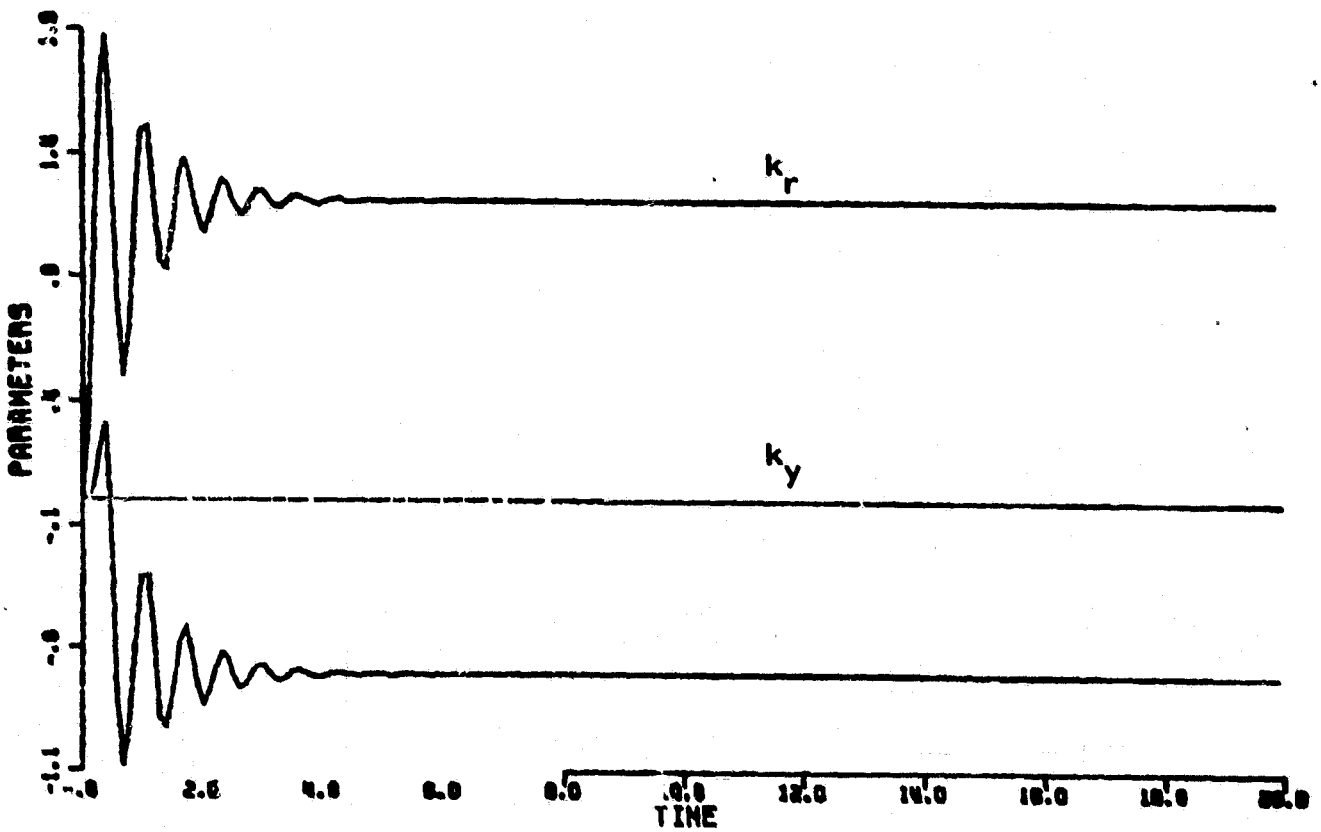

Figure 3-6. Parameters from simulation of CA1 with r=5.0.

desired set of parameters for the case where the plant's order and relative degree are different from what was assumed when the controller was designed. The immediate discussion will consider the case where the plant consists of a nominal first order system plus a high frequency pole pair which is unmodeled in the sense that its presence is not taken into account in the adaptive controller design. These results will be expanded in Section 3.3.6 to include more general unmodeled dynamics.

Assume that the reference model as given by eqn. (3-3) as in Section 3.3.2 but that now the actual plant is represented by:

$$y(t) = \left(\frac{g_p}{s+a} \quad \frac{a_{u1}a_{u2}}{(s+a_{u1})(s+a_{u2})} \right) [u(t)] \tag{3-21}$$

where a_{u1}, a_{u2}, are either real numbers or complex conjugates with $|a_{u1}|>|a_M|$ and $|a_{u2}|>|a_M|$. The adaptive system is designed using CAl with the assumption that the plant is first order with no zero so it is described by eqns. (3-2) to (3-8). The error equation can be deduced from Table 2-1 and is as follows:

$$e(t) = \left(\frac{g^*B^*}{A^*} - \frac{g_M B_M}{A_M} \right) [r(t)] + \frac{g^*B^*}{A^*} \left[\frac{\tilde{k}^T(t)w(t)}{k_r^*} \right] \tag{2-24}$$

where, in view of eqn. (2-22)

$$\frac{g^*B^*}{A^*} = \frac{k_r^* g_p a_{u1} a_{u2}}{(s+a)(s+a_{u1})(s+a_{u2}) - g_p a_{u1} a_{u2} k_y^*} \tag{3-22}$$

The analysis that follows is valid for any choice of k_y^* and k_r^*. The motivating choice, however, one that is consistent with the idea of k_y^* and k_r^* being the desired values, is to pick k_y^* and k_r^* so that $\frac{g^*B^*}{A^*}$ matches $\frac{g_M B_M}{A_M}$ over as large a low-frequency range as possible. This approach will be demonstrated later in an example.

Assume that k_r^* and k_y^* have been chosen and represent $\frac{g^*B^*}{A^*}$ as:

$$\frac{g^*B^*}{A^*} = \frac{g^*}{s^3+a_2^*s^2+a_1^*s+a_0^*} \tag{3-23}$$

Let

$$e_d(t) = \left(\frac{g^*B^*}{A^*} - \frac{g_M B_M}{A_M}\right)\left[r(t)\right] \tag{3-24}$$

be the driving term of the error equation. Note that if r(t) consists mostly of low frequencies and $\frac{g^*B^*}{A^*}$ is chosen to match the model over low frequencies, the signal $e_d(t)$ will correspond to a small perturbation term. The error system can now be derived from eqns. (2-24), (2-12), and (3-23) and is as follows:

$$\frac{d}{dt}\begin{bmatrix} e(t) \\ \dot{e}(t) \\ \ddot{e}(t) \\ \tilde{k}_y(t) \\ \tilde{k}_r(t) \end{bmatrix} = \begin{bmatrix} 0 & 1 & 0 & 0 & 0 \\ 0 & 0 & 1 & 0 & 0 \\ -a_0^* & -a_1^* & -a_2^* & \frac{g^*}{k_r^*}y(t) & \frac{g^*}{k_r^*}r(t) \\ -\gamma y(t) & 0 & 0 & 0 & 0 \\ -\gamma r(t) & 0 & 0 & 0 & 0 \end{bmatrix}\begin{bmatrix} e(t) \\ \dot{e}(t) \\ \ddot{e}(t) \\ \tilde{k}_y(t) \\ \tilde{k}_r(t) \end{bmatrix} + \begin{bmatrix} 1 \\ 0 \\ 0 \\ 0 \\ 0 \end{bmatrix} e_d(t) \qquad (3\text{-}25)$$

Equation (3-25) can be linearized around the zero error condition as was done in eqn. (3-14), which again simply replaces y with $y^*=y_M$. Assuming that r and, consequently, y^* are constant, renders the system linear and time-invariant. The resulting characteristic equation is:

$$s(s(s^3+a_2^*s^2+a_1^*s+a_o^*) + \frac{g^*}{k_r^*}\gamma d^*)=0 \qquad (3\text{-}26)$$

with $d^* \triangleq r^2+y^{*2}$ (3.17) as before.

Again, there is a pole of the system (3-25) fixed at the origin associated with a subspace in the parameter space where no further adaptation occurs. Now, however, the d^*-root locus of eqn. (3-26) contains a third-order pattern so that, for d^* large enough, the

error system will not only be oscillatory but will also become unstable. This is true even when r and y^* are constant and the system starts near the desired parameter set.

3.3.5 Numerical Example of a First Order Nominal System with Unmodeled Dynamics

For this example, we add an unmodeled pole pair at $s=-15\pm 2j$ to the plant considered earlier in Section 3.3.3. The plant is then described by:

$$y(t) = \left(\frac{2}{s+1}\right)\left(\frac{229}{s^2+30s+229}\right)\left[u(t)\right] \qquad (3\text{-}27)$$

Let the model be as before:

$$y_M(t) = \left(\frac{3}{s+3}\right)\left[r(t)\right]$$

3.3.5.1 Linearizing about a Desired System

One reasonable way to pick the point in parameter space about which to analyze the system is to choose k_y^* so that $\frac{g^*B^*}{A^*}$ has one pole which matches the model pole at $s=-3$, and to let the high frequency poles go as they may (assuming, as is the case, that they will remain well within the stable region and at a higher frequency than the poles of the model).

Substituting the values of eqn. (3-27) into eqn. (3-22) yield the equation of the nominal system for this example

$$\frac{g^*B^*}{A^*} = \frac{k_r^* 458}{s^3+31s^2+259s+229-459k_y^*} \tag{3-28}$$

The root locus on k_y^* for the poles of eqn. (3-28) is shown in Figure 3-7. At a value of $k_y^* = -0.65$, the dominant pole of the nominally controlled plant will match the model pole. Substituting the value $k_y^* = -0.65$ into eqn. (3-28), the poles of the nominally controlled plant are found to be located at

$$s=-3;\ s=-9.4;\ s=-18.6$$

Two poles have remained at relatively high frequencies so with the proper choice of k_r^*, the nominally controlled plant, matches the model closely over a broad range of low frequencies. A value of $k_r^* = 1.14$ will produce the desired unity d.c. gain, and the nominal controlled plant then becomes:

$$\frac{g^*B^*}{A^*} = \frac{525}{s^3+31s^2+259s+525} \tag{3-29}$$

Using this as the desired system, the characteristic equation of the error system becomes, according to eqn. (3-26)

$$s(s^4+31s^3259s^2+525s+458\gamma d^*)=0 \tag{3-30}$$

A value of $\gamma=1$ will be used in the sequel. The d^*-root locus of eqn. (3-30) is given in Figure 3-8.

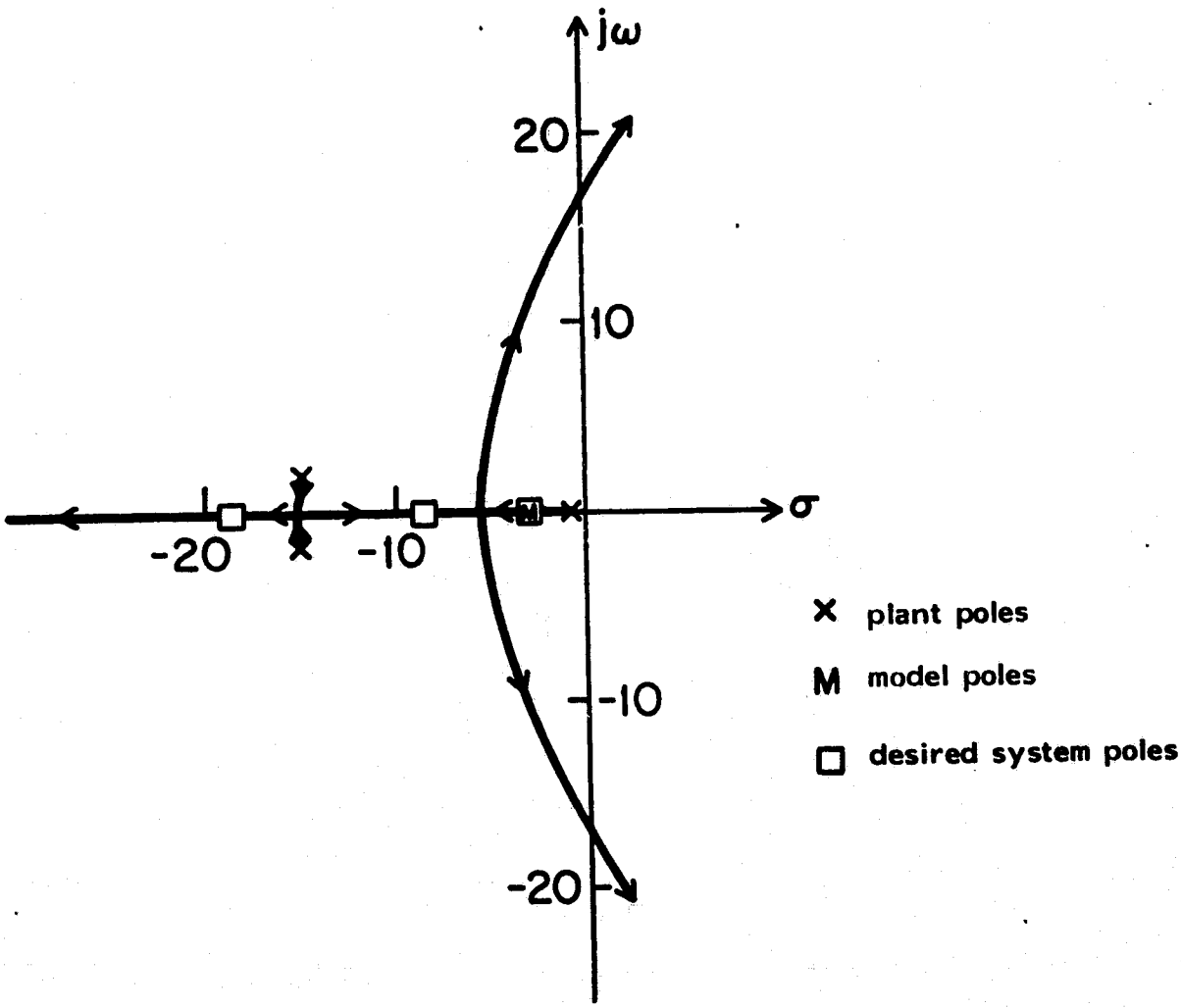

Figure 3-7. k_y^*-root locus of eqn. (3-28).

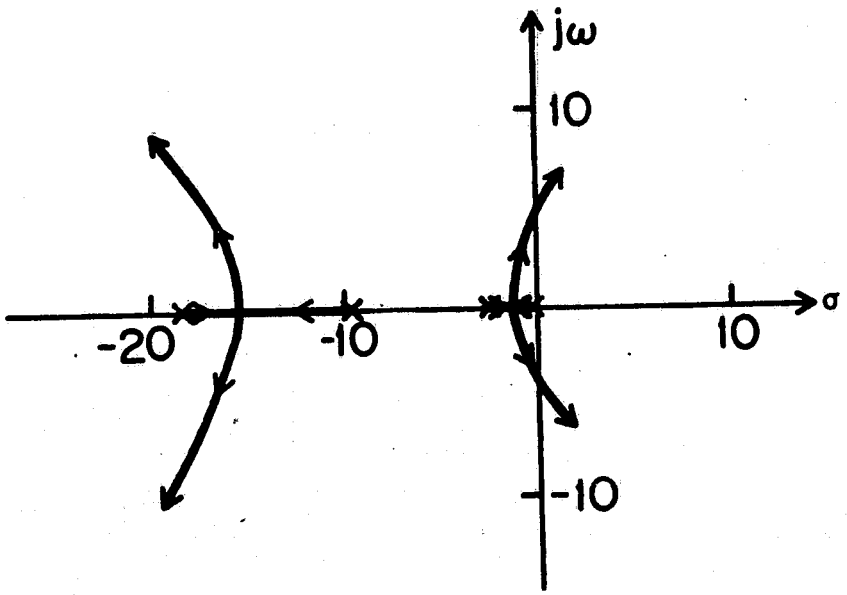

Figure 3-8. d^*-root locus of eqn. (3-30).

The linearization about this particular choice of k_y^*, k_r^* predicts instability when $d^* > 8.95$ which will occur when the reference input, r, is such that $r > 2.11$. Figure 3-9 shows the outputs and the parameters of a simulation run with r=2.5. The initial conditions of the simulation were k_y=-0.6, k_r=1.0, γ=1.0, and the plant and model states had zero initial conditions. The linearization with the desired system given by eqn. (3-29) predicts error system poles at $0.34 \pm j4.7$ and $-15.8 \pm j2.7$. The simulation results of Figure 3-9 indicate a stable system with an oscillation at the frequency of around ω=5 rad/sec. The results also indicate that the parameters have converged to the values $k_y^* = -1.57$ and $k_r^* = 2.08$. Thus the linearization around the initial set of parameters, $k_y^* = -0.65$ and $k_r^* = 1.14$, does not give an accurate prediction of the system behavior when the parameters have moved to the values $k_y^* = -1.57$ and $k_r^* = 2.08$.

Note that with the system converging to $k_y^* = -1.57$ and $k_r^* = 2.08$ the poles of the nominal control system as defined by eqn. (3-28) have moved to

$$s=-20.7;\ s=-5.15 \pm j4.4;\ s=-5.15-j4.4$$

so that the nominal control loop no longer matches the reference model but is of a higher bandwidth.

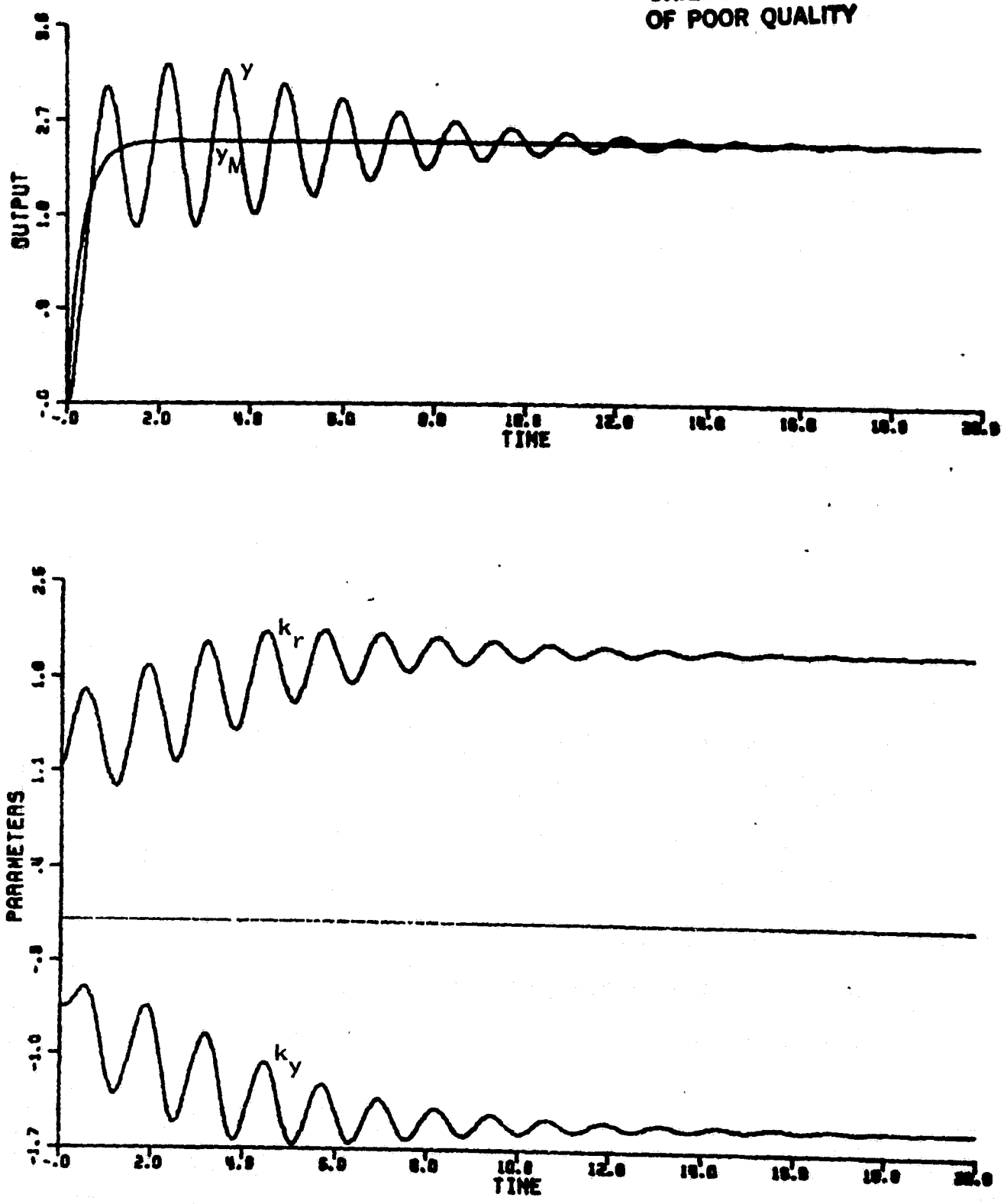

Figure 3-9. Simulation of CA1 with unmodeled dynamics and r=2.5.

Thus the analysis of this subsection show that although the control may remain stable for constant reference inputs that are larger than r=2.11, it cannot be expected to match the reference model for inputs of this size. If a reference input larger than r=2.11 is used, the linearization around the set of parameters which will produce good model matching is unstable, so the system must necessarily move away from this set of parameters.

3.3.5.2 Linearizing about the New Parameters

By linearizing the plant around the parameters

$$k_y^* = -1.57;\ k_r^* = 2.08 \tag{3-31}$$

to which the simulation of Section 3.3.5.1 eventually converged the asymptotic behavior of this simulation can be explained. With the parameters of eqn. (3-31), the nominal controlled plant of eqn. (3-28) is

$$\frac{g^*B^*}{A^*} = \frac{950}{s^3+31s^2+259s+950} \tag{3-32}$$

Substituting the proper values for the nominal controlled plant and $d^*=12.5$, corresponding to r=2.5, into eqn. (3-26) yields the characteristic equation for the error system linearized around the parameters of eqn. (3-31) with r=2.5

$$s(s^4+31s^3+259s^2+950s+5725)=0$$

This equation has a dominant pole pair at $s=-0.3\pm j5.2$ which corresponds well to the results of the simulation.

3.3.5.3 Using Linearization to Predict Instability

As was mentioned in Section 3.2, a linearization technique is, in its essence, a local technique. If a linearization about a specific set of parameters is unstable, then it shows only that the adaptive system will not converge to that set of parameters. If a reference input can be found so that the linearization around any set of parameters is unstable, then it follows that the adaptive system will not converge to any constant set of parameters. It is possible that the algorithm may maintain stability by moving among parameters sets. However, it is the experience of the author, attained through simulations, that this phenomenon does not occur. Thus, the derivation of the numerical value of a constant reference input, for which no set of parameters which produce a stable linearization, can be found, will be taken as a prediction of instability. Such a prediction must be verified by simulation.

For the example of this section (Section 3.3.5), a reference input (equivalently, a value of d^*), for which there is no set of parameters which produce a stable linearization, can be found analytically by applying the Routh-Hurwitz test for stability to the following equation

$$s^4+31s^3+259s^2+(229-458k_y^*)s + 458d^*=0 \qquad (3\text{-}33)$$

This equation (3-33) is derived from eqn. (3-26) for this example. Its roots are the poles of the error system linearized around k_y^*.

The Routh-Hurwitz test leads to three stability conditions, all of which must be satisfied.

$$229-458k_y^* > 0$$

$$(259)(31)-(229-458k_y^*) > 0 \qquad (3\text{-}34)$$

$$\frac{-(229-458k_y^*)^2}{31} + 259(229-458k_y^*) \geq (31)\ 458d^* \qquad (3\text{-}35)$$

From eqns. (3-33) and (3-34), one finds

$$-17.03 < k_y^* < 0.5 \qquad (3\text{-}36)$$

The left hand side of ineq. (3-35) is maximized for $k_y^* = -8.26$ which in turn implies

$$d^* < 36.62 \qquad (3\text{-}37)$$

Equations (3-36) and (3-37) must be satisfied simultaneously in order for the error system to have a stable linearization.

When $k_y^* > 0.5$ the nominal system is unstable and the d^*-root locus of the error system cannot return the poles to the left-hand plane.

Figure 3-10b shows that when k_y^* is negative and small in magnitude, the d^*-root locus moves the poles arising from the modeled portion of the plant and the adaptation mechanism into the right-half plane. When k_y^* gets too large and negative, either the d^*-root locus moves the "unmodeled" poles over the $j\omega$-axis as shown in Figure 3-10c, or, k_y^* is large enough to have already created unstable poles out of the "unmodeled" poles.

The marginally stable condition of $d^*=36.62$ corresponds to a constant reference input $r=4.28$. The marginally stable oscillation will occur at $\omega=11.4$ rad/sec.

The nominal system for this most stable configuration is obtained from eqn. (3-28)

$$\frac{q^*B^*}{A^*} = \frac{3996}{(s+27)(s+2+j12)(s+2-j12)} \qquad (3\text{-}38)$$

Thus, the nominal system has moved to a high bandwidth system in order to maintain stability in the error system.

Figure 3-11 shows the output and parameters of a simulation with the same initial conditions as the simulation of Section 3.3.5.1 but with $r=4.1$, which should lead to a stable system. Note the characteristic frequency of about 11 rad/sec in the plant output and the convergence of the parameters to $k_y=-8$ and $k_r=8$. This is as predicted as k_y^* is within the small range of values satisfying eqn. (3-35) for the value of d^* used.

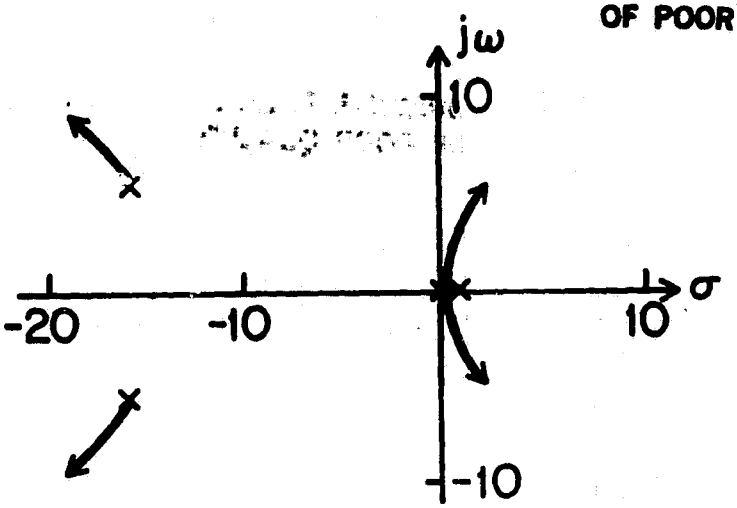

Figure 3-10a. $k_y^* > 0.5$.

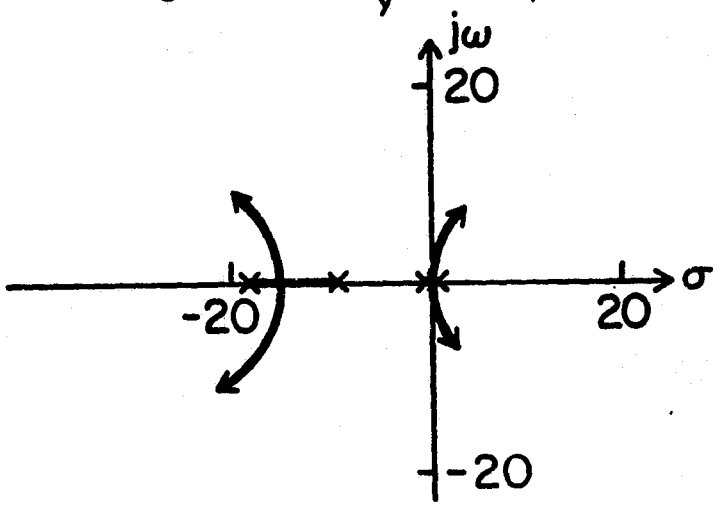

Figure 3-10b. k_y^* small and negative.

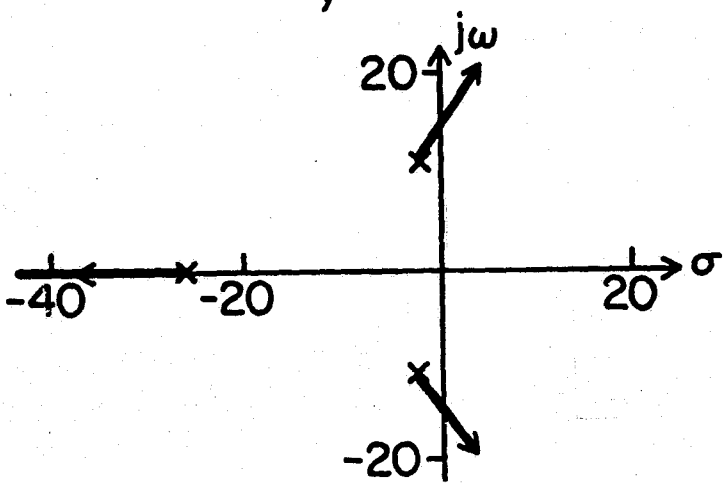

Figure 3-10c. k_y^* large and negative.

Figure 3-10. d^*-root loci of eqn. (3-33) for different k_y^* conditions.

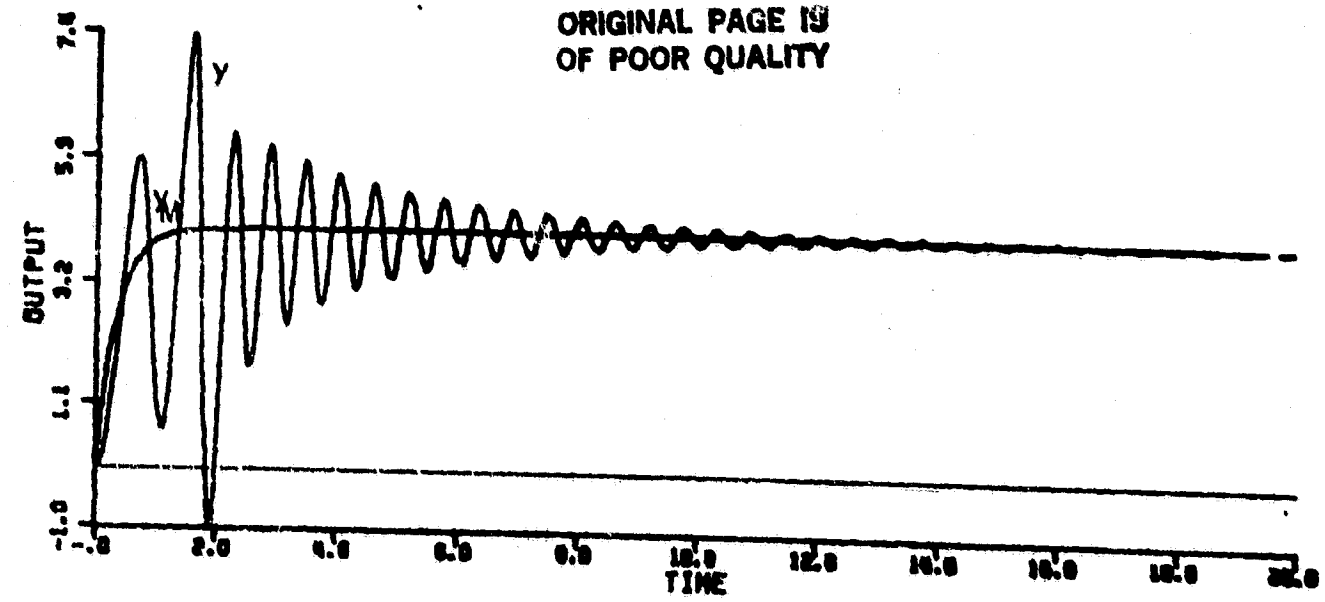

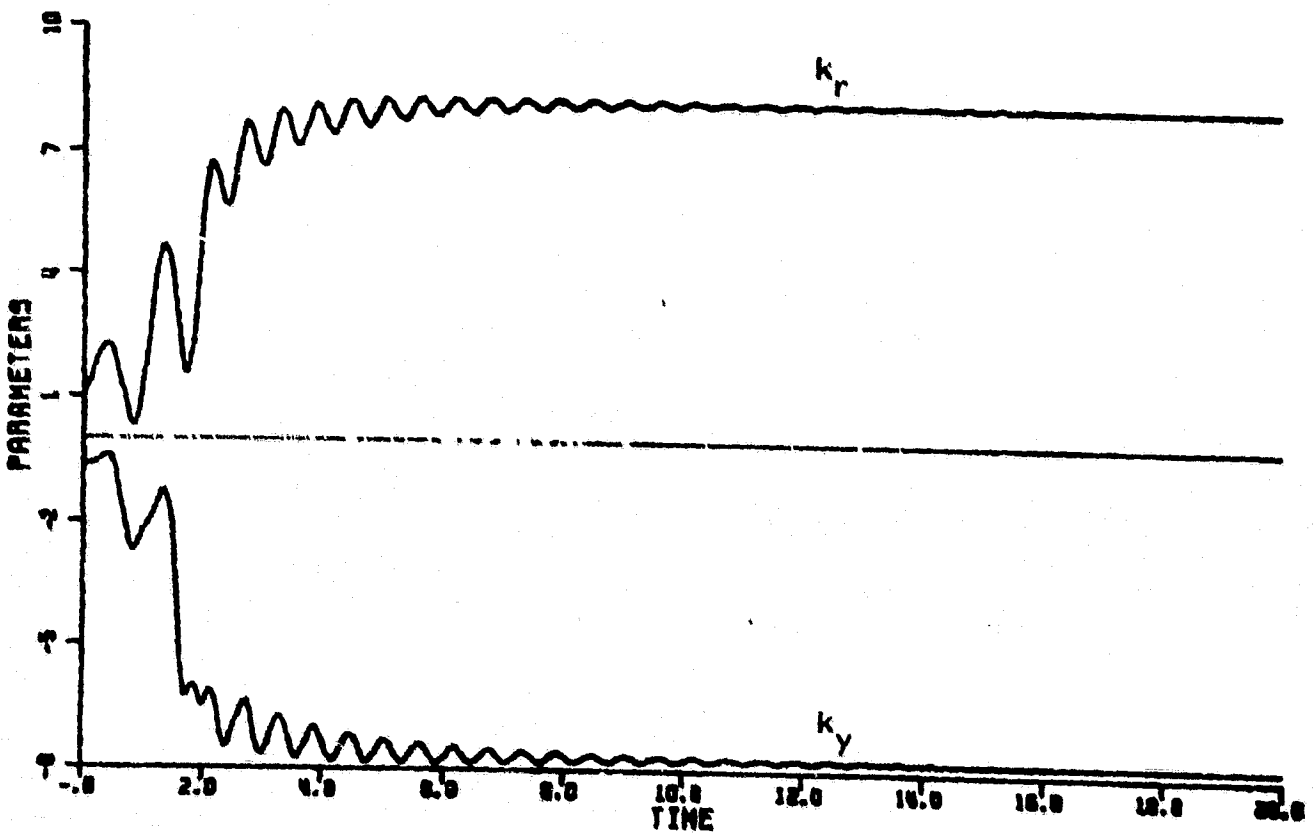

Figure 3-11. Simulation of CA1 with unmodeled dynamics and r=4.1.

Figure 3-12 shows the output of a simulation with a constant reference input r=4.3 for which the Routh-Hurwitz test predicts that there is no nominal system for which the error system is stable. The oscillations in the output decrease in the earlier stage, as the parameters move to a more stable configuration but, since all configurations are unstable, the error system eventually becomes unstable. Only the onset of instability is shown in Figure 3-12 but a continuation of the simulation shows that all signals "blow up" quite rapidly.

3.3.5.4 Summary of Results

Through the use of an example, for CA1, we have demonstrated that the linearization technique of Section 3.3.4 is a powerful tool in the study of adaptive control algorithms with constant inputs and no disturbances. The following use of the linearization technique has been demonstrated in this example:

- The linearization technique can be used to establish if an adaptive system can possibly converge to a particular set of parameters as was done in Section 3.3.5.1.
- The linearization technique can be used to predict the asymptotic behavior of the plant output and parameters as the parameters approach constant limits as was done in Section 3.3.5.2.

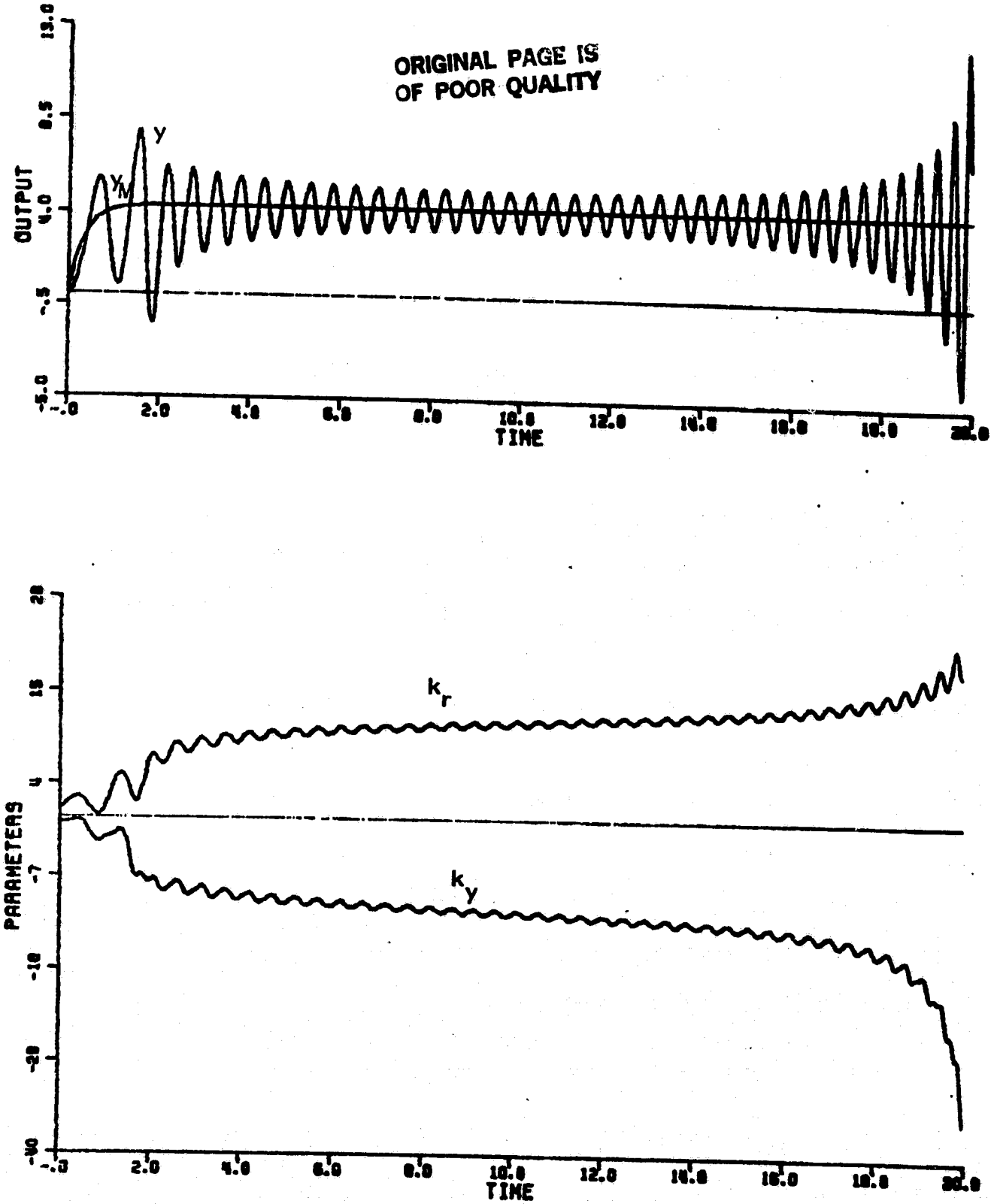

Figure 3-12. Simulation of CA1 with unmodeled dynamics and r=4.3.
(System eventually becomes unstable.)

- The linearization technique can be used to predict possible system instabilities for certain constant reference inputs as was done in Section 3.3.5.3.

Instability is predicted by finding reference inputs such that there is no set of parameters which produce a stable linearization. Such a reference input may or may not exist depending upon the actual dynamics of the plant, the design of the controller and the reference model. If such a reference input does exist, it may be found by the following method:

1. Find the characteristic polynomial of the error system in terms of the adaptive system parameters and the reference input as was done in eqn. (3-33) in Section 3.3.5.3 (where the equations is in term of $d^*=2r^2$).
2. Find conditions on the parameters and reference input that are necessary so that the characteristic equation of the error system has only left-half plane zeroes, using the Routh-Hurwitz test.
3. Find the values of reference input for which the conditions found in Step 2 cannot be satisfied.

This method may require a great deal of computational effort for higher order systems, but will always produce all the values of reference input for which no set of parameters which produce stable

linearizations exist. Other methods, such as that used in Section 5.1.2.2.1, may be used to demonstrate that a particular value of reference input will not be able to produce a stable linearization.

In addition to the demonstration of the use of the linearization technique, the example of this section demonstrated certain problems with the algorithm CA1. These are summarized as follows:

- In the presence of high frequency unmodeled dynamics, the algorithm CA1 may become unstable when a constant reference input, which is too large, is used.
- In the presence of high frequency unmodeled dynamics, there may be a class of reference inputs which are not large enough to cause instability but which <u>are</u> large enough so that the algorithm CA1 will be unable to match the reference model, (thus defeating the entire philosophy of model reference adaptive control).

3.3.6 Analysis of Higher Order Systems Using CA1

The linearization technique which was used on nominally first order systems is now extended to high order systems. The adaptive controller is designed assuming that the plant has n poles and m=n-1 zeroes, so that the relative degree of the system is assumed to be $n^*=1$, allowing the use of CA1. The system is then analyzed using the actual plant, $\frac{q_p B}{A}$, which contains unmodeled dynamics as well as the nominal system.

The error system is shown in Figure 2-3 and the relevant equations appear in Table 2-1.

As in the first-order case of Sections 3.3.2 and 3.3.4 the analysis consists of first linearizing the adaptive system around some nominal set of parameters and signals.

Assume that

$$y(t) = y^*(t) + \delta y(t) \tag{3-39}$$

where

$$y^*(t) = \frac{g^* B^*}{A^*} [r(t)] \tag{3-40}$$

so that $$y^*(t) = y_M(t) \tag{3-41}$$

Then $$\underline{w}_y(t) = \underline{w}_y^*(t) + \delta \underline{w}_y(t) \tag{3-42}$$

where $$w_{yi}^*(t) = \frac{s^{i-1}}{p^{(n-1)}} [y^*(t)] \tag{3-43}$$

Also assume that

$$u(t) = u^*(t) + \delta u(t) \tag{3-44}$$

where $u^*(t)$ is such that

$$y^*(t) = \frac{g_p B}{A} [u^*(t)] \tag{3-45}$$

Then

$$\underline{w}_u^*(t) = \underline{w}_u^*(t) + \delta \underline{w}_u(t) \tag{3-46}$$

Linearizing the error system of Figure 2-2 around $\underline{w}^*(t)$, $\underline{k}^*(t)$ simply replaces $\underline{w}(t)$ with $\underline{w}^*(t)$. Further assuming that the reference input, r, is constant, so that y^* is constant and $\underline{w}^*$ is constant allows the error system to be manipulated into the form of Figure 3-13. Remembering that the magnitude of the scalar

$$\gamma d^* = \underline{w}^{T^*} \underline{\Gamma} \underline{w}^* \geq 0 \qquad (3\text{-}47)$$

is controlled by the magnitude of r and, therefore, that γd^* can assume any value, one is led to the following theorem.

Theorem 3.1: The algorithm of CA1 is globally asymptotically stable only if there exists a $\underline{k}^*$ such that $\frac{g^*B^*}{A^*}$ is positive real.

Proof: For the nonlinear error system to be globally asymptotically stable, the linearized error system of Figure 3-13 must be asymptotically stable for all values of $d^* = \underline{w}^{*T} \underline{\Gamma} \underline{w}^*$. Note first that if A^* has unstable poles, there exists a d^* small enough so that the system of Figure 3-12 is unstable. If A^* is stable, the Nyquist Criterion shows that, in order for the system to be stable for all d^*, the Nyquist plot of $\frac{g^*B^*}{k_r^* A^* s}$ must never cross the negative real axis; for this to be true, the Nyquist plot of $\frac{g^*B^*}{A^*}$ must never cross into the left-half plane so that $\frac{g^*B^*}{A^*}$ must necessarily be positive real.

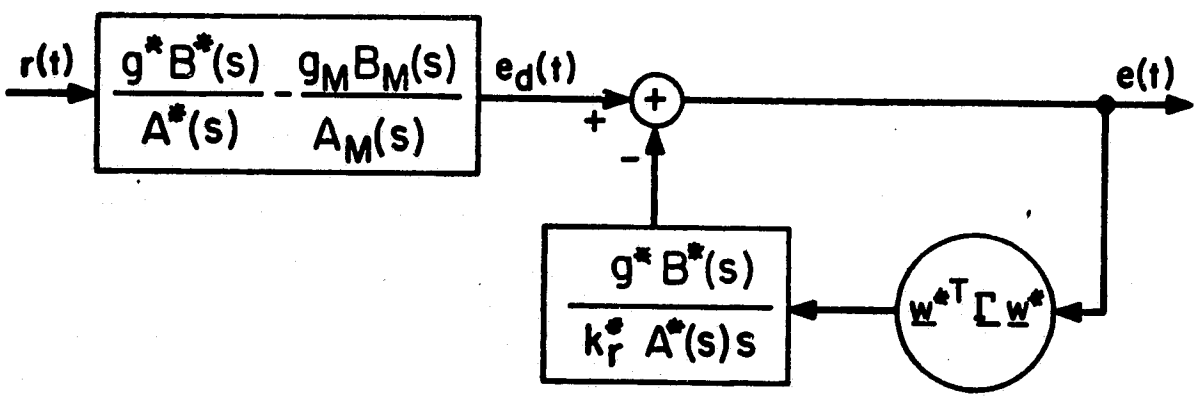

Figure 3-13. Linearized error system of CA1 with $\underline{w}^*$ constant.

Remark 1: There are many proofs, e.g. [3-6], of the sufficiency of a positive real condition for global asymptotic stability of adaptive control algorithms. This is the first proof of the necessity of this condition.

Remark 2: From eqn. (2-22) it is seen that the relative degree of $\frac{g^*B^*}{A^*}$ is equal to the relative degree of the plant. Thus the plant must have relative degree equal to 0,1, or -1 in order to have global asymptotic stability. This will not occur for physically realizable plants since physically realizable plants must be of at least relative degree two to satisfy the Horowitz criteria [64].

Besides showing that there are some inputs for which global asymptotic stability is lost, the analysis leading to Figure 3-13 also can be used for a local analysis of the behavior of the adaptive system with constant inputs as did the specific analysis, performed earlier in this section, for a first order plant. In fact, Figure 3-13 provides the basis for the generalization of the d^*-root locus analysis considered earlier. This analysis will include the CA1 adaptive system where the design is carried out as if the plant has relative degree equal to one, while, in actuality, the real plant consists of a relative degree one system in series with a set of stable unmodeled dynamics.

It can be seen from Figure 3-13, eqn. (3-47) and the definition of $\underline{w}$ from Table 2-1 that the gain of the error system loop of CA1 is roughly proportional to the square of the magnitude of the reference input. It is when the gain of the error loop becomes large that the bandwidth of the error system becomes large, and the unmodeled dynamics of the nominally controlled system can become excited, causing instability. The gain of the error system loop could be set independently of the size of the reference input, if the adaptation gain matrix of eqn. (3-47) were made to contain a normalizing factor, such as

$$\underline{\Gamma}(t) = \frac{\gamma}{\underline{w}^T(t)\underline{w}(t)}\,\underline{I}; \quad \gamma>0$$

Such a normalizing factor would allow the prudent system designer, with some knowledge about the unmodeled dynamics present in the plant, to design a linearized error loop gain which would maintain stability for all constant reference inputs, if there were no disturbances.*

Unfortunately, the stability proof of CA1 does not allow for such time-varying adaptation gain matrices. Algorithms CA3 and CA4 do include such a normalizing factor and have much improved stability properties for constant reference inputs and no disturbances, as will be seen in in Section 3.5 and Section 3.6.

---

*The case where more general reference inputs and disturbances are allowed does not allow for such a simple modification to improve stability properties, as will be seen in Chapter 4.

3.3.7 Numerical Example with Nonminimum Phase High Frequency Unmodeled Dynamics

The following example illustrates the use of this analysis when the unmodeled dynamics are non-minimum phase. This is of interest since such unmodeled dynamics may represent time delays. It is also of interest since now Assumption A2 of Section 2.2.1, as well as Assumption A3, is violated by the unmodeled dynamics.

Consider the same first order system considered in Section 3.3.3, given by eqn. (3-19) but let the plant include unmodeled dynamics represented as:

$$P_u = \frac{-(s-10)}{(s+10)} \tag{3-48}$$

The system (3-48) happens to be a first order Pade approximation of a 0.2 second time delay, but it will be considered here for its own sake as a non-minimum phase system. (Time delays can be handled directly from Figure 3-13 by use of Nyquist concepts or direct transfer function calculations).

The actual plant is then described by

$$\frac{g_p B}{A} = \frac{-2(s-10)}{(s+1)(s+10)} \tag{3-49}$$

while the model is given by:

$$\frac{g_M B_M}{A_m} = \frac{3}{(s+3)} \tag{3-50}$$

With the degrees of freedom that we have, the relative degree $n^*=1$ assumption allows us to define the nominal controlled plant.

$$\frac{g^* B^*}{A^*} = \frac{-2k_r^*(s-10)}{s^2+11s+10+2k_y^*(s-10)} \tag{3-51}$$

The k_y^*-root locus for the desired system appear in Figure 3-14. The d^*-root locus is shown in Figure 3-15 starting with the "desired" poles represented by boxes on Figure 3-14.

As was the case in the example of Section 3.3.5, the nominal system which is "desired" to closely match the model may lead to an unstable error system whereas another nominal system may have stable error dynamics. In order to predict instability, one must find a value of d^* for which no nominal system is stable. The poles of the linearized error system shown in Figure 3-13 are derived from that figure using eqn. (3-51):

$$s^3 + (11+2k_y^*)s^2 + (10-20k_y^*-2d^*)s + 20d^*=0 \tag{3-52}$$

Performing the Routh-Hurwitz test on eqn. (3-52) shows that all linearizations will be unstable independent of k_y^* and k_r^* if

$$d^* > 11.7 \tag{3-53}$$

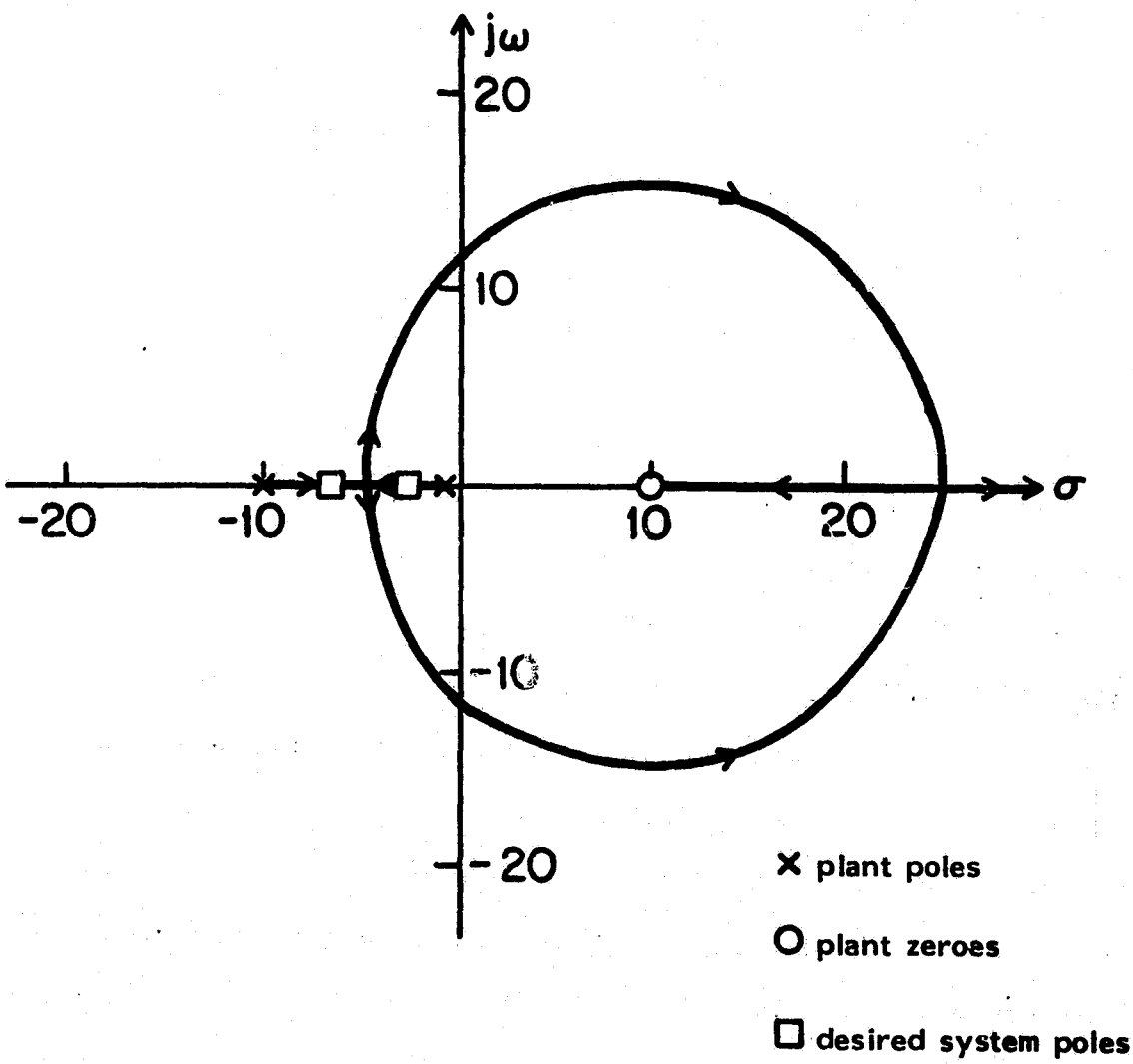

Figure 3-14. k_y^*-root locus of eqn. (3-51).

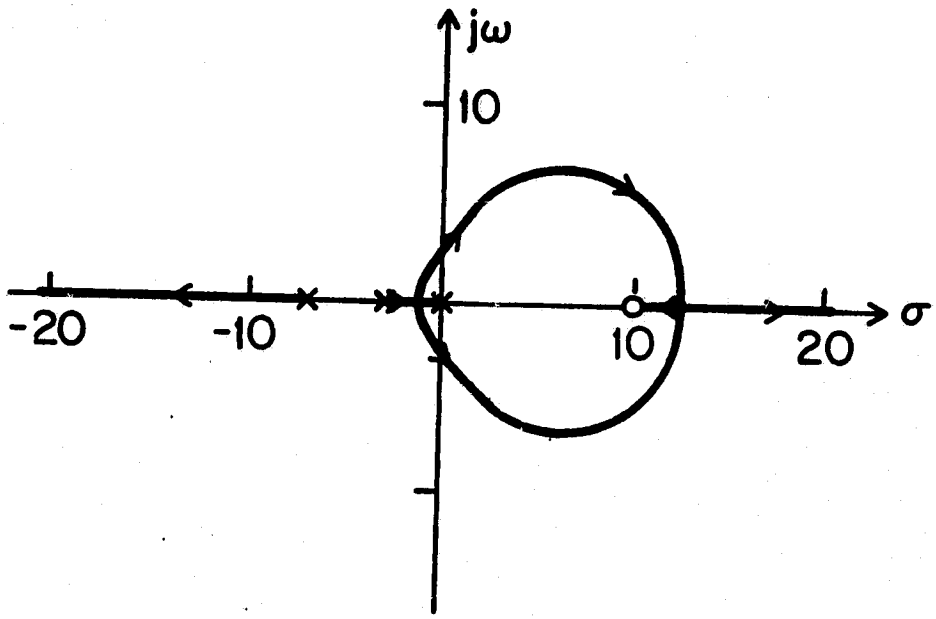

Figure 3-15. d^*-root locus for numerical example of Section 3.3.7.

The value of d^* given in eqn. (3-53) can be translated into the value of reference input r for which there will be no values of k_y^* and k_r^* which can produce a stable linearization. The eqn. (3-47) and the condition $\gamma=1$, shows that the value of r corresponding to eqn. (3-53) is

$$r > 2.4$$

If the value, $d^*=11.7$ is used, eqn. (3-52) shows that a stable linearization is produced only if

$$k_y^* = -3.1$$

Figure 3-16 shows the results of a simulation run with r=1.0. The parameters converge to $k_y^* = -.3$, $k_r^* = .8$ and the error system shows a characteristics frequency of $\omega=2.1$ rad/sec. as predicted by eqn. (3-50) with the above value for k_y^* and $d^*=2$.

Figure 3-17 shows the results of a simulation with r=2.0. This value of r is getting close to one for which there is no stable linearization. Note how after the initial non-minimum phase behavior the parameters rapidly settle to levels which will maintain stability. The parameter k_y^* cannot converge to the value $k_y^* = -0.54$ which would make the controlled plant match the model because for this large a reference input the linearization around $k_y^* = -0.54$ is unstable. Naturally the oscillation frequency of the error system is much higher in this case as the linearization predicts.

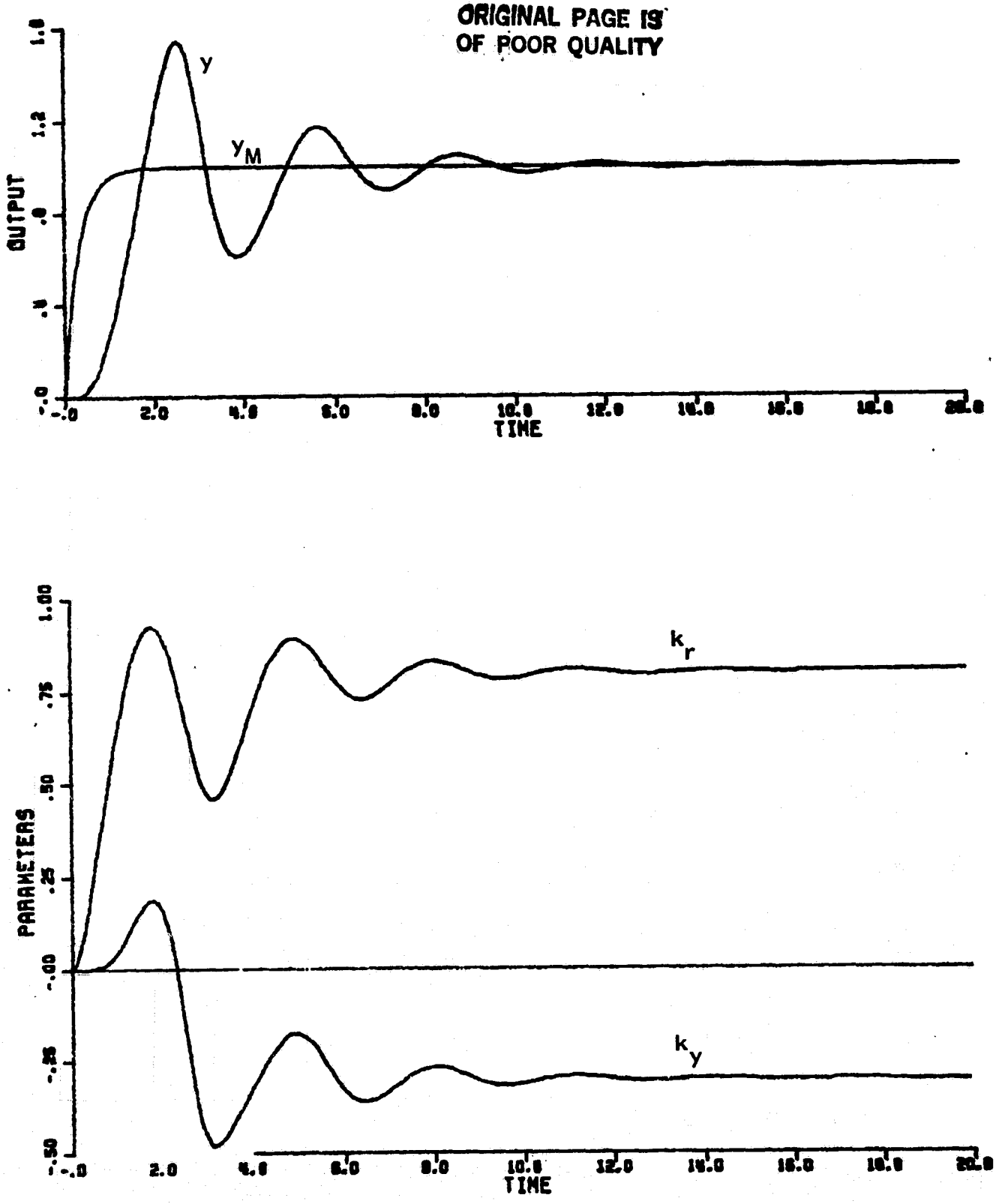

Figure 3-16. Simulation of CA1 with non-minimum phase unmodeled dynamics and r=1.0.

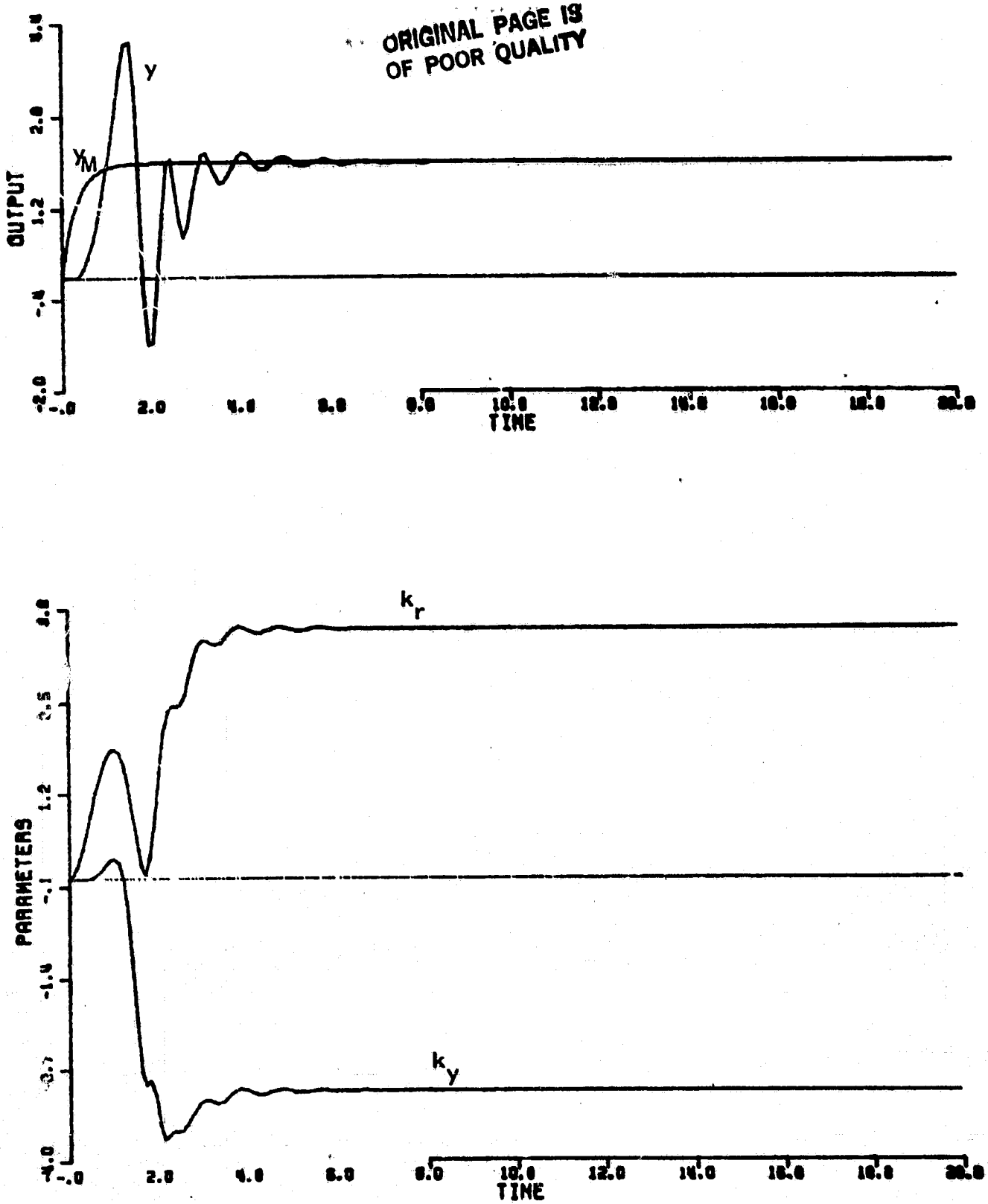

Figure 3-17. Simulation of CA1 with non-minimum phase unmodeled dynamics and r=2.0.

In attempting to simulate the system close to the stability limit of r=2.4, it was found that the system went unstable during the large overshoot in the transient phase not covered by the linearization. When the initial parameters were picked to be closer to what must be their final values if the system is to converge, the linearization technique predicted the behavior well. Figure 3-18 shows the results of a simulation with r=2.3 and the initial values of the parameters, $k_y = -2.0$ and $k_r = 2.5$. The simulation shows that there is indeed a stable linearization possible with r=2.3.

This experience with the simulation converging for some initial values of parameters but not for other values of the parameters reminds us that the analysis used here is a local analysis. By the existence of an unstable linearization we may conclude that the system cannot converge to the parameter and signal values around which the linearization was made; however, by the existence of a stable linearization we may not conclude that the system will indeed converge to the parameter and signal values around which the linearization was made, because the system may never enter the subset of parameter and signal space around which the linearization is valid. Thus the linearization analysis of this chapter may be used to determine possible situations of poor behavior but it cannot ensure good behavior for the non-linear adaptive system.

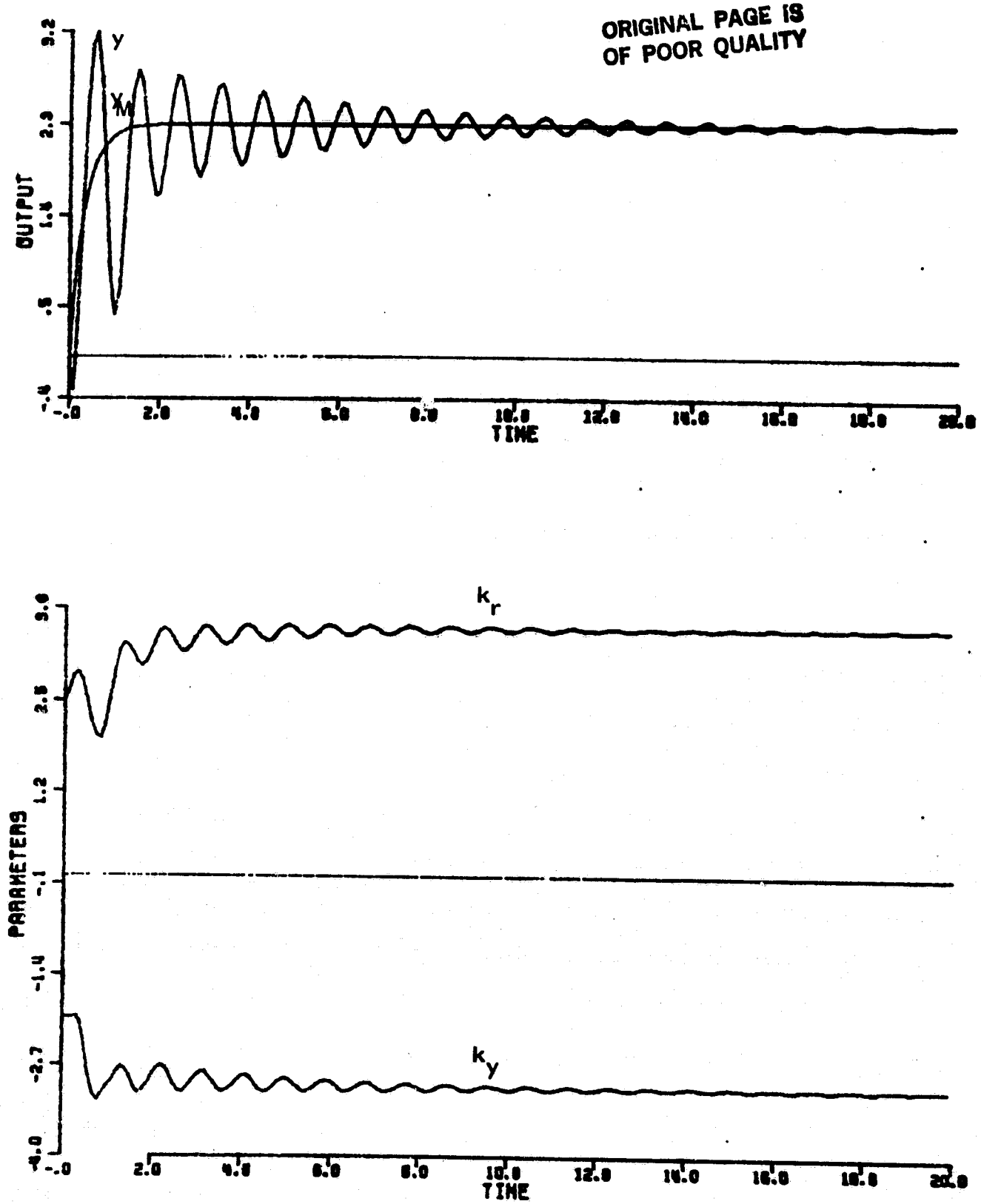

Figure 3-18. Simulation of CA1 with non-minimum phase unmodeled dynamics, $r=2.3, k_y(0)=-2.0$, and $k_r(0)=2.5$.

From the example of this subsection, we have seen that the linearization-based analysis can be extended to include cases where the unmodeled dynamics of the plant include non-minimum phase characteristics and the results in this case are very similar to the results when the unmodeled dynamics are minimum phase.

3.3.8 Summary of Section 3.3 on CA1

In Section 3.3, we have shown that the linearization technique introduced in Section 3.2 is a valuable tool in the study of algorithm CA1 when the reference input is constant and there are no disturbances. The linearization analysis, verified by simulation leads us to the following conclusion about CA1:

- Even when the plant model upon which the adaptive design is based is a perfect description of the plant dynamics, large constant reference inputs may cause high frequency control activity.
- When there are unmodeled dynamics present in the plant, large constant reference inputs may cause the algorithm CA1 to be unable to perform its main task of following a change in reference input in the same manner that a reference model does. As the reference input further increases, instability may result.

- The two properties mentioned above are caused by the fact that the error loop gain and thus the bandwidth of the error loop increases with increasing reference input. It is not allowable within the constraints of the CAl algorithm to counteract the increasing error loop gain by including a normalizing factor in the adaptation gain matrix.

3.4 Analysis of CA2

3.4.1 Introduction

In this section, the linearization analysis which was introduced in Section 3.2 and applied to algorithm CA1 in Section 3.3, will be used to investigate algorithm CA2. The major difference in the stability analysis between algorithms CA1 and CA2 is due to the added feedback loop in CA2 as shown in Figure 2-7. This inner loop feeds the auxiliary error signal, $\epsilon(t)$, back through a gain,

$$\rho \underline{v}^T(t) \Gamma \underline{v}(t),$$

where ρ is a positive constant chosen by the designer, and then back to $\epsilon(t)$ through the positive real system,

$$\frac{g_M B_M L}{A_M M}$$

The additional loop was included in CA2 in order that the first derivative of the adjustable parameter be square integrable, satisfying a technical condition in the stability proof [5]. From the analysis of this section, we will be able to make the following conclusions about CA2:

- The inner error loop provides the designer with a parameter, ρ, with which he can tradeoff improved stability properties in the presence of unmodeled dynamics against the speed of adaptation.

- The algorithm CA2 can, for a specific set of unmodeled dynamics, be made to have a stable linearized error system for all values of constant reference inputs.
- By selecting the value of ρ conservatively, the algorithm CA2 can be made to have stable linearized error systems for all constant reference inputs in the presence of a wide range of unmodeled dynamics. However, a conservative choice of ρ will cause the adaptive system to adapt very slowly.

It is important to remember that the existence of stable linearized error systems for all constant reference inputs does not guarantee that the non-linear error system will be stable for constant references inputs. Instabilities may still result if the initial values of the parameters and signals in the system are too far from the values about which the linearization is performed.

3.4.2 Unity Relative Degree Analysis

We consider the special case of CA2 where the adaptive controller is designed assuming that the relative degree of the plant is unity, i.e., $n^*=1$. It can be seen from Figure 2-7 and the equations of Table 2-3 that in this case CA2 differs from CA1 only in the additions of an inner feedback loop in the error system.

3.4.2.1 The Linearized Error System

Using the same technique of linearization with constant input as in Section 3.3, the error system is reduced to that of Figure 3-19a. In Figure 3-19b, the system is redrawn, incorporating the usual definition

$$\gamma d^* = \underline{w}^{*T} \underline{\Gamma} \underline{w}^* \tag{3-54}$$

and showing that, for constant inputs, the effect of the additional feedback loop is to replace $\frac{g^*B^*}{k_r^*A^*s}$ from CA1, with

$$S_E = \frac{g^*B^*}{k_r^*A^*s} + \frac{\rho g_M B_M}{A_M} = \frac{g^*B^*A_M + \rho g_M k_r^* B_M A^* s}{k_r^* A^* A_M s} \tag{3-55}$$

in the linearized error feedback loop.

3.4.2.2 Discussion of the Inner Loop

There are two important properties of the inner loop of Figure 3-19a, which give rise to the second term in eqn. (3-55).

1) There is no integrator in the inner loop.

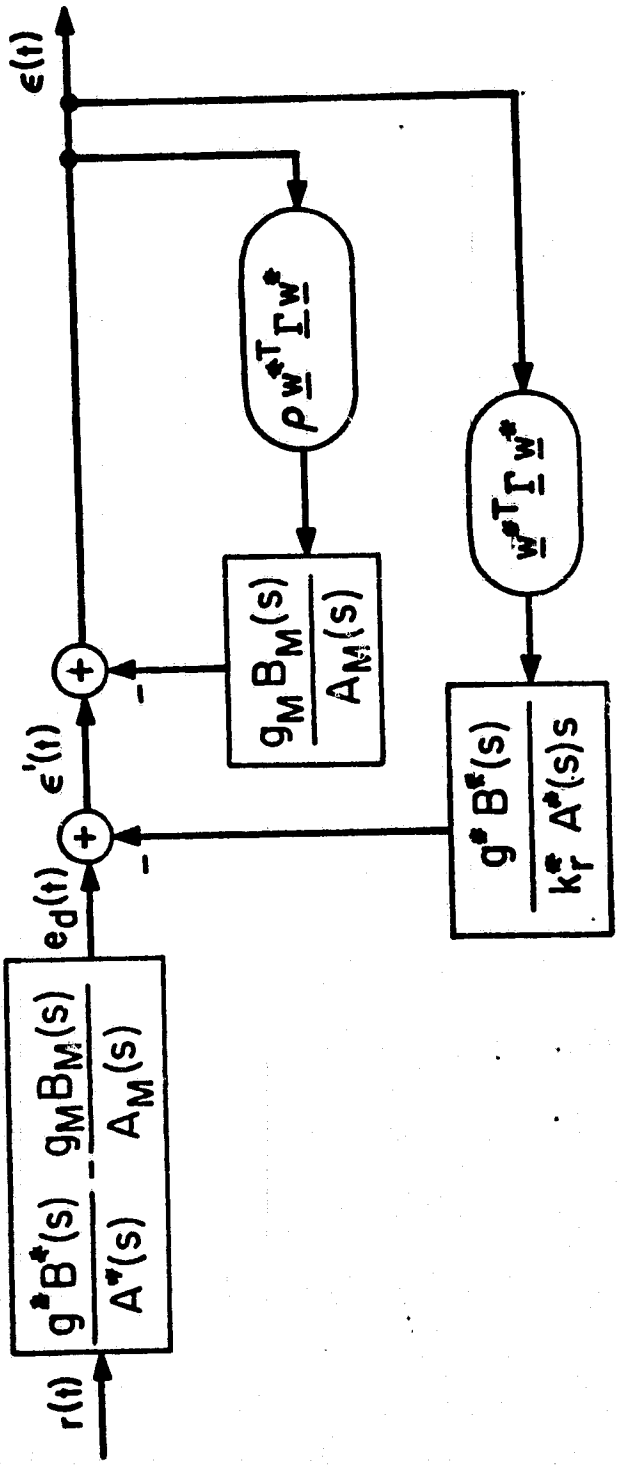

Figure 3-19a

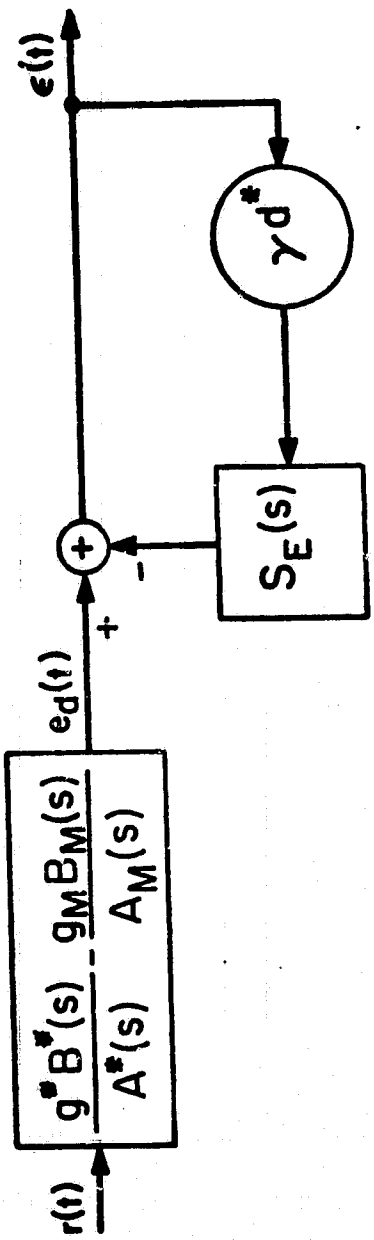

Figure 3-19b

Figure 3-19. Linearized error systems for CA2 with constant input and $n^*=1$.

Even in the case where there are no unmodeled dynamics, the outer loop of Figure 3-18a which CA2 has in common with CA1 must have a loop transfer function with a pole excess of at least two- one from the nominal controlled plant and one from the integrator. The proportional feedback term of the inner loop will give rise to a zero in the error system which was not present in the solely integral loop of CA1.

2. The inner loop does not feedback through the nominal controlled plant which contains unmodeled dynamics but it feeds back through the model.

Since the model is chosen to have relative degree of unity, the system, S_E of eqn. (3-55) and Figure 3-19b will have relative degree of unity. Therefore, the system will not become unstable due to a large gain.

Indeed, the model is chosen to be positive real. For any given nominal control system, $\frac{g^*B^*}{k_r^*A^*}$, ρ can be chosen large enough so that the second term of eqn. (3-55) will dominate the first term to the point that the system of Figure 3-19b will be stable for any constant d^*. In practice, this means that, by choosing ρ large enough, the linearized error system can be made stable for a large class of unmodeled dynamics and a large class of <u>constant</u> reference inputs.

C-3

It is important to notice, however, that the increased ability to maintain stability in the presence of unmodeled dynamics attained by increasing ρ is not attained without a tradeoff. As ρ increases, the size of the error becomes smaller for any nominal control system due to the larger inner loop gain. From Figure 3-19a we can derive that

$$e(t) = \frac{1}{1+\rho \frac{d^* g_M B_M}{A_M}} \left[e'(t) \right] .$$

The signal $e'(t)$ reflects how well the plant is matching the model. The above equation shows that as ρ increases the signal $e(t)$ which drives the adaptation mechanism becomes small even if the actual error represented by $e'(t)$ is large. Thus, large values of ρ will cause slow adaptation.

3.4.3 A First Order System with No Unmodeled Dynamics

3.4.3.1 Analysis

Examine first the case where the plant is really first order so that Assumption A3 is satisfied and the model is

$$\frac{g_M B_M}{A_M} = \frac{g_M}{s+a_M} \qquad (3\text{-}56)$$

Then $\frac{g^*B^*}{A^*}$ can be made equal to the [illegible]. Linearizing about this nominal system yields.

$$S_E = \left(\frac{1}{k_r^* s} + \rho\right)\frac{g_M B_M}{A_M} \qquad (3\text{-}57)$$

The characteristic equation of the error system is:

$$s^2 + a_M s + \gamma d^*\left(g_M \rho s + \frac{g_M}{k_r^*}\right) \qquad (3\text{-}58)$$

The d^*-root locus now contains a zero, whose location can be controlled by ρ, using some a priori knowledge of g_p. The zero is located at

$$s = \frac{-1}{k_r^* \rho} = \frac{-g_p}{g_M \rho} \qquad (3\text{-}59)$$

A typical d^*-root locus of eqn. (3-58) is shown in Figure 3-20. Note that as ρ is increased, the zero controlled by ρ moves toward the origin and the problem of high frequency oscillations in the error system and the plant input is alleviated. However, as ρ is increased, it begins to limit the speed of response of the error system, because, as the zero moves close to the origin, a pole of the error system will then be trapped near the origin producing an extremely sluggish adaptation mechanism. It is important to stress that the zero controlled by ρ is not a transmission zero of the error

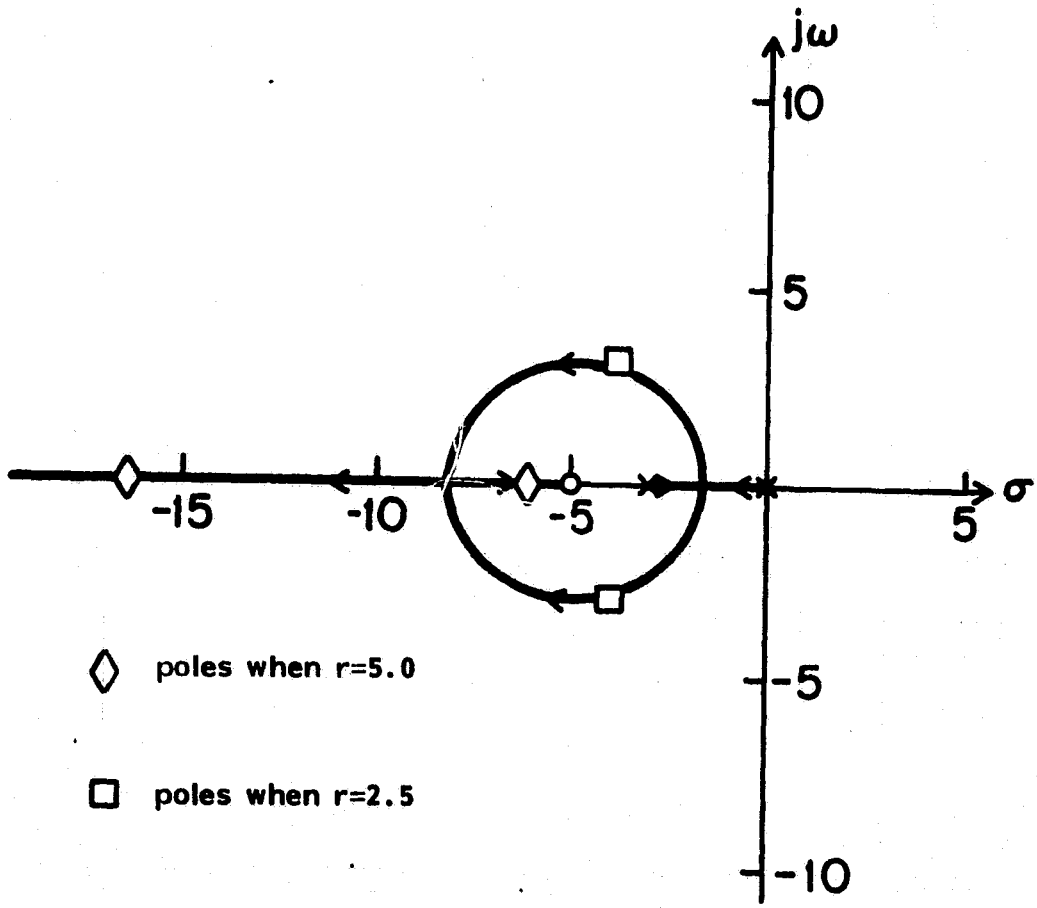

Figure 3-20. d^*-root locus for numerical example of Section 3.4.2.2.

system which can cancel an errcr system pole. Rather, it is a zero only in the context of determining the d*-root locus of eqn. (3-58).

3.4.2.2. Numerical Example with No Unmodeled Dynamics

The example of Section 3.3.3 was simulated using the algorithm CA2 with ρ=.13. For this example, this value of ρ places the d*-root locus zero at about s=-5, so that the locus is as in Figure 3-20. The result where r=2.5 is shown in Figure 3-21.

Compared with Figures 3-2 and 3-3 the system oscilates more slowly and is better damped as expected from the analysis. Figure 3-22 shows that when the input is turned up to r=5.0, the system behaves better rather than worse, particularly in contrast to what it did in Figure 3-4 as explained from the position of the poles in the error system in the d*-root locus of Figure 3-20.

3.4.4 A First Order System with Unmodeled Dynamics

3.4.4.1 Analysis

When there are unmodeled dynamics in the plant, the poles of the linearized error system are determined by the characteristic equation upon which a d*-root locus can be performed

$$A^*A_M s + \gamma d^* \rho g_M \left(B_M A^* s + \frac{g_p}{\rho g_M} B^* A_M \right) = 0 \qquad (3\text{-}60)$$

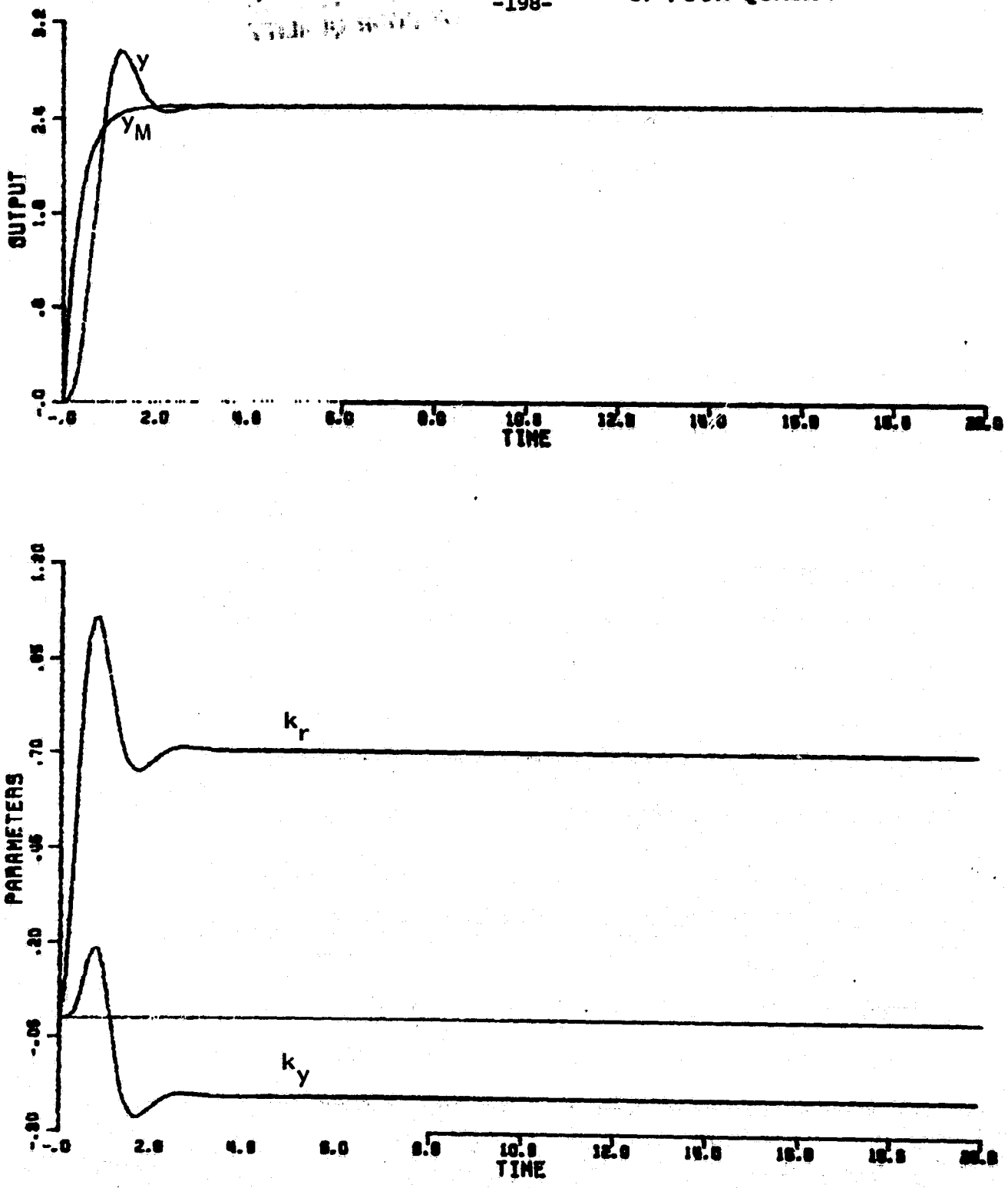

Figure 3-21. Simulation of CA2 with r=2.5.

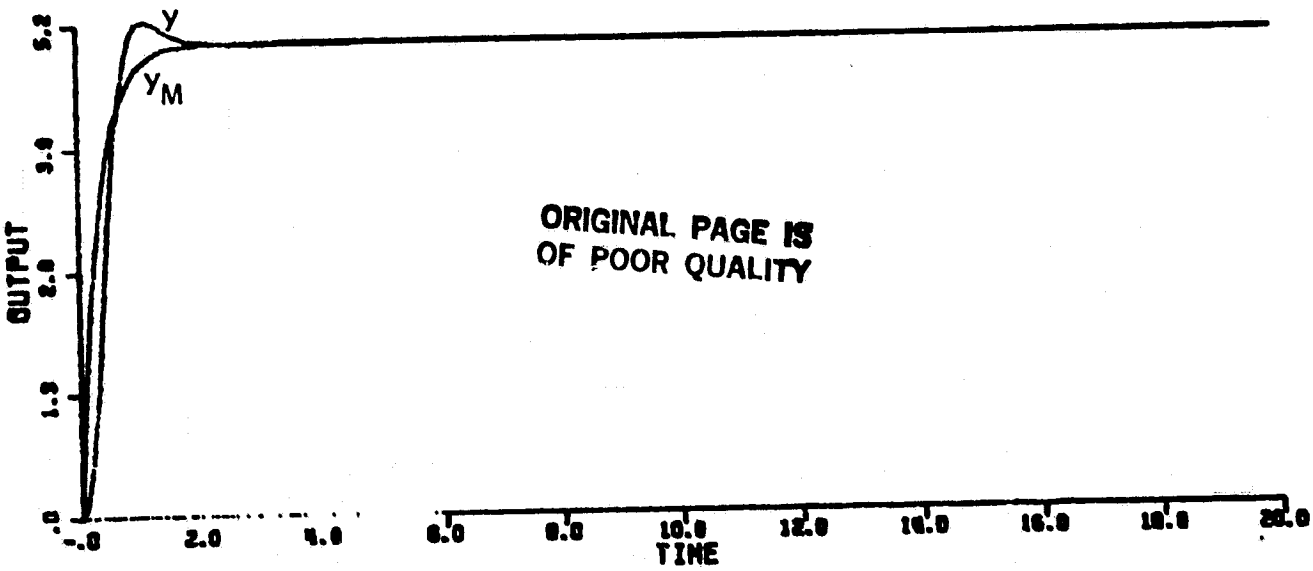

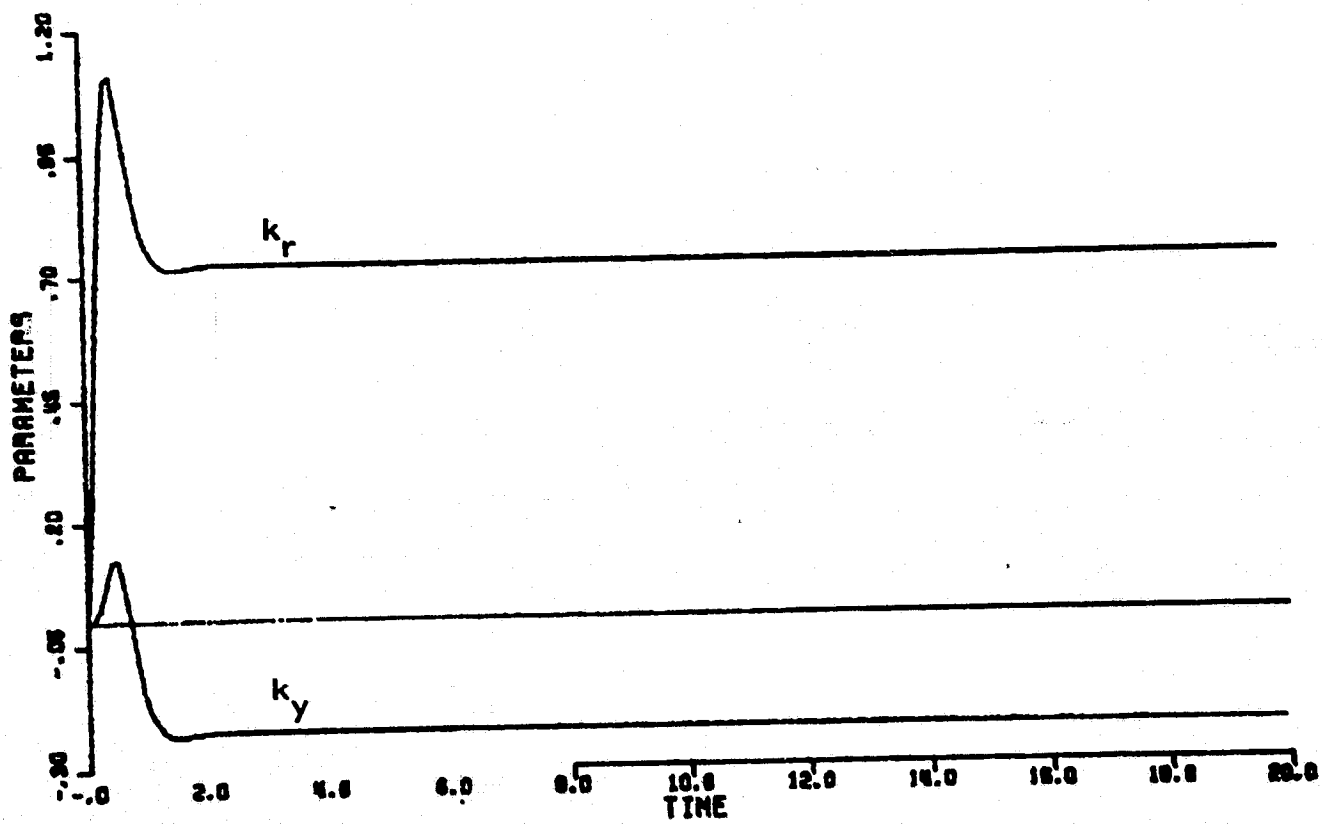

Figure 3-22. Simulation of CA2 with r=5.0.

The zeroes of the first term of eqn. (3-60) are the poles of the d^*-root locus. The zeroes of the d^*-root locus are found by finding the solutions of

$$B_M A^* s + \frac{g_p}{\rho g_M} B^* A_M = 0 \qquad (3\text{-}61)$$

The effects of the choice of ρ upon the zeroes of the d^*-root locus can be investigated by performing a root locus on eqn. (3-61) using ρ (or, equivalently, $1/\rho$) as a parameter.

Through these root locus techniques the designer is guided how to choose the parameter ρ in order to maintain stability in the presence of a specific set of unmodeled dynamics provided that the system is in the neighborhood of a specific linearization point. The designer must use engineering judgement in applying the root locus techniques to a number of different sets of unmodeled dynamics and to analyze each around a number of linearization points so that the behavior of the algorithm is understood for all possible sets of unmodeled dynamics and operating points.

3.4.4.2 Numerical Example with Unmodeled Dynamics

The example with unmodeled poles from Section 3.3.5 is now repeated using CA2. First ρ is picked to give favorable zero positions in the d*-root locus. The $1/\rho$-root locus of eqn. (3-61) is shown in Figure 3-23. Note that there will be zeroes in the right-half plane if $\frac{1}{\rho}$ is too large (ρ too small). Using Figure 3-23 ρ is picked to be

$$\rho = .5$$

which places the zeroes of the d*-root locus at

$$s=-3.67,\ s=-4.57,\ s=-20;\ s=-2.71$$

Note that a designer would not know exactly where the unmodeled poles lie and would thus have to estimate a reasonable value for ρ.

The d*-root locus is then given in Figure 3-24.

The error system should be stable for all values of d^* and should be dominated by the pole which lies between zero and -2.71. Figure 3-25 shows the output of a simulation with r=5.0. Remember that such an input drove the CA1 algorithm unstable. Here the system is not only stable but well behaved. Similar results were achieved with r=50.0.

Thus, we have seen that by including an additional feedback loop in the error system, the algorithm CA2 can, if its parameters are chosen correctly, remain stable and well behaved for all constant inputs even in the presence of some unmodeled dynamics.

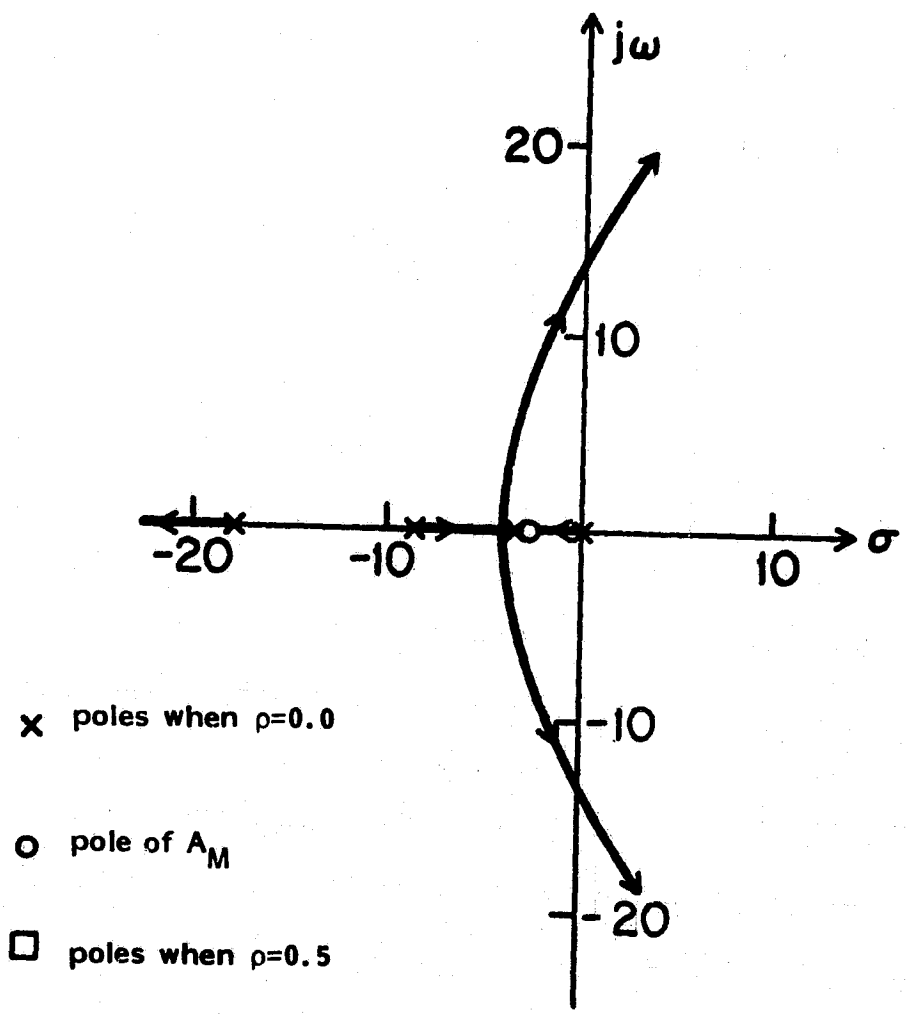

Figure 3-23. $\frac{1}{\rho}$-root locus for numerical example of Section 3.4.4.2.

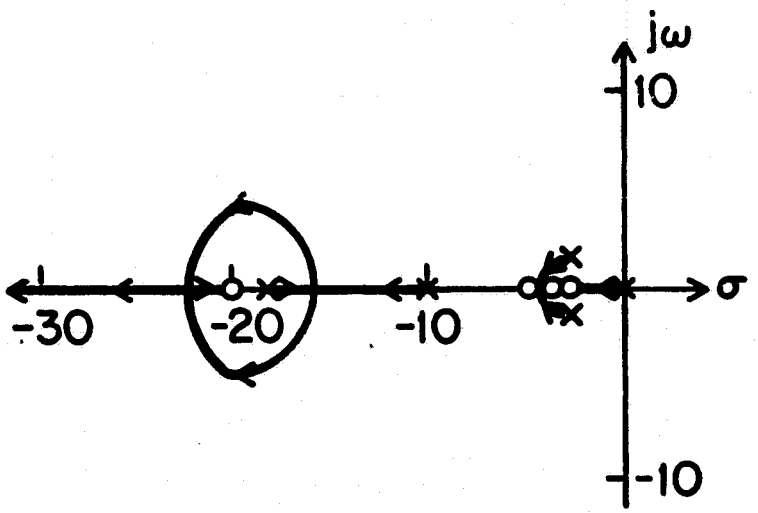

Figure 3-24. d^*-root locus for example of Section 3.4.4.2 with $\rho=0.5$.

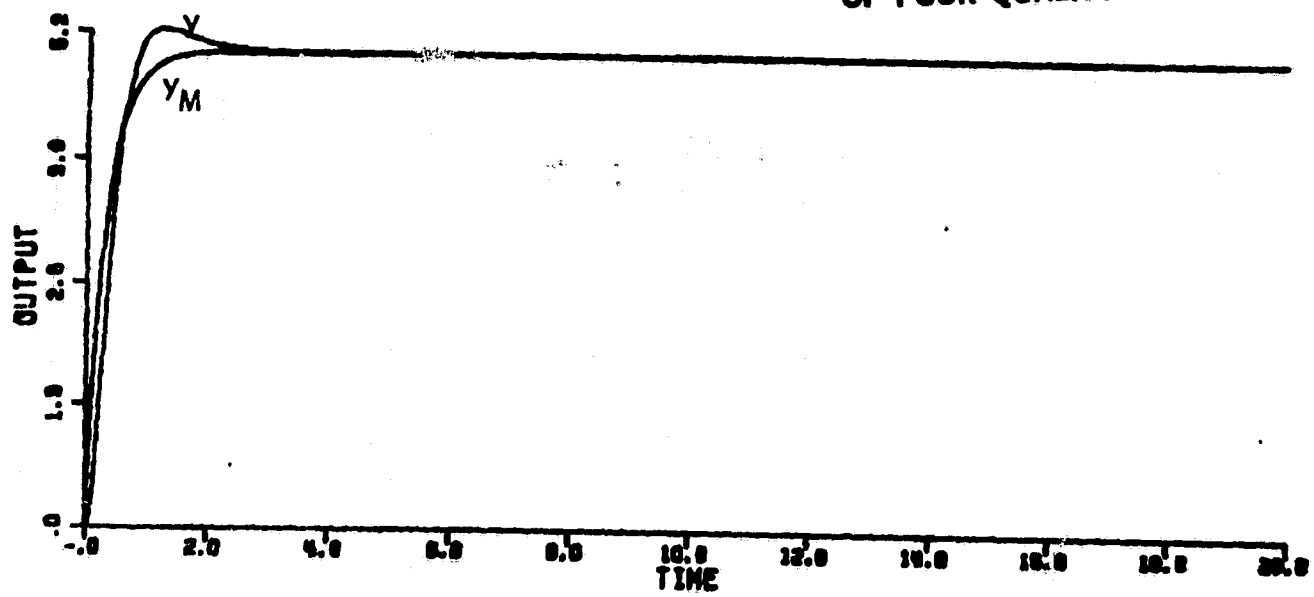

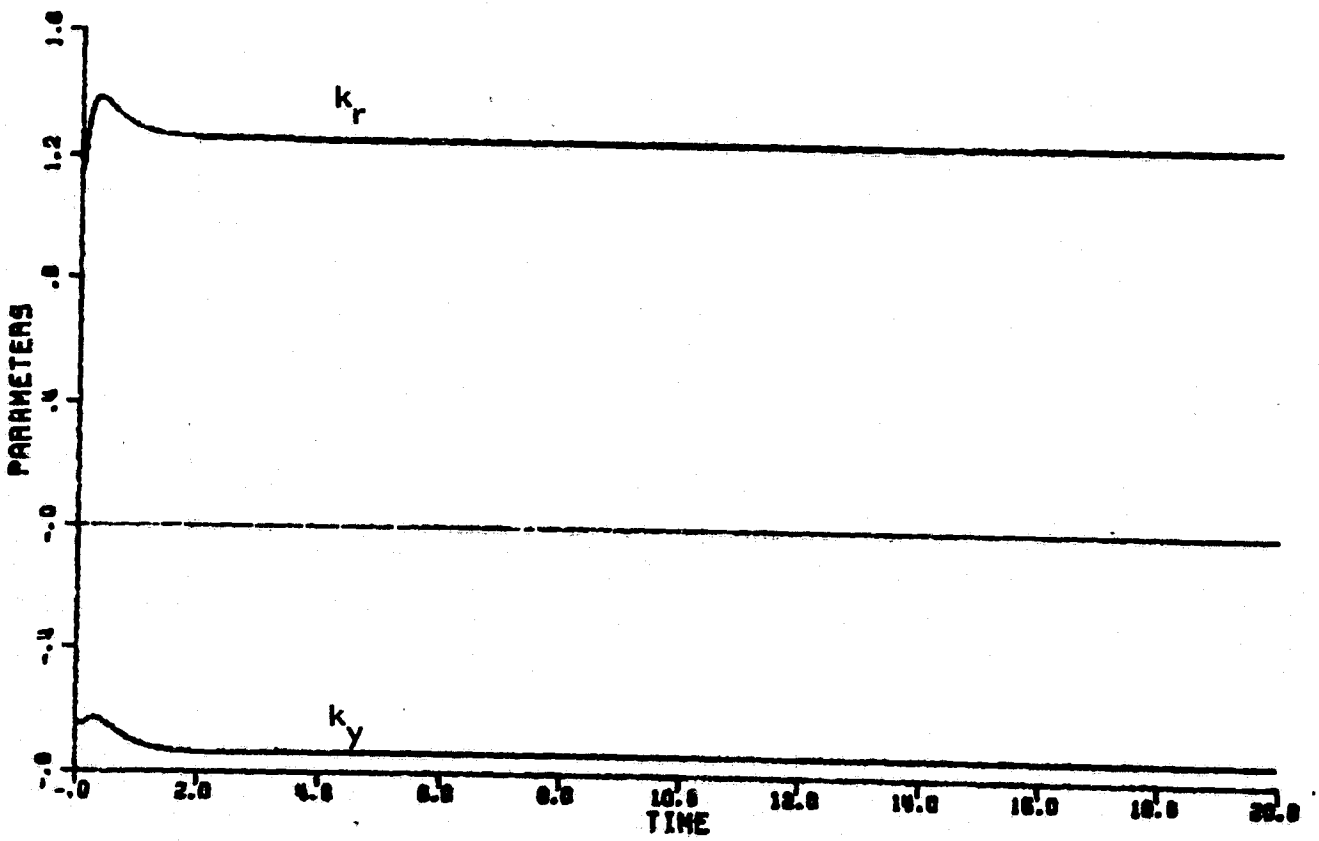

Figure 3-25. Simulation of CA2 with unmodeled dynamics and r=5.0.

3.4.5 Analysis of CA2 for Higher Order Systems

The analysis of CA2 will now completed for the case where the control system is designed for a plant with relative degree greater than unity ($n^*>1$). Linearization is still the tool used and the reference input again will be assumed constant. The equations of Table 2-2 and Figure 2-6 then apply.

The linearization proceeds as in the $n^*=1$ case. Let

$$\underline{w}(t) = \underline{w}^* + \delta\underline{w}(t) \tag{3-63}$$

$$\underline{v}(t) = \underline{v}^* + \delta\underline{v}(t) \tag{3-64}$$

with $\underline{w}^*$ defined as it was in eqns. (3-39)-(3-46) of Section 3.3.6 and $\underline{v}^*$ the output of eqn. (2-34) using $\underline{w}^*$ as an input. Also assume that

$$\underline{k}(t) = \underline{k}^* + \tilde{\underline{k}}(t) \tag{3-65}$$

$$h(t) = h^* + \tilde{h}(t) \tag{3-66}$$

and that all errors and perturbations are small. Recall eqn. (2-41) repeated below:

$$\psi(t) = \frac{M}{L}\left[\tilde{\underline{k}}^T(t)\underline{w}(t)\right] - \tilde{\underline{k}}^T(t)\underline{v}(t) \tag{2-41}$$

which, when linearized becomes

$$\psi(t) = \frac{M}{L}\left[\tilde{\underline{k}}^T(t)\underline{w}^*\right] - \tilde{\underline{k}}^T(t)\underline{v}^* \tag{3-67}$$

This shows that ψ is small when $\tilde{\underline{k}}$ is small so that the $h\psi$ term in Figure 2-6 is of second order and, hence, does not appear in the linearization. The rest of Figure 2-6 survives the linearization intact with $\underline{w}^*$ and $\underline{v}^*$ replacing $\underline{w}$ and $\underline{v}$.

Assume further, without loss of generality, that $\frac{M}{L}$ has unity d.c. gain. Then, from eqn. (2-34), if $\underline{w}^*$ is constant

$$\underline{v}^* = \underline{w}^* \tag{3-68}$$

Also using the assumption that $\underline{w}^*$ is constant and setting $\underline{\Gamma} = \gamma \underline{I}$ for simplicity, Figure 2-6 is reduced to Figure 3-26. Notice that again the d^*-root locus will have one less zero than pole since $\frac{g_M B_M L}{M A_M}$ is chosen to have relative degree equal to unity. Also, since $\frac{g_M B_M L}{A_M M}$ is chosen to be positive real, the parameter ρ can, as in the $n^*=1$ case, be chosen large enough so that the positive real term will dominate the error loop and the loop will be stable for all values of constant reference input. Again, as in the $n^*=1$ case, too large a choice of ρ will cause the error to be small and insensitive to parameter changes so that the adaptation will be slow.

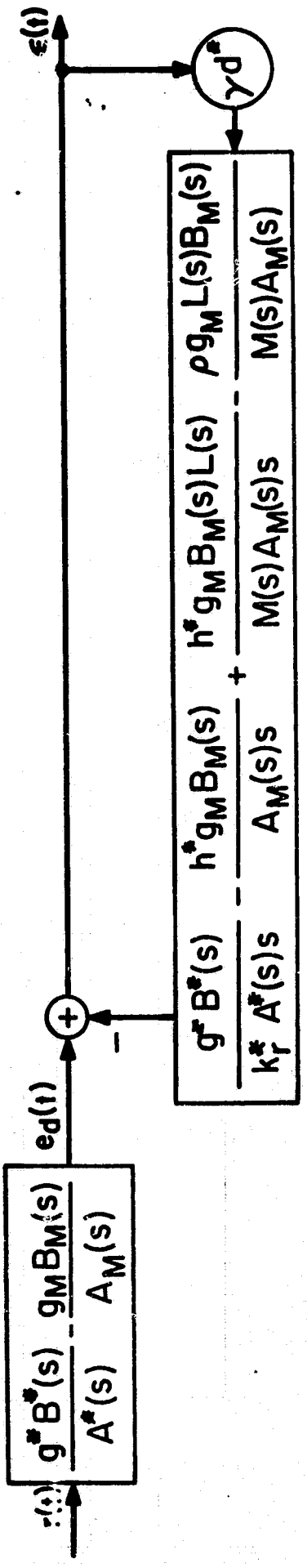

Figure 3-26. Linearized error system for CA2 with constant $\underline{w}^*$.

3.4.6 Conclusion

We have demonstrated analytically that the algorithm CA2 contains a parameter, ρ, by which the designer of the adaptive system can trade off improved stability properties in the presence of unmodeled dynamics against the speed of adaptation achieved.

The analysis method presented aids the designer in establishing how large ρ must be for the linearized error system to be stable for a specific set of unmodeled dynamics, a specific point of linearization and a range of constant reference inputs. It also provides information on how fast the adaptation mechanism will react under such specific conditions by displaying the poles of the linearized error system. The designer must couple this tool with engineering judgement, if he is to create a system which will perform satisfactorily in the presence of any possible unmodeled dynamics, at all possible operating points and for all constant reference inputs.

We stress here that none of the linearized analysis in this section can ensure stability. Also, all the analysis was performed assuming constant reference inputs and no disturbances. More general reference inputs and arbitrary disturbances can cause instabilities as will be seen in Chapter 4.

3.5 The Analysis of CA3

3.5.1 Introduction

As was mentioned in the discussion of Section 3.3.6, it is desirable to have a time-varying adaptation gain of the form

$$g_{d^*}(t) = \frac{\gamma}{\lambda_o + \gamma' d^*(t)} \qquad (3\text{-}62)^*$$

where $d^*(t) = \underline{w}^{*T}(t)\underline{w}^*(t)$, to enable the designer to approximately place the poles of the linearized error system independently of the size of the signals in the system. Such a gain is not allowed in CA1 or CA2 due to the nature of the associated stability proofs.

Luckily, normalizing gains of the type given by eqn. (3-62) in the adaptation process are suggested by various identification schemes such as least squares and stochastic approximation [65]. As a result, adaptive control algorithms have been developed using such a normalizing factor and it can be seen from eqn. (2-49) that CA3 is such an algorithm. The normalizing factor of eqn. (3-62) provides control of how far along the d*-root locus the poles of the error system can travel. This establishes the region in which the poles of the linearized error system can lie, again under the assumption that only constant inputs are applied.

*The parameters γ and γ' control the nominal size of the gain while the parameter λ_o is present to avoid possible division by zero.

In order to incorporate the normalization factor of eqn. (3-62) into a stability proof for CA3, two changes are made in the CA2 algorithm. The inner loop of the error system shown in Fig. 2-7 is removed and the auxiliary filter with transfer function $\frac{L}{M}$ is chosen so that $\frac{L}{M}$ has unity d.c. gain and so that $\frac{g_M B_M L}{A_M M}$ is a constant memoryless system. With this realization, the auxiliary signal loop is present even when $n^*=1$ and, furthermore, it takes the place of the inner loop of CA2 shownin Figure 2-7 in placing zeroes of the d^{*}-root locus.

3.5.2 Analysis

Proceeding with the exact same linearization-constant input analysis as in Section 3.2, Figure 2-8 is reduced to Figure 3-27 where

$$\gamma d^* = \underline{w}^{*T} \underline{\Gamma} \underline{w}^* \tag{3-63}$$

and

$$\gamma' d^* = \underline{w}^{*T} \underline{\Gamma}' \underline{w}^* \tag{3-64}$$

The new parameter matrix, Γ', is a weighting matrix providing extra flexibility over the normalization factor of eqn. (3-62).

The linearized analysis proceeds as usual except that, for this algorithm, the gain of the d^*-root locus is:

$$\frac{\gamma d^*}{\lambda_o + \gamma' d^*} \tag{3-65}$$

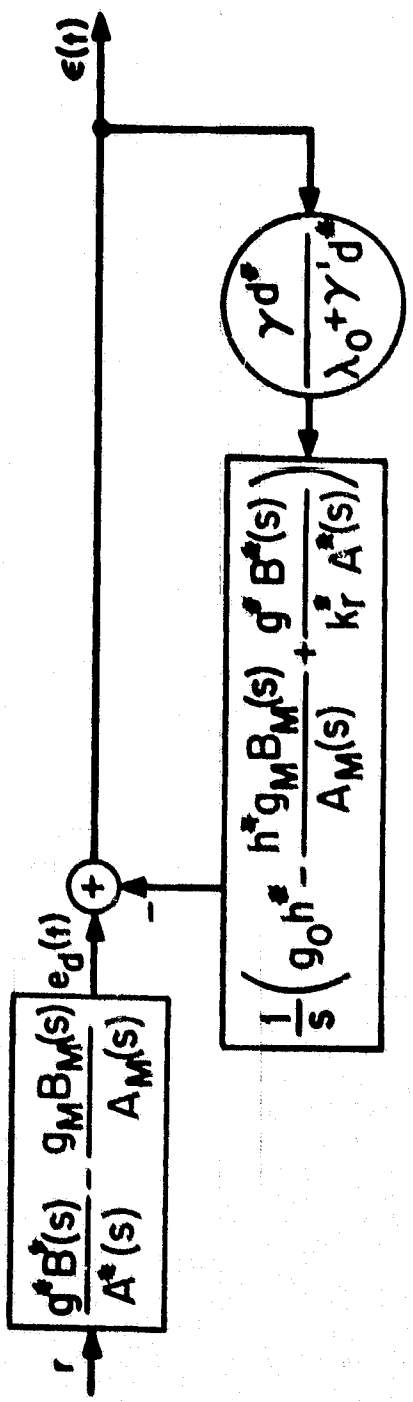

Figure 3-27. Linearized error system for CA3 with constant $\underline{w}^*$.

When the reference input is large so that $\gamma' d^* > \lambda_o$ the gain of the d^*-root locus given by eqn. (3-65) will not itself become large but will saturate at the value $\frac{\gamma}{\gamma'}$. The quantity $\frac{\gamma}{\gamma'}$ is picked by the designer so that he can control how far along the d^*-root locus the poles of the linearized error system can travel, in a manner independent of the magnitude of the constant reference input.

3.5.3 A Numerical Example with Unmodeled Poles

The example of Section 3.3.5 with an unmodeled pole pair is considered here for CA3. The plant is given by

$$y(t) = \frac{2}{s+1} \left(\frac{229}{s^2+30s+229} \right) [u(t)] \qquad (3\text{-}27)$$

with the usual model described by:

$$y_M(t) = \frac{3}{s+3} [r(t)] \qquad (3\text{-}28)$$

When the linearization is performed around

$$k_r^* = 1.14 \qquad k_y^* = -0.65 \qquad h^* = .88$$

a point in the parameter space where the $\frac{g^* B^*}{A^*}$ of eqn. (2-118) system nearly matches the model, the system d^*-root locus is obtained from Figure 3-27 with

$$S_E = \frac{.88(s+20.8)(s+3.6+j3.5)(s+3.6-j3.5)}{(s+18.6)(s+9.4)(s+3)s} \qquad (3\text{-}66)$$

where

$$S_E = \frac{1}{s}\left(g_o h^* - \frac{h^* g_M B_M}{A_M} + \frac{g^* B^*}{k_r^* A^*}\right)$$

The d*-root locus for this system is shown in Figure 3-28. The normalized adaptation gain of eqn. (3-62) is not actually needed here for stability although it could be used to keep the linearized error system from becoming oscillatory.

Figure 3-29 shows the results of a simulation with r=10.0 and $\frac{\gamma}{\gamma'} = 1.0$ Figure 3-30 shows the results of a simulation with r=10.0 and $\frac{\gamma}{\gamma'} = 0.3$. We notice from Figure 3-30 that the lower gain in the d^*-root locus slows down the system and increases its damping. The same results occurred with r=50.0 in both cases. This is not surprising, since the d^*-root locus gain remains at approximately $\frac{\gamma}{\gamma'}$.

When simulations were tried with r=100.0, both systems became unstable during the initial transient period. This reinforces the fact that the linearized analysis used throughout this chapter is a <u>local</u> analysis. If either the parameters or the signals in $\underline{w}(t)$ are too far from the values around which the linearization is performed,

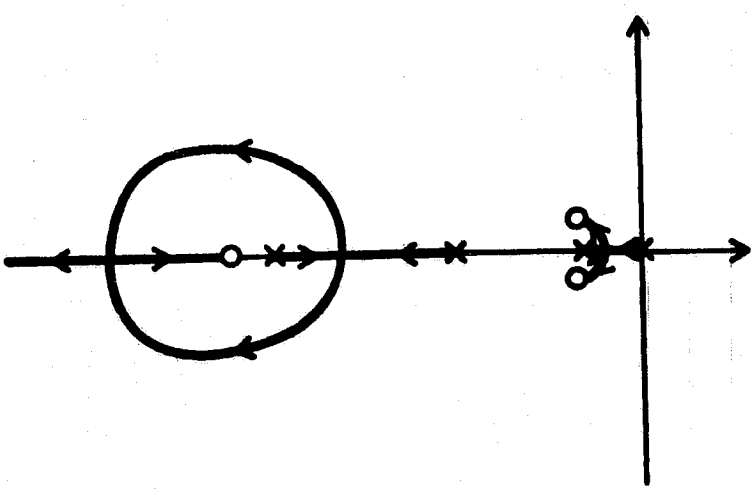

Figure 3-28. d^*-root locus for numerical example of Section 3.5.3.

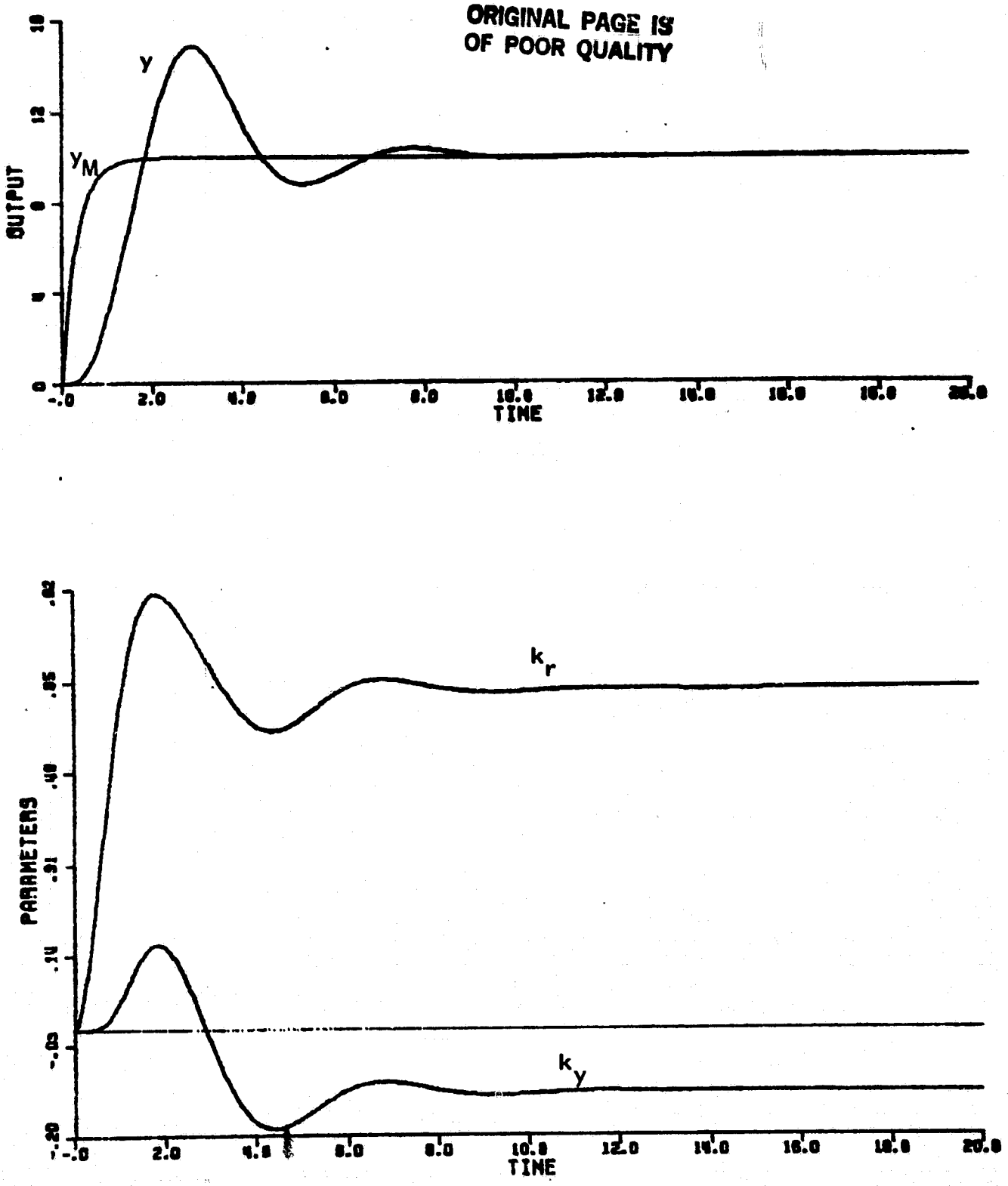

Figure 3-29. Simulation of CA3 with unmodeled dynamics, r=10.0, and $\frac{\gamma}{\gamma'}$=1.0.

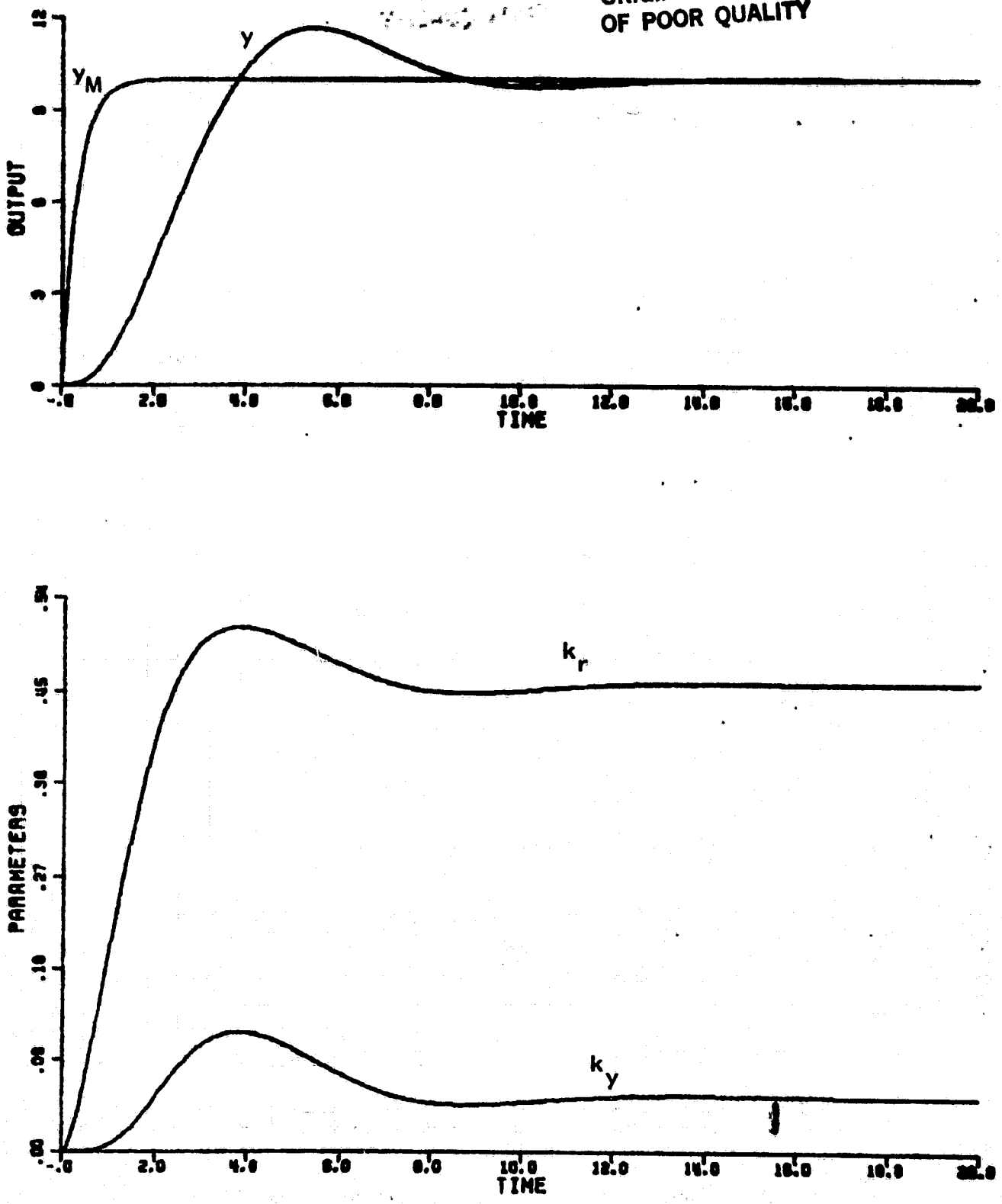

Figure 3-30. Simulation of CA3 with unmodeled dynamics, . .
r=10.0, and $\frac{\gamma}{\gamma'}$=0.3.

the results of the linearization analysis may not be valid. Thus, all the results of this chapter based upon the linearization technique must be validated by simulation.

3.5.4 Conclusions

It has been shown in Section 3.5 with the use of linearization techniques that with the normalization of the adaptation gain as given in eqn. (3-62) and the proper setting of the parameters in this gain, the algorithm CA3 can be designed so that the linearized error system is stable for all constant reference inputs in the presence of a specific set of unmodeled dynamics. In addition, the poles of the linearized error system can be positioned at a point along the d^*-root locus for a large range of constant reference inputs.

Although the linearized analysis is a local analysis which cannot guarantee global stability, simulations indicate that there is a reasonably large range of values for which the linearized analysis provides an accurate prediction of the adaptive system behavior.

3.6 The Analysis of CA4

3.6.1 Introduction and Development of the Linearized Error System

The final continuous-time algorithm analyzed in this dissertation is the CA4 algorithm of Egardt [11]. As was mentioned in Section 2.2.4, this algorithm uses extra filtering in the control loop (see Figure 2-10).

The algorithm is analyzed by linearizing the error system of the algorithm about a nominal set of parameters and constant signals $\underline{w}^*$ produced by a constant reference input. Linearizing the error system of Figure 2-11 produces the system of Figure 3-31. In the special case when $n^*=1$, the error system of Figure 2-12 applies and the linearization of this system produces the system of Figure 3-32.

Notice that the algorithm CA4 does include a normalizing factor in the gain as given by eqn. (2-58). This produces the d^*-root locus gain which is the same as in CA3, given by eqn. (3-62)

$$g_{d^*}(t) = \frac{\gamma d^*(t)}{\lambda+\gamma' d^*(t)} \qquad (3\text{-}62)$$

as shown in Figures 3-31 and 3-32. Such a gain allows the designer to control the placement of the poles of the linearized error system over a wide range of constant reference inputs. The situation is similar to that discussed in Section 3.5.2.

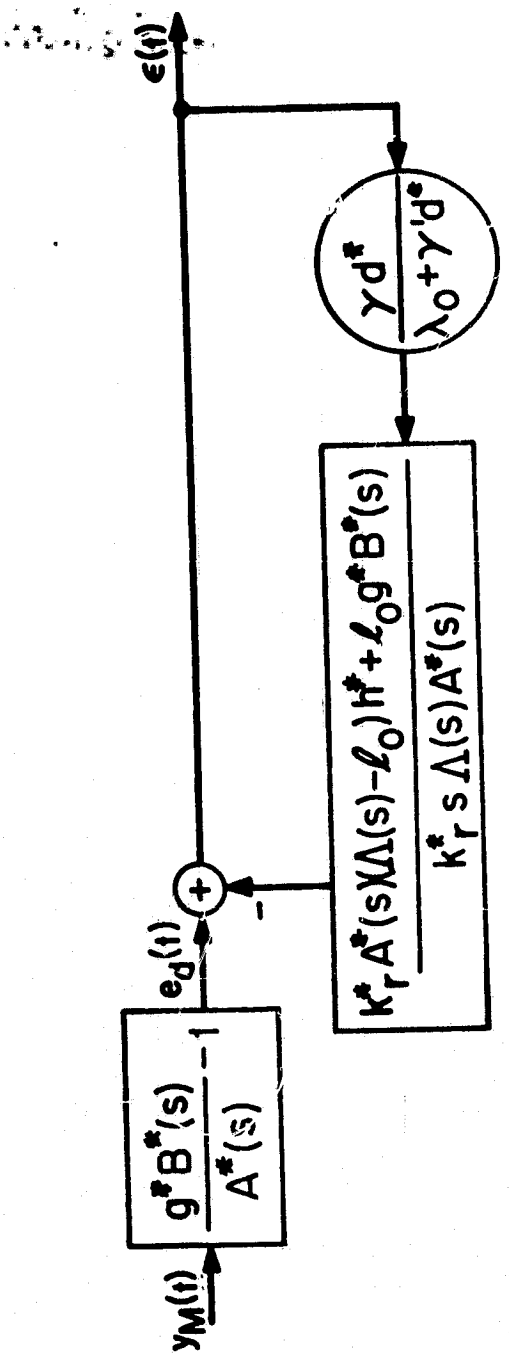

Figure 3-31. Linearized error system for CA4 with constant $\underline{w}^*$.

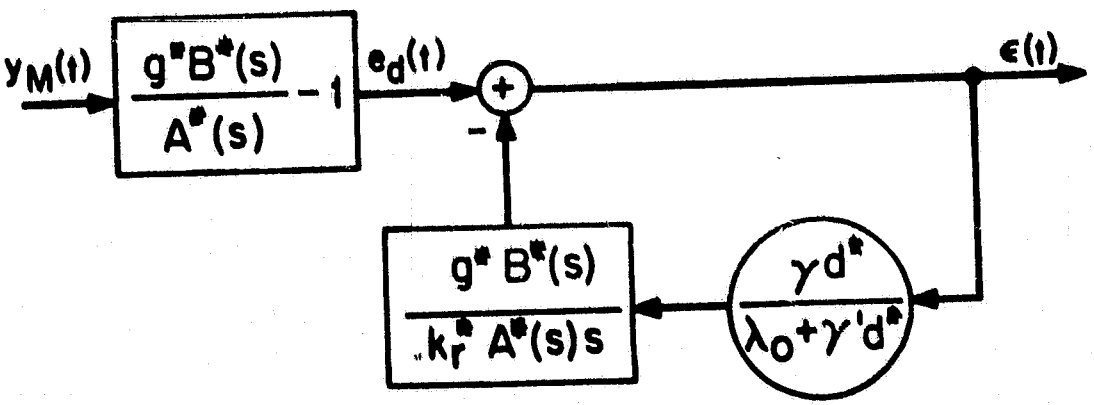

Figure 3-32. Linearized error system for CA4 with constant $\underline{w}^*$ and $n^*=1$.

3.6.2 The Case $n^*=1$

First, examine the algorithm for the case $n^*=1$. Note that in this case the inner loop of Figure 2-11 is not used, so there is no way to place zeroes of the d^*-root locus. The algorithm of CA4 is an improvement over CA1 both in the normalizing factor limiting the gain of the d^*-root locus and in the fact that, with the added filtering, the nominal controlled plant, $\frac{q^*B^*}{\Lambda^*}$, of eqn. (2-63) will have a relative degree that is one less than the relative degree of the corresponding nominal controlled plant of CA1 given in eqn. (2-23). Here, from eqn. (2-64), it can be seen that $\frac{q^*B^*}{\Lambda^*}$ can be made to be a memoryless system. The d^*-root locus will have a pole excess of one and thus no oscillatory high frequency error signals can result.

When there are unmodeled dynamics, $\frac{q^*B^*}{\Lambda^*}$ will have the same pole excess as the unmodeled dynamics. If this pole excess is greater than one, the d^*-root locus of the linearized error system will exhibit a Butterworth pattern of order three or greater causing the linearized error system to be unstable, if the d^*-root locus gain is allowed to become toolarge. This situation is worse than the situation of CA3 where the pole excess of the d^*-root locus is one, independent of the unmodeled dynamics.

3.6.3 The Case $n^* > 1$

When the adaptive control system CA4 is designed for a plant with $n^*>1$, the inner loop of Figure 2-11 is now present and the error loop of the d^*-root locus given in Figure 3-31 will have a single pole excess independent of the relative degree of the unmodeled dynamics. This is similar to the situation of CA3. Whether or not the zeroes of the d^*-root locus will be such that the linearized error system remains stable for all values of the d^*-root locus gain is something that must be determined by analyzing each case individually. If necessary, the normalization of the gain of eqn. (3-62) can limit the distance that the poles travel along the d^*-root locus.

3.6.4 A Numerical Example with Unmodeled Dynamics

The usual example of Section 3.3.5 with an unmodeled pole pair is carried out for CA4. The filter used was

$$\frac{1}{L} = \frac{1}{s+3} \qquad (3\text{-}67)$$

The d^*-root locus gain was allowed to saturate at unity ($\frac{\gamma}{\gamma'} = 1$ in the notation of Section 3.3). Figure 3-33 shows the results when r=5.0. Curves of the exact same shape were obtained for r=10.0, since in both cases the d^*-root locus gain was near one.

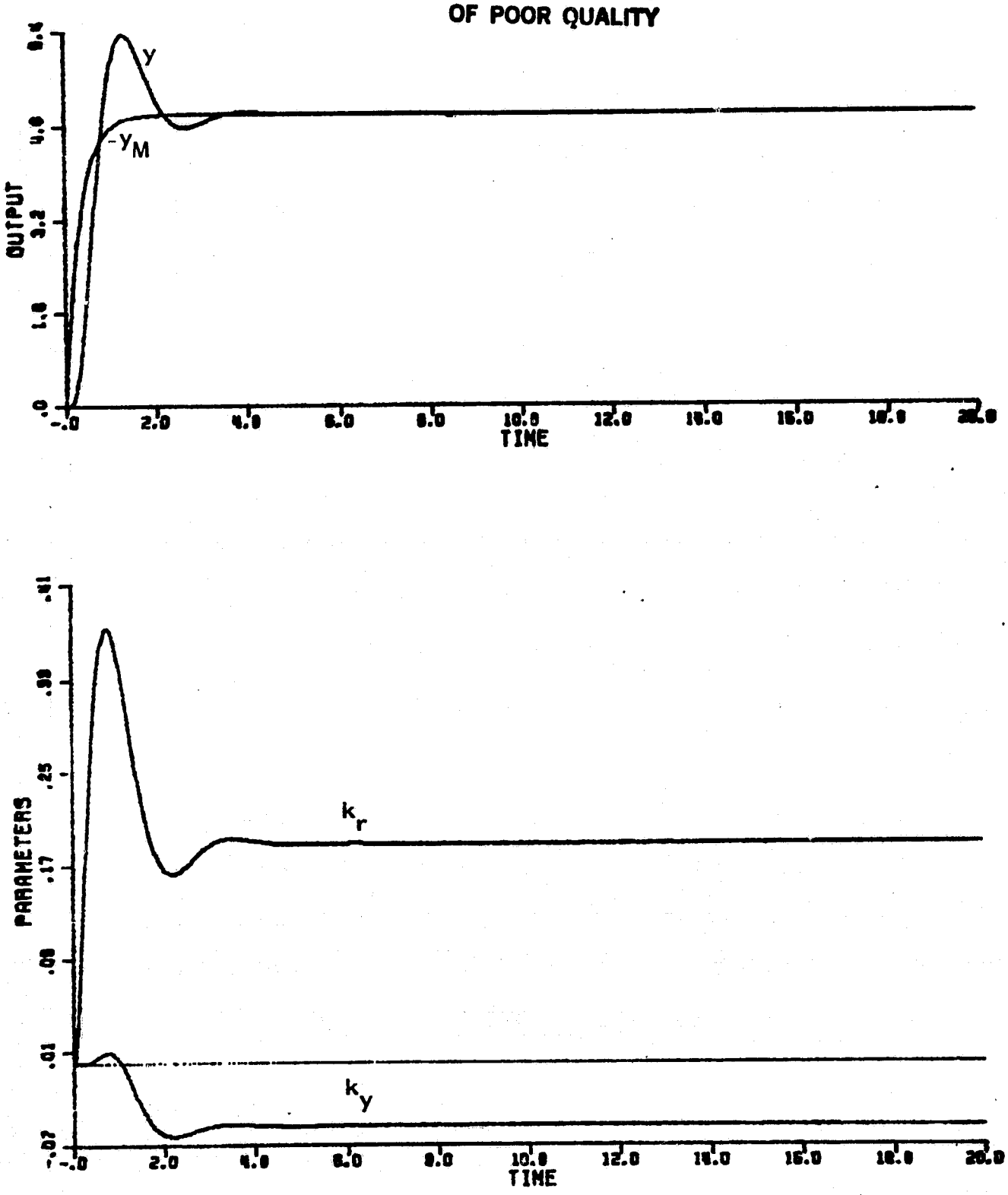

Figure 3-33. Simulation of CA4 with unmodeled dynamics and r=5.0.

When the system was simulated with r=50.0, we observed a bad transient similar to the one which caused instability in CA3 when too large a reference input was used in that adaptive system. The results are shown in Figure 3-34. The system is driven by the overshoot to a point in the parameter space far beyond what could be a reasonable desired parameter set. (Here, the desired parameter which would let the nominal controlled plant of eqn. (2-63) match the model as closely as possible is $k_y^* = -0.65$). Fortunately, for CA4, in this case, the parameters manage to stay in a region where the linearized error system still remains stable. In the simulation of Figure 3-34 the parameters converge to $k_y^* = -7.4$, $k_r^* = 2.6$ which result in a d^*-root locus system of

$$\frac{g^*B^*}{A^*} = \frac{458}{s(s+27.4)\,(s+1.8+j11.3)\;\;(s+1.8-j11.3)} \qquad (3\text{-}68)$$

The normalized d^*-root locus gain kept the error system stable even at these high signal levels so that the system could converge after the transient had died down. If the reference input used is increased to r=100, the transient drives the parameter into a region where even the linearized system with normalized gains is unstable. Recovery is then hopeless.

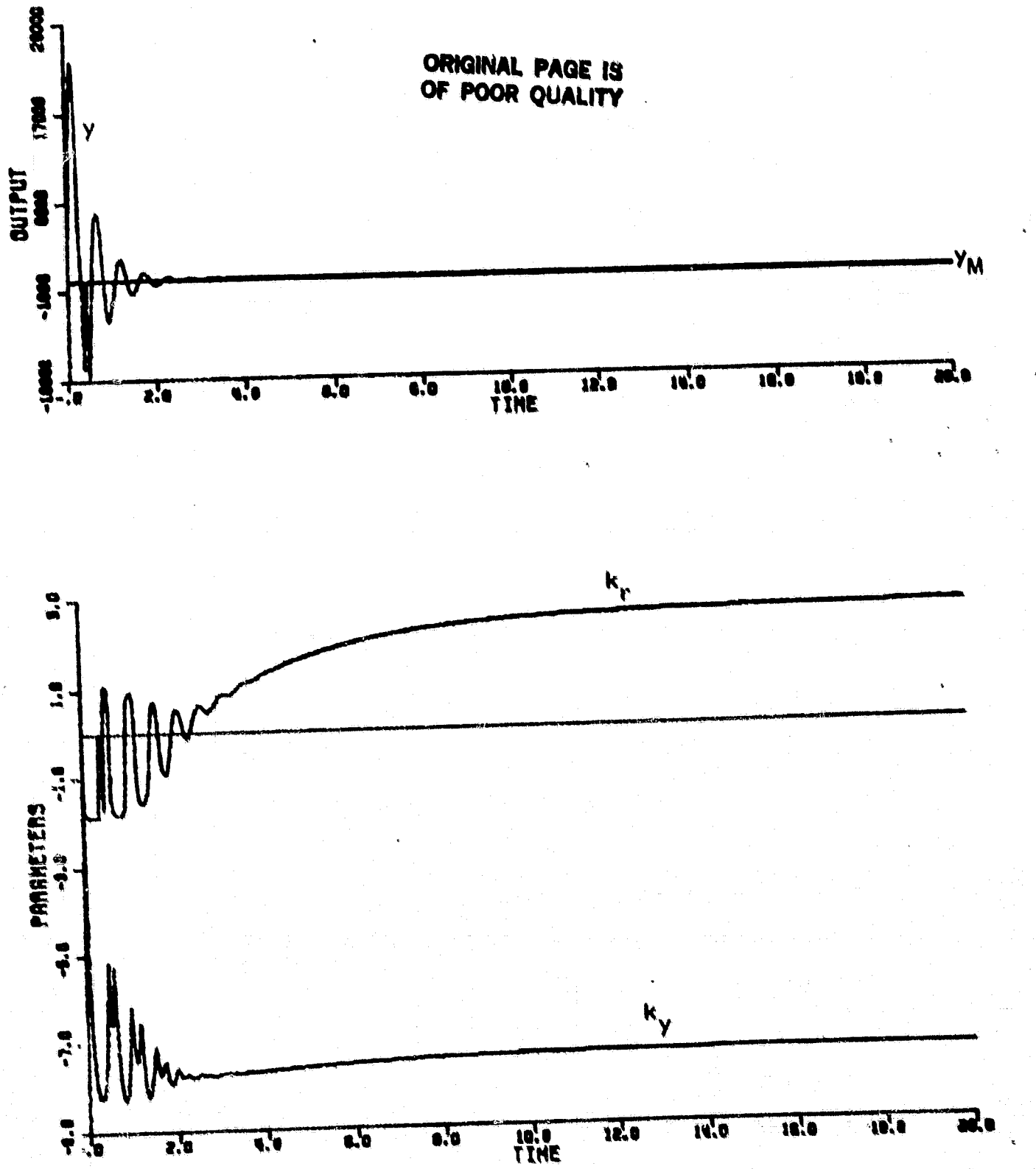

Figure 3-34. Simulation of CAS with unmodeled dynamics and r=50.0.

In this subsection, it has been shown in the context of CA4 that even when the error system is stable for all values of reference input when linearized around a set of desired parameters, normalized adaptation gains are still useful in enhancing its robustness when the system is driven into an undesirable region by the transient phase.

3.7 Conclusions

It has been shown in this chapter that linearization techniques are useful for the study of the behavior of continuous-time adaptive control algorithms when such algorithms are implemented in the presence of unmodeled dynamics under constant reference inputs with no disturbances.

Using this technique various general properties of the algorithms CA1 to CA4 have been displayed.

- In Section 3.3.6 it was shown that the gain and bandwidth of the error system loop of CA1 depend upon the magnitude of the reference inputs. In the presence of unmodeled dynamics, a large bandwidth can cause instability.
- A modification in CA2 provides for an inner loop in the error system. As described in Section 3.4.2.2, a gain parameter, ρ, in the inner loop allows the

designer of the adaptive system to create a situation where the linearized error system of CA2 is stable for a wide range of unmodeled dynamics and a wide range of values of constant reference inputs. The increased stability in the presence of unmodeled dynamics is attained at the expense of slowing down the adaptation mechanism.

- In algorithms CA3 and CA4, the adaptation gain is normalized as in eqn. (3-62). This enables the designer of the adaptive system to achieve the increased stability in the presence of unmodeled dynamics versus a speed of adaptation tradeoff by controlling the placement of poles of the linearized error system on the d^*-root locus.

Although the linearization technique provides valuable insights into the behavior of the adaptive systems, it does have the following limitations:

- As a linearization technique, the method can produce only <u>local</u> stability results, as discussed in Section 3.2. Results from the analysis are valid only for values of parameters and signals near those

used for the linearization. Results of the linearized analysis must be verified by simulation. An example demonstrating the limits of the linearization is discussed in Section 3.6.4.

- The technique of this chapter provides a method for analyzing a system implemented in the presence of a specific set of unmodeled dynamics. Engineering judgement must be exercised to use this analysis for a number of sets of unmodeled dynamics and, thus, create a system that will perform acceptably in the presence of any possible unmodeled dynamics.

Finally, we iterate that the analysis of the chapter is concerned only with constant reference inputs and no disturbances. It will be seen in Chapter 4 that even a system designed to maintain stability for constant reference inputs will be unstable in the presence of unmodeled dynamics, when excited with certain sinusoidal reference inputs or with constant or sinusoidal disturbances.

CHAPTER 4

THE RESPONSE OF CONTINUOUS-TIME ADAPTIVE CONTROL SYSTEMS TO SINUSOIDAL REFERENCE INPUTS AND DISTURBANCES

4.1 Introduction

In the last chapter, it was shown that, with a proper choice of the design parameters, the continuous-time adaptive algorithms CA2-CA4 could be made to be locally stable in the presence of a large class of unmodeled dynamics provided that the reference inputs are kept constant and no disturbances are allowed.

In this chapter we analyze the response of the algorithms CA1-CA4 to sinusoidal reference inputs and to deterministic disturbances in the presence of unmodeled dynamics. The following conclusions can be drawn from the contents of this chapter:

- All of the algorithms CA1-CA4 contain an infinite gain operator in their error system. This infinite gain operator gives rise to two mechanisms of possible instability when sinusoidal reference inputs and disturbances are present along with unmodeled dynamics.
- In the presence of unmodeled dynamics, the adaptive systems CA1-CA4 do become unstable if sinusoidal reference inputs at certain frequencies are introduced.

- In the presence of unmodeled dynamics, the adaptive systems CA1-CA4 become unstable in the presence of even a small sinusoidal disturbance of any frequency.

The results of the chapter are developed as follows:

Section 4.2 describes the infinite gain operators present in the error loops of the algorithms. In Section 4.2.4, it is argued that these infinite gain operators are generic to the adaptive control problem. Such infinite gains are usually handled in stability proofs by assuming the high frequency phase properties of the plant are known. These phase properties can then be used to stabilize the error system. However, it is the high frequency phase properties of a plant that are most affected by unmodeled dynamics. Section 4.3 shows two mechanisms for instability of the adaptive control system in the presence of unmodeled dynamics.

In Section 4.3.2 the first mechanism for instability in the adaptive algorithms is given. This mechanism uses the combination of the infinite gain operator and the phase shift introduced by the unmodeled dynamics to produce instability.

In Section 4.3.3, the second instability mechanism is explained. This mechanism occurs when there is a steady output error due to

either a disturbance or a controlled plant-model mismatch at some frequency. Such instabilities are usually ruled out in the published stability proofs by assuming that the controlled plant has no unmodeled dynamics and that it can match the model perfectly; it is furthermore assumed that no disturbances are present.

Section 4.4 shows, through digital simulations, that the adaptive systems (CA1-CA4) do indeed become unstable when faced with certain combinations of sinusoidal reference inputs and unmodeled dynamics. The instabilities arise in the manner predicted by the analysis of Section 4.3.

Section 4.5 shows that, even though the stability problems of Section 4.4 are caused by the presence of a high frequency output error signal, the use of additional filters on the plant output or output error do not alleviate the problem. The filters, themselves, lower the frequency of the output error which is necessary to produce instability.

Section 4.6 presents the most damaging of all evidence for the adaptive control algorithms CA1-CA4. In Section 4.6 it is verified by digital simulation that, for a large class of unmodeled dynamics, the adaptive controllers CA1-CA4 will become unstable in the presence of a small amplitude sinusoidal disturbance of any frequency. While a designer can control the reference inputs that will be introduced

into his system, he has no control over what disturbances are present. Since sinusoidal disturbances are common in many applications, e.g. 60 Hz noise, these algorithms will lead to unstable systems.

Section 4.7 summarizes the conclusions of this chapter.

4.2 The Infinite Gain Operator

4.2.1 Quantitative Proof of Infinite Gain for the Operator of CA1

The simplest adaptive control error system, that of CA1, appears in Figure 2-3 and is repeated here as Figure 4-1. It consists of a forward linear time-invariant operator representing the nominal controlled plant complete with unmodeled dynamics, $\frac{g^*B^*}{k_r^*A^*}$, and a time-varying feedback operator. It is this feedback operator which is of immediate interest. The operator, reproduced in Figure 4-2 for the case where w is a scalar and Γ=1, is parameterized by the function w(t) and can be represented mathematically as:

$$u(t) = G_{w(t)}[e(t)] = u(o) + w(t) \int_0^t w(\tau)e(\tau)d\tau \qquad (4\text{-}1)$$

In order to make the notion of the gain of the operator $G_{w(t)}[\cdot]$ precise, the following operator theoretic concepts are introduced. For further development see [66].

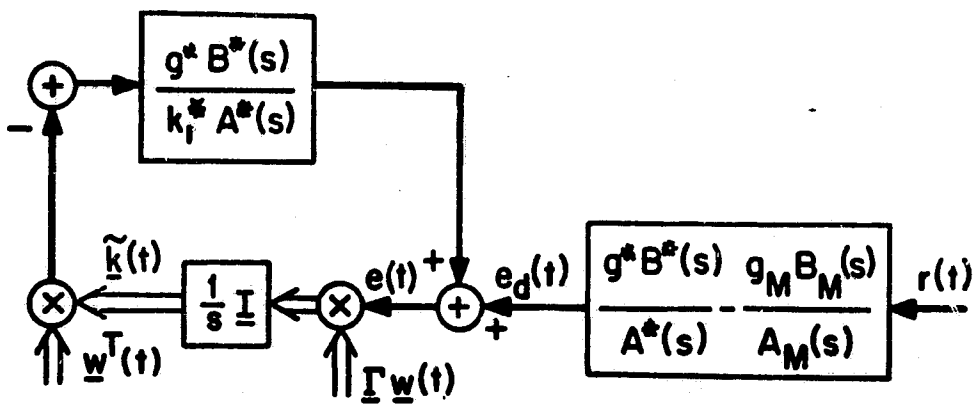

Figure 4-1. Error system for CA1.

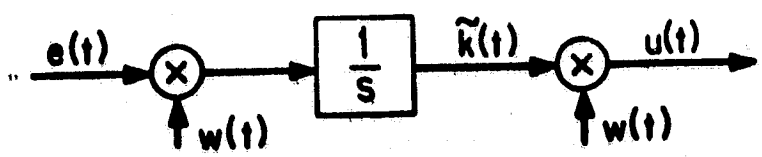

Figure 4-2. Infinite gain operator of CA1

Definition 4.1: A function f(t), from $[0,\infty)$ to R is said to be in L_2 if it is integrable and

$$||f(t)||_{L_2} \triangleq \left(\int_0^\infty f^2(\tau)d\tau\right)^{1/2} < \infty \qquad (4\text{-}2)$$

The quantity $||\cdot||_{L_2}$ is called the norm of the function.

Definition 4.2: A function f(t) from $[0,\infty)$ to R is said to be in L_{2e} if the truncated norm

$$||f(t)||_{L_2}^T \triangleq \left(\int_0^T f^2(\tau)d\tau\right)^{1/2} \qquad (4\text{-}3)$$

is finite for all finite T.

Definition 4-3: The gain of an operator G[f(t)], which takes functions in L_{2e} into functions in L_{2e} is defined as

$$||G|| = \sup_{\substack{f(t)\in L_{2e} \\ T\in[0,\infty)}} \frac{||G[f(t)]||_{L_2}^T}{||f(t)||_{L_2}^T} \qquad (4\text{-}4)$$

If there is no finite number satisfying eqn. (4-4), then G is said to have infinite gain.

Theorem 4-1: If w is given by

$$w(t) = b + c \sin\omega_o t \tag{4-5}$$

for any positive constants b, c, ω_o the operator, of eqn. (4.1), G_w, has infinite gain.

Proof: The proof consists of constructing a signal, e(t), such that

$$\lim_{T\to\infty} \frac{||G_w[e(t)]||^T_{L_2}}{||e(t)||^T_{L_2}}$$

is unbounded.

Let $e(t) = a \sin\omega_o t$

with a an arbitrary positive constant and ω_o the same constant as in eqn. (4.5).

These signals produce:

$$w(t)e(t) = ab \sin\omega_o t + \frac{1}{2} ac - \frac{1}{2} ac \cos 2\omega_o t \tag{4-7}$$

$$\tilde{k}(t) \triangleq \tilde{k}_o + \int_0^t w(\tau)e(\tau)d\tau$$

$$= \tilde{k}_o + \frac{1}{2} act + \frac{ab}{\omega_o} - \frac{ab}{\omega_o} \cos\omega_o t - \frac{ac}{4\omega_o} \sin 2\omega_o t \tag{4-8}$$

$$u(t) = G_{w(t)}[e(t)] = u_0 + w(t)\int_0^t w(t)e(\tau)d\tau =$$

$$= u_o + \frac{1}{2}abc\ t + \frac{ab^2}{\omega_o} + \left(\frac{1}{2}ac^2t + \frac{abc}{\omega_o}\right)\ \sin\omega_o t +$$

$$+ \left(\frac{ac^2}{8\omega_o} - \frac{ab^2}{\omega_o}\right)\cos\omega_0 t - \frac{3abc}{4\omega_o}\sin 2\omega_o t + \frac{ac^2}{8\omega_o}\cos 3\omega_o t \quad (4\text{-}9)$$

Now, using standard norm inequalities,* we obtain

$$||u(t)||_{L_2}^T \geq \left|\left|\frac{1}{2}abc\ t + \frac{1}{2}ac^2t\ \sin\omega_o t\right|\right|_{L_2}^T -$$

$$-||u_o||_{L_2}^T - \left|\left|\frac{ab^2}{\omega_o}\right|\right|_{L_2}^T - \left|\left|\frac{abc}{\omega_o}\sin\omega_o t\right|\right|_{L_2}^T -$$

$$-\left|\left|\left(\frac{ac^2}{8\omega_o} - \frac{ab^2}{\omega_o}\right)\cos\omega_o t\right|\right|_{L_2}^T - \left|\left|\frac{3abc}{4\omega_o}\sin 2\omega_o t\right|\right|_{L_2}^T -$$

$$- \left|\left|\frac{ac^2}{8\omega_o}\cos 3\omega_o t\ \right|\right| \quad (4\text{-}10)$$

$$> \left|\left|\frac{1}{2}abc\ t + \frac{1}{2}ac^2t\ \sin\omega_o t\right|\right|_{L_2}^T - \left(K_1' T\right)^{1/2} \quad (4\text{-}11)$$

with

$$K_1' = u_o^2 + \left(\frac{ab^2}{\omega_o}\right)^2 + \left(\frac{abc}{\omega_o}\right)^2 + \left\{\frac{ac^2}{8\omega_o} - \frac{ab^2}{\omega_o}\right\}^2 + \left\{\frac{3abc}{4\omega_o} + \frac{ac^2}{8\omega_o}\right\}^2 < \infty \quad (4\text{-}12)$$

---

*Specifically $||A-B|| \geq ||A||-||B||$

and $||A+B|| \geq ||A||-||B||$.

Now

$$\left|\left|\frac{1}{2}\,abc\;t + \frac{1}{2}\,ac^2 t\,\sin\omega_o t\right|\right|_{L_2}^{T^2}$$

$$= \int_0^T \left(\frac{a^2b^2c^2}{4}\,t^2 + \frac{a^2c^4}{4}\,t^2\sin^2\omega_o t + \frac{a^2bc^3}{2}\,t^2\sin\omega_o t \right) dt = \tag{4.13}$$

$$= \left[\frac{a^2b^2c^2}{12}\,t^3\right]_0^T + \frac{a^2c^4}{4\omega_o^2}\left[\left(\frac{\omega_o t}{6\omega_o}\right)^3 - \left\{\left(\frac{\omega_o t}{4\omega_o}\right)^2 - \frac{1}{8\omega_o}\right\}\sin 2\omega_o t - \frac{t\cos 2\omega_o t}{4}\right]_0^T +$$

$$+ \frac{a^2bc^3}{2\omega_o^2}\left[\left(\frac{2}{\omega_o} - \omega_o t^2\right)\cos 2\omega_o t + 2t\sin\omega_o t\right]_0^T \tag{4-14}$$

$$\geq \left(\frac{a^2b^2c^2}{12} + \frac{a^2c^4}{24}\right)T^3 - K_2T^2 - K_1T^2 - K_0 \tag{4-15}$$

where

$$K_2 = \left(\frac{a^2c^4}{16\omega_o^2}\right)^2 + \left(\frac{a^2bc^3}{2\omega_o}\right)^2 < \infty \tag{4-16}$$

$$K_1 = \left(\frac{a^2c^4}{16\omega_o^2}\right)^2 + \left(\frac{a^2bc^3}{\omega_o^2}\right)^2 < \infty \tag{4-17}$$

$$K_0 = \left(\frac{a^2c^4}{32\omega_o^3}\right)^2 + \left(\frac{a^2bc^3}{\omega_o^3}\right)^2 < \infty \tag{4-18}$$

Combining ineqs. (4-11) and (4-15) we arrive at:

$$\left(\left|\left|u(t)\right|\right|_{L_2}^T\right)^2 \geq \left(\frac{a^2b^2c^2}{12} + \frac{a^2c^4}{24}\right)T^3 - K_2T^2 - K_1T - K_0 \tag{4-16}$$

$$\left(||e(t)||_{L_2}^{T}\right)^2 = a^2 \int_0^T \sin 2\omega_o t \;\leq\; a^2 T \qquad (4\text{-}17)$$

Therefore,

$$\frac{||u(t)||_{L_2}^{T}}{||e(t)||_{L_2}^{T}} \geq \left[\frac{\left(\frac{a^2b^2c^2}{12} + \frac{a^2c^4\omega_o}{24}\right)T^3 - K_2T^2 - K_1T - K_0}{a^2T}\right]^{1/2} \xrightarrow{T\to\infty} \infty$$

and G_w for w as in eqn. (4-5) has infinite gain. Q.E.D.

In addition to the fact that the operator $G_{w(t)}$ from e(t) to u(t) has infinite gain, we show next that the operator, $H_{\underline{w}}$, from e(t) to $\tilde{k}(t)$ in Figure 4-2 has infinite gain. This operator is described by:

$$H_{w(t)}[e(t)] = \tilde{k}_o + \int_0^t w(\tau)e(\tau)d\tau \qquad (4\text{-}18)$$

Theorem 4.2: The operator $H_{w(t)}$ with w(t) given in eqn. (4-5) has infinite gain.

Proof: Choose e(t) as in eqn. (4-6); then $\tilde{k}(t) = H_{w(t)}[e(t)]$ is given by eqn. (4-8)

$$||\tilde{k}(t)||_{L_2}^T \geq ||\tfrac{1}{2} ac\ t||_{L_2}^T - ||\tilde{k}_o||_{L_2}^T - ||\tfrac{ab}{\omega_o}||_{L_2}^T$$

$$- ||\tfrac{ab}{\omega_o} \cos\omega_o t||_{L_2}^T - ||\tfrac{ac}{4\omega_o} \sin 2\omega_o t||_{L_2}^T \qquad (4\text{-}19)$$

$$\geq ||\tfrac{1}{2} act||_{L_2}^T - (KT)^{1/2} \qquad (4\text{-}20)$$

where

$$K = (\tilde{k}_o)^2 + 2\left(\frac{ab}{\omega_o}\right)^2 + \left(\frac{ac}{4\omega_o}\right)^2 \qquad (4\text{-}21)$$

Then

$$||\tilde{k}(t)||_{L_2}^T \geq \left(\frac{1}{2} ac \frac{T^3}{3}\right)^{1/2} - (KT)^{1/2} \qquad (4\text{-}22)$$

Using ineqs. (4-22) and (4-17)

$$\frac{||\tilde{k}(t)||_{L_2}^T}{||e(t)||_{L_2}^T} \geq \frac{\left(\frac{1}{2} ac \frac{T^3}{3}\right)^{1/2} - (KT)^{1/2}}{a\ T^{1/2}} \xrightarrow{T\to\infty} \infty \qquad (4\text{-}23)$$

and, hence, H_w has infinite gain for w as in eqn. (4-5) Q.E.D.

4.2.2 Qualitative Explanation of the Infinite Gain of G_w and H_w

An explanation of the mechanism which results in the infinite gain of the operators $G_{w(t)}$ and $H_{w(t)}$ can be constructed as follows:

If w(t) and e(t) contain sinusoids of the same frequency, as they do in eqns. (4-5) and (4-6), and if these sinusoids do not have a phase difference of exactly 90°, the multiplication of w(t) and e(t) in both $G_{w(t)}$ and $H_{w(t)}$ will produce a constant correlation term, the second term in eqn. (4-7). The signal w(t)e(t) is then integrated; the integration of this constant correlation produces the infinite gain. Since the integral of a constant is a ramp, the output signal of the integrator (which is also the output of $H_{w(t)}$) increases in amplitude indefinitely with time. The output of $G_{w(t)}$ is formed by multiplying the output of the integrator by w(t), producing a sinusoid with increasing amplitude at the frequency assumed present in w(t).

Finally, we note that both the operators G_w and H_w will also be infinite gain for vectors $\underline{w}(t)$, since the operators' infinite gains can arise from any component of the vector $\underline{w}(t)$.

4.2.3. The Infinite Gain Operator for CA2, CA3 and CA4

The infinite gain operators for CA2, CA3, and CA4 have been isolated from the error systems of Figures 2-8, 2-9 and 2-11 and appear in Figures 4-3 a,b and c respectively. Remember that each figure captures two operators; one from $e(t)$ to $\underline{k}(t)$ and one from $e(t)$ to $u(t)$. That these operators indeed have infinite gain will be argued by modifying the qualitative argument of Section 4.2.2. Mathematical proofs such as those presented for Theorem 4.1 and 4.2 in Section 4.2.1 could be constructed for each of these operators but do not prove very instructive, and, hence, are omitted.

The infinite gain operators of CA2, depicted in Figure 4-3a differ from the operators of CA1 only in that the first multiplication is by $\underline{\Gamma}\ \underline{v}(t)$ instead of $\underline{\Gamma}\ \underline{w}(t)$. If it is assumed that $\underline{v}(t)$ contains a sinusoid at the same frequency, ω_o, as $\underline{w}(t)$ does, then the infinite gain of the operators of Figure 4-3a follows from the arguments of Section 4.2.2. We note that $\underline{v}(t)$ and $\underline{w}(t)$ will contain sinusoids of the same frequency in practice since $\underline{v}(t)$ is merely $\underline{w}(t)$ passed through a linear time-invariant system.

The operators of CA3 depicted in Figure 4-3b differ from those of CA2 only in that there is a normalizing factor, $\lambda_0+\underline{v}^T(t)\underline{\Gamma}\ \underline{v}(t)$, in the first multiplication of Figure 4-3b. As long as the first multiplication produces a constant term, the following integrator will produce an infinite gain.

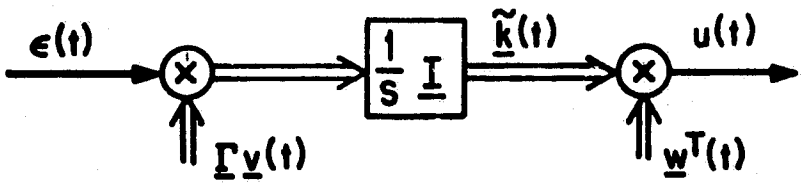

Figure 4-3a. The infinite gain operator of CA2.

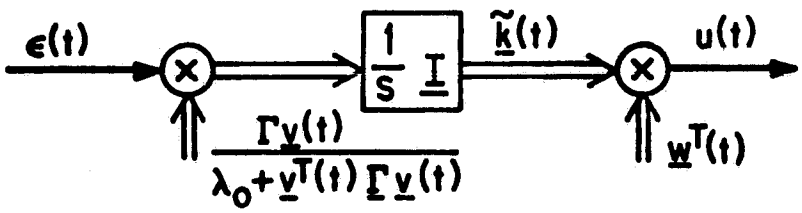

Figure 4-3b. The infinite gain operator of CA3.

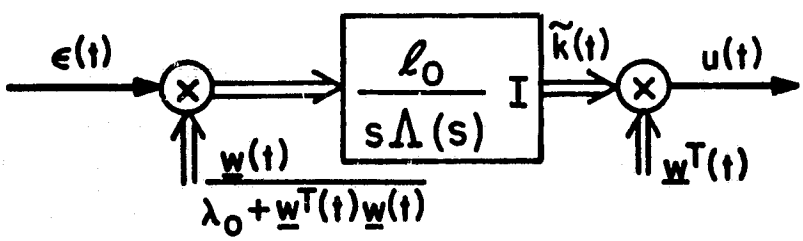

Figure 4-3c. The infinite gain operator of CA4.

Figure 4-3. The infinite gain operators of CA2, CA3, and CA4.

If a component of $\underline{v}(t)$ contains a dominant sinusoid at ω_o, so will a component of $\frac{\Gamma\,\underline{v}(t)}{\lambda_o+\underline{v}^T(t)\Gamma'\underline{v}(t)}$. This component will correlate with the sinusoid assumed present in $\epsilon(t)$ producing the constant input to the integrator which will in turn generate the infinite gain.

The operators of CA4 shown in Figure 4-3c differ from the operators of CA3 in that the original signal $\underline{w}(t)$ has returned in the first multiplication replacing $\underline{v}(t)$, a change of no consequence to the infinite gain nature of the operators, and the pure integrators of the previous algorithms have been replaced by the linear time-invariant operator $\frac{\ell_o}{s\Lambda(s)}$. This operator, $\frac{\ell_o}{s\Lambda(s)}$, still has infinite gain when its input is constant. Since infinite d.c. gain is all that is needed of the integrators in the argument of Section 4.2.2, the same arguments carry forward for the system of Figure 4-3c. Thus it can be concluded that the two operators for the CA4 algorithm shown in Figure 4-3c are also infinite gain.

4.2.4 The Generic Nature of the Infinite Gain Operator in Adaptive Control

As mentioned in Section 4.2.3, the infinite gain system of Figure 4-1 appears in various equivalent forms in all algorithms considered. Also, it should not come as a surprise that all the adaptive stability proofs available to date are centered around accomodating this operator. The following discussion is offered as a supportive argument to the statement that infinite gain operators of this type are in some sense generic to the adaptive control problem and its associated "learning" or "adaptation" mechanism.

One of the basic premises of adaptive control is that the control input to the plant is synthesized via multiplication by some time-varying gains of feedback signals generated from the plant output and the plant input as in Figure 4-4, according to:

$$u(t) = \underline{k}^T(t)\ \underline{C}[y(t),u(t)] \qquad (4\text{-}21)$$

where $\underline{C}$ is a linear time-invariant system representing an observer or an auxiliary variable generator. The gains, $\underline{k}(t)$, which will produce the desired closed-loop controller must be either estimated directly or derived from other estimated parameters. In

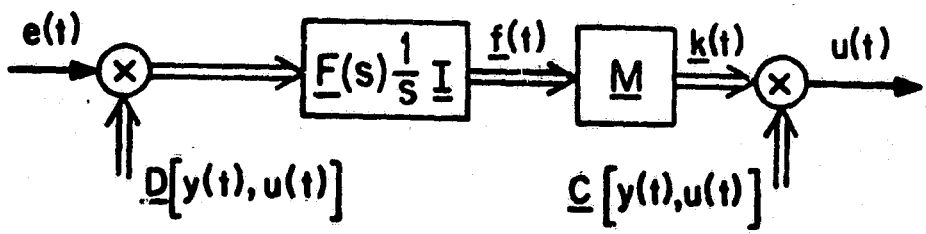

Figure 4-4. Infinite gain operator generically present in adaptive control.

general, one can write for these parameters the equation:

$$\underline{k}(t) = \underline{M}[\underline{f}(t)] \tag{4-22}$$

where $\underline{M}$ is usually a memoryless map, often the identity map, as it is in CA1-CA4. The only information available for identification is the plant input, the plant output and the error between the plant output and either a desired or expected plant output. All the usual methods of parameter identification (see, e.g., [65]) use this information by first correlating or multiplying the output error with signals generated from the plant input and output by a linear time-invariant system; the outcome of these operations is represented by the vector $\underline{D}[y(t),u(t)]$ in Figure 4-4.

Since the parameter to be estimated must ideally be able to move towards the correct values and converge there in the absence further input, the correlation must be followed by an operator that contains an integrator, i.e.

$$\underline{f}(t) = \underline{F}\,\frac{1}{s}\,\underline{I}[e(t)\underline{D}[y(t),u(t)]] \tag{4-23}$$

where $\underline{F}$ is a linear time-invariant system.

If y(t) and e(t) consist of a dominant sinusoid of a particular frequency, in addition to other small signals, the system of Figure 4-4 can be shown to have infinite gain by the arguments of Section 4.2.2.

We note here that Ioannou [52] has relaxed the requirement that the parameters be able to converge to match the model exactly and has replaced the integrator, the $\frac{1}{s}$ of eqn. (4-23), with

$$\frac{1}{s+\sigma}$$

If σ is kept small, the parameters may be able to remain close to the desired values while the infinite gain operator of Figure 4-4 is reduced to a high gain operator. (The gain will be proportional to $\frac{1}{\sigma}$). The change allowed Ioannou to prove local stability of the modified CAl algorithm when the adaptive system is driven by low frequency sinusoids in the presence of unmodeled dynamics whose poles are at a much larger frequency than the properly modeled poles of the plant. Such a result is consistent with the analysis of this chapter.

If σ were made too large, all the variable feedback parameters in the nominal control system would be constantly drawn toward zero. Only a large output error would be able to drive the parameters towards their desired values.

Thus, the adaptive system would at best settle with a large magnitude steady-state error. The reference model would not be matched at all.

Finally, we note that the infinite gain operator as a non-linear system only exhibits its infinite gain for certain classes of inputs and signals, $\underline{w}(t)$. In particular, signals which are dominated by distinct sinusoids will cause infinite gain while signals with flat power spectrum will not. This can be seen by analyzing the system of Figure 4.2 while assuming different frequency profiles for e(t) and w(t). We note, however, that in Section 4.3.1 it is shown that the types of signals that do give rise to infinite gain arise in practical situations.

4.3 Two Mechanisms of Instability

In the last section, it was shown that all the continuous-time adaptive control algorithms studied in this thesis contain an infinite gain operator. In this section, we use the algorithm CA1 to introduce and delineate two mechanisms which may cause unstable behavior in the adaptive system CA1 when it is implemented in the presence of unmodeled dynamics and excited by sinusoidal reference inputs or by disturbances. The arguments made for CA1 are valid for algorithms CA2, CA3, and CA4 *mutatis mutandis*. Since the arguments of instability are heuristic in nature, they must be verified by simulation. This will be done in Section 4.4.

4.3.1 The Causes of Possible Instability

In order to demonstrate the infinite gain nature of the feedback operator of the error system of CA1 in Section 4.2.1, it was assumed that a component of $\underline{w}(t)$ had the form

$$w_i(t) = b + c \sin\omega_o t \tag{4-5}$$

and that the error had the form

$$e(t) = a \sin\omega_o t \tag{4-6}$$

The arguments of Section 4.3.2 indicate that, if $e(t)$ and a component of $\underline{w}(t)$ have distinct sinusoids at a common frequency,

the operator $G_{\underline{w}(t)}$ of eqn. (4-1) and the operator $H_{\underline{w}(t)}$ of eqn. (4-18) will have infinite gains. Two possibilities for e(t) and $\underline{w}(t)$ to have the forms of eqn. (4-6) and eqn. (4-5) are now considered.

Case (1): If the reference input consists of a sinusoid and a constant, e.g.

$$r(t) = r_1 + r_2 \sin\omega_o t \qquad (4\text{-}24)$$

where r_1, and r_2 are constants, then the plant output y(t) will contain a constant term and a sinusoid at frequency ω_o. Since

$$\underline{w}(t) = \begin{bmatrix} r(t) \\ \underline{w}_u(t) \\ \underline{w}_y(t) \end{bmatrix}$$

and $$w_{ui}(t) = \frac{s^{i-1}}{p} \quad [u(t)]; \quad i=1,2,\ldots,n-1 \qquad (2\text{-}4)$$

and $$w_{yi}(t) = \frac{s^{i-1}}{p} \quad [y(t)]; \quad i=1,2,\ldots,n \qquad (2\text{-}5)$$

all components of the vector $\underline{w}(t)$ will contain a constant and a sinusoid of frequency ω_o.

If the controlled plant matches the model at d.c. but not at the frequency ω_o, the output error

$$e(t) = y(t) - y_M(t) \qquad (2\text{-}13)$$

will contain a sinusoid at frequency ω_o. Thus, the conditions for infinite gain in the feedback path of Figure 4-1 have been attained.

Case (2): If a sinusoidal disturbance, d(t), at frequency ω_o enters the plant output, as shown in Figure 4-5, the sinusoid will appear in $\underline{w}(t)$ through the following equation which replaces eqn. (2-5) in the presence of an output disturbance

$$w_{yi}(t) = \frac{s^{i-1}}{P} [y(t)+d(t)]; \; i=1,2,\ldots,n \qquad (4\text{-}25)$$

The following equation replaces eqn. (2-13) when an output disturbance is present

$$e(t) = y(t) + d(t) - y_M(t) \qquad (4\text{-}26)$$

Any sinusoid present in d(t) will also enter e(t) through eqn. (4-26).

Thus the signals e(t) and $\underline{w}(t)$ will contain sinusoids of the same frequency and the operators $H_{\underline{w}(t)}$ and $G_{\underline{w}(t)}$ will display an infinite gain.

We note here that while the frequencies present in the reference input can be controlled by the designer of the adaptive system, there is no control over what disturbances are present. Sinusoidal disturbances, in fact, are extremely common from a number of sources.

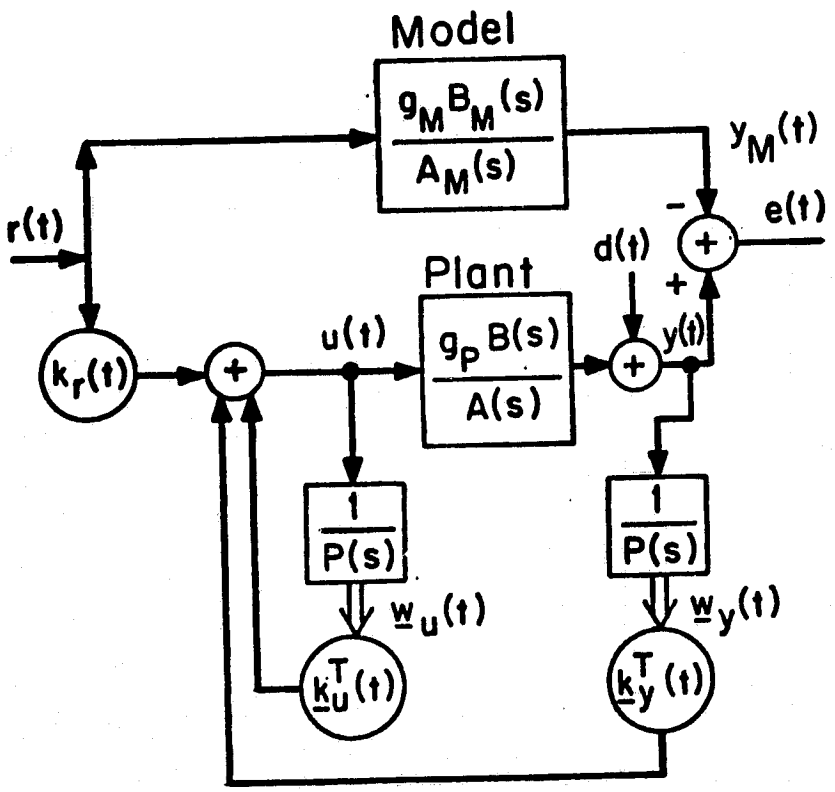

Figure 4-5. Controller structure of CA1 with additive output disturbance, d(t).

4.3.2 Instability Due to the Gain of the Operator $G_{\underline{w}}$ of Equation (4-1)

The operator $G_{\underline{w}}$ of eqn. (4-1) is not only an infinite gain operator but its gain influences the system in such a manner as to allow arguments using linear systems concepts, as outlined below.

Assume, initially, that the error signal is of the form of eqn. (4-6), i.e., a sinusoid at frequency ω_o. Assume also that a component of $\underline{w}(t)$ is of the form of eqn. (4-5), i.e., a constant plus a sinusoid at the same frequency ω_o as the input. The output of the infinite gain operator, $G_{\underline{w}(t)}$ of eqn. (4-1), as given by eqn. (4-9) consist of a sinusoid at frequency ω_o with a gain which increases linearly with time plus other terms at 0 radians/sec (i.e. d.c.) and other harmonics of ω_o; i.e.

$$u(t) = \frac{1}{2} ac^2 t \sin\omega_o t + \quad \text{other terms.}$$

Then the infinite gain operator manifests its large gain by producing at the output a sinusoid at the same frequency, ω_o, as the input sinusoid but with an amplitude which increases linearly with time plus some other signals. By concentrating on the signal at frequency ω_o and viewing the operator $G_{\underline{w}(t)}$ as a simple time-increasing gain with no phase shift at the frequency ω_o and very

small gain at other frequencies, we will be able to come up with a mechanism for instability of the error system of Figure 4-1, redrawn in Figure 4-6 which emphasizes the impact of the operator $G_{\underline{w}(t)}$.

If the forward path, $\frac{g^*B^*}{k_r^*A^*}$, of the error loop of Figure 4-6 has less than $\pm$ 180° phase shift at the frequency ω_o, and if the gain of $G_{\underline{w}(t)}$ were indeed small at all other frequencies, then the high gain of $G_{\underline{w}(t)}$ at ω_o would not affect the stability of the error loop.

If, however, the forward loop, $\frac{g^*B^*}{k_r^*A^*}$, does have 180° phase shift at ω_o, the combination of this phase shift with the sign reversal will produce a positive feedback loop around the operator $G_{\underline{w}(t)}$, thereby reinforcing the sinusoid at the input of $G_{\underline{w}(t)}$. The sinusoid will then increase in amplitude linearly with time, as the gain of $G_{\underline{w}(t)}$ grows, until the <u>combined gain</u> of $G_{\underline{w}(t)}$ and $\frac{g^*B^*}{k_r^*A^*}$ exceeds unity at the frequency ω_o. At this point, the loop itself will become unstable and all signals will grow without bound very quickly (as the effects of the unstable loop and continually growing gain of $G_{\underline{w}(t)}$ compound.)

Since the infinite gain of $G_{\underline{w}(t)}$ can be achieved at any frequency ω_o, if $\frac{g^*B^*}{k_r^*A^*}$ has $\pm$ 180° phase shift at any frequency

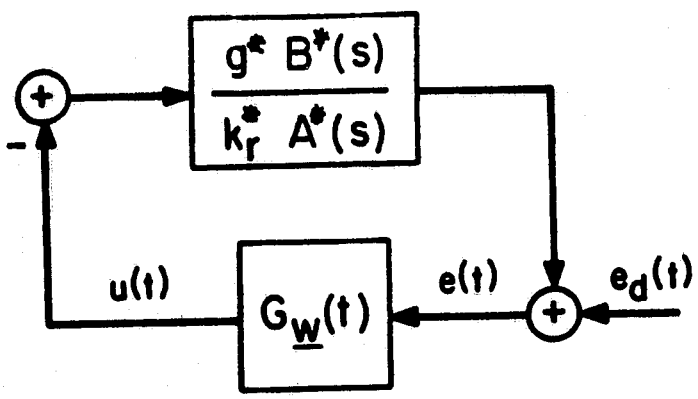

Figure 4-6. Error system of CA1 emphasizing role of $G_{\underline{w}}$

the adaptive system is susceptible to instability from either a reference input or a disturbance as shown in Section 4.3.1.

Thus the importance of the Relative Degree Assumption A3 of Section 2.2.1.2 which allows one to assume that $\frac{g^*B^*}{k_r^*A^*}$ is strictly positive real is seen. The stability proof of CA1 hinges on the assumption that $\frac{g^*B^*}{k_r^*A^*}$ is strictly positive real and that $G_{\underline{w}(t)}$ is passive, i.e.

$$\int_0^\infty G_{w(t)}[e(t)]\, e(t)dt \geq 0 \qquad (4\text{-}27)$$

Both properties of positive realness and passivity are properties which are independent of the gain of the operator involved. However, it is always the case that, due to the inevitable unmodeled dynamics, only a bound is known on the gain of the plant at high frequencies. Therefore, for a large class of unmodeled dynamics in the plant, including all unmodeled dynamics with relative degree two or greater, the operator, $\frac{g^*B^*}{k_r^*A^*}$, will have $\pm$ 180° phase shift at some frequency and be susceptible to unstable behavior, if subjected to sinusoidal reference inputs and/or disturbances in that frequency range.

4.3.3 Instability Due to the Gain of the Operator $H_{\underline{w}}$ of Equation (4-18)

In the previous subsection, the situation was examined where the amplitude of the sinusoidal error e(t) grew with time due to a positive feedback mechanism in the error loop. In this subsection, we explore the situation where the sinusoidal error, e(t), is not at a frequency where it will grow due to the error system but rather when there exist persistent steady-state errors. Such a persistent error could arise from either or both of the two mechanisms discussed in Section 4.3.1.

1) A reference input with a number of frequencies is applied and the controlled plant with unmodeled dynamics cannot match the model in amplitude and phase for all reference input frequencies involved. This will cause a persistent sinusoid in <u>both</u> the error e(t), through eqn. (2-18), <u>and</u> the signals $\underline{w}(t)$, through eqns. (2-4) and (2-5)

and/or

2) An output sinusoidal disturbance, d(t), enters as shown in Figure 4-5, causing the persistent sinusoid directly on e(t), through eqn. (4-26), and $\underline{w}(t)$ through eqn. (4-25).

Assume that, through one of the above or any other mechanism, a component of $\underline{w}(t)$ contains a sinusoid at frequency ω_o as in eqn. (4-5) and that e(t) contains a sinusoid of the same frequency. Then the operator $H_{\underline{w}(t)}$ has infinite gain and the norm of the output signal of this operator, $\tilde{k}(t)$, increases without bound. The signal, $\tilde{k}(t)$, will take the form of eqn. (4-8), repeated here:

$$\tilde{k}(t) = \tilde{k}_o + \frac{1}{2} ac\ t + \frac{ab}{\omega_o} - \frac{ab}{\omega_o} \cos\omega_o t - \frac{ac}{4\omega_o} \sin 2\omega_o t \qquad (4\text{-}8)$$

From the second term one can see that <u>the parameters of the controller</u>

$$\underline{k}(t) = \underline{k}^* + \underline{\tilde{k}}(t) \qquad (2\text{-}14)$$

<u>will increase without bound.</u>

If there are any unmodeled dynamics at all, increasing the size of the nominal feedback controller's parameters without bound will cause the adaptive system to become unstable. Indeed, since it is the gains of the nominal feedback loop that are unbounded, the system will become unstable for a large class of plants including all those whose relative degree is three or more even if no unmodeled dynamics are present.

4.4 Simulations with Time-Varying Inputs

4.4.1 Introduction

In this section, the response of the various continuous-time adaptive algorithms is explored through the use of simulation. First, it is demonstrated that the heuristic argument of Section 4.3.2 which explains the instability caused by sinusoidal inputs of a certain frequency is valid. This is followed with a short demonstration and discussion of the response of the algorithms to sinusoidal reference inputs which are of a frequency other than that at which $\frac{g^*B^*}{k_r^*A^*}$ of Figure 4-6 has $\pm$ 180° phase shift.

4.4.2 Simulations of Algorithms CA1, CA2 and CA3 with Sinusoidal Reference Inputs

The simulations were generated using the usual plant with unmodeled dynamics

$$y(t) = \frac{2}{(s+1)} \quad \frac{229}{(s^2+30s+229)} [u(t)] \qquad (3\text{-}27)$$

and the usual reference model

$$y_M(t) = \frac{3}{s+3} [r(t)] \qquad (3\text{-}20)$$

The simulations were all started out with the initial conditions

$$k_y(0) = -0.65 \qquad k_r(0) = 1.14 \qquad (4\text{-}28)$$

For all three of these algorithms the nominal controlled plant is the same, given by eqn. (2-22) and for the parameters of eqn. (4-28) equals

$$\frac{g^*B^*}{A^*} = \frac{527}{s^3+31s^2+259s+527} \qquad (4\text{-}29)$$

The reference input signal was chosen based upon the discussion of Section 4.3.2:

$$r(t) = 0.3 + 1.85 \sin 16.1t \qquad (4\text{-}30)$$

The frequency 16.1 rad/sec is the frequency at which the plant and, for all three algorithms CA1, CA2, and CA3, the transfer function $\frac{g^*B^*}{k_r^*A^*}$ has 180° phase lag. A small d.c. offset was provided so that the linearized system would be asymptotically stable (see Section 3.3.5). The relatively large amplitude, 1.85, of the sinusoid in eqn. (4-11) was chosen so that the unstable behavior would occur over a reasonable simulation time. A smaller sinusoidal amplitude could be used with the effect that the instability would occur at a much later time.

Note that the reference input (4-30) is not large from the point of view of the stability of the linearized system as discussed in Section 3.3.5 (where it was shown that a constant reference input

of r=4.2 was necessary to cause instability for CA1). The linearization for algorithms CA2 and CA3 was stable for all size inputs.

Adaptation gains of γ=1.0 were used for CA1 and CA2 and an adaptation gain of γ=3.0 was used in CA3 to offset the total gain reduction caused by the normalization of the adaptation gain in that algorithm.

Figures 4-7, 4-8, and 4-9 show respectively the simulation results for CA1, CA2, and CA3. The plant output and the parameters $k_r(t)$ and $k_y(t)$ are plotted. All three algorithms show the instability phenomena predicted in Section 4.3.2.

The amplitude of the plant output at the critical frequency (ω_o=16.1 rad/sec) and the parameters grow linearly with time, until the loop gain of the error system becomes larger than unity. At this point in time, even though the parameters are well within the region of stability for the linearized system, highly unstable behavior results.

Figure 4-10 shows the results of a simulation of the algorithm CA1 with

$$r(t)=0.3 + 2.0 \sin 8.0t \qquad (4\text{-}31)$$

This simulation demonstrates that, if the sinusoidal input is at a frequency for which the nominal controlled plant does not generate a large phase shift-(at ω_o=8.0, the phase shift of eqn. (4-29) is -133°), the algorithm may stabilize despite the high gain operator. Similar results were achieved with simulations of algorithms CA2 and CA3.

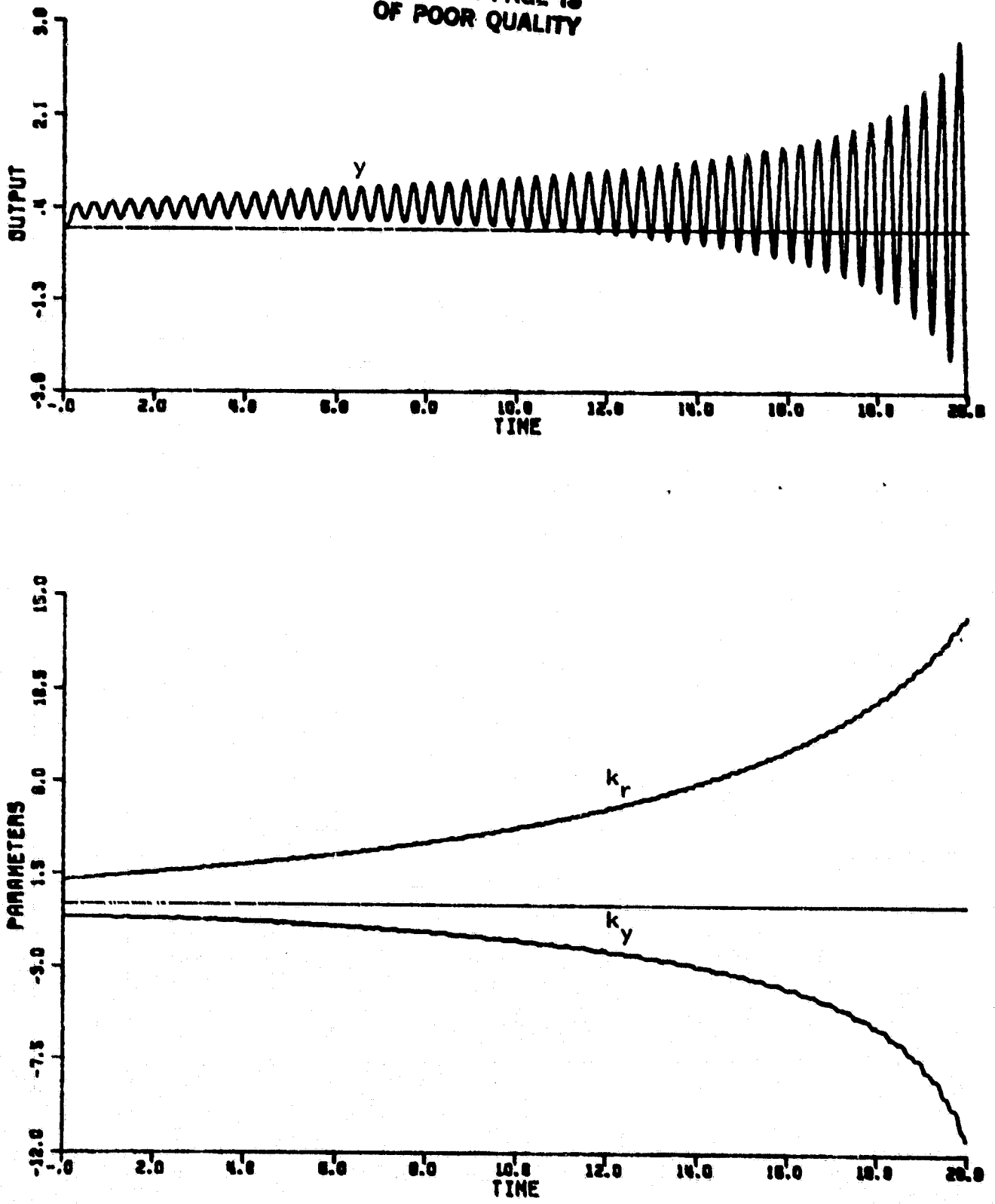

Figure 4-7. Simulation of CA1 with unmodeled dynamics and $r(t)=0.3 + 1.85\sin 16.1t$
(System eventually becomes unstable.)

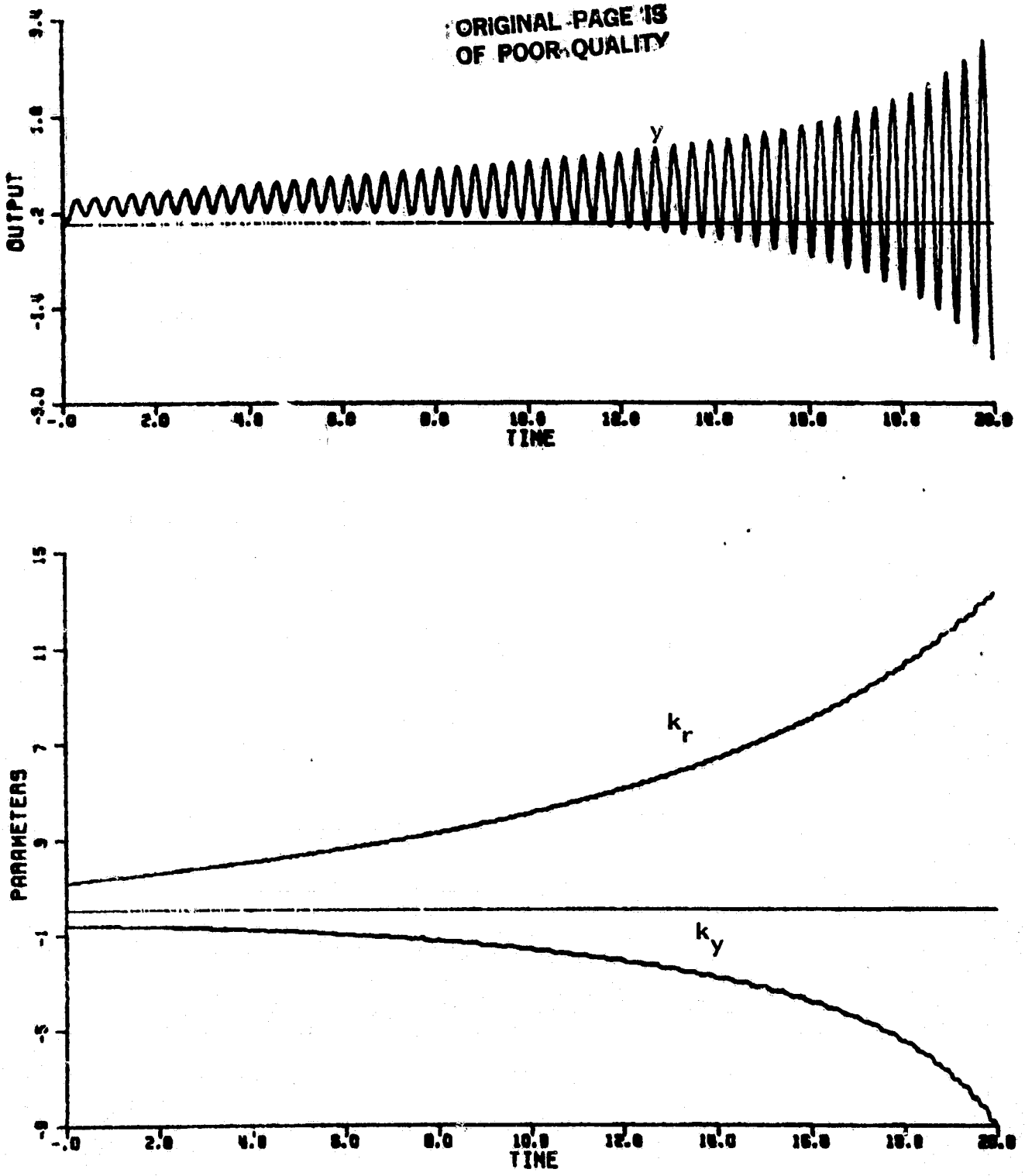

Figure 4-8. Simulation of CA2 with unmodeled dynamics and $r(t)=0.3 + 1.85\sin 16.1t$
(System eventually becomes unstable.)

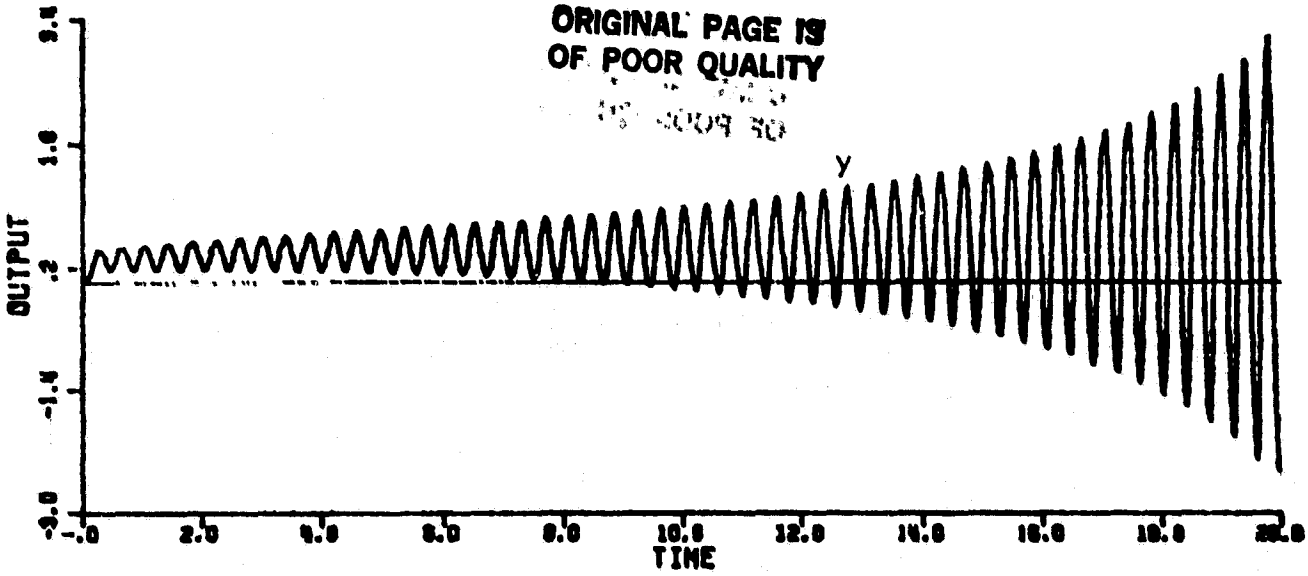

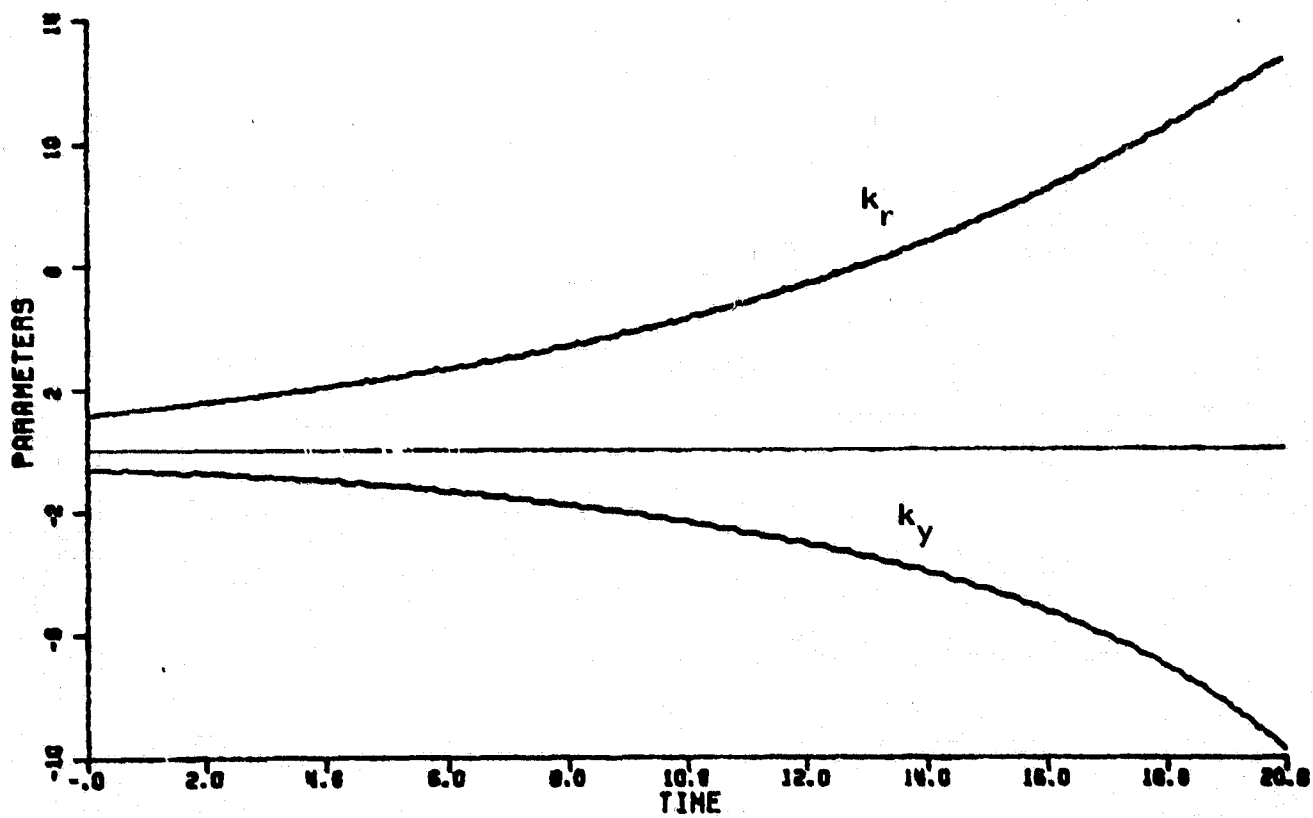

Figure 4-9. Simulation of CA3 with unmodeled dynamics and $r(t)=0.3 + 1.85\sin 16.1t$
(System eventually becomes unstable.)

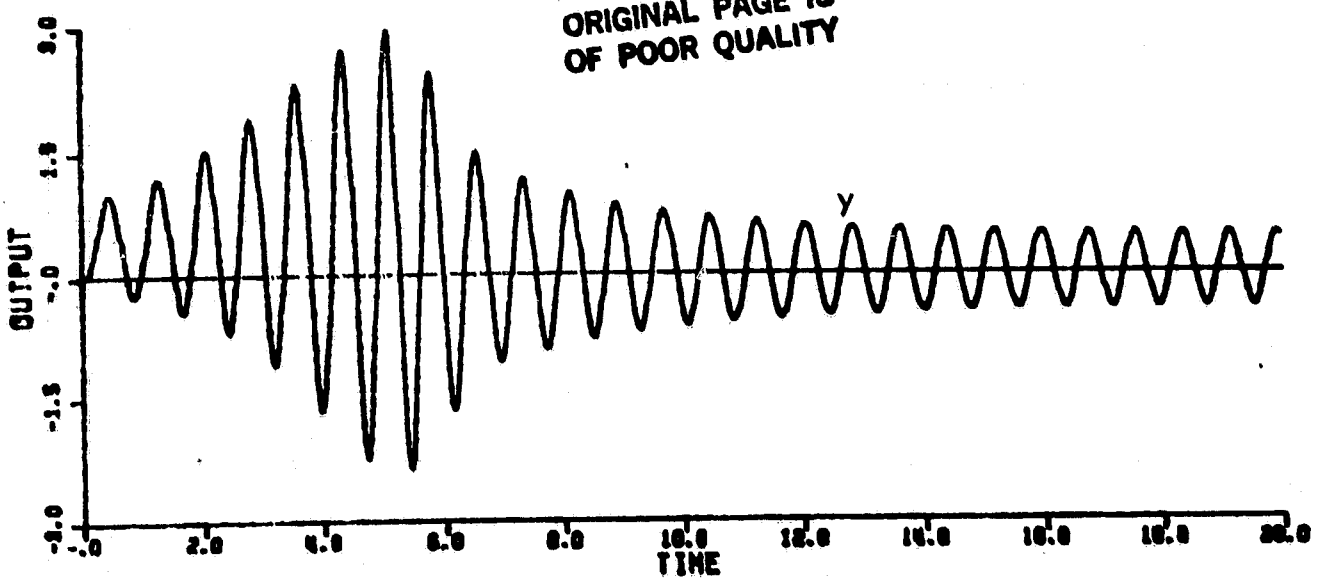

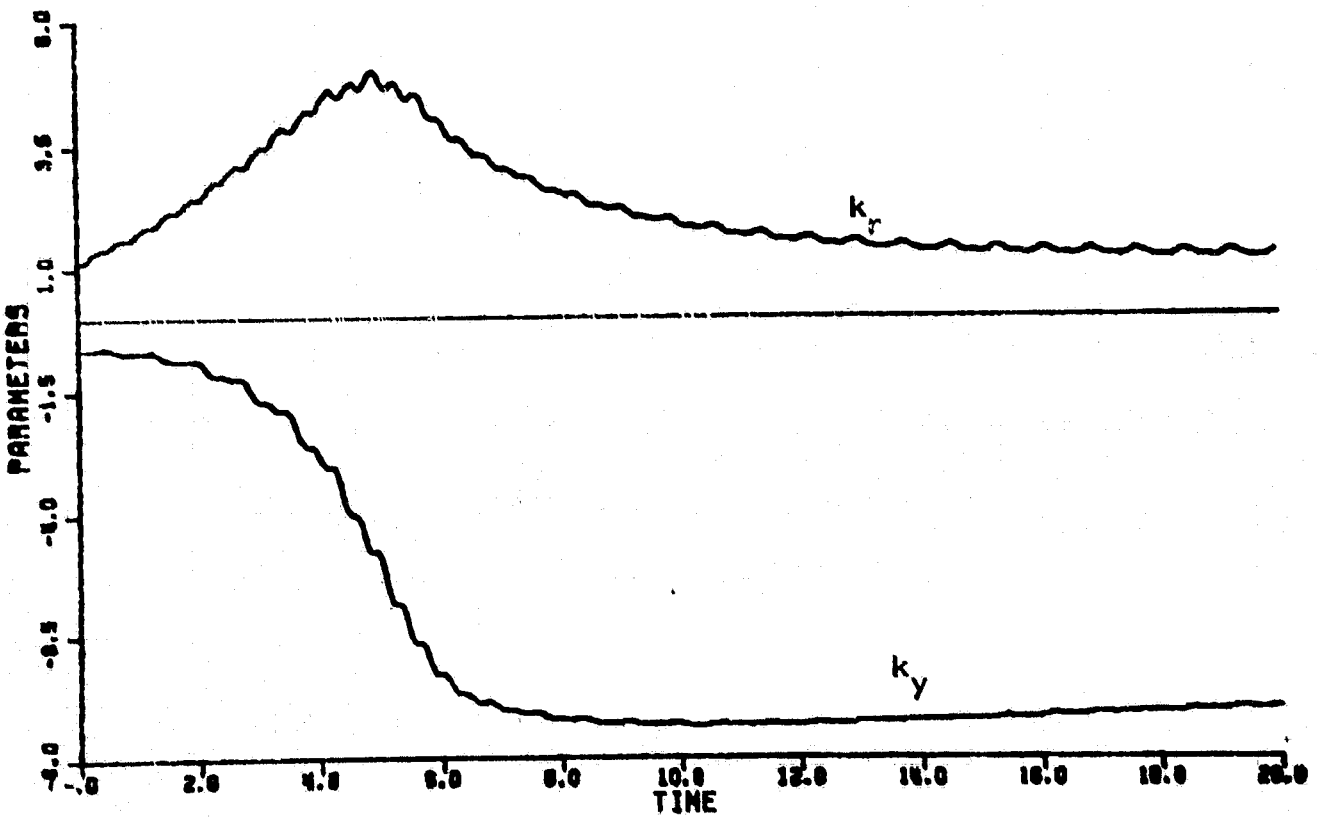

Figure 4-10. Simulation of CA1 with unmodeled dynamics and $r(t)=0.3 + 2.0\sin 8.0t$

(No instability observed).

4.4.3 Simulation of the Algorithm CA4 with Sinusoidal Reference Inputs

The algorithm CA4 requires a slight modification of the analysis. Due to the addition of a zero, from the filtering of L in this algorithm, (eqn. (2-63)), the phase of $\frac{g^*B^*}{k_r^*A^*}$ for CA4 is always less than 180° degrees. The same filtering, however, produces an added 90° phase lag in w_y and thus in the high gain operator.

Figure 4-11 shows the simulation results of running CA4 with

$$L = s+3 \tag{4-32}$$

and

$$r(t) = 0.3 + 1.85 \sin 16.1t \tag{4-33}$$

At this frequency (ω_o=16.1), $\frac{g^*B^*}{k_r^*A^*}$ has 90° phase shift while another 90° is generated by the high gain operator through the multiplication by w_y which has been shifted 90° from y by the filtering of $\frac{1}{L}$. Thus, the overall error loop has 180° phase shift, and the system becomes unstable just like the other algorithms for the reference input (4-33). An adaptation gain of γ=10 was used in the simulation to offset the attenuation of the additional filtering inherent in the CA4 algorithm.

An interesting effect occurs when we simulated CA4 with the reference input

$$r(t) = 0.3 + 2.0 \sin 8.0t \tag{4-34}$$

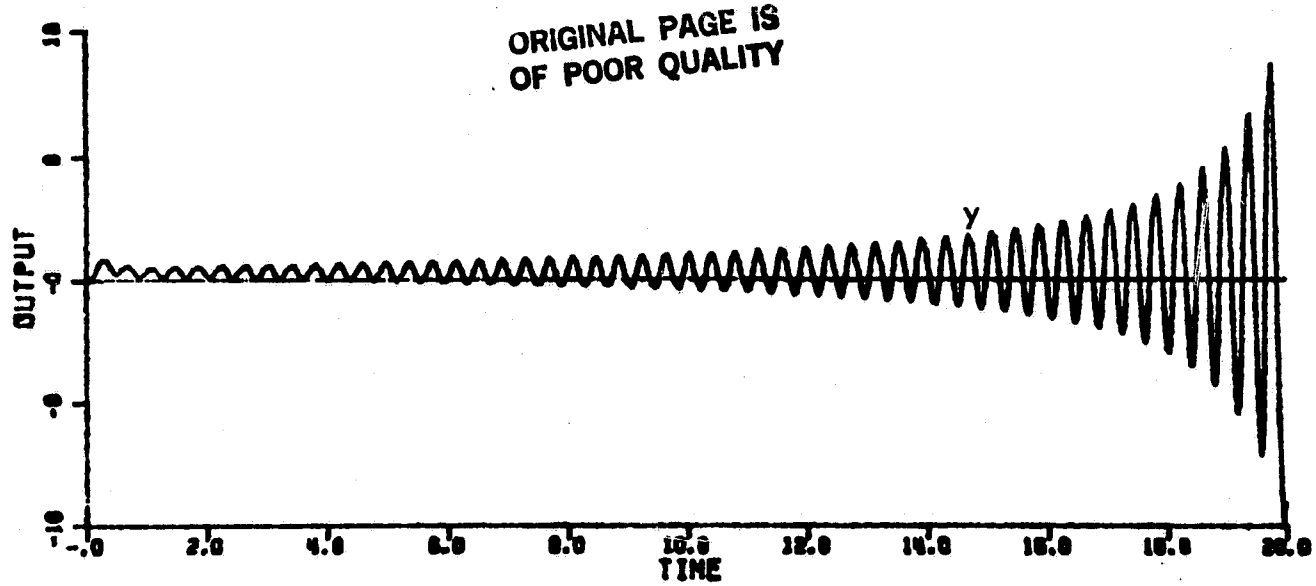

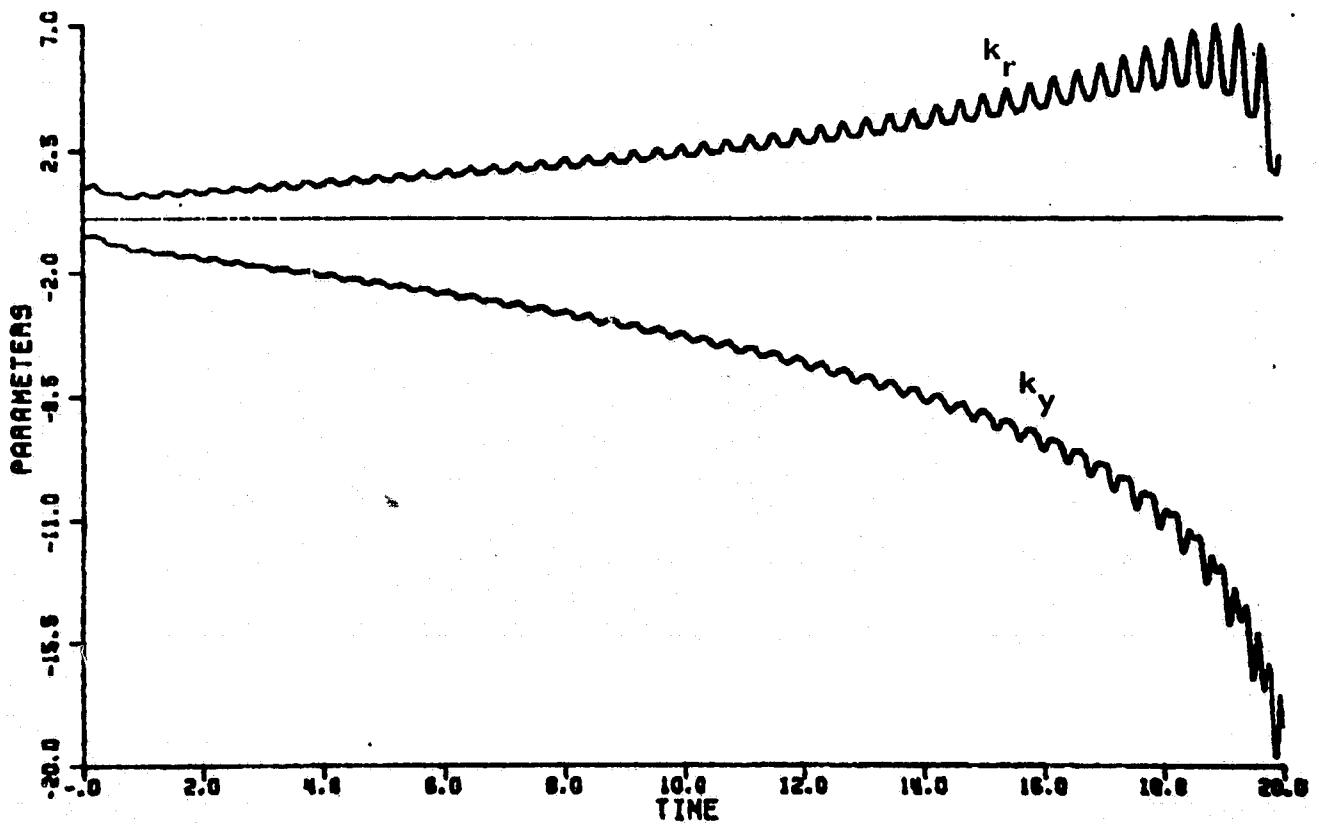

Figure 4-11. Simulation of CA4 with unmodeled dynamics and $r(t)=0.3+1.85\sin 16.1t$.
(System eventually becomes unstable.)

The total phase shift of the error system at this frequency (ω_o=8.0) is less than 180° but still greater than 90°. Figure 4-12 shows that the output appears to be converging.

However, the k_y parameter continues to drift as a correlation still exists between w_y and ϵ. When the simulation was allowed to run longer than shown in Figure 4-12, the parameter $k_y(t)$ continued to drift away until it moved to the point where the linearized error system was no longer stable. At this point the system broke wildly and suddenly into instability, because of the mechanism of Section 4.3.3.

Finally, Figure 4-13 shows the simulation of CA4 with

$$r(t)=0.3 + 2.0 \sin 1.5t \qquad (4\text{-}35)$$

At this frequency the filtering $\frac{1}{L}$ provides only -26° phase shift and $\frac{g^*B^*}{k_r^*A^*}$ provides only -40° phase shift. The system converges nicely.

4.4.4. Conclusions

The simulations of this section verify that the mechanisms for instability which were hypothesized by our heuristic arguments do indeed occur. The following statements about the continuous-time algorithms CA1-CA4, operating in the presence of unmodeled dynamics with sinusoidal reference inputs can be made:

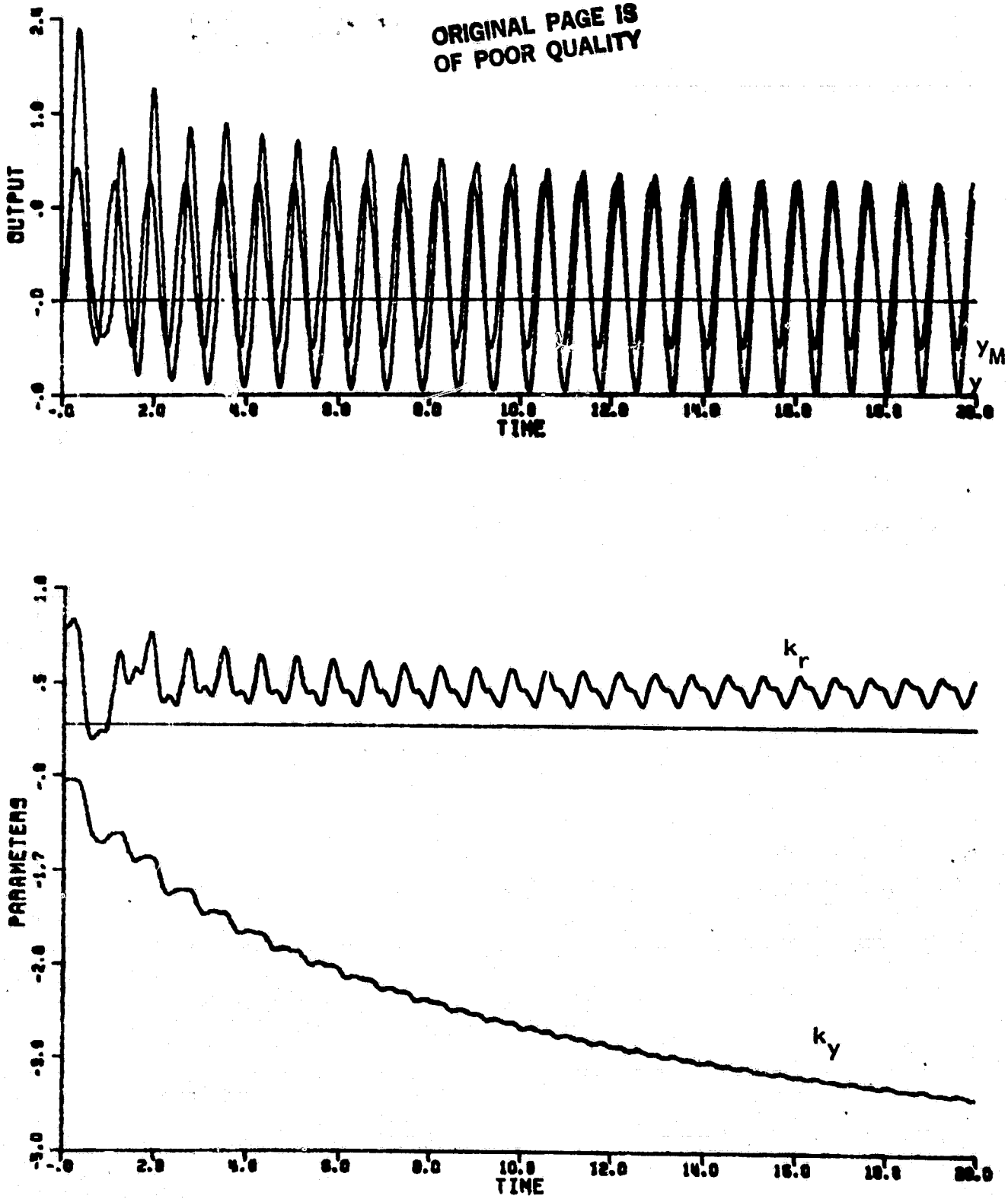

Figure 4-12. Simulation of CA4 with unmodeled dynamics and $r(t)=0.3 + 2.0\sin 8.0t$.
(System eventually becomes unstable.)

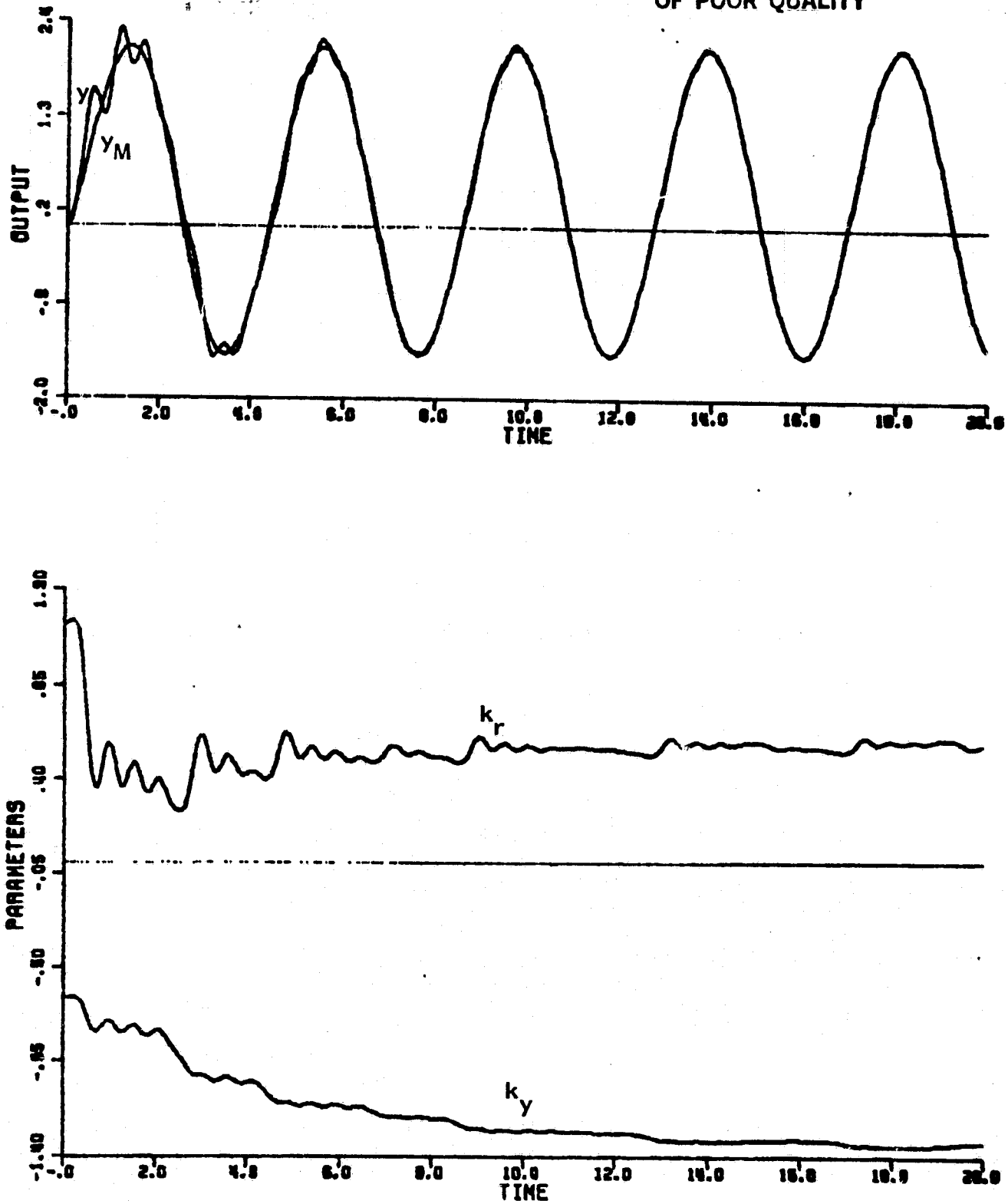

Figure 4-13. Simulation of CA4 with unmodeled dynamics and
$r(t)=0.3 + 2.0\sin 1.5t$
(No instability occurs.)

- When faced with certain frequency sinusoidal reference inputs in the presence of unmodeled dynamics the algorithms CA1-CA4 will produce an error function which is a growing sinusoid and will become unstable via the mechanism described in Section 4.3.2.
- Instability via the mechanism of Section 4.3.2 requires a high frequency reference input, i.e., it is highly likely to occur when the frequency of the reference inputs is at a frequency where the nominal controlled plant, ($\frac{g^*B^*}{k_r^*A^*}$ of eqn. (2-22) for CA1-CA3 and of eqn. (2-63) for CA4) has $\pm$ 180° phase shift. Instability can still occur when the sinusoidal reference input is at a frequency where $\frac{g^*B^*}{k_r^*A^*}$ has more than $\pm$ 90° phase shift, as the feedback operator, $G_{\underline{w}(t)}$ of eqn. (4-1), can provide up to $\pm$ 90° phase shift. This effect occurred in the simulation of Figure 4-11. When the frequency of the reference input is at a frequency where $\frac{g^*B^*}{A^*}$ has less than $\pm$ 90° phase shift, stability is not guaranteed but instability will not occur by the mechanism of Section 4.3.2.

- If the reference input is such that the controlled plant cannot match the model for all frequencies present in the reference input, instability can occur by the mechanism of an unbounded parameter gain, as described in Section 4.3.3. Instability of this type is shown in the simulation of Figure 4-12.

Finally, we note that the results of this section merely verify that some situations for possible instability which were argued heuristically in the previous section to be part of continuous-time algorithms do indeed occur. However, there is no proof that instability will occur in these situations nor is there any guarantee that instability will not occur in situation where the heuristic arguments do not indicate instability.

4.5 The Use of Filters on the Output

4.5.1 Introduction

Since the infinite gain behavior of the adaptive control system is most disruptive at high frequencies, it appears possible that better behavior can be attained by using low pass filters either on the plant output or the error signal. It has been argued by several researchers that such filtering will allow the adaptation mechanism to ignore high frequency components and, therefore, not be fooled by them. We disagree with such conjectures: Rather, we argue that what constitutes a high frequency signal is determined by the amount of phase shift present in the system; "tricks" such as the introduction of low pass filters merely add to that phase shift and, thereby, lower the frequency of the reference signal which will cause the adaptive system to become unstable.

4.5.2 Filters on the Plant Output

The effect of filters used directly on the plant output as shown, for example, in Figure 4-14 of CA1 is easily explained. The filter is simply considered as part of the plant. The designer either ignores the filter in the adaptive design, a strategy which

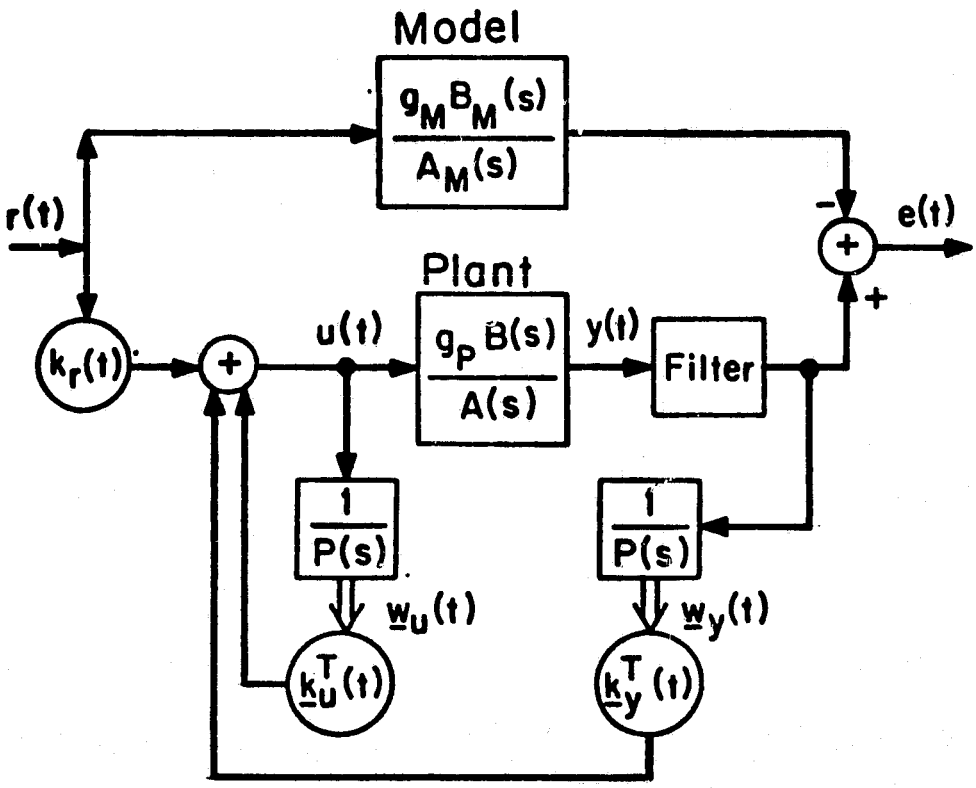

Figure 4-14. Controller structure for CA1 with filter on plant output.

reduces the filter itself to the realm of unmodeled dynamics, or he increases the order of the adaptive system and adapts around the filter as well as the plant. This latter strategy takes the system back to the beginning as far as unmodeled dynamics in the plant-filter combination are concerned.

Thus, adding a filter to the output of the plant does nothing to change the basic stability problem discussed in Section 4.3.2.

4.5.3 Filters on the Output Error

Filtering the output error is slightly different in that the filtering no longer appears in the primary control loop around the plant, but it only appears in the adaptation mechanism as shown in Figure 4-15. A possible analysis is as follows.

Assume some kind of filter, $\frac{F}{G}$, were used on the error signal of the CAl algorithm. Then the error system of Figure 2-2 becomes the error system of Figure 4-15. Instead of the debilitating sinusoid explained in Section 4.1 being at the frequency where the phase of $\frac{g^*B^*}{k_r^*A^*}$ is $\pm$ 180°, it is now simply where the phase of $\frac{g^*B^*F}{k_r^*A^*G}$ is $\pm$ 180° degrees. If $\frac{F}{G}$ is a low pass filter, then the destabilizing input will be at a lower frequency.

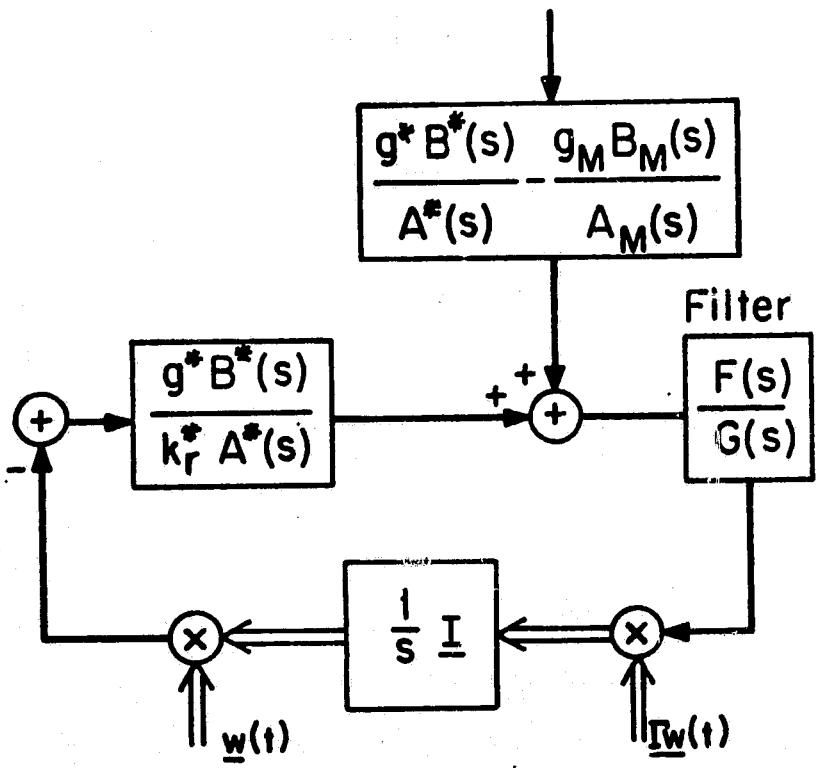

Figure 4-15. Error system of CA1 with filtering on output error.

Thus, we see that filtering the output error, like filtering the plant output itself, does nothing to change the basic stability problem outlined in Section 4.3.2.

4.6 Simulations of Responses to Disturbances

4.6.1 Introduction

It was mentioned in Section 4.3.1 that the sinusoid that drives the error system to instability could arise either from the reference input or from an output disturbance. In this section, it is shown that the instability mechanism explained in Section 4.3.2 does indeed occur when there is an output disturbance at the wrong frequency, entering the system as in Figure 4-5. In addition, the instability mechanism of Section 4.3.3, which will drive the algorithms unstable when there is a sinusoidal disturbance at any frequency, is also shown to actually take place.

The simulations of this section were generated with the usual plant with unmodeled dynamics.

$$y(t) = \frac{2}{(s+1)} \quad \frac{229}{s^2+30s+229} [u(t)] \qquad (3\text{-}27)$$

and the usual reference model

$$y_M(t) = \frac{3}{s+3} \quad [r(t)] \qquad (3\text{-}20)$$

The simulations were all started out with:

$$k_y(0) = -0.65 \qquad k_r(0)=1.14$$

For these parameters the nominal controlled plant of eqn. (2-22) is:

$$\frac{g^*B^*}{A^*} = \frac{527}{s^3+31s^2+259s+527} \tag{4-29}$$

4.6.2 Instability via the Mechanism of Section 4.3.2

Figure 4-16 shows the simulation results when algorithm CA1 is driven by

$$r = 0.3 \tag{4-36}$$

with a disturbance

$$d(t) = 5.59\times10^{-6} \sin 16.1t \tag{4-37}$$

At the frequency, $\omega_o=16.1$, $\frac{g^*B^*}{k_r^*A^*}$ of eqn. (4-29) has 180° phase shift. The by now expected growing instability occurs due to the mechanism of Section 4.3.2. The only surprise may be the minuteness of the disturbance ($\sim10^{-6}$) which will cause instability. The same unstable response was obtained with all the other algorithms considered.

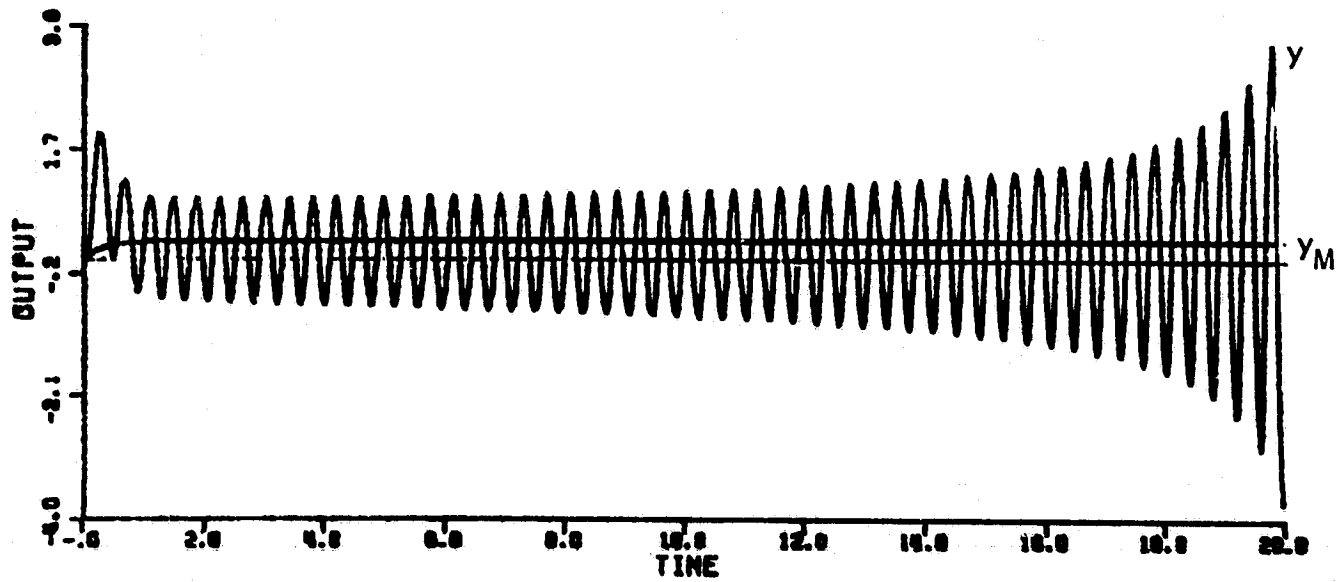

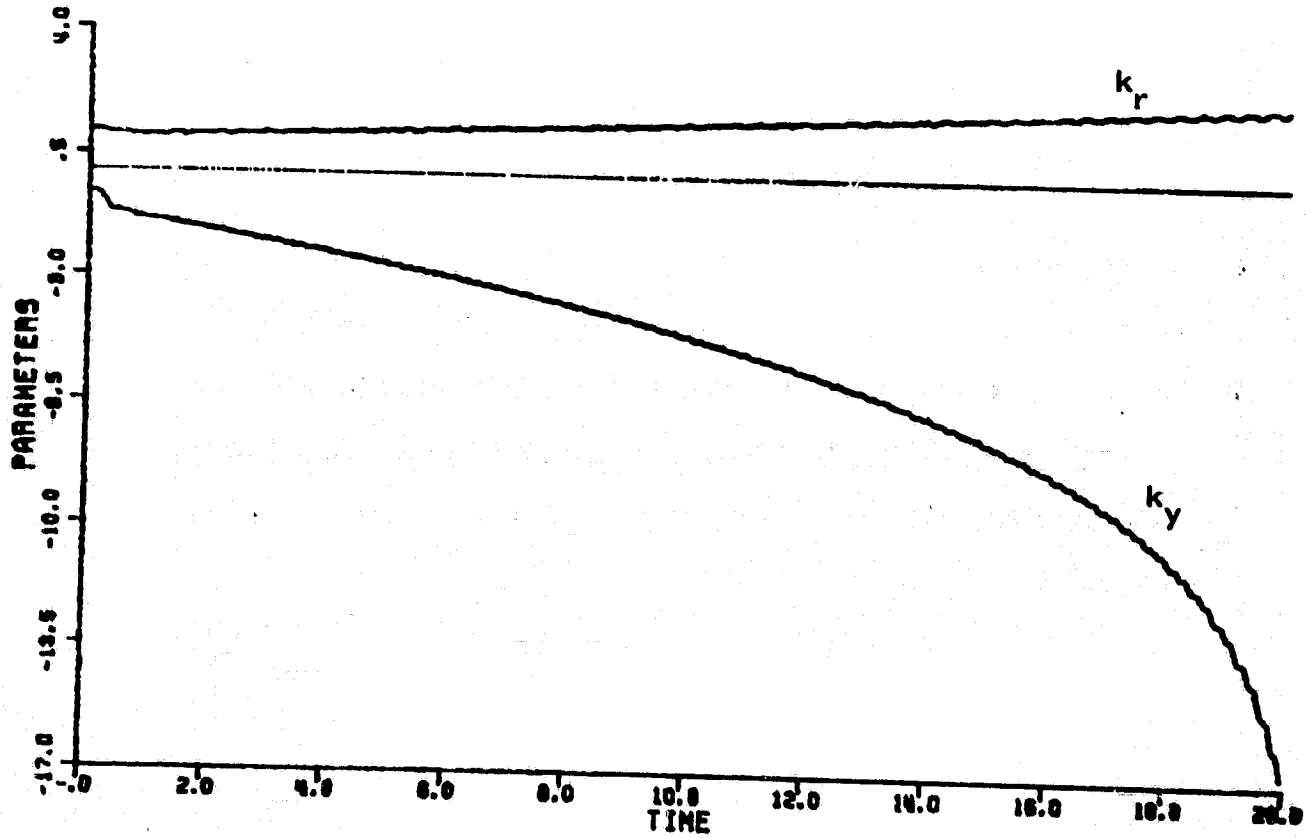

Figure 4-16. Simulation of CA1 with unmodeled dynamics, $r(t)=0.3$, and $d(t)=5.59\times10^{-6}\sin 16.1t$.

4.6.3 Instability via the Mechanism of Section 4.3.3

Figure 4-17 shows the results of a simulation of CA1 that was generated with

$$r=0.3 \tag{4-36}$$

but the disturbance was changed to

$$d(t) = 8.0\times10^{-6} \sin 5t \tag{4-38}$$

At $\omega_o=5$, $\frac{g^*B^*}{k_r^*A^*}$ of eqn. (4-29) provides only -102° phase shift so the sinusoidal error signal of increasing amplitude, which is characteristic of instability via the mechanism of Section 4.3.2, is not seen in Figure 4-17. What is seen is that the system becomes unstable by the mechanism of Section 4.3.3; while the output appears to settle down to a steady state sinusoidal error, the k_y parameter drifts away until the point where the controller becomes unstable. (Only the onset of unstable behavior is shown in Figure 4-17 in order to maintain scale.) We note also that, even when the error appeared settled its value represented a large disturbance amplification rather than rejection.

The most disconcerting part of this analysis is that none of the systems analyzed have been able to counter this parameter drift for a sinusoidal disturbance at any frequency tried!

Indeed, Figure 4-18 shows the results of a simulation run with reference input

$$r = 0.0 \tag{4-39}$$

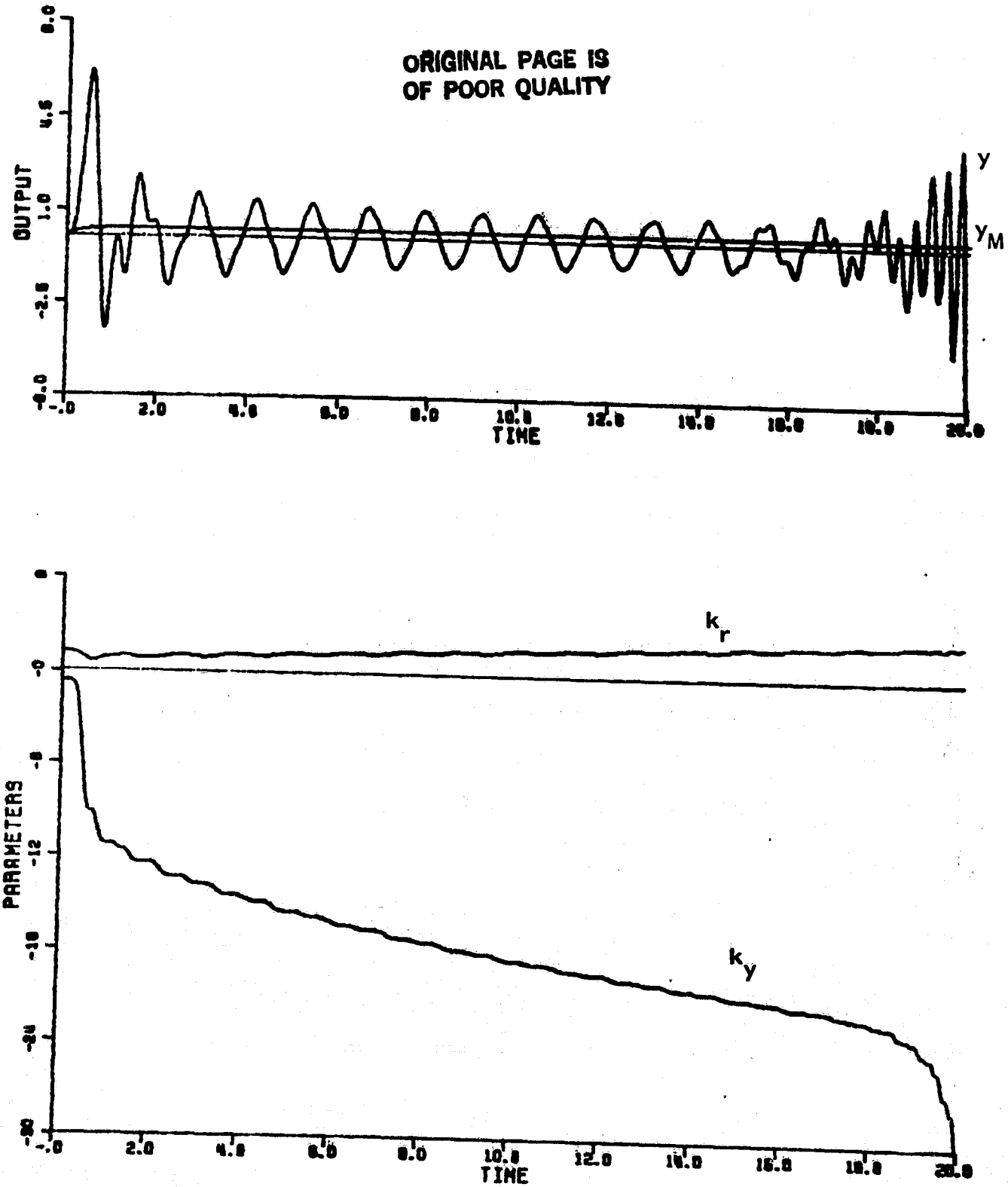

Figure 4-17. Simulation of CA1 with unmodeled dynamics, $r(t)=0.3$, and $d(t)=8.0\times10^{-6}\sin 5.0t$. (System eventually becomes unstable.)

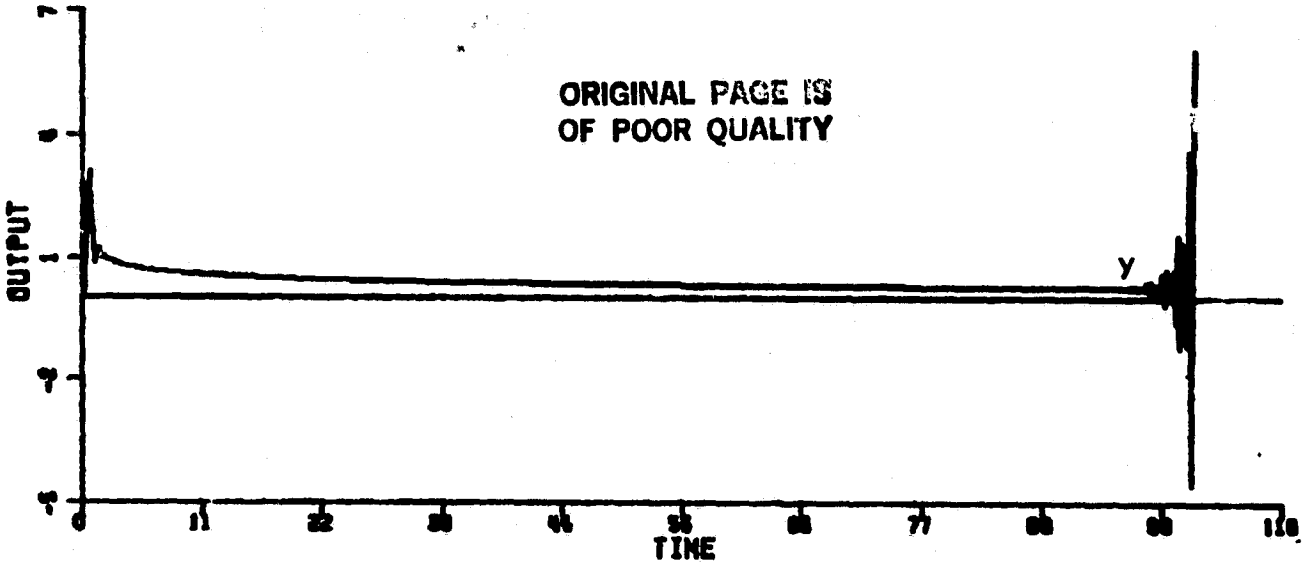

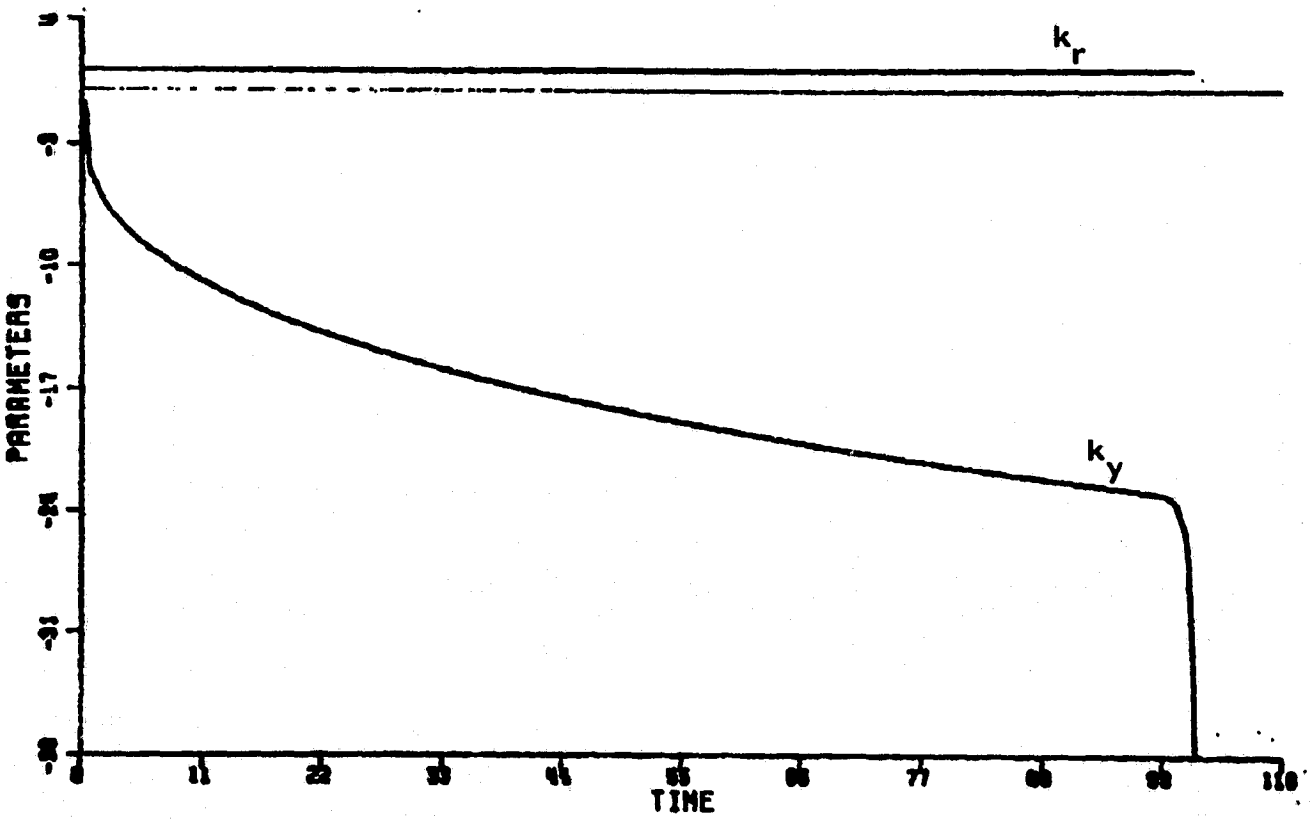

Figure 4-18. Simulation of CA1 with unmodeled dynamics, $r(t)=0.0$, and $d(t)=3.0\times10^{-6}$. (System eventually becomes unstable.)

and constant disturbance

$$d = 3.0 \times 10^{-6} \tag{4-40}$$

The simulation results show that the output again settles for a long time, again with disturbance amplification, but the parameter k_y increases in magnitude until instability ensues.* Thus the adaptive algorithm shows no ability to act even as a regulator when there are output disturbances.

4.6.4 Egardt's Modifications

The only one of the continuous-time algorithms in which disturbances are even mentioned during the development of the algorithm for the properly modeled case is CA4.

Egardt [11] gives a possible modification of CA4 in the presence of disturbances. The modifications considered consist of two fairly unsatisfactory alternatives. One of Egardt's modification assumes that there is an upper bound for the size of the disturbance at any time (an assumption that cannot be guaranteed in practice). Egardt suggests that all parameter adaptation be stopped when the error is less than this upper bound. The second of Egardt's

---

*The analysis of Iaonnou [66] shows that, if there were no disturbance in this case, the output would converge to zero. Iaonnou's thesis contains no analysis in the presence of disturbances.

modifications introduces a term into the parameter adjustment law which will arbitrarily decrease the magnitude of the parameter when the magnitude of the parameters gets too large. In this way, Egardt achieves bounded parameters and can then prove stability in the face of disturbances when there are no unmodeled dynamics.

It is not clear that either of the proposed modifications would work if unmodeled dynamics are present.

Even in the properly modeled case, these modification are designed to produce some kind of boundedness result with no assurance that the adaptive algorithm will produce a result with anywhere near the original intent.

4.6.5 Conclusions

In this section it has been shown that the adaptive control algorithms CA1-CA4, when operated in the presence of unmodeled dynamics and output disturbances at any frequency, display the traits of disturbance amplification and instability.

Unless something is done about this adverse reaction to disturbances in the presence of unmodeled dynamics, the adaptive algorithms examined cannot be considered as serious practical alternatives to other methods of control.

4.7 Conclusions

In this chapter it was shown by analytical methods, and verified by simulation results, that the adaptive algorithms CA1-CA4 have imbedded in their adaptation mechanisms infinite gain operators which, in the presence of unmodeled dynamics, will cause:

- instability, if the reference input is a high frequency sinusoid.
- disturbance amplification and instability, if there is a sinusoidal output disturbance at any frequency including d.c.

While the first problem can be alleviated by proper limitations on the class of permissible reference inputs, the designer has no control over the additive output disturbances which impact his system. Sinusoidal disturbances are extremely common in practice and can produce disastrous instabilities in the adaptive algorithms considered.

CHAPTER 5

ANALYSIS OF DISCRETE-TIME ALGORITHMS

In this chapter the discrete-time algorithms introduced in Section 2.3 will be analyzed. The constant input analysis that was performed for continuous-time algorithms in Chapter 3 will be performed for discrete-time algorithms in Section 5.1. In Section 5.2, it will be shown that the discrete-time algorithms also become unstable for certain types of sinusoidal inputs and disturbances. This exactly parallels the development for continuous-time algorithms that was presented in Chapter 4.

The following results are presented in this chapter:

- In the presence of unmodeled dynamics and constant reference inputs all the discrete-time algorithms considered will become unstable if the design parameters are not carefully chosen. The analysis of Section 5.1 provides a design tool for choosing the parameters properly.
- In the presence of unmodeled dynamics, high frequency reference inputs will cause all the adaptive systems studied to become unstable.
- A sinusoidal output disturbance <u>at any frequency</u> will cause the feedback parameters in all the

algorithms studied to increase without bound. This will cause the adaptive system to become unstable if any unmodeled dynamics are present.

In addition to the above results which parallel the results obtained for continuous-time systems, in Chapter 3 and 4, it is shown in this chapter that instabilities due to constant or sinusoidal reference inputs in the presence of unmodeled dynamics can be eliminated, if the system is sampled slowly enough. A slow sampling rate, however, does not help the stability properties in the presence of an output disturbance.

5.1 Analysis of Discrete-Time Algorithms with Constant Reference Inputs

5.1.1 Introduction

The development in this section parallels the development given in Chapter 3 for continuous-time algorithms. The same assumptions will be made, i.e., that the system is close to some nominal set of parameters, that the reference input and the nominal signals in the system are constant, and that the system is free from noise and disturbances. The system will be linearized around the nominal parameters and signals and the behavior of this linearized error system will be examined.

5.1.2 Analysis of DA2

The analysis of DA2 (see Section 2.3.3) is undertaken first since this is the simplest of the discrete-time algorithms and provides the clearest view of the issues involved.

The equations of DA2 (see Table 2-8) are analyzed by linearizing the system about a nominal set of parameters as was done for the continuous-time algorithms in, e.g., Section 3.3.6. Assume that $\underline{w}(t)$ from eqns. (2-94)-(2-96) is represented as follows:

$$\underline{w}(t) = \underline{w}^*(t) + \underline{\delta w}(t) \tag{5-1}$$

and that the parameters, $\underline{k}(t)$, are represented as follows:

$$\underline{k}(t) = \underline{k}^* + \underline{\delta k}(t) \tag{5-2}$$

Linearizing the system about $\underline{w}^*(t)$, $\underline{k}^*$ reduces the error system of Figure 2-16 to the linearized error system of Figure 5-1. If, in addition, the reference input, r, is assumed constant, then the signal $\underline{w}^*$ can be taken as a constant and the linearized error system of Figure 5-1 becomes linear and time-invariant. In Figure 5-1

$$\frac{g^*B^*q^{-d_p}}{k_r^*A^*} = \frac{k_r^*g_pq^{-d_p}B}{A(1-q^{-1}K_u)-g_pq^{-d_p}BK_y} \qquad (2\text{-}103)$$

The local dynamics of the error system are determined by first establishing a nominal system and then performing a d*-root locus on the error system of Figure 5-1. Note that the DA2 algorithm has a normalizing factor in the adaptive gain. The definition

$$d^* = \frac{\underline{w}^{*T}\underline{w}^*}{1+\underline{w}^{*T}\underline{w}^*} \qquad (5\text{-}3)$$

is used so that $0 \leq d^* \leq 1$.

The error system can then be represented as in Figure 5-2 with

$$G_E(q^{-1}) = \frac{g^*B^*q^{-d_p}}{(1-q^{-d})k_r^*A^*} \qquad (5\text{-}4)$$

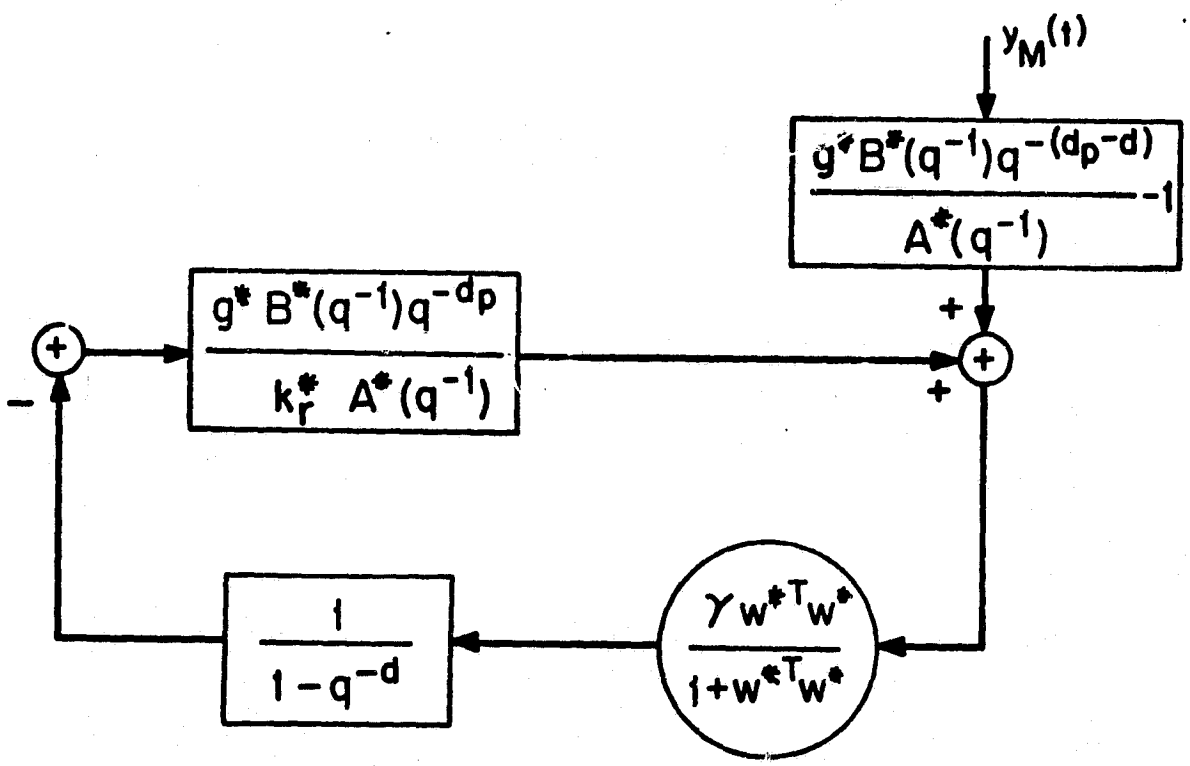

Figure 5-1. Linearized error system for DA2.

Using eqns. (5-4) and (2-103) it can be seen from Figure 5-2 that the roots of the linearized error system will be given by the solutions of the equation

$$\left(1-q^{-d}\right)\left(A\left(1-q^{-1}K_u\right)-g_p q^{-d_p} BK_y\right)+\gamma\, d^* g_p q^{-d_p} B=0 \qquad (5-5)$$

5.1.2.1 Analysis of System with No Unmodeled Dynamics

Consider first the case when the system is modeled properly As was mentioned in Section 2.3.3.2, it is possible to achieve

$$\frac{q^* B^* q^{-d_p}}{A^*} = q^{-d} \qquad (2-104)$$

with

$$K_r^* = \frac{1}{g_p} \qquad (5-6)$$

Substituting eqns. (2-104) and (5-6) into eqn. (5-4) yields:

$$G_E = \frac{g_p q^{-d}}{1-q^{-d}} \qquad (5-7)$$

The d*-root loci for the error system of Figure 5-2 with G_E as in eqn. (5-7) are given in Figure 5-3a for d=1 and in Figure 5-3b for d=3. In both cases, it can be seen that the linearized system is stable if

$$0 < \gamma d^* g_p < 2 \qquad (5-8)$$

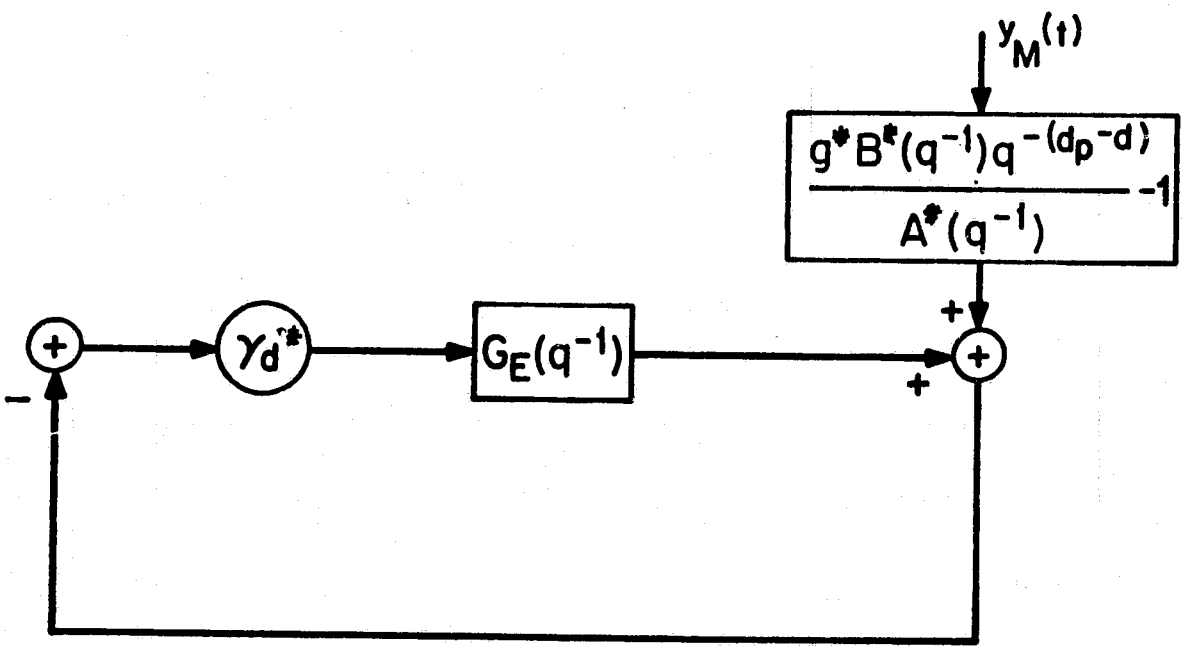

Figure 5-2. Reduced linearized error system for DA2.

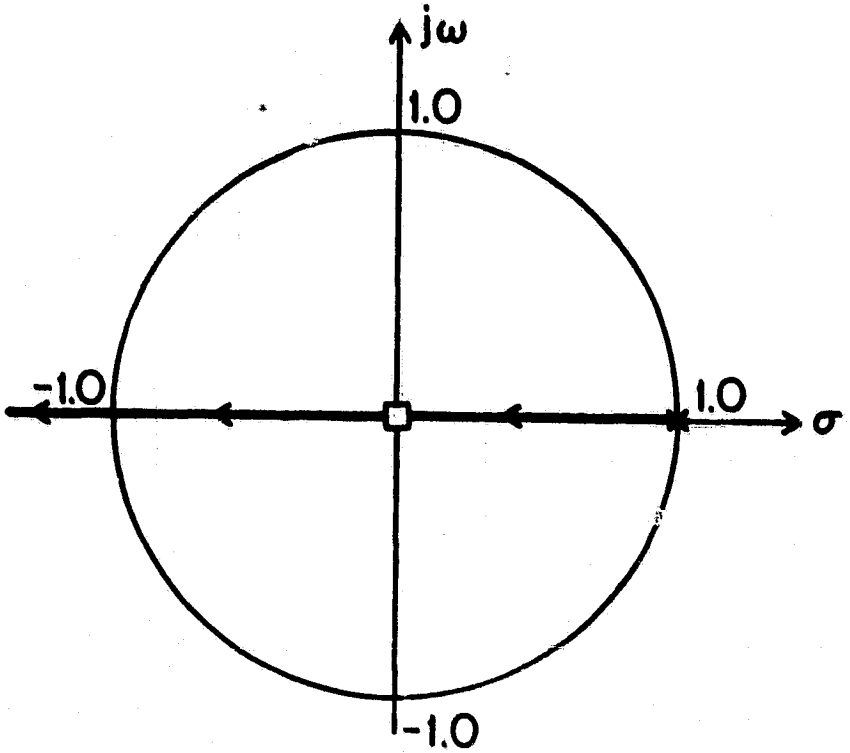

Figure 5-3a. The case d=1.

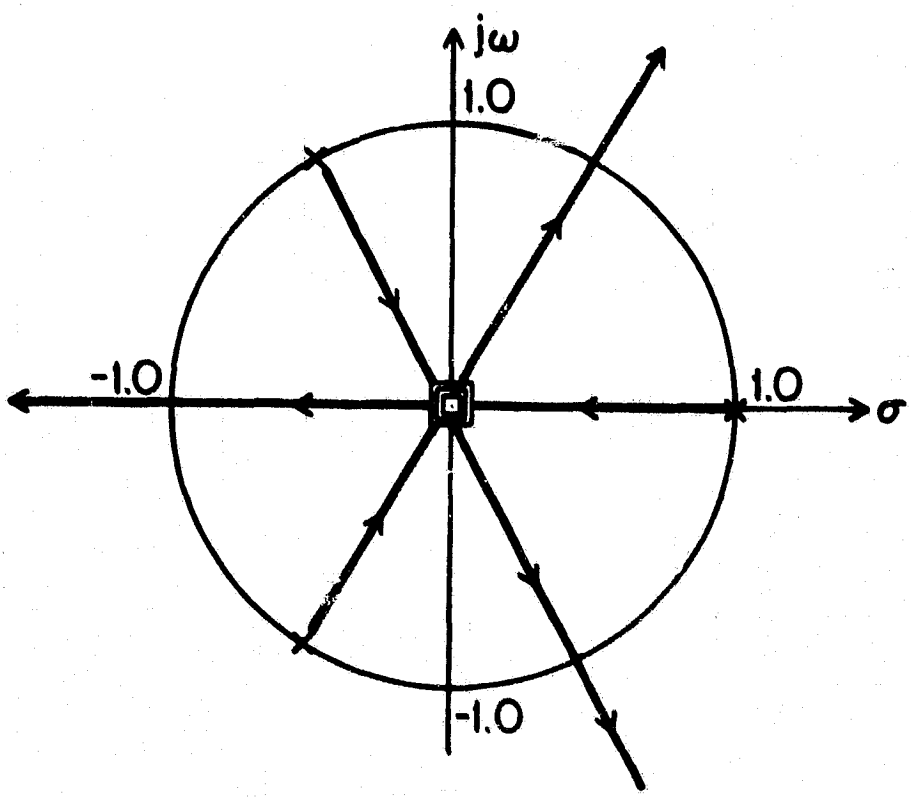

Figure 5-3b. The case d=3.

Figure 5-3. d^*-root loci for DA2 with no unmodeled dynamics.

Indeed, this is exactly the condition for global stability given in [10]. Thus, for the DA2 algorithm with no unmodeled dynamics, the local stability analysis performed in this section gives the same condition as the global stability proof performed in [10].

If one could choose γ so that

$$\gamma d^* g_p = 1 \tag{5-9}$$

the error system itself would be deadbeat, i.e., the error would become zero after d_p steps where d_p is the properly modeled pure plant delay.

From eqn. (5-2), one can see that d^* is close to unity for a large range of reference inputs. Therefore, if the plant gain g_p is known, eqn. (5-9) can be satisfied for a large range of reference inputs by choosing

$$\gamma = \frac{1}{g_p} \tag{5-10}$$

Indeed the choice of γ given by eqn. (5-10) is implied as the proper way to choose the adaptation gain for DA2 in [10]. Although this choice of gain produces a very fast and well behaved error system when no unmodeled dynamics are present, we will see in Section 5.1.2.2.3 that the gain of eqn. (5-10) will be far too large in the presence of unmodeled dynamics. Large gains in the presence of unmodeled dynamics will produce unstable adaptive systems.

5.1.2.2. A Numerical Example of a System with Unmodeled Dynamics

When there are unmodeled dynamics present in the plant, the analysis follows along very similar lines as in Section 3.3.4. The key issues will be examined by example.

Although this section provides analysis for only a specific example, conclusions can be drawn from this example which are true more generally.

Any type of unmodeled dynamics can be studied using the techniques of this section. In particular, an important consideration in discrete-time systems are errors in the determination of the delay. Errors in time delay specifications can be handled just like any other unmodeled dynamics. In this case, the unmodeled dynamics consist of poles at the origin but no zeroes.

The example used in this section will consist of the first order plant with second order unmodeled dynamics that has been used throughout this thesis.

$$y(t) = \left(\frac{2}{s+1}\right)\left(\frac{229}{s^3+30s+229}\right) u(t) \qquad (3\text{-}27)$$

In order to obtain a discrete-time system which is equivalent to the system (3-27), the standard technique of discrete-time control system analysis called hold equivalence was used (see [68], Section 3.4). The continuous-time plant of eqn. (3-27) is preceded by a

zero-order hold and followed by an impulse sampler which is synchronized with the zero-order hold. The resulting discrete-time system is equivalent to the original continuous-time system in that both systems will produce the same output at the sampling instants, if the input to each system is constant from one sampling instant to the next.

Although anti-aliasing filters (see [68]) are usually included in discrete-time controller designs, such filters are not specifically treated here. Any filter, such as an anti-aliasing filter, operating upon the plant output can be considered as part of the plant. Indeed, since the presence of an anti-aliasing filter is often ignored when designing the adaptation mechanism, it is reasonable to consider an anti-aliasing filter as part of the unmodeled dynamics of the plant.

For our initial investigation a sampling period of T=0.04 seconds was used. This represents fairly fast sampling, since it is approximately ten times as fast as the fastest dynamics in the plant.*

The discrete-time description of the plant is:

$$y(t) = \frac{(0.00361)(1+0.196q^{-1})(1+2.763q^{-1})q^{-1}}{(1-0.961q^{-1})(1-(0.547+j0.044)q^{-1})(1-(0.547-j0.044)q^{-1})} \left|u(t)\right| \qquad (5\text{-}11)$$

*The importance of the sampling interval in determining the stability of the adaptive control system in the presence of unmodeled dynamics is discussed in Section 5.1.2.3.

The model was chosen as the discrete-time equivalent of eqn. (3-20).

$$y_M(t) = \frac{(.12)q^{-1}}{1-(.88)q^{-1}}\,[r(t)] \qquad (5\text{-}12)$$

Note the presence of the non-minimum phase zero at -2.763 in the discrete-time version of the plant as predicted in [69]. The validity of the linearized analysis is unaffected by this non-minimum phase zero.

5.1.2.2.1 Stability Analysis

Figure 5-4 shows a k_y^*-root locus which determines the poles of the nominal controlled plant of eqn. (2-103) for the plant of eqn. (5-11).

A set of gains which will produce a stable nominal controlled system is given by:

$$k_y^* = -0.8; \quad k_r^* = 1.32 \qquad (5\text{-}13)$$

The position of the poles of $\frac{q^*B^*}{A^*}$ with the parameters of eqn. (5-13) is indicated by boxes (□) in Figure 5-4.

The γd^*-root locus of the error system poles given by eqn. (5-4), using the parameters of eqn. (5-13), is shown in Figure 5-5. From Figure 5-5 it can be seen that the linearized error system is unstable for

$$\gamma d^* > .35 \qquad (5\text{-}17)$$

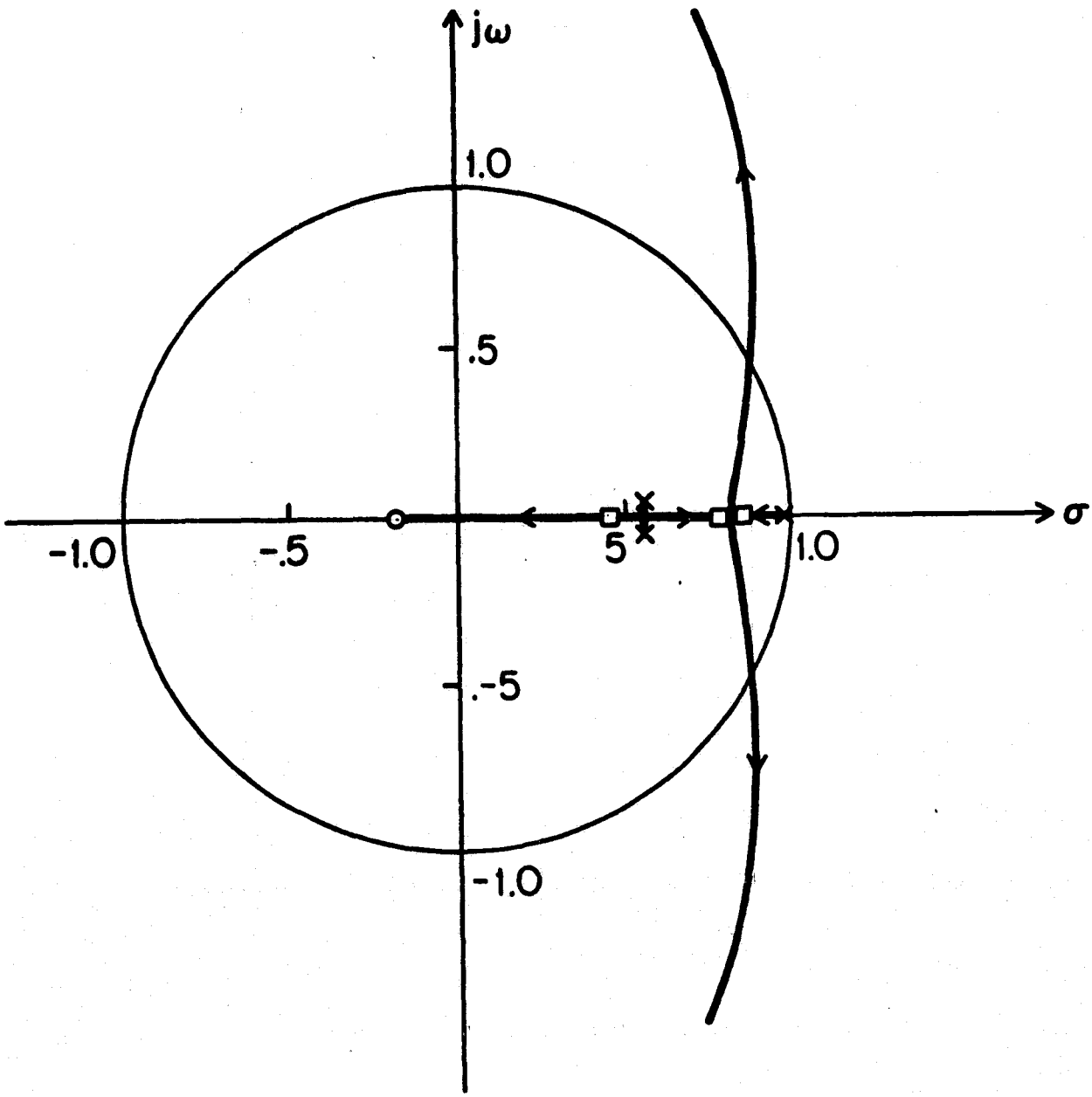

Figure 5-4. k_y^*-root locus for numerical example of Section 5.1.2.2. (Zero at z=-2.76 not shown.)

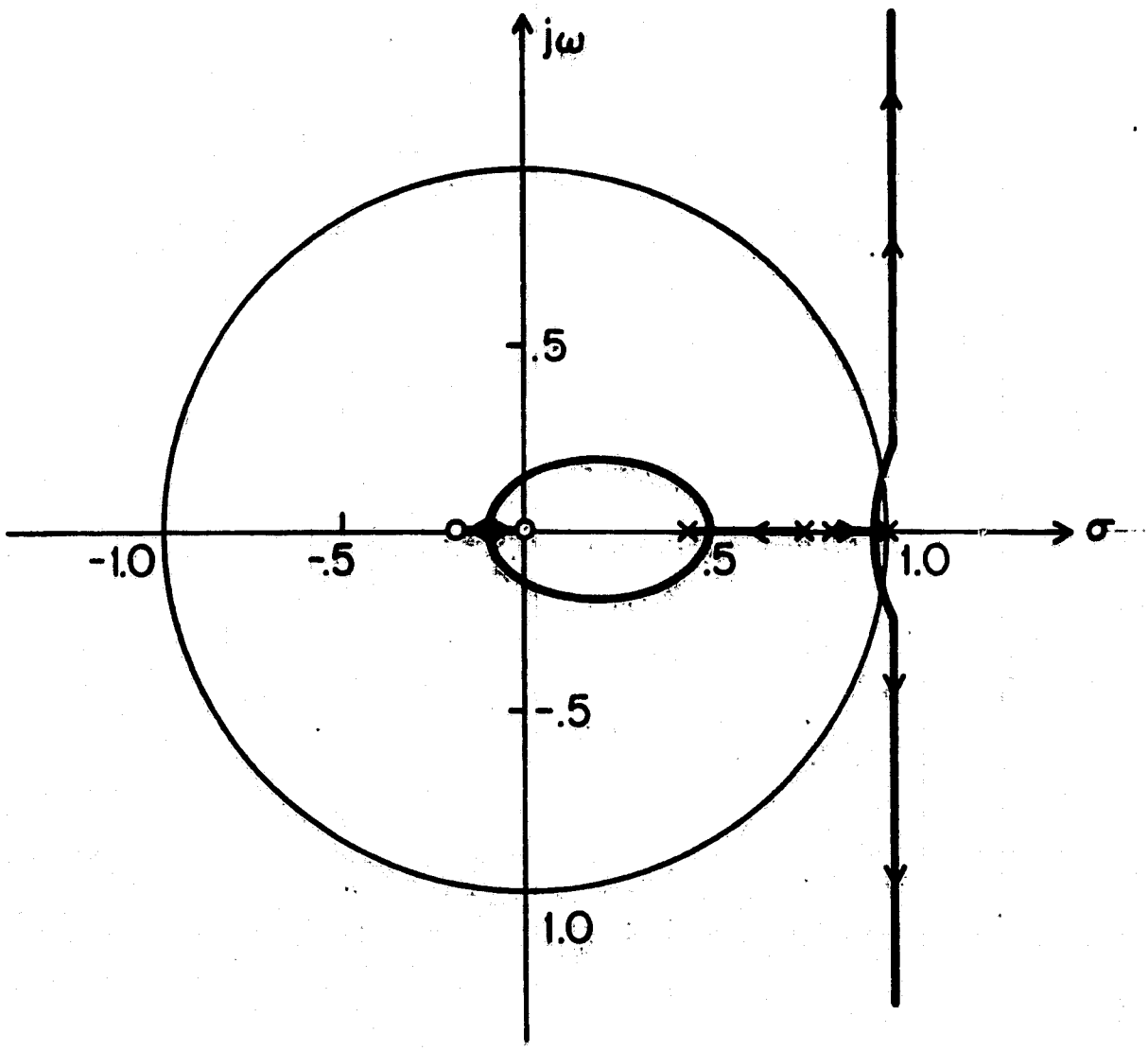

Figure 5-5. d^*-root locus of numerical example of Section 5.1.2.2 with $k_y^* = -0.8$. (Zero at $z=-2.76$ not shown.)

Figure 5-6 shows the results of a simulation generated with the parameters initialized at the values given in eqn. (5-13) and with

$$\gamma=0.2; \quad r=0.1; \quad \gamma d^*=0.04 \tag{5-14}$$

The system is well-behaved.

Figure 5-7 shows the results of the same simulation but with

$$\gamma=0.2, \quad r=10.0 \quad \gamma d^*=.199 \tag{5-15}$$

As expected from the γd^*-root locus of Figure 5-5, the system is oscillatory.

If γd^* is too large, then there exists no nominal system for which the error system is stable. This is shown in Figure 5-8 which gives the k_y^*-root locus of the linearized error system of Figure 5-2 with

$$\gamma d^* = .94 \tag{5-16}$$

The root locus analysis of Figure 5-8 replaces the Routh-Hurwitz analysis of Section 3.3.5.3 in establishing for which values of γd^* there does not exist a set of parameters which lead to a stable linearized system. This root-locus type of analysis is not as exact as the Routh-Hurwitz analysis, since it only establishes whether or not there exists a stable linearization for particular

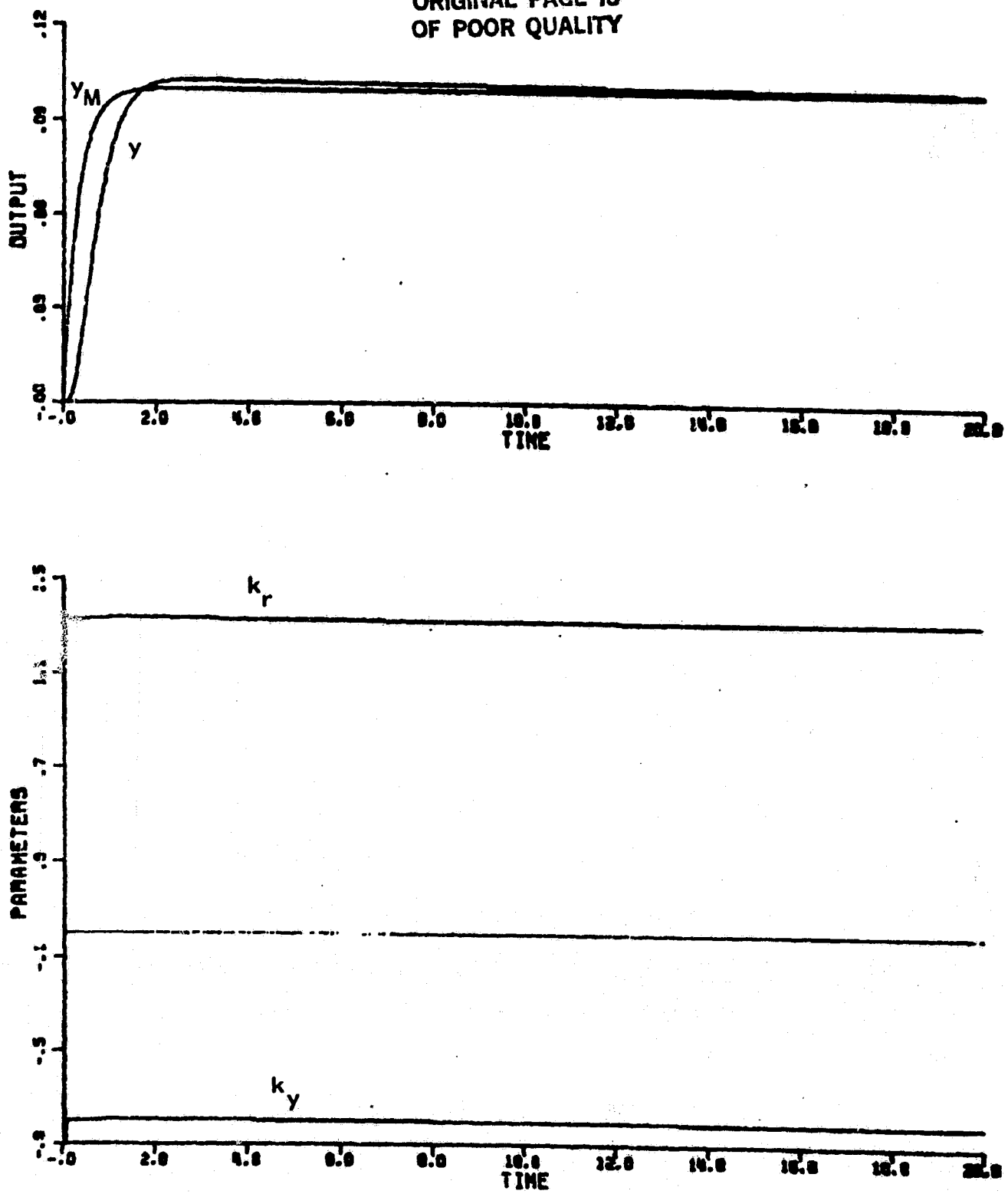

Figure 5-6. Simulation of DA2 with unmodeled dynamics, $r=0.1$, and $\gamma=0.2$.

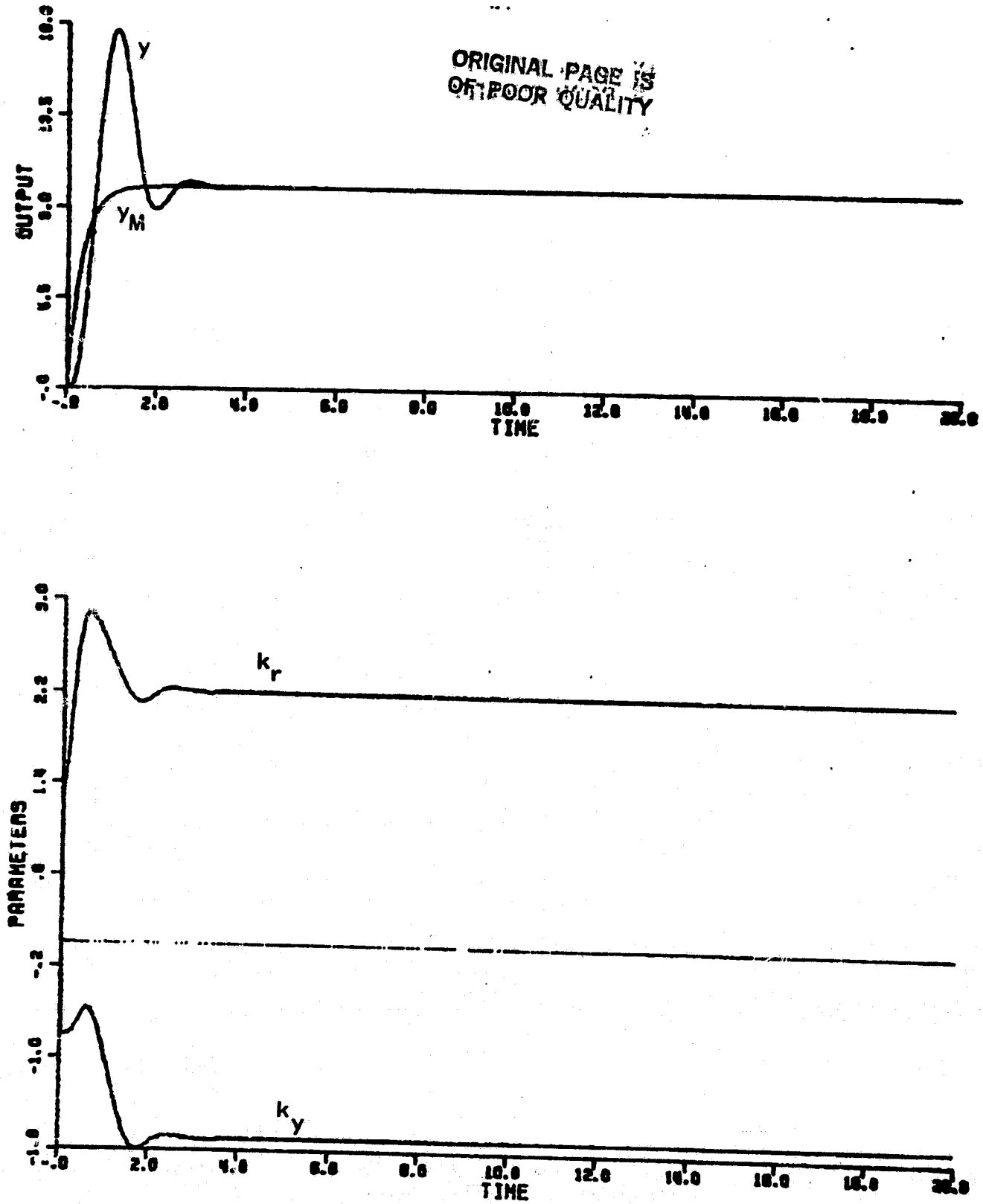

Figure 5-7. Simulation of DA2 with unmodeled dynamics, r=10.0, and γ=0.2

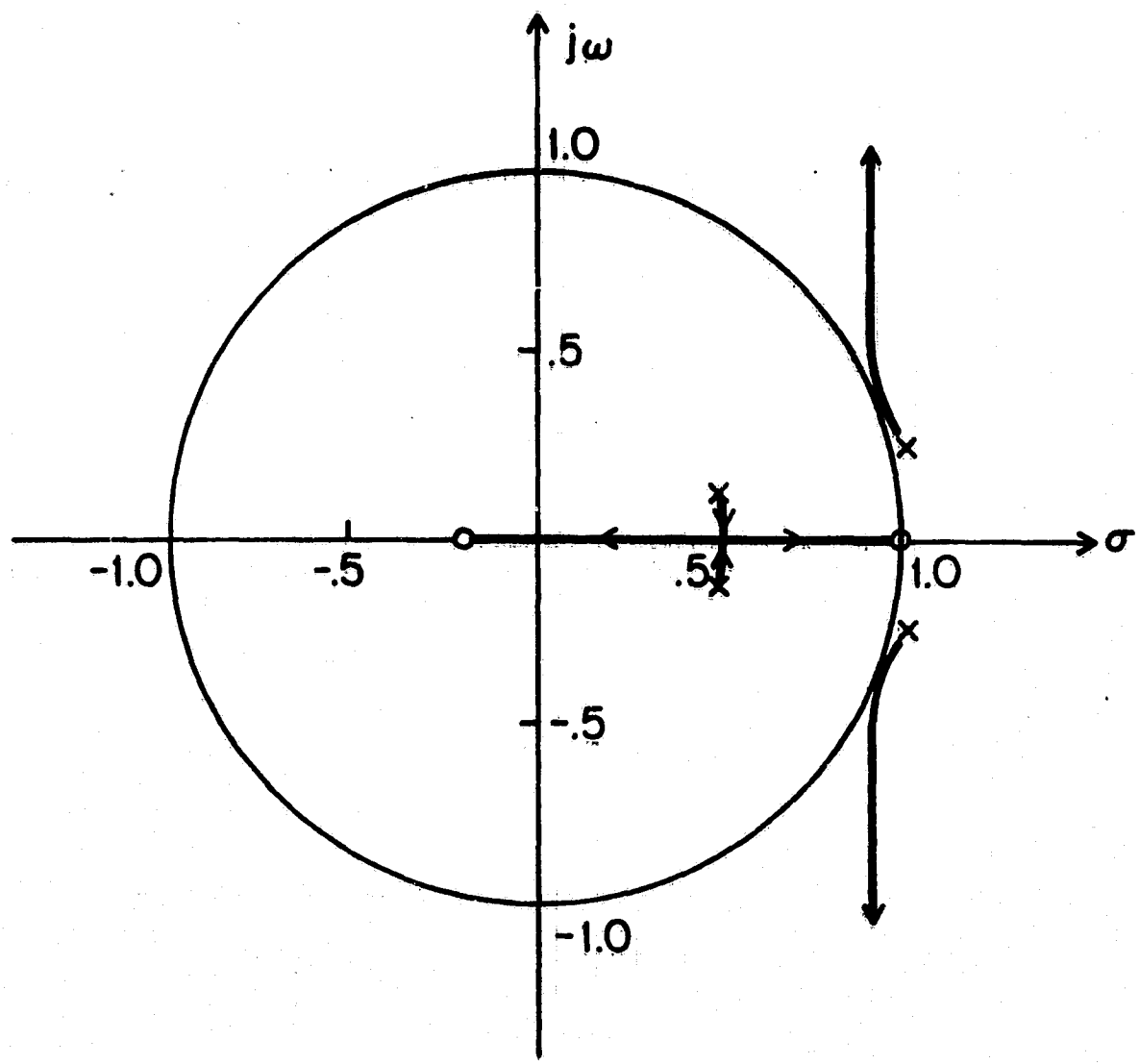

Figure 5-8. k_y^*-root locus for numerical example of Section 5.1.2.2 with $\gamma d^* = 0.94$. (Zero at z=-2.76 not shown.)

values of γd^*. It is, however, much simpler to perform in the case of discrete time systems and still provides the designer with a good idea of how large his adaptation gain can be in order to maintain stability.

For this numerical example, the analysis shows that, if γd^* is close to 0.94, instability problems will ensue, while if the value of γd^* is smaller that of eqn. (5-16), the γd^*-root locus of Figure 5-8 will pass through the unit disk indicating that a set of parameters for which the linearized system is stable exists.

Thus, if we let $\gamma=1$ and r is increased, γd^* will approach 0.94 and the system will go unstable.

Figure 5-9 shows the simulation result with

$$\gamma=1.0, \quad r=1.5 \tag{5-17}$$

The value r=1.5 corresponds, through eqn. (5-3), to $d^*=.81$. In this case, there are sets of parameters for which the linearized system is stable. The parameters of the simulation converge to such a set of parameters.

Figure 5-10 shows the results of a simulation with r increased to

$$r=3.1 \tag{5-18}$$

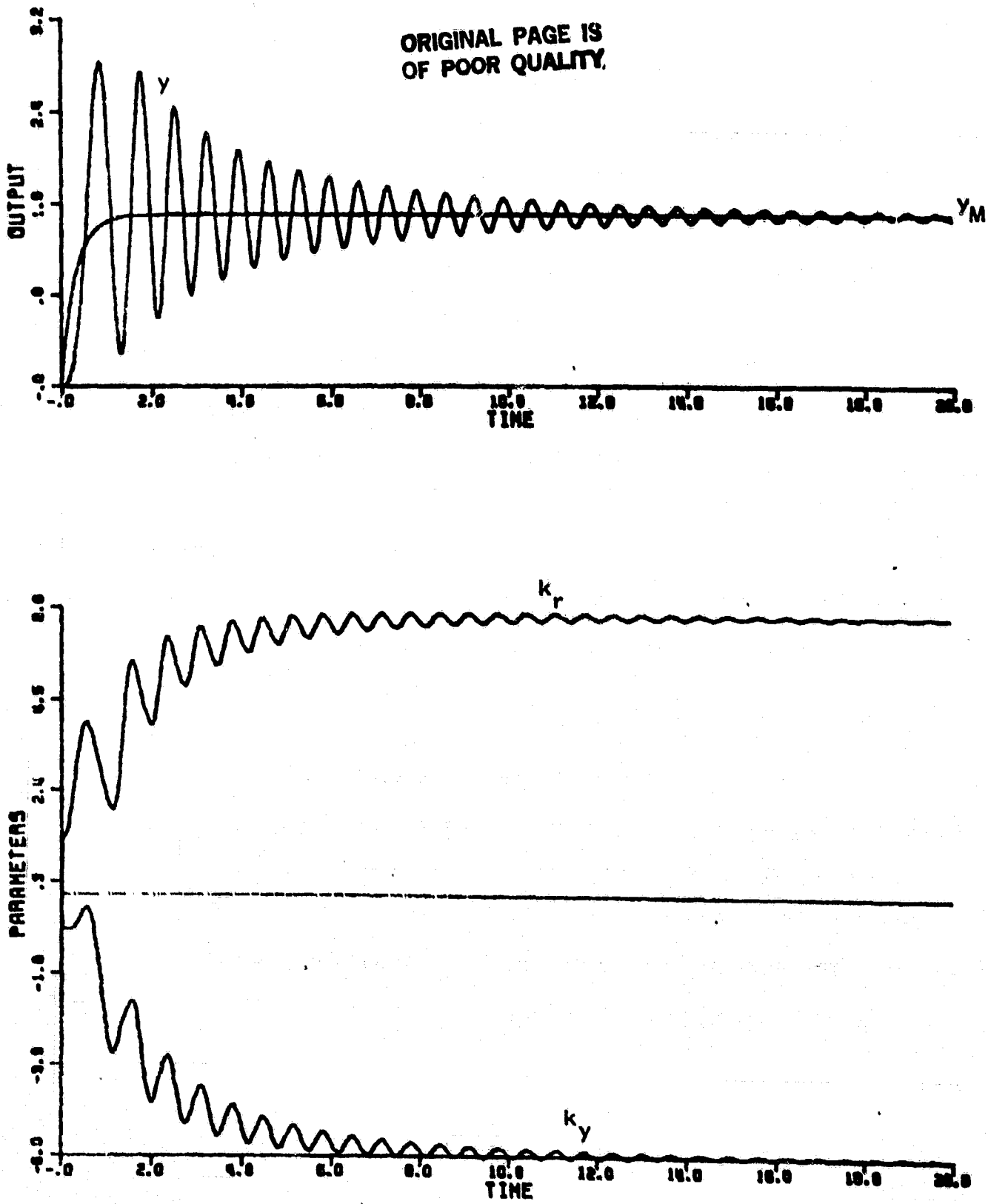

Figure 5-9. . Simulation of DA2 with unmodeled dynamics, r=1.5, and γ =1.0.

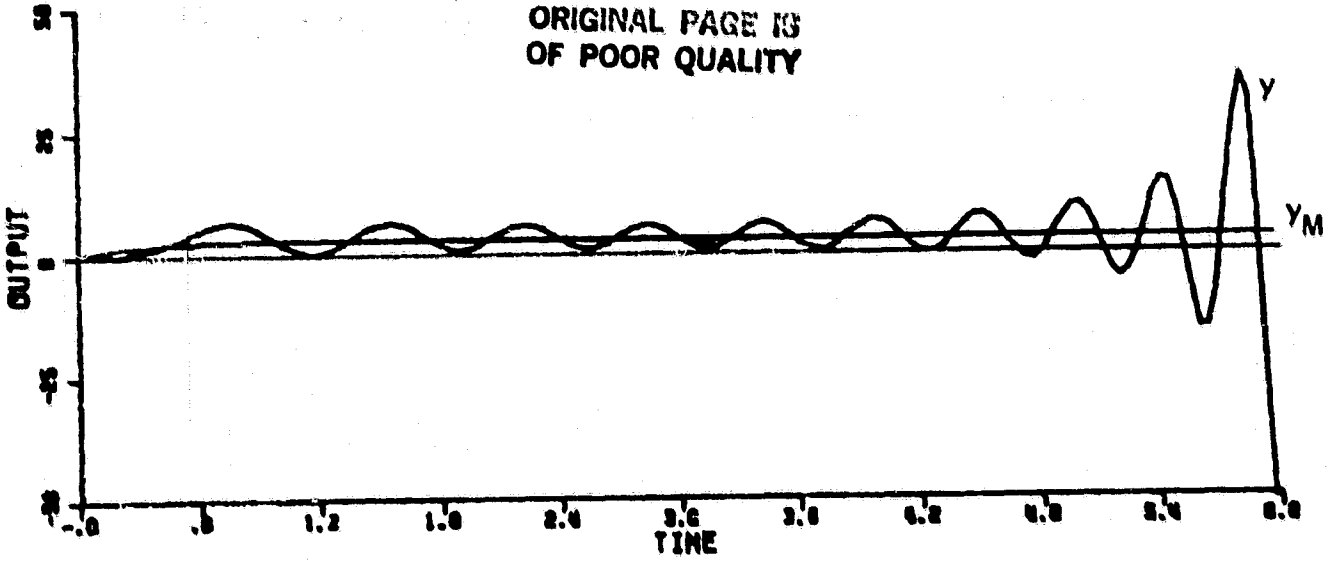

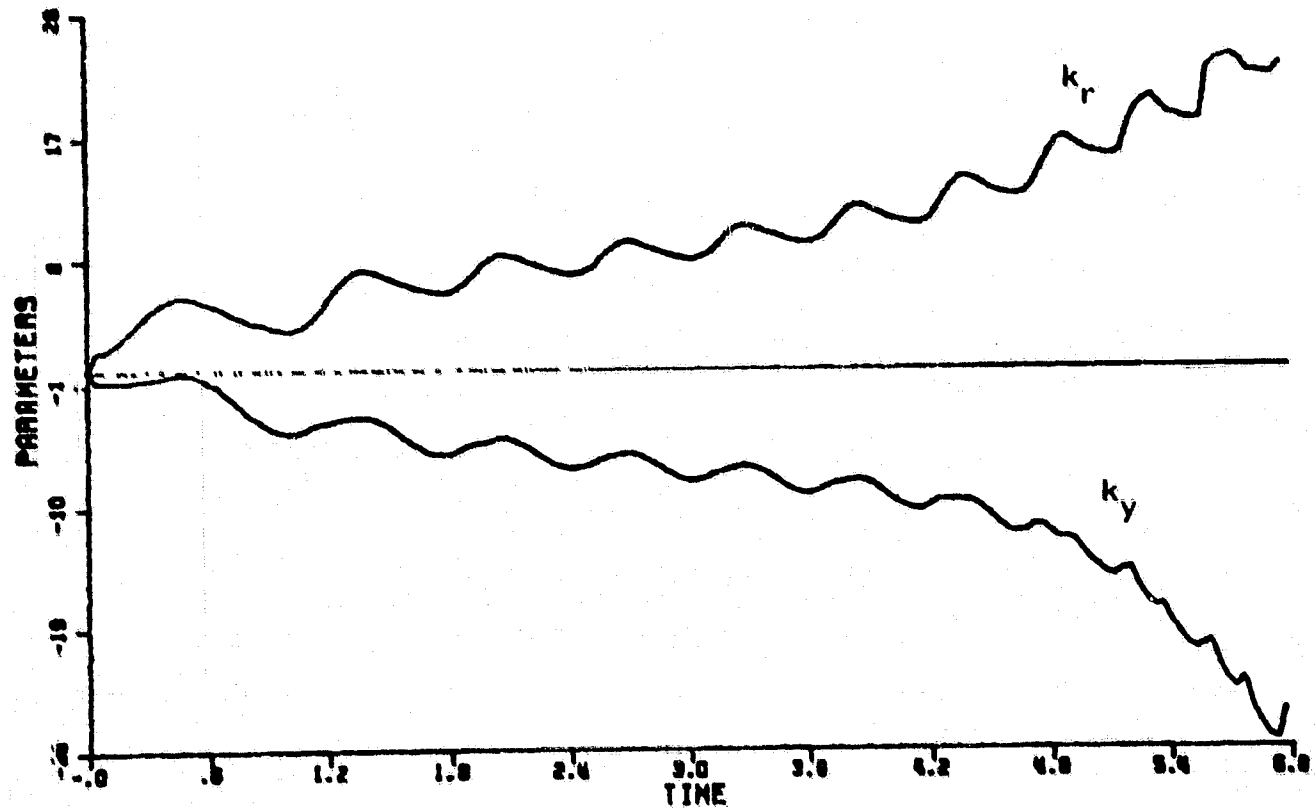

Figure 5-10. Simulation of DA2 with unmodeled dynamics, $r=1.62$, and $\gamma=1.0$
(System eventually becomes unstable.)

This value of the reference input corresponds, through eqn. (5-3), to $d^*=.95$. Now there is no set of parameter values for which the error system is stable and the plant output blows up.

The stability behavior of discrete-time systems which has been discussed so far has been very similar to the behavior of the continuous-time systems. If the gain of the adaptation mechanism is made too large the system becomes oscillatory and unstable. This is the same conclusion that was reached for CA3 in Section 3.4 and for CA4 in Section 3.5 as these algorithms both have the normalizing factor creating an error system gain similar to that of eqn. (5-3).

5.1.2.2.2 Model Matching in the Presence of Unmodeled Dynamics

In order to study the ability of the DA2 algorithm to match the reference model in the presence of unmodeled dynamics, we return to study the nominal controlled system of eqn. (2-103) when the nominal parameter values of eqn. (5-13) are in effect along with the plant of eqn. (5-11) and the model of eqn. (5-12).

The nominal controlled system with the parameters of eqn. (5-13)

$$\frac{q^*B^*q^{-d}}{A^*} = \frac{(.0046)q^{-1}(1+0.196q^{-1})(1+2.763q^{-1})}{(1-.82q^{-1})(1-.79q^{-1})(1-.45q^{-1})}$$

allows the nominal closed-loop controller of Figure 2-15,

$$y(t) = \frac{(.0046)(.12)q^{-1}(1+0.196q^{-1})(1+2.763q^{-1})}{(1-.88q^{-1})(1-.82q^{-1})(1-.79q^{-1})(1-.45q^{-1})}\ [r(t)]$$

to match the model's d.c. gain but does not provide an overall reasonable match of the model. In fact, no values for the parameters, k_y^* and k_r^*, will allow model matching. Due to the deadbeat structure of the DA2 algorithms all the poles of $\frac{q^*B^*}{A^*}$ must be moved near the origin to provide for good model matching. This cannot occur for this example as Figure 5-4 shows. Even approximate model matching will not occur for the algorithm DA2 in the presence of a large class of unmodeled dynamics.*

---

*In Section 5.1.3.3 we will see that a modification of DA2 present in DA3 allows approximate model matching in the presence of unmodeled dynamics.

5.1.2.2.3 The Effects of Design Parameters Chosen Without Consideration of Unmodeled Dynamics

In this section, we investigate what the effects would be on a system with unmodeled dynamics if the design parameters of the adaptive controller were chosen as if there were no unmodeled dynamics. We find that, due to the structure of the DA2 system (which prefilters the reference input through the model's dynamics and follows with a deadbeat controller), the feedback and adaptation gains suggested by an analysis which ignores unmodeled dynamics are excessively large.

Thus the lesson that the designer of an adaptive controller must take into account unmodeled dynamics in his design is stressed. The analysis that takes place here is only for DA2 where the effects of ignoring unmodeled dynamics in the design process is especially evident but the lesson should be heeded no matter what algorithm is used.

If there were no unmodeled dynamics and the plant followed the equation

$$y(t) = \frac{.078q^{-1}}{1-.961q^{-1}} \left[u(t)\right] \qquad (5\text{-}19)$$

the desired values of parameters for the algorithm DA2 necessary to match the model could be attained from eqn. (2-104) and (2-103) as:

$$k_y^* = -12.32 \qquad k_r^* = 12.82 \tag{5-20}$$

and the suggested adaptive gain from eqn. (5-10) would be:

$$\gamma = 12.82 \tag{5-21}$$

If the parameters of the linear system were chosen as in eqn. (5-20), the nominal controlled plant would be unstable with poles at

$$z = .88+j.52; \quad z = .88-j.52; \quad z=.25 \tag{5-22}$$

Thus, an analysis of the DA2 system which were performed without taking unmodeled dynamics into account would lead a designer to pick a nominal parameter set which would produce an unstable controller in the presence of even very high frequency unmodeled dynamics.

In addition, we have seen from Figure 5-8 that the error system of this example will be unstable for a large range of constant reference inputs if the adaptation gain is chosen to be larger than 0.94. We stress that the gain of eqn. (5-21) suggested by an analysis ignoring unmodeled dynamics is more than an order of magnitude larger than the gain which would produce a stable system for all values of constant reference input.

Thus we see that it is critical that a designer have some idea of what unmodelled dynamics may be present in a plant and choose the design parameters so that the adaptive system behaves well in the presence of unmodeled dynamics. After all, this is always done in classical non-adaptive designs!

5.1.2.3 The Effects of the Sampling Interval

There is an additional design parameter in discrete-time systems not present in continuous-time systems which can increase tolerance to unmodeled dynamics. That parameter is the sampling interval.

Let the system of eqn. (3-27) be sampled at a rate of T=.4, instead of T=.04. Such a sampling rate is fairly slow in that it represents five times the speed of the modeled pole; however, sampling of the unmodeled dynamics occurs at barely once per cycle. The equivalent discrete time system is now given by

$$y(t) = \frac{(0.629)(1+.0399q^{-1})(1+.0048q^{-1})q^{-1}}{(1-.67q^{-1})(1-(.0017+j.0018)q^{-1})(1-(.0017-j.0018)q^{-1})}[u(t)] \qquad (5\text{-}23)$$

We note there is no longer a non-minimum phase zero, as was the case in eqn. (5-11) where the plant was sampled faster. Indeed, the poles and zeroes of the unmodeled dynamics are very close to each other so that their effects almost cancel.

Figure 5-11 shows the k_y^*-root locus of the nominal controlled plant of eqn. (2-103) when the open loop plant is described by eqn. (5-23). From Figure 5-11, we notice that all the nominal control system poles can be placed close to the origin and that the nominal closed-loop controller of Figure 2-15 can be made to match the model fairly closely.

The γd^*-root locus of Figure 5-12 then shows that the unmodeled dynamics hardly come into play allowing the full $\gamma d^*=2$ of eqn. (5-8) gain with retention of stability.

Figure 5-13 shows the results of a simulation made with the system sampled at $T=.4$ and

$$\gamma = \frac{1}{g_p} = 1.58; \quad r=10.0 \tag{5-24}$$

The parameters were started at what would be their desired values if no unmodeled dynamics were present

$$k_y^* = -1.06; \quad k_r^* = 1.58$$

The system behaves as if there were no unmodeled dynamics at all. The plant and the model output in Figure 5-13 coincide.

Figure 5-14 shows the same type of simulation but with the parameters started out at zero. The system adjusts quickly to follow the model again as if no unmodeled dynamics were present.

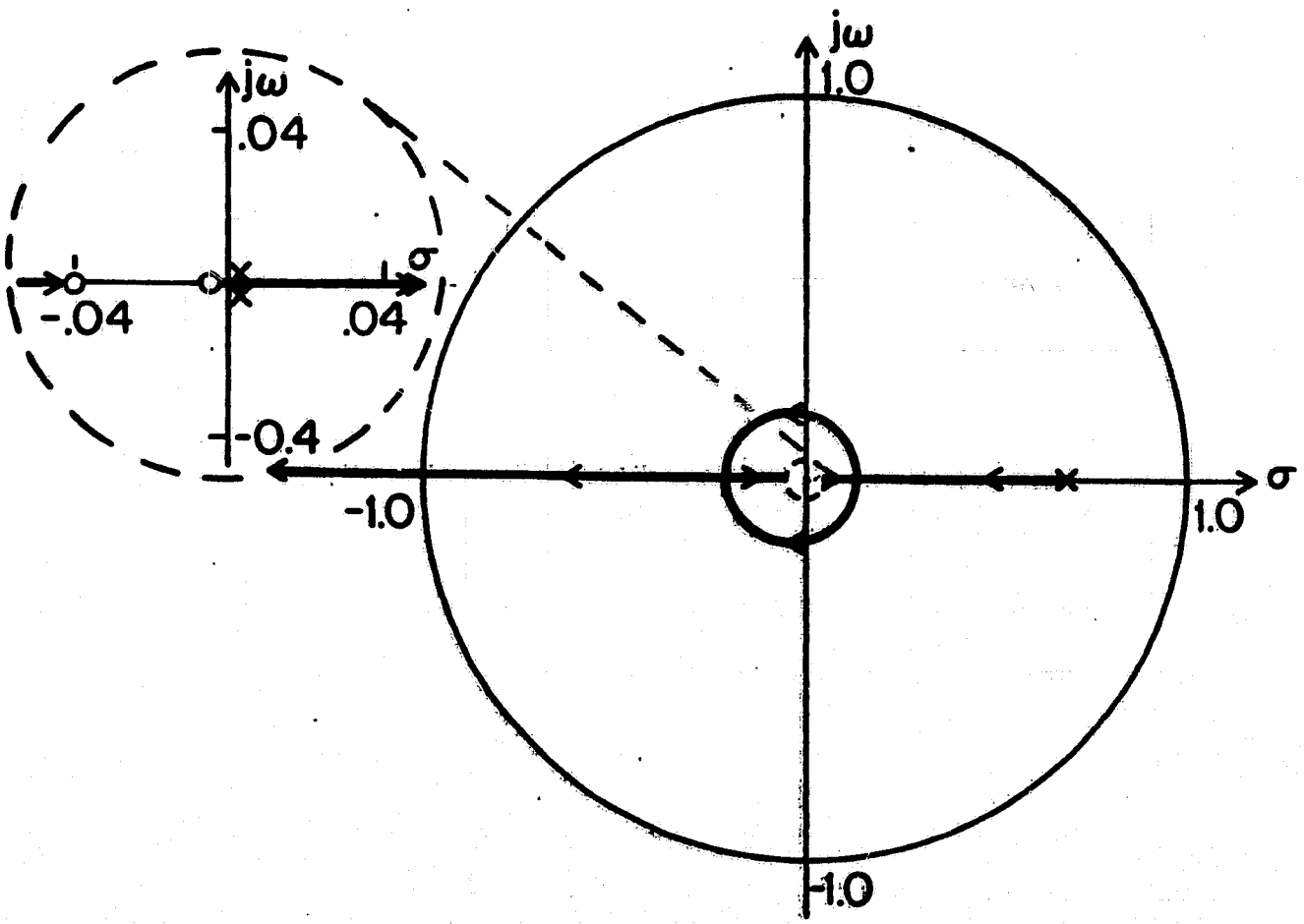

Figure 5-11. k_y^*-root locus for numerical example of Section 5.1.2.3.

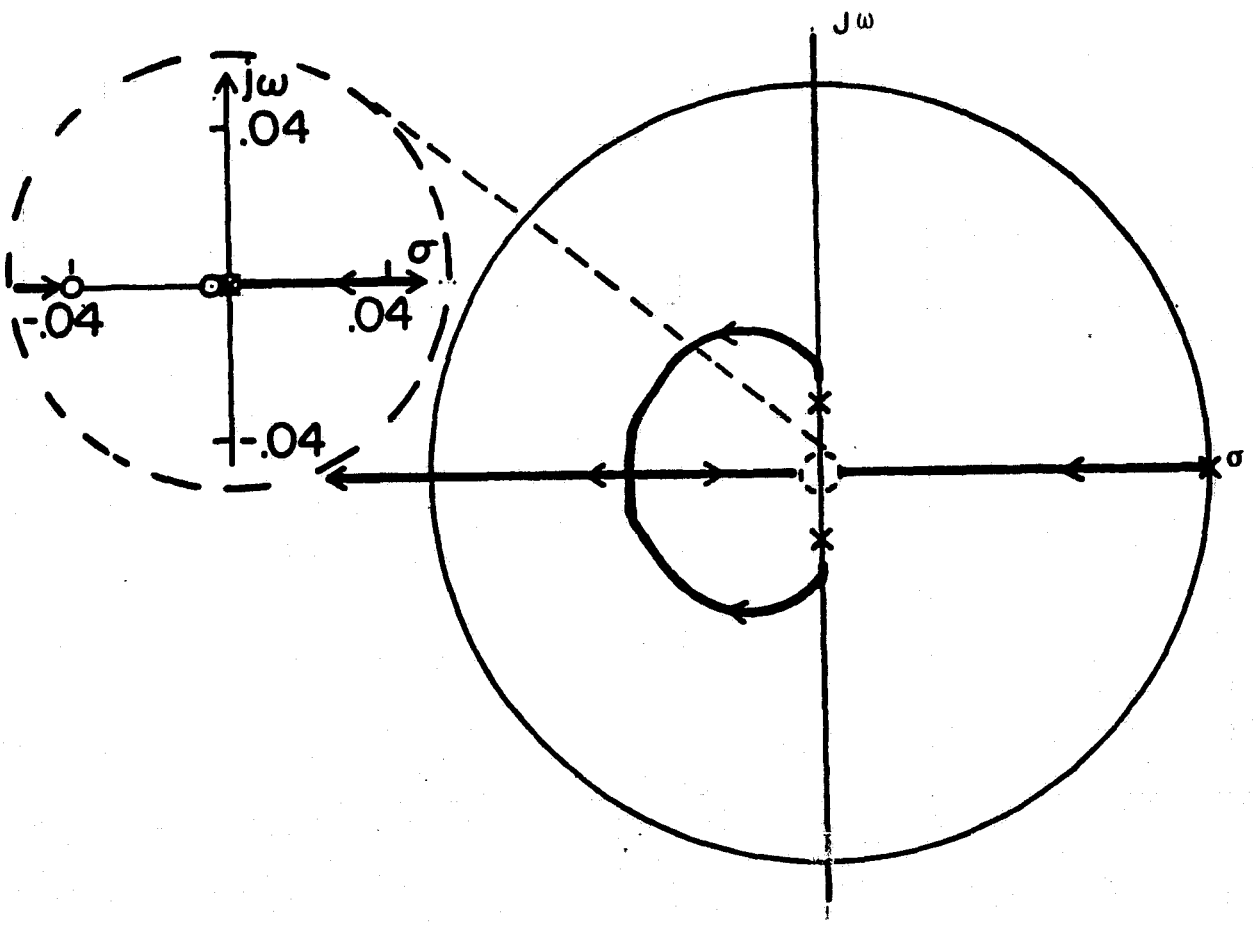

Figure 5-12. d^*-root locus for numerical example of Section 5.1.2.3.

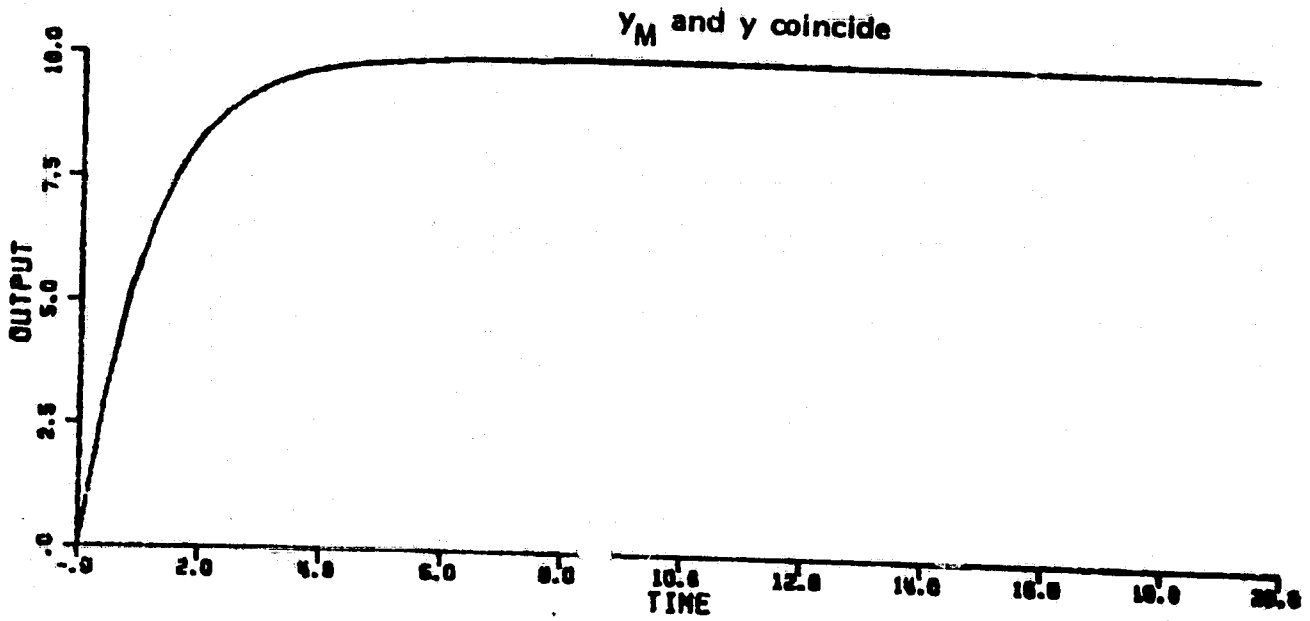

Figure 5-13. Simulation of DA2 with unmodeled dynamics, slow sampling, $k_y(0) = -1.06$, and $k_r(0) = 1.58$.

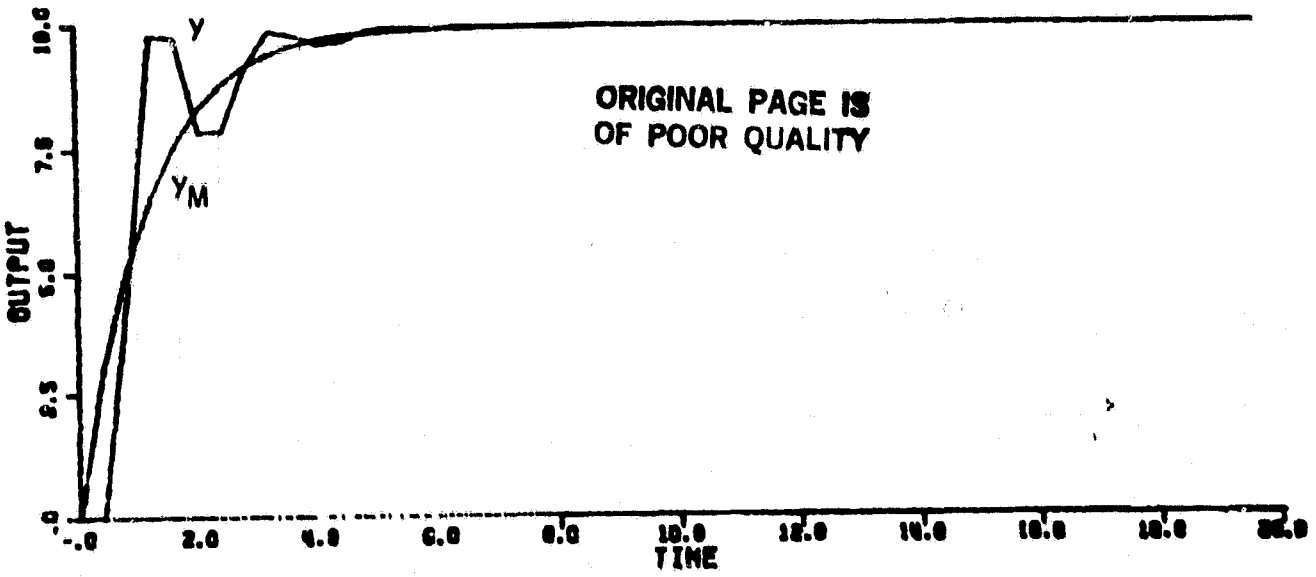

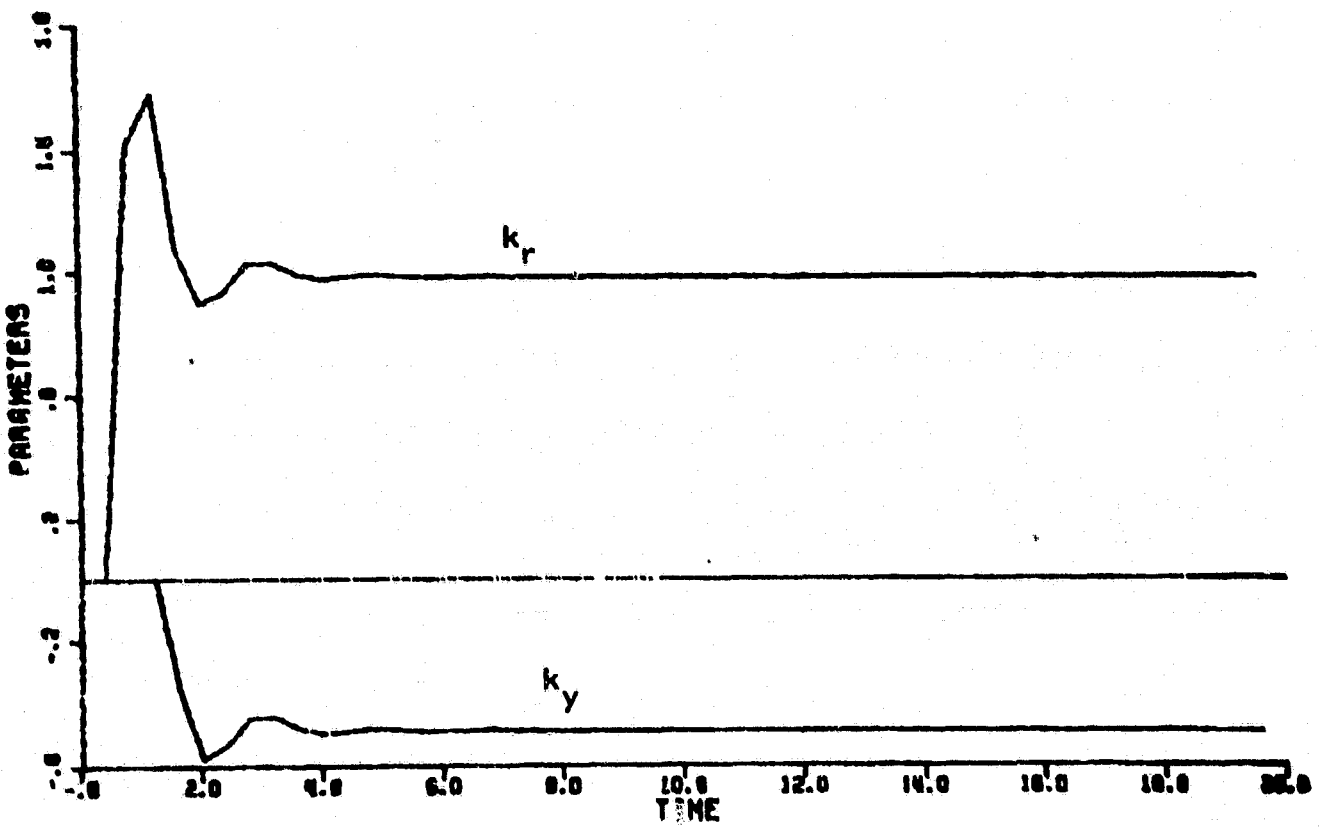

Figure 5-14. Simulation of DA2 with unmodeled dynamics, slow sampling, and $k_y(0)=k_r(0)=0.0$.

Thus we have seen that, if a discrete-time adaptive system with high frequency unmodeled dynamics is designed for constant inputs and with a slow enough sampling interval, the system can be made to behave almost as if there were no unmodeled dynamics at all. Although this is shown only for a numerical example using DA2, the conclusion arises from the fact that, in the slowly sampled system, the poles and zeroes of the unmodeled dynamics almost cancel and thus the result will be true for more general plants with high frequency unmodeled dynamics and for all discrete-time adaptive control algorithms.

5.1.3 The Analysis of DA3

As was mentioned in Section 2.3.4, the algorithm DA3 is very similar to DA2. Its stability properties as analyzed in Section 5.1.3.2 are fundamentally the same as those of DA2 in that, if the adaptation gain is chosen small enough, the linearized error system will be stable for all constant reference inputs for a large class of unmodeled dynamics. However, too large an adaptation gain will lead to an unstable error system for a large class of constant reference inputs and unmodeled dynamics.

There is, however, one important addition in DA3 not present in DA2, the added filter L of Figure 2-17. We will see in Section 5.1.3.2 that, with this filter as part of the nominal controlled

plant, $\frac{g^*B^*q^{-d_p}}{A^*}$ of Figure 2-17, the reference model can still be fairly closely matched in the presence of high frequency unmodeled dynamics, unlike the DA2 algorithm.

In Section 5.1.3.3, it is pointed out that, with a proper choice of L, the model can be matched in the structure of DA3 with no feedback at all. This observation makes clear a weakness of the problem formulation of all the model reference adaptive control algorithms. The only objective of these algorithms is to have the controlled plant match a reference model. This should be but one objective of a control system.

Finally, we note here that slowing the sampling rate will cause the effects of high frequency unmodeled dynamics upon the adaptive system DA3 to be greatly reduced as was the case with DA2.

5.1.3.1 Analysis

The tool for analysis once more consists of linearizing around a nominal set of parameters and assuming that the input is constant.

Following this approach, the error system of Figure 2-16 is reduced to that of Figure 5-15 where

$$\frac{g^*q^{-d_p}B^*}{k_r^*A^*} \quad \frac{g_p q^{-d_p} PLB}{(P-q^{-1}K_u)A-g_p q^{-d_p} BK_y} \tag{2-118}$$

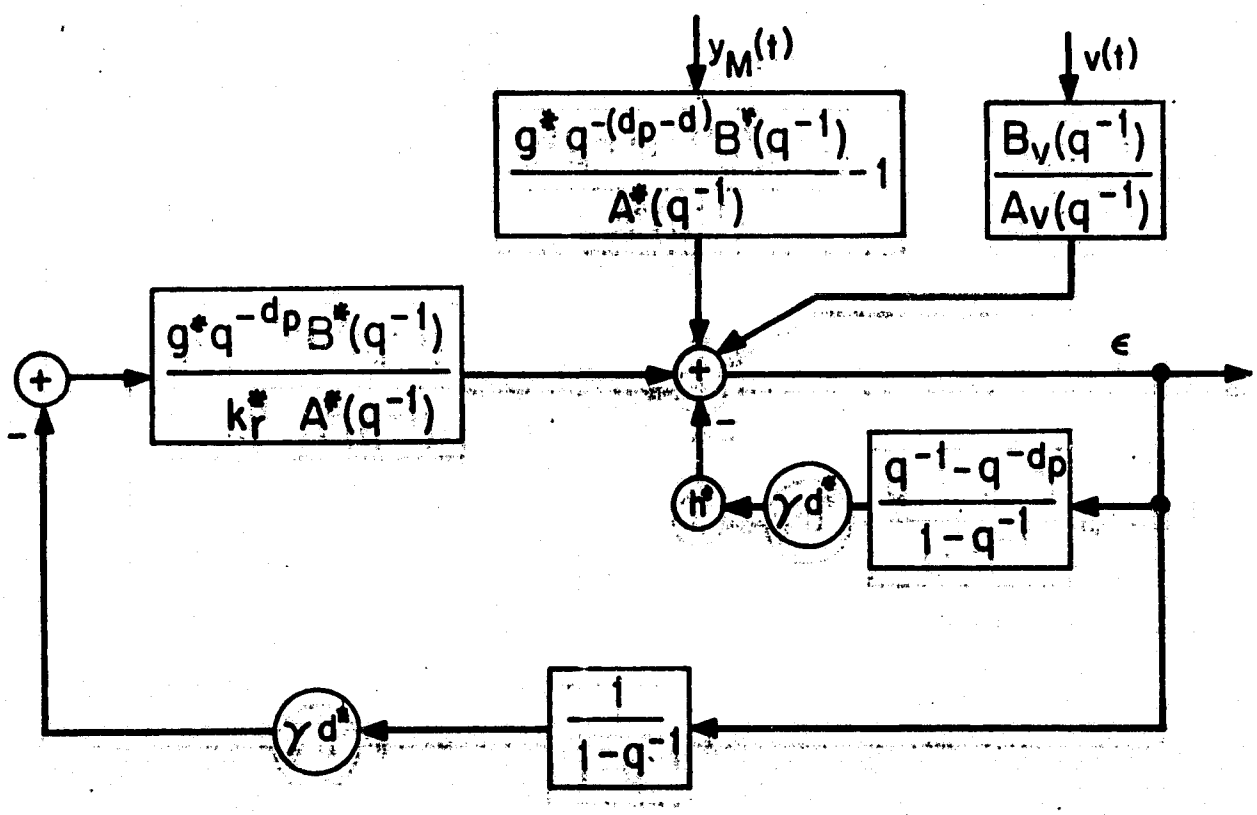

Figure 5-15. Linearized error system for DA3.

and

$$d^* = \frac{\underline{w}_d^T \underline{w}_d}{\lambda_o + \underline{w}_d^T \underline{w}_d} \qquad (5\text{-}25)$$

If the delay, d_p, is unity, the system further reduces to that of Figure 5-16 where

$$G_E = \frac{g^* q^{-d_p} B^*}{k_r^* A^* (1-q^{-1})} \qquad (5\text{-}26)$$

5.1.3.2 A Numerical Example with Unmodeled Dynamics

In this section, we apply the algorithm DA3 to the example of Section 5.1.2.2 with the fast sampling rate T=.04 secs.

The plant with unmodeled dynamics is described by eqn. (5-11) and the model by eqn. (5-12). Since the system is designed as a first order system, the filter P of eqn. (2-108) is not used. Choose

$$L = A_M = 1-.88q^{-1} \qquad (5\text{-}26)^*$$

It is assumed that there is no disturbance so n_c, the degree of C in eqn. (2-106), is set to zero and through eqn. (2-109) w_r and, hence, k_r are scalars.

---

*The choice of L is discussed in Section 5.1.3.3.

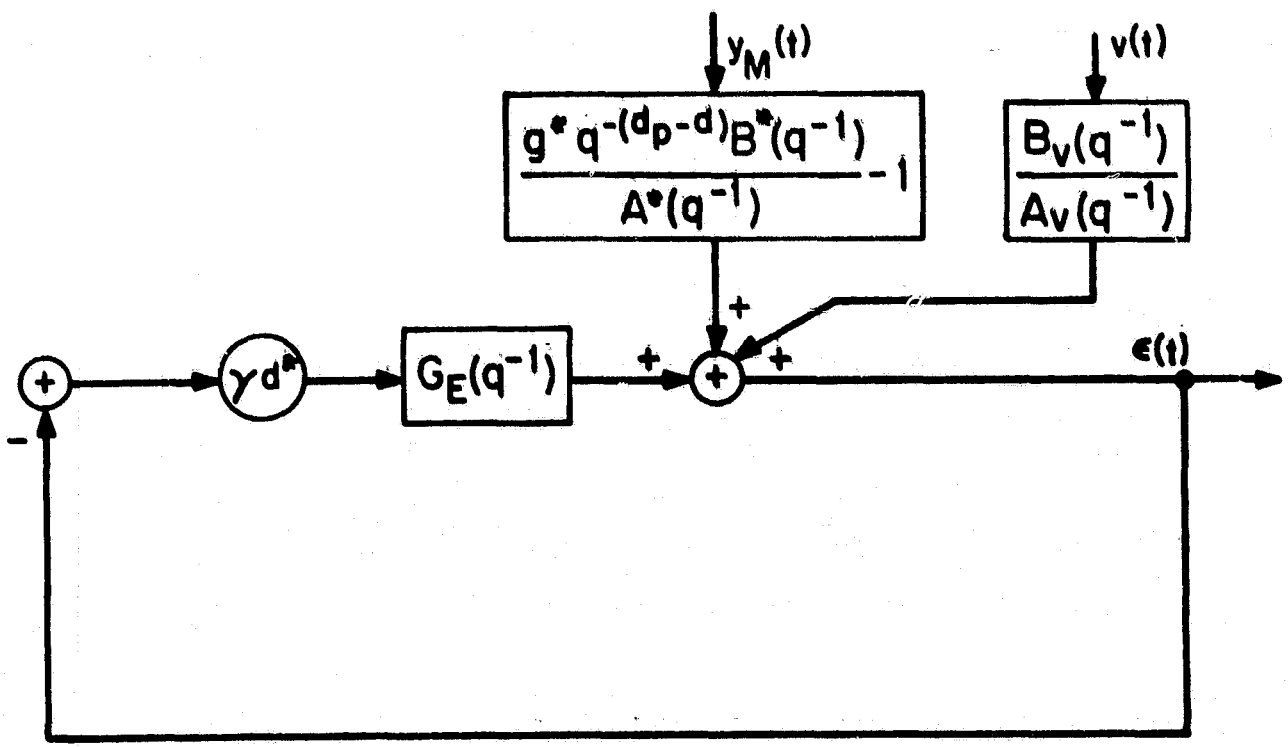

Figure 5-16. Linearized error system for DA3 when $d_p = 1$.

The system is linearized about the parameters.

$$k_y^* = -0.615 \qquad k_r^* = 1.16 \tag{5-27}$$

leading to a nominal controlled plant which is calculated from eqn. (2-118).

$$\frac{g^* q^{-1} B^*}{A^*} = \frac{(.035)q^{-1}(1+0.196q^{-1})(1+2.763q^{-1})}{(1-.71q^{-1})(1-.46q^{-1})} \tag{5-28}$$

The pole at z=.88 is cancelled by the zero due to L at z=.88. Thus the nominal closed loop controller of Figure 2-17 for the parameter of eqn. (5-27) matches the reference model over the frequency range of zero rad/sec. to about 8.5 rad/sec where the pole of eqn. (5-28) at z=.71 takes effect.*

The d^*-root locus for the error system of Figure 5-16 linearized about the parameters of eqn. (5-27) with G_E from eqn. (5-26) and (5-28),

$$G_E = \frac{(.035)q^{-1}(1+0.196q^{-1})(1+2.763q^{-1})}{(1-.71q^{-1})(1-.46q^{-1})(1-q^{-1})}$$

is shown in Figure 5-17. With a gain of

$$\gamma d^* < 6.9$$

---

*This is much better than the model matching ability of DA2 shown in Section 5.2.2.2 which does not have the additional filtering L to cancel the low frequency pole.

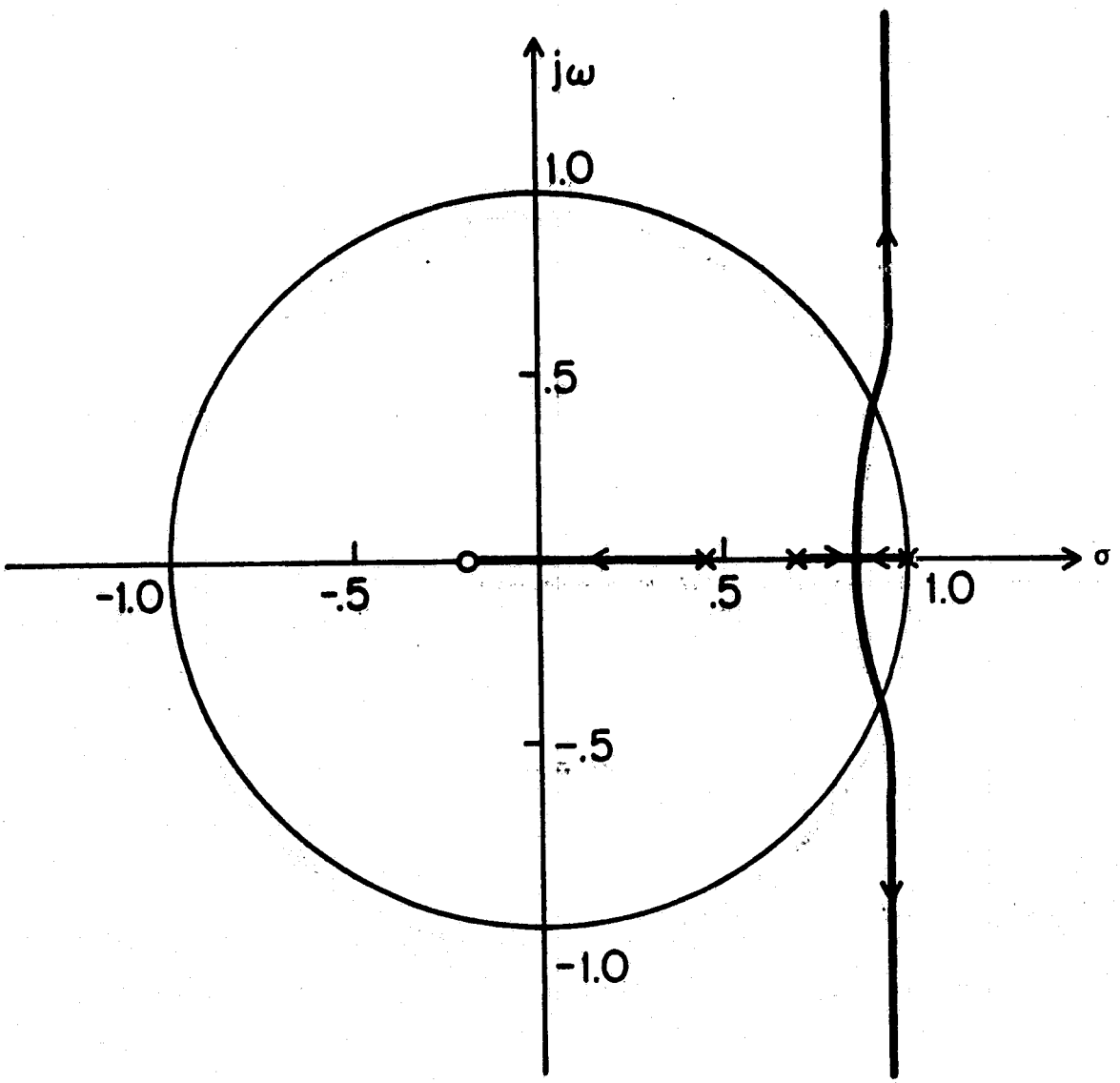

Figure 5-17. γd^*-root locus for numerical example of Section 5.1.3.2. (Zero at z=-2.76 not shown.)

the linearized error system of Figure 5-16 will be stable*.

Figure 5-18 shows the results of a simulation started with the parameters at their nominal values given by eqn. (5-27) and with

$$\gamma = 3.0; \quad r = 10.0; \quad \gamma d^* = 2.98 \tag{5-29}$$

The system behaves well as the linearized analysis predicts it would.

Figure 5-19 shows the results of a simulation with

$$\gamma = 13.98; \quad r = 10.0; \quad \gamma d^* = 13.91 \tag{5-30}$$

There is a set of parameters which produces a stable error system for γd^* as in eqn. (5-30). However, the system parameters must move to values which produce a stable linearized error for such a large adaptation gain as in eqn. (5-30). In Figure 5-19, the parameters move to

$$k_y^* = -7.5 \quad k_r^* = 67 \tag{5-31}$$

The nominal closed loop controller of Figure 2-17 for the parameters of eqn. (5-31) is

$$y(t) = \frac{(.03)(.12)(1+.196q^{-1})(1+2.763q^{-1})}{(1-.88q^{-1})(1-.3q^{-1})(1-(.86+j.41)q^{-1})(1-(.86-j.41)q^{-1})}[r(t)] \tag{5-32}$$

*The system of DA2 would not have a stable linearization for this example if $\gamma d^* > .94$ (Fig. 5-16). Thus the added filter, L, in DA3 has made DA3 able to remain stable at higher adaptation gains then DA2.

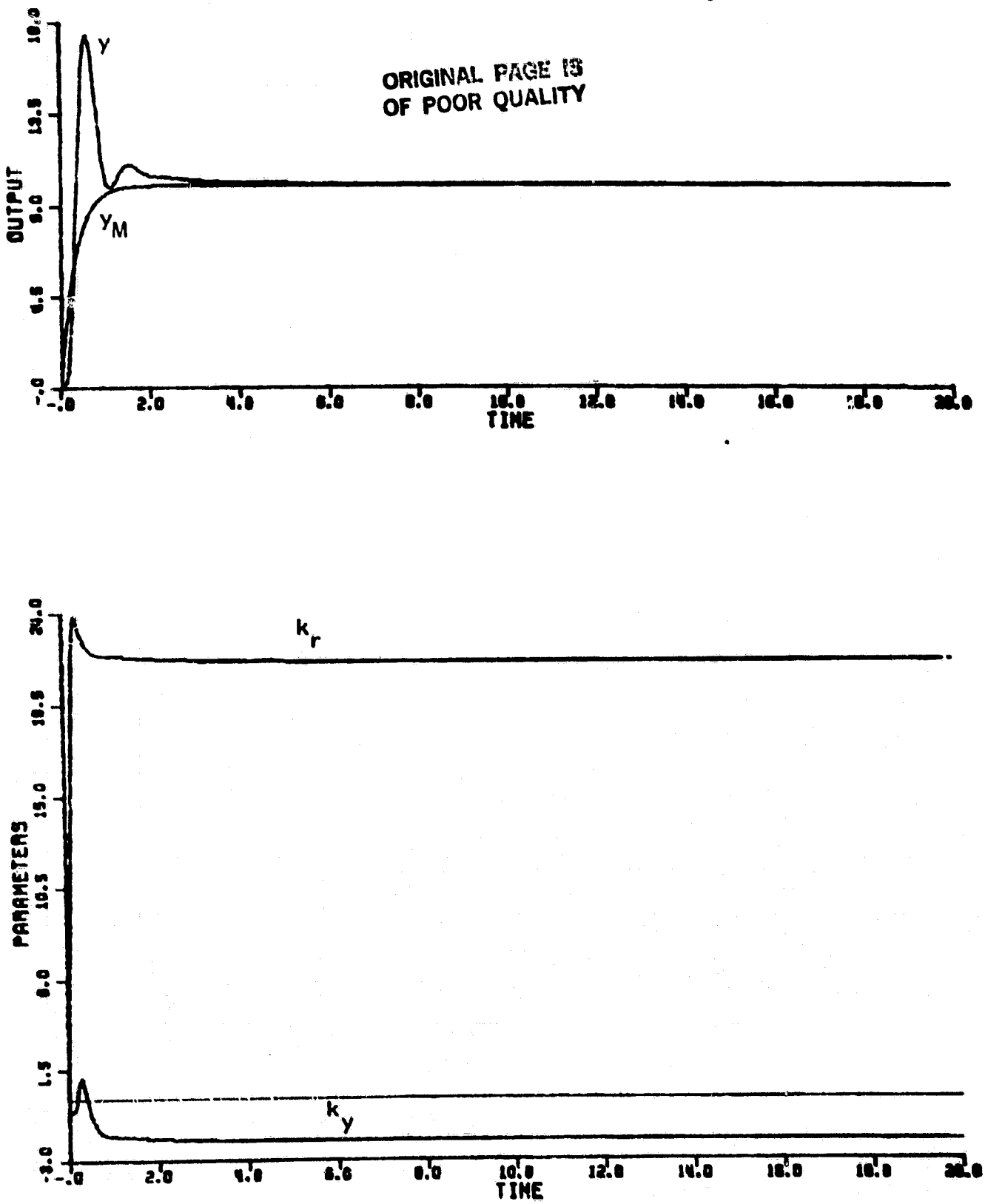

Figure 5-18. Simulation of DA3 with unmodeled dynamics and $\gamma=3.0$.

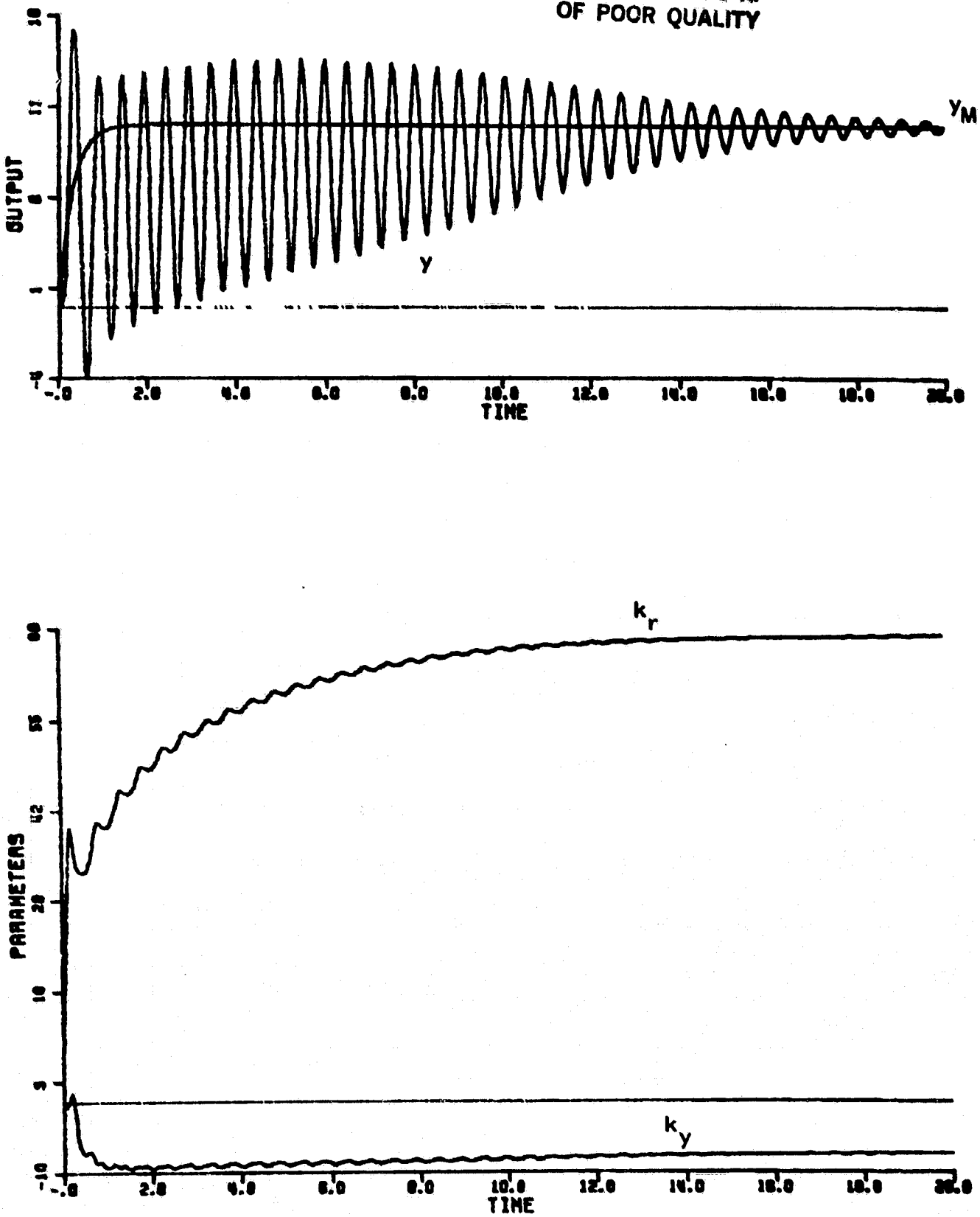

Figure 5-19. Simulation of DA3 with unmodeled dynamics and $\gamma = 13.98$.

This does not come close to matching the model of eqn. (5-12). Thus, as is the case with all the algorithms, if the adaptive gain is too large, the adaptive controller of DA3 may not be able to match the model even if it can maintain stability in the presence of unmodeled dynamics.

Although there is a stable linearization for γd^* as in eqn. (5-30), this value for γd^* represents as large a value of γd^* for which there is a stable linearization. When the parameters are increased to

$$\gamma = 13.981; \quad r = 10.0; \quad \gamma d^* = 13.912 \tag{5-33}$$

there is no longer a value of k_y^*, which will produce a stable linearized system. The simulation of Figure 5-20, with the parameter values set as in eqn. (5-33), becomes unstable as predicted.

Thus, in this subsection, it has been shown that the algorithm DA3 reacts essentially the same as the other algorithms with some advantage over DA2 due to the added filtering of L. It is clear that a slower sampling rate would help DA3 in exactly the same way it helped DA2.

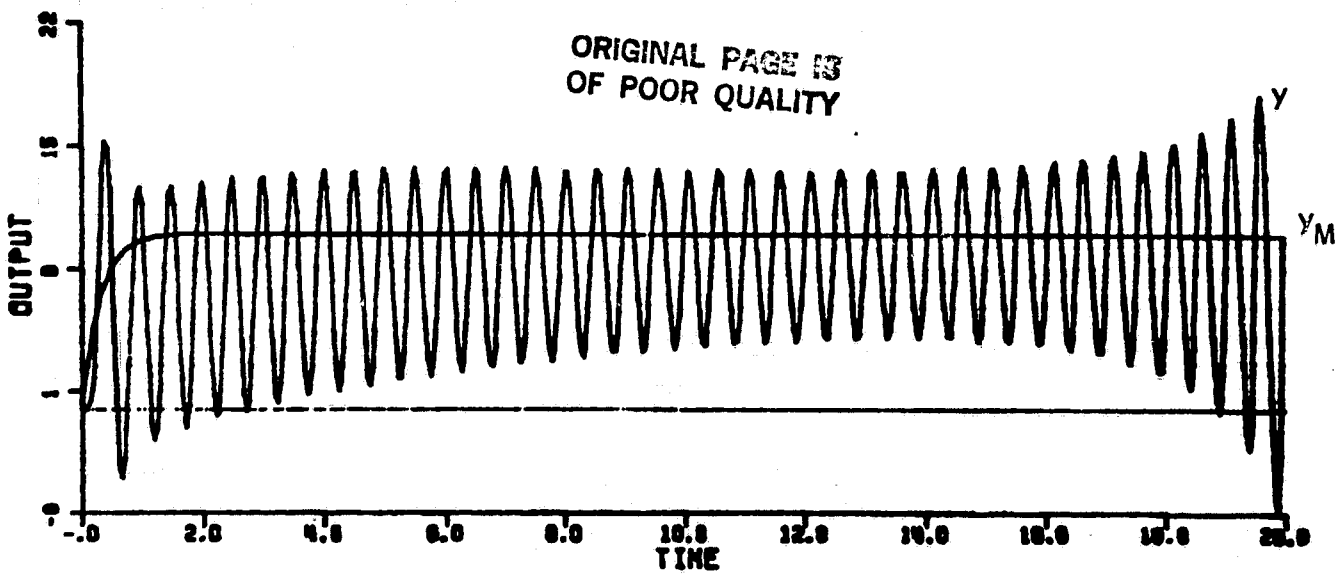

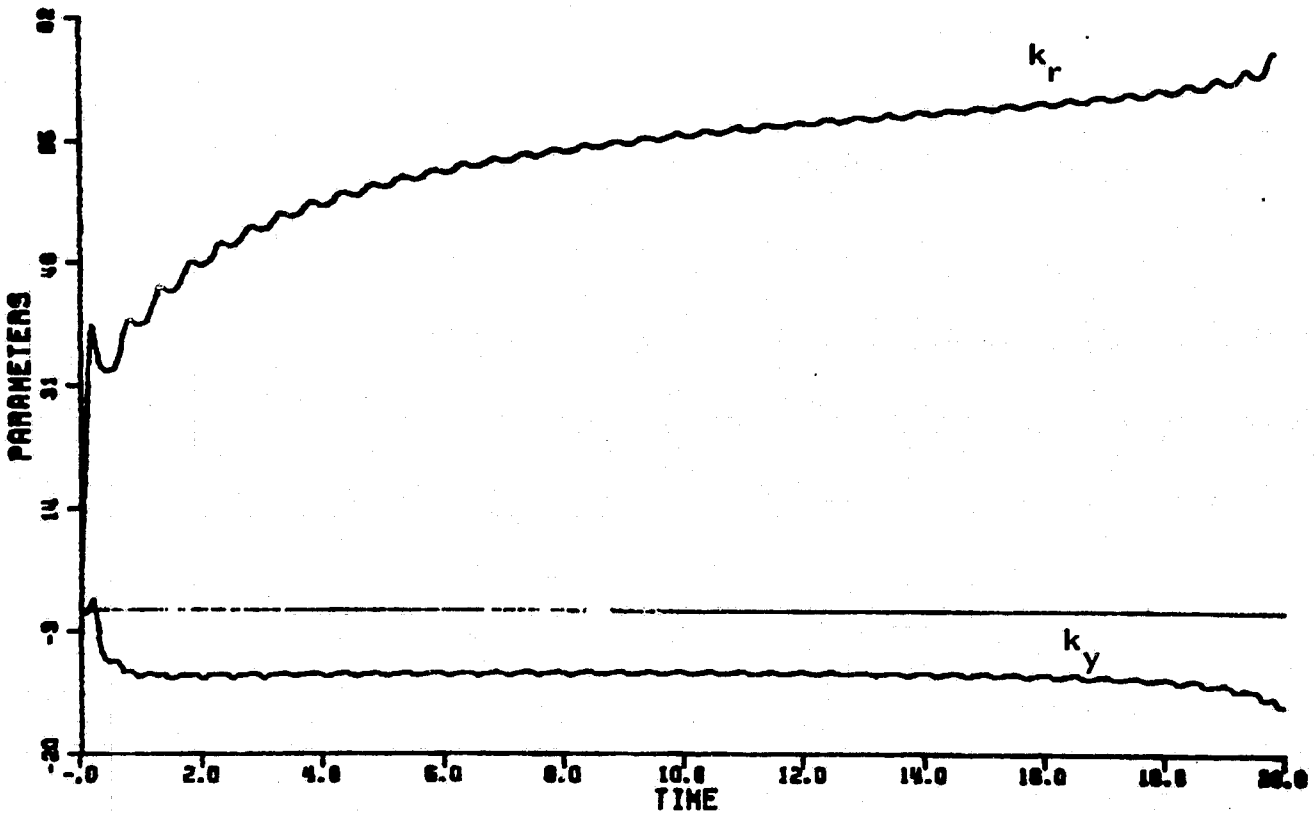

Figure 5-20. Simulation of DA3 with unmodeled dynamics and γ=13.981. (System eventually becomes unstable.)

5.1.3.3 The Need to Design the Nominal Controller Well

In this section we show that if the filter, L, is chosen properly in DA3, the nominal control system can be made to match the reference model with no feedback at all. Such an open loop control design is clearly not desirable. This points out the need for the adaptive system designer to consider the design of the nominal control system carefully in the context of the model reference problem formulation where the only criterion of performance involves the systems response to reference input. It is left to the designer to try to construct the system so that, if it converges as desired, the resulting nominal control system will perform all the functions usually expected of a control system such as disturbance rejection and sensor noise reduction.*

In the sequel, we assume that the plant contains no unmodeled dynamics and is given by

$$y(t) = \frac{.078q^{-1}}{1-.961q^{-1}}\,[u(t)] \qquad (5\text{-}19)$$

with the reference model of eqn. (5-1)

$$y_M(t) = \frac{.12q^{-1}}{1-.88q^{-1}}\,[r(t)] \qquad (5\text{-}11)$$

---

*In Chapter 4 and Section 5.2 it is seen that at this point, the design process is a losing battle since, even if the nominal controller has good disturbance rejection properties, the adaptive system is extremely sensitive to disturbances.

If L could be chosen so that

$$L = A = 1-.961q^{-1} \tag{5-34}$$

then the nominal closed-loop controller of Figure 2-7 is

$$y(t) = \frac{.078k_r^*(1-.961q^{-1})}{(1-.88q^{-1})(1-.961q^{-1}-.078k_y^*q^{-1})}\,[r(t)] \tag{5-35}$$

Thus the nominal controller will match the reference model with $k_y^*=0$, i.e., with no feedback. While such a controller would provide the desired response for reference inputs, it would provide no disturbance rejection at all. Even if the adaptive controller converged as desired, the resulting controller could hardly be considered adequate.

This discussion of a possible solution with DA3 points out the more general danger of the present adaptive control problem formulation which states as its only objective the open loop property of model following. The designer must supply the additional reasoning necessary to obtain closed-loop objectives such as disturbance rejection, and noise reduction while retaining robustness.

5.1.4 The Analysis of DA1

The algorithm DA1 does not simplify when the delay is unity as the algorithm DA2 does. This makes its analysis slightly more involved although conceptually the same as the other algorithms.

5.1.4.1 Analysis

Assume that the parameters and signals of the system remain near nominal values and that the input is constant. Using the same arguments as in Section 3.2 for CA2, the continuous-time counterpart to DA1, the error system for DA1 given in Figure 2-12 reduces to that of Figure 5-21, where now

$$G_E = -\frac{q^{-1}}{1-q^{-1}}\left[\frac{q^*B^*q^{-d}\rho}{k_r^*A^*} - \frac{h^*g_N B_N q^{-d}}{A_N} + \frac{h^*g_N B_N L}{NA_N}\right] + \rho\frac{g_N L B_N}{NA_N} \tag{5-36}$$

and

$$d^* = \underline{w}^T\underline{w}, \quad \underline{\Gamma} = \gamma\underline{I} \tag{5-37}$$

Due to the last term in eqn. (5-37) the system G_E will have as many zeroes as poles.

If ρ is chosen large enough, the system will be stable for all values of d^*. However, choosing ρ too large will cause ϵ_1 to be small whether the closed loop system matches the model or not, since G_E will be dominated by the ρ term. Physically, what happens is that, when ρ is too large, the loop containing ρ in the controller structure of Figure 2-13 dominates the loop that contains the nominal controlled plant. Hence, the error becomes insensitive to changes in the controller parameters and adaptation proceeds very slowly.

The linearized error system of DA1 is fairly complicated and will be analyzed in the context of specific examples.

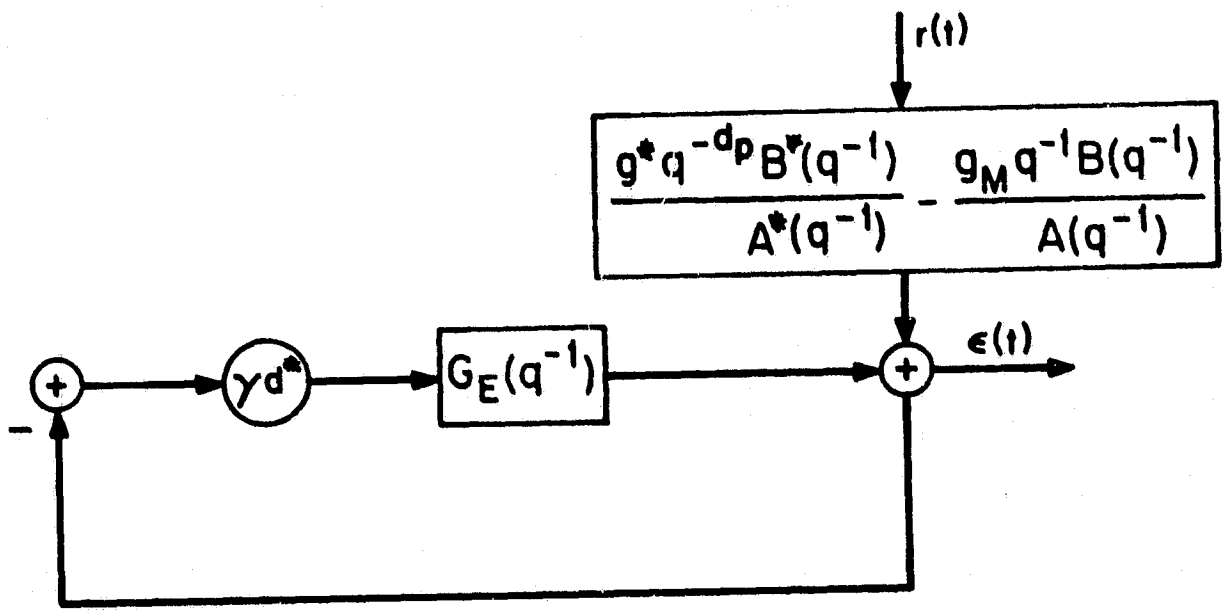

Figure 5-21. Linearized error system for DA1.

5.1.4.2 A Numerical Example with No Unmodeled Dynamics

The same example that has been used throughout will be used again. First, assume that the system is modeled correctly. The plant is

$$y(t) = \frac{.078q^{-1}}{1-.961q^{-1}}\left[u(t)\right] \tag{5-19}$$

and the model is

$$y_M(t) = \frac{(.12)q^{-1}}{1-(.88)q^{-1}}\left[r(t)\right] \tag{5-11}$$

Cancel the first two terms of eqn. (5-36) by choosing the desired nominal system to be

$$\frac{q^*B^*q^{-d_p}}{A^*} = \frac{g_M B_M q^{-d}}{A_M} \tag{5-38}$$

$$h^* = \frac{1}{k_r^*} \tag{5-39}$$

Equation (5-38) is achieved with the following numerical values.

$$k_y^* = -1.02 \qquad k_r^* = \frac{g_M}{g_p} = 1.54 \tag{5-40}$$

Since the system is designed as a first order system, the filter P in eqn. (2-70) vanishes. Choose the auxiliary filter of eqn. (2-75) as

$$\frac{M}{L}\, q^{-d} = \frac{q^{-1}}{1-.88q^{-1}} \tag{5-41}$$

Then the equation for G_E for this examples is:

$$G_E = \frac{g_p q^{-1}}{1-q^{-1}} + \rho g_M$$

$$= \frac{\rho g_M \left(1 - \left(1 - \frac{g_p}{\rho g_M}\right) q^{-1}\right)}{1-q^{-1}} \qquad (5\text{-}42)$$

and the system will be stable for all d^* if

$$\rho \geq .5 \frac{g_p}{g_M} \qquad (5\text{-}43)$$

This is indeed the condition given for stability of the algorithm in [7] (where it is assumed that $g_p = g_M$). Thus, for the algorithm DA1 the local linearized analysis gives the same stability condition on ρ as the global stability proof.

The analysis above suggests a rule of thumb for choosing ρ. The value

$$\rho = \frac{g_p}{g_M} \qquad (5\text{-}44)$$

should provide the fastest error system without allowing oscillation when d^* gets large,as the zero in eqn. (5-42) will be located at the origin and the pole of the d^*-root locus will be trapped near the origin for large values of d^*.

5.1.4.3 A Numerical Example with Unmodeled Dynamics

Use the same plant with unmodeled dynamics as in Section 5.2.2.

$$y(t) = \frac{(0.00361)(1+0.196q^{-1})(1+2.763q^{-1})q^{-1}}{(1-0.961q^{-1})(1-(0.547+j.044)q^{-1})(1-(0.547-j.044)q^{-1})}[u(t)] \tag{5-10}$$

The model and the auxiliary filter will be chosen as in the properly modeled case.

Choose the nominal parameters to be

$$k_y^* = -0.615; \quad k_r^* = 1.16; \quad h^* = \frac{1}{k_r^*} = .86 \tag{5-45}$$

leaving $\frac{g^*B^*}{A^*}$ with poles at

$$z = 0.88; \quad z = 0.71 \quad \text{and} \quad z = 0.46 \tag{5-46}$$

and unity dc gain, approximately matching the model.

In order to find a value of ρ so that the error system is stable for all values of d^*, eqn. (5-36) is broken up as follows

$$G_E = G_E\Big|_{\rho=0} + g_M\rho \tag{5-47}$$

The discrete-time Nyquist plot of $G_E\Big|_{\rho=0}$ for the nominal system given by eqn. (5-45) is given in Figure 5-22. The term ρg_M merely

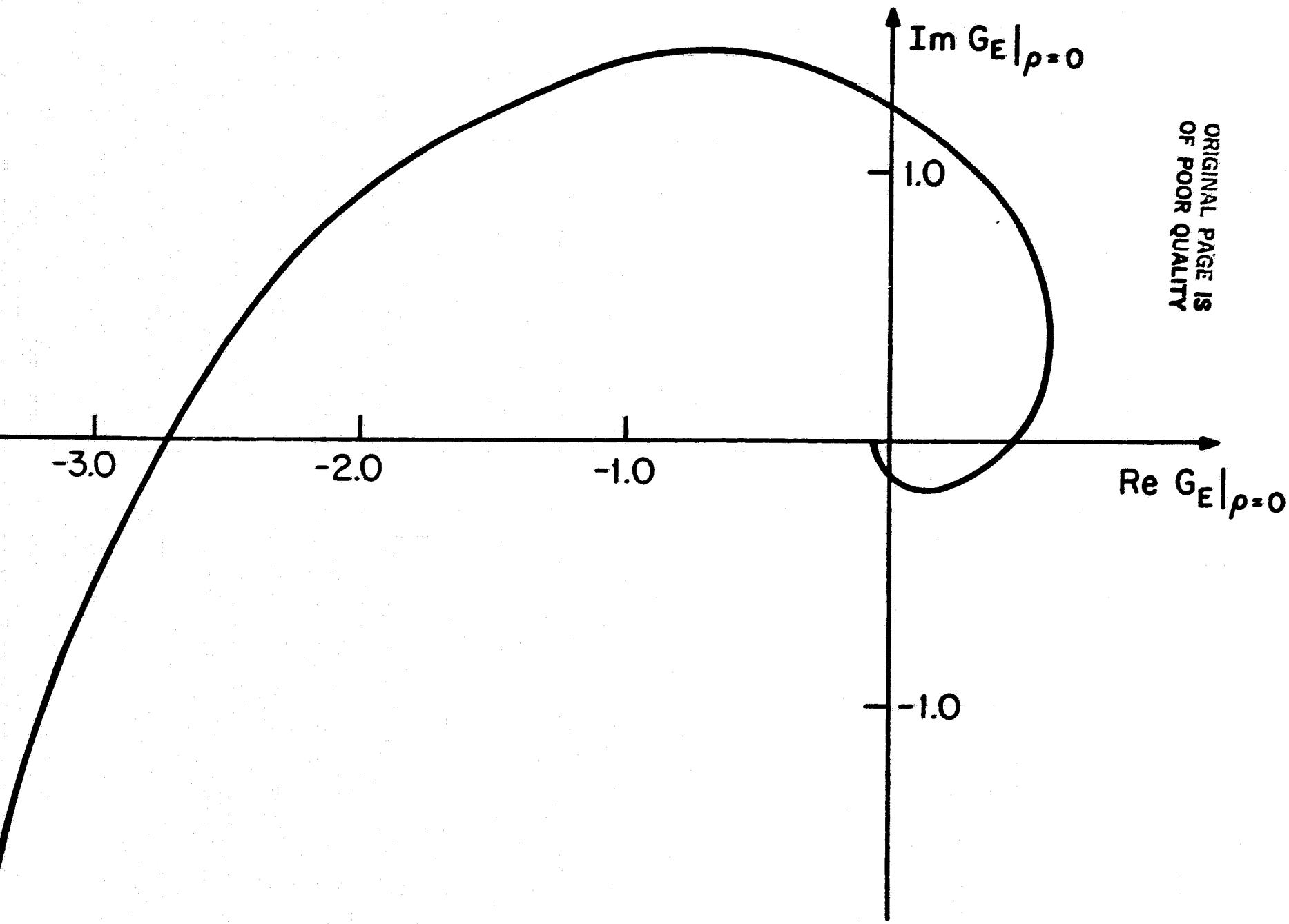

Figure 5-22. Discrete-time Nyquist plot for $G_E|_{\rho=0}$.

shifts this plot to the right. The error system will be stable for all values of d^* if

$$\rho \geq \frac{2.7}{g_M} = 22.5 \qquad (5\text{-}48)$$

This is much larger than the value of ρ which would be picked if unmodeled dynamics were ignored. With no unmodeled dynamics, eqn. (5-44) using g_p from eqn. (5-12) and g_M from eqn. (5-11) would give a suggested value for ρ,

$$\rho = 0.65 \qquad (5\text{-}49)$$

In this example, we will see that for ρ as in eqn. (5-48) the adaptive system DA1 behaves well. However, when ρ is lowered to values somewhat below that of eqn. (5-49), the adaptive system will become oscillatory and then, as ρ is further reduced, unstable.

Figure 5-23 shows the results of a simulation with the parameters initialized according to eqn. (5-44) and with

$$\rho = 23.0; \quad r = 10.0; \quad d^* = 200.0 \qquad (5\text{-}50)$$

The system behaves well for this value of ρ as predicted in the preceeding analysis. If ρ is chosen smaller than the value given by eqn. (5-48), the error system may remain stable but the parameters will move to a more stable configuration and model matching will be compromised. Figure 5-24 demonstrates this with a simulation generated with

$$\rho = 0.319 \qquad (5\text{-}51)$$

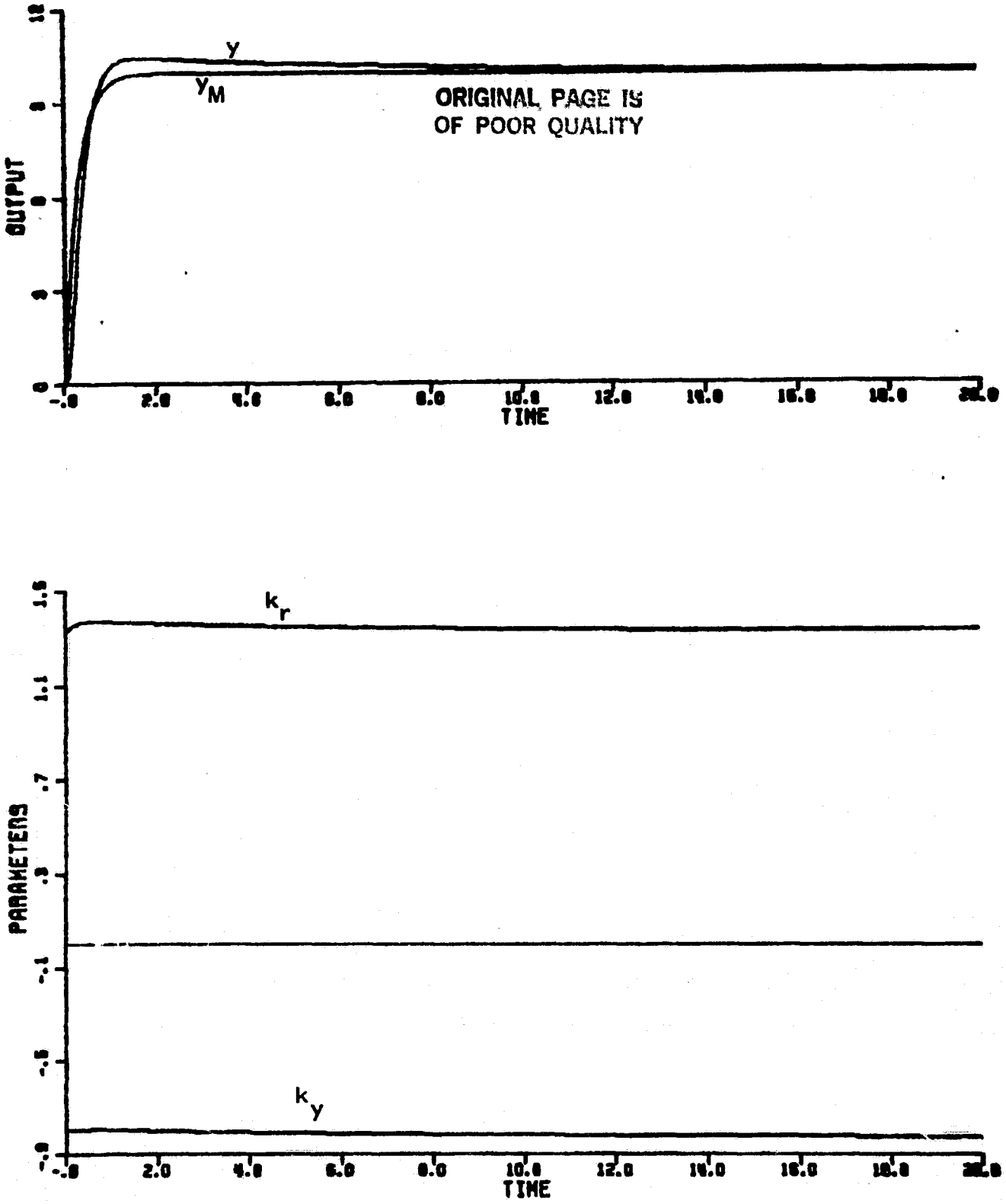

Figure 5-23. Simulation of DA1 with unmodeled dynamics and γ=15.0.

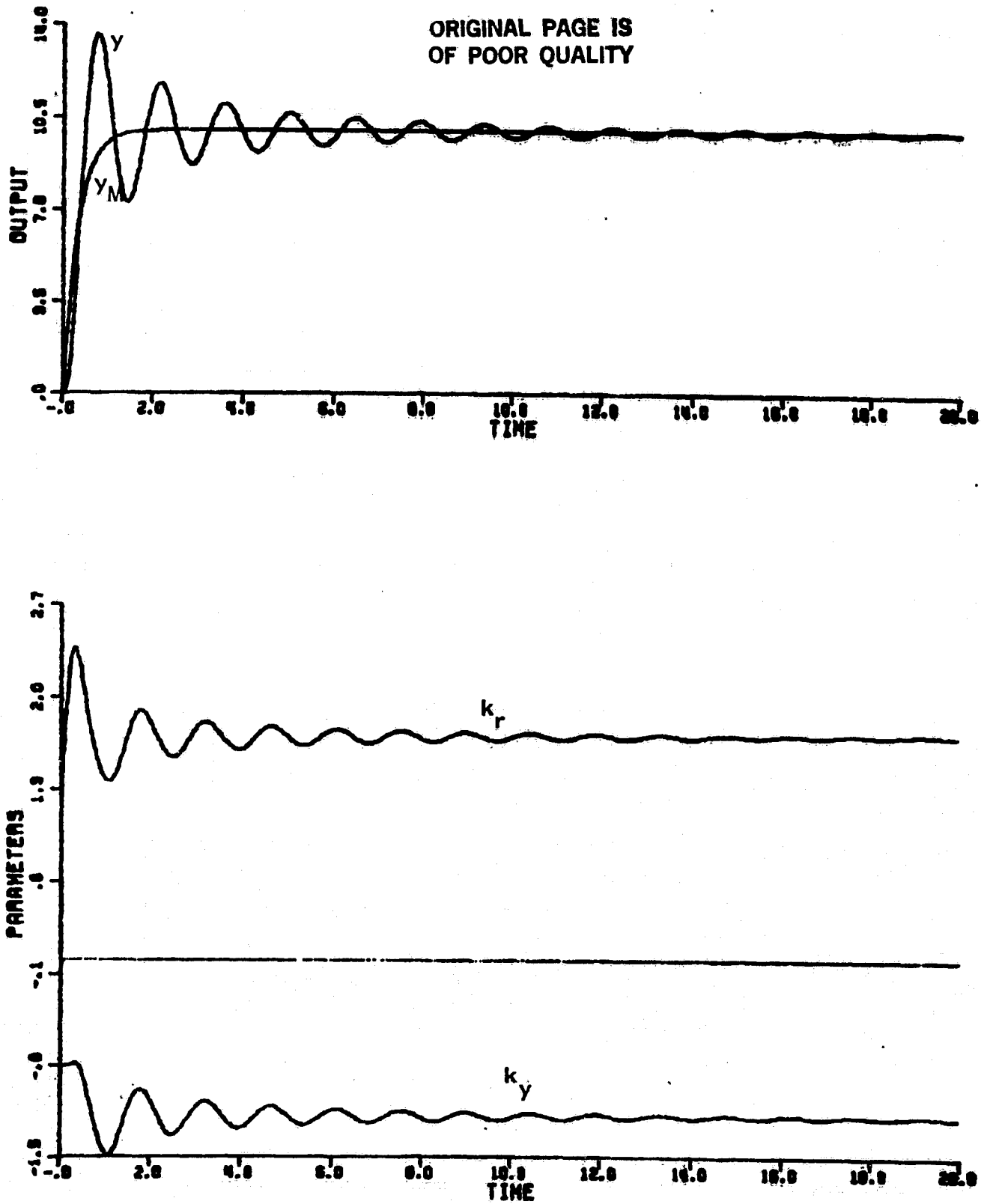

Figure 5-24. Simulation of DA1 with unmodeled dynamics and $\gamma = 0.319$.

The parameters move to

$$k_y^* = -1.2; \quad k_r^* = 1.7; \quad h^* = 0.03 \tag{5-52}$$

The oscillations in Figure 5-24 are harbingers of impending doom. As Figure 5-25 shows, when ρ is lowered to

$$\rho = 0.31828 \tag{5-53}$$

and all other values remain the same, the system is unstable.

Again, it is noted that if the system were sampled at a slow rate the unmodeled poles and zeroes would almost cancel and this system would behave in a manner close to the properly modeled case as explained in Section 5.1.2.3.

5.1.5 Conclusions

In this section, it has been shown that the linearization with constant input method, developed in this thesis, is an extremely useful technique for analyzing the behavior of discrete-time adaptive control system as well as for continuous-time adaptive control systems.

Using this technique, it was shown

- If adaptive controllers are designed without regard for unmodeled dynamics, unstable systems are likely to result.

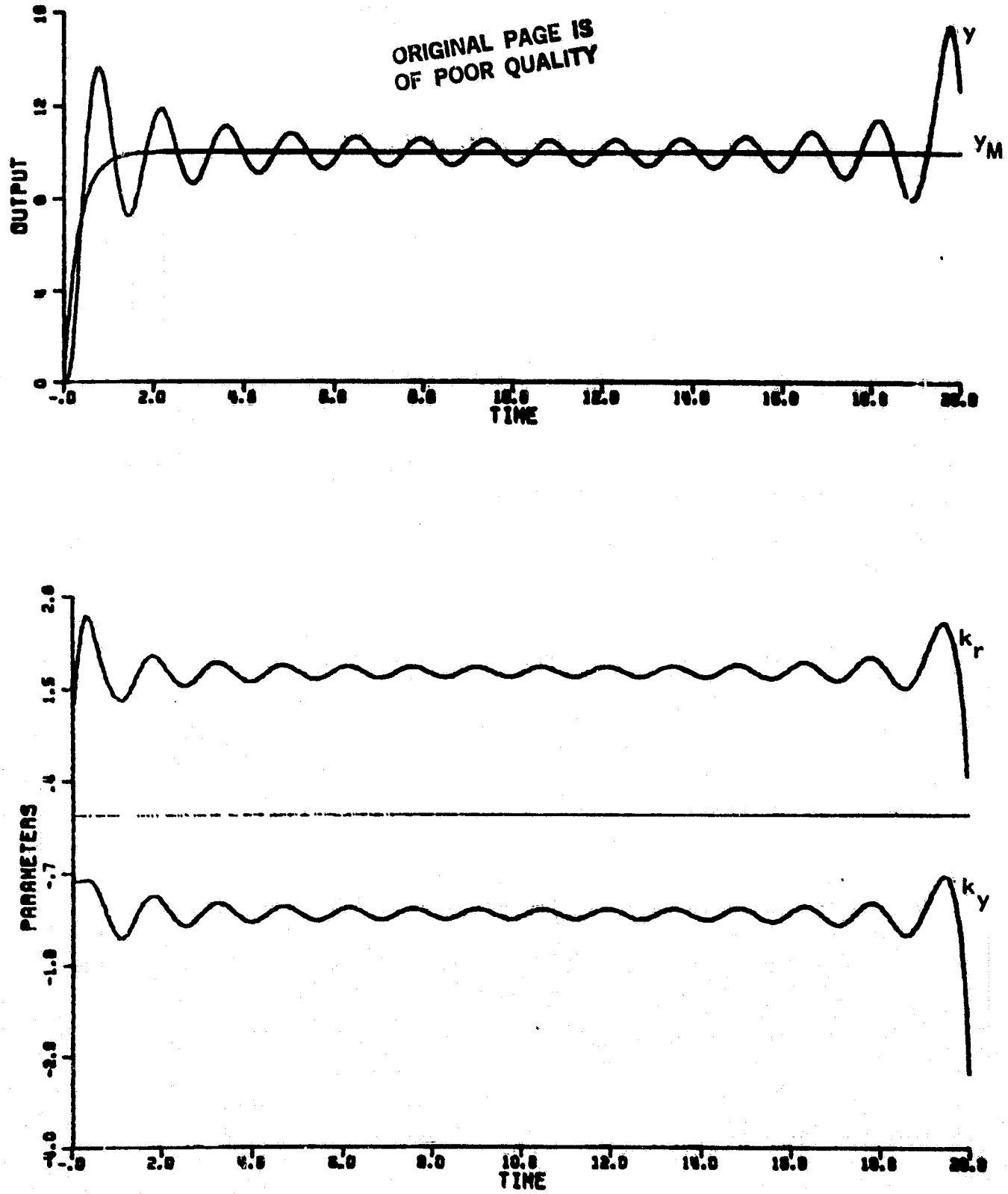

Figure 5-25. Simulation of DA1 with unmodeled dynamics and $\gamma = 0.31828$. (System eventually becomes unstable.)

- Using the linearization analysis of Section 5.2, adaptive systems can be designed which behave well locally when presented with constant reference inputs and no disturbances in the presence of certain classes of unmodeled dynamics.
- In Section 5.2.2.4, it was shown that much of the problem of high frequency unmodeled dynamics is alleviated, if the discrete-time system is created with a slow enough sampling rate.

5.2 Analysis of Discrete-Time Algorithms with Sinusoidal Inputs and Disturbances

5.2.1 Introduction

This section provides for discrete-time systems the analog of the analysis in Chapter 4 for continuous-time systems.

Subsection 5.2.2 shows that an infinite gain feedback operator is present in all the discrete-time systems investigated and Subsection 5.2.3 shows that this infinite gain operator can result in unstable behavior in response to certain sinusoidal inputs and all persistent sinusoidal disturbances.

Subsection 5.2.4 contains the simulations which show that the adaptive algorithms will indeed become unstable in the presence of unmodeled dynamics for certain sinusoidal reference inputs.

Subsection 5.2.5 deals with the response of the systems to sinusoidal disturbances. It is shown there that such disturbances

lead to parameter drift and instability. Finally, Subsection 5.2.6 deals with a phenomenon unique to discrete-time system. In it, the choice of the sampling interval and its effect on the ability of the system to deal with sinusoidal inputs and disturbances is examined.

5.2.2 The Infinite Gain Operators

5.2.2.1 Quantitative Proof of Infinite Gain for the Operator of DA1

In the discrete-time adaptive control systems studied there are infinite gain operators present in the error loop which exactly parallel the infinite gain operators in continuous-time adaptive system which were discussed in Section 4.2.

The infinite gain operators of DA1 are isolated from the error system of Figure 2-12 in Figure 5-26a. The signals w(t) and v(t) are assumed to be scalars. The infinite gain operators of DA2 and DA3 are identical. These are isolated from the systems of Figures 2-16 and 2-18 and are represented in Figure 5-26b.

In this subsection we will prove that two operators which will be defined from Figure 5-26a are indeed of infinite gain. The proof for the operators of Figure 5-26b is analogous and is omitted. The proof of infinite gain, if $\underline{w}(t)$ is a vector, follows from the proof for scalar w(t) since the operator infinite gain can arise from any component of the vector $\underline{w}(t)$.

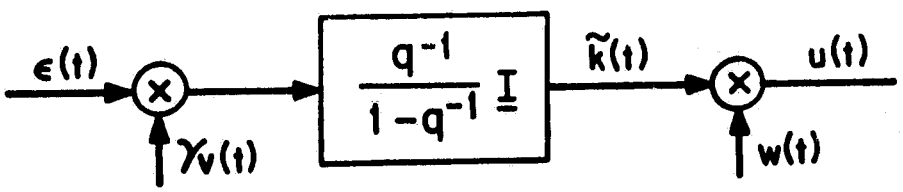

Figure 5-26a. Infinite gain operator for DA1

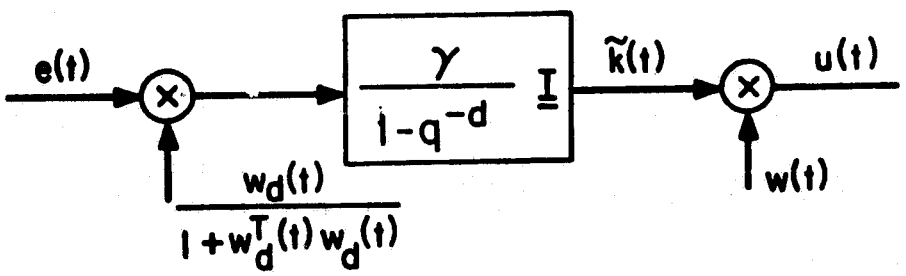

Figure 5-26b. Infinite gain operator for DA2 and DA3.

Figure 5-26 Infinite gain operators for discrete-time algorithms.

The operators of interest are defined from Figure 5-26a as follows:

$$G_{w(t),v(t)}\ [e(t)] = u_o + w(t) \sum_{\tau=1}^{t} \gamma v(\tau-1) e(\tau-1) \tag{5-54}$$

$$H_{v(t)}[e(t)] = \tilde{k}_o + \sum_{\tau=1}^{t} \gamma v(\tau-1) e(\tau-1) \tag{5-55}$$

The following operator theoretic concepts are introduced. For further development of these concepts see [66].

Definition 5-1: A function f(t) from $\mathbb{Z}^+$, the non-negative integers, to R is said to be in ℓ_2 if the following sum exists:

$$||f(t)||_{\ell_2} \triangleq \left(\sum_{t=0}^{\infty} f^2(t) \right)^{1/2} < \infty \tag{5-56}$$

The quantity $||\cdot||_{\ell_2}$ is called the norm of the function.

Definition 5-2: A function f(t) from $\mathbb{Z}^+$ to R is said to be in ℓ_{2e} if the truncated norm

$$||f(t)||_{\ell_2}^{T} \triangleq \left(\sum_{t=0}^{T} f^2(t) \right)^{1/2} \tag{5-57}$$

is finite for all finite T.

Definition 5-3: The gain of an operator G[f(t)] which takes functions in $\mathcal{L}_{2e}$ into functions in $\mathcal{L}_{2e}$ is defined as

$$||G|| = \sup_{\substack{f(t)\in\mathcal{L}_{2e} \\ T\in\mathbb{R}^+}} \frac{||G[f(t)]||^T_{\mathcal{L}_2}}{||f(t)||^T_{\mathcal{L}_2}} \tag{5-58}$$

If there is no finite number satisfying eqn. (5-58), then G is said to have infinite gain.

Theorem 5-1: If w(t) is given by

$$w(t) = b + c \sin\omega_o t \tag{5-59}$$

and v(t) is given by

$$v(t) = b + c \sin\omega_o (t+1) \tag{5-60}$$

for any positive constants b, c, ω_o, the operator $G_{w(t),v(t)}$ of eqn. (5-54) has infinite gain.

Proof: The proof consists of finding a signal, e(t), such that

$$\lim_{T\to\infty} \frac{||G_{w(t),v(t)}[e(t)]||^T_{\mathcal{L}_2}}{||e(t)||^T_{\mathcal{L}_2}}$$

is unbounded.

Throughout the proof, all k_i's will represent finite positive constants, all d_{ij}'s will represent finite constants, while all ϕ_{ij}'s will be constant phase angles, $0 \leq \phi_{ij} \leq 2\pi$.

Let

$$\epsilon(t) = a \sin\omega_o(t+1) \tag{5-61}$$

with a an arbitrary positive constant, and ω_o the same constant as in eqns. (5-59) and (5-60). These signals produce:

$$v(t-1)\epsilon(t-1) = \frac{1}{2} ac + d_{11}\sin(\omega_o t+\phi_{11}) + d_{12}\sin(2\omega_o t+\phi_{12}) \tag{5-62}$$

$$\tilde{k}(t) = H_{v(t)}[\epsilon(t)] \triangleq \tilde{k}_o + \sum_{\tau=1}^{t} \gamma v(\tau-1)\epsilon(\tau-1)$$

$$= k_0 + \gamma\left(\frac{1}{2} ac\, t + d_{21}\sin(\omega_o t+\phi_{21}) + d_{22}\sin(2\omega_o t+\phi_{22})\right) \tag{5-63}$$

$$u(t) = G_{w(t),v(t)}[\epsilon(t)] \triangleq u_0 + w(t) \sum_{\tau=1}^{t} \gamma v(\tau-1)\epsilon(\tau-1)$$

$$= u_0 + \frac{1}{2}\gamma abc\, t + \frac{1}{2}\gamma ac^2 t \sin\omega_o t$$

$$+ d_{31} + d_{32}\sin(\omega_o t+\phi_{32}) + d_{33}\sin(2\omega_o t+\phi_{33})$$

$$+ d_{34}\sin(2\omega_o t+\phi_{34}) + d_{35}\sin(2\omega_o t+\phi_{35})$$

$$+ d_{36}\sin(2\omega_o t+\phi_{36}) \tag{5-64}$$

Using standard norm inequalities* we obtain

$$||u(t)||_{\ell_2}^T \geq || \frac{1}{2} \gamma abct + \frac{1}{2} \gamma ac^2 t \sin\omega_o t||_{\ell_2}^T$$

- (sum of the norms of the remaining terms of eqn. (5-64))

$$\geq || \frac{1}{2} \gamma abct + \frac{1}{2} \gamma ac^2 t \sin\omega_o t||_{\ell_2}^T - (K_1)^{1/2} - (K_2 T)^{1/2} \qquad (5\text{-}65)$$

Now

$$||\frac{1}{2} \gamma abct + \frac{1}{2} \gamma ac^2 t \sin\omega_o t||_{\ell_2}^{T\ 2}$$

$$= \sum_{t=0}^{T} \frac{1}{4} \gamma^2 c^2 b^2 t^2 + \frac{1}{2} \gamma^2 a^2 bc^3 t^2 \sin\omega_o t + \frac{1}{4} \gamma^2 a^2 c^4 t^2 \sin 2\omega_o t$$

$$= \sum_{t=0}^{T} \left(\frac{1}{4} \gamma^2 a^2 b^2 c^2 + \frac{1}{2} \gamma^2 a^2 c^4\right) t^2 + \frac{1}{2} \gamma^2 a^2 bc^3 t^2 \sin\omega_o t - \frac{1}{\gamma} \gamma^2 c^2 c^4 t^2 \cos 2\omega_o t$$

$$\geq \frac{1}{3}\left(\frac{1}{4} \gamma^2 a^2 b^2 c^2 + \frac{1}{2} \gamma^2 a^2 c^4\right) T^3 - K_3 T^2 - K_4 T - K_5 \qquad (5\text{-}66)$$

Also

$$||e(t)||_{\ell_2}^{T\ 2} = a^2 \sum_{t=1}^{T} \sin 2\omega_o (t-1) \leq a^2 T \qquad (5\text{-}67)$$

---

*Specifically

$$||A-B|| \geq ||A|| - ||B||$$

and

$$||A+B|| \geq ||A|| + ||B||$$

Therefore, using eqns. (5-65), (5-66) and (5-67)

$$\frac{||u(t)||^T_{\ell_2}}{||e(t)||^T_{\ell_2}} = \frac{\left(\left(\frac{\gamma^2 a^2 b^2 c^2}{12} + \frac{\gamma^2 a^2 c^4}{24}\right) T^3 - K_3 T^2 - (K_2+K_4)T - (K_1+K_5)\right)^{1/2}}{aT^{1/2}} \xrightarrow{T\to\infty} \infty$$

and hence, $G_{v(t),w(t)}$ for w(t) as in eqn. (5-59) and v(t) as in eqn. (5-60) has infinite gain

Q.E.D.

Theorem 5.2: The operator $H_{v(t)}$ with w(t) given in eqn. (5-59) and v(t) given in eqn. (5-60) has infinite gain.

Proof: Choose $e(t)$ as in eqn. (5-61). Then

$k(t) = H_{v(t)}[e(t)]$ is given by eqn. (5-63)

$$\tilde{k}(t) = \tilde{k}_o + \frac{1}{2}\gamma act + d_{21}\gamma \sin(\omega_o t+\phi_{21}) + d_{22}\gamma \sin(\omega_o t+\phi_{22}) \quad (5\text{-}63)$$

where, as in the proof of Theorem 5-1, all d_{ij}'s are finite constants and all ϕ_{ij} are constant phase angles $0 \le \phi_{ij} \le 2\pi$, and all K_i's will be finite positive constants. Using norm inequalities, we obtain

$$||\tilde{k}(t)||^{T\ 2}_{\ell_2} \ge \sum_{t=0}^{T} \frac{1}{4}\gamma^2 a^2 c^2 t^2 - K_1 T \quad (5\text{-}69)$$

$$\ge \frac{\gamma^2 a^2 c^2 T^3}{12} - K_2 T^2 - K_3 T - K_4 \quad (5\text{-}70)$$

Using eqn. (5-70) and eqn. (5-67) which states:

$$||e(t)||_{\ell_2}^{T\ 2} \leq a^2 T, \tag{5-67}$$

we obtain

$$\frac{||\tilde{k}(t)||_{\ell_2}^{T}}{||e(t)||_{\ell_2}^{T}} \geq \frac{\left(\frac{\gamma^2 a^2 c^2}{12}\ T^3 - K_2 T^2 - K_3 T - K_4\right)^{1/2}}{aT^{1/2}} \xrightarrow{T\to\infty} \infty$$

and, hence, $H_{v(t)}$ has infinite gain for v(t) as in eqn. (5-60).

Q.E.D.

5.2.2.2 Qualitative Explanation of the Infinite Gain of $G_{w,v}$ and H_v

The qualitative explanation of the mechanism which results in the infinite gain of the operators $G_{w(t),v(t)}$ and $H_{v(t)}$ is a discrete-time analogue to the discussion of Section 4.2.2.

If v(t) and e(t) contain sinusoids of the same frequency and if these sinusoids do not have a phase difference of exactly 90°, the multiplication of v(t) and e(t) will produce a constant correlation term. The signal v(t)e(t) then enters an accumulator; the accumulation of the constant correlation term produces the infinite gain. Since the output of an accumulator with constant

input is a ramp, the output signal of the accumulator (which is also the output of $H_{v(t)}$) increases in amplitude indefinitely with time. The output of $G_{w(t),v(t)}$ is formed by multiplying the output of the accumulator by w(t), producing a sinusoid with increasing amplitude at the frequency assumed present in w(t).

The explanation of infinite gain given in this subsection can be applied to explain the infinite gain of the operators which may be defined analogously to eqns. (5-54) and (5-55) from Figure 5-26b.

5.2.3 Two Mechanisms of Instability

Two mechanisms of instability for discrete-time algorithms are now examined. These mechanisms are parallels to the mechanism discussed in Section 4.3 for continuous-time algorithms.

These mechanisms depend on the infinite gain nature of the operators $G_{w(t),v(t)}$ and $H_{v(t)}$ as discussed in Section 5.2.2. In order to demonstrate infinite gain of these operators, it was assumed that $\epsilon(t)$ and a component of $\underline{w}(t)$ and $\underline{v}(t)$ have distinct sinusoids at a common frequency as in eqns. (5-59), (5-60) and (5-61).

The discussion of Section 4.3.1 shows that the equivalent signals of $\epsilon(t)$, $\underline{w}(t)$, $\underline{v}(t)$ in the continuous-time system will have a distinct sinusoid at a common frequency if either:

1) The reference input has a distinct sinusoid, or

2) There is a sinusoidal disturbance.

The points of the discussion of Section 4.3.1 hold also for the discrete-time systems and the discussion will not be repeated here.

5.2.3.1 Instability Due to the Gain of the Operator G of Equation (5-54)

The first instability mechanism for discrete-time algorithms is the same mechanism which was discussed in Section 4.3.2. The mechanism will be explained here using the error system of DA2 shown in Figure 2-16. The error system is redrawn in Figure 5-27 which emphasizes the role of the infinite gain operator

$$G_{\underline{w}(t)}[e(t)] = \gamma \underline{w}(t) \sum_{\tau=0}^{t} \frac{\underline{w}_d(\tau) e(\tau)}{1+\underline{w}_d^T(\tau)\underline{w}_d(\tau)} \qquad (5\text{-}72)$$

Assume $\underline{w}(t)$ consists of a sinusoid of frequency ω_o and a constant. The signal $\underline{w}_d(t)$ is simply a delayed version of $\underline{w}(t)$. Assume that $e(t)$ is a sinusoid of frequency ω_o. Then, just as in the continuous time case, the operator $G_{\underline{w}(t)}$ will manifest its infinite gain by producing at the output a sinusoid at the same frequency, ω_o, as the sinusoidal error signal, but with an amplitude which increases linearly with time, plus some other signals. By concentrating on the signal at frequency ω_o and viewing the operator

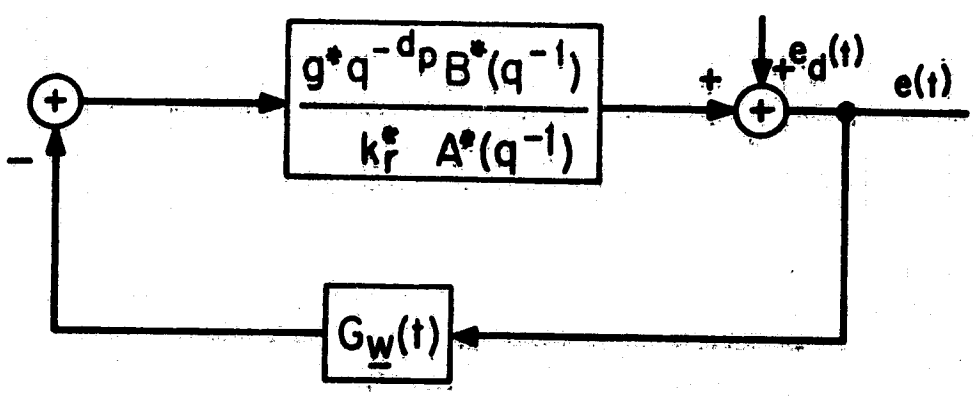

Figure 5-27. Error system for DA2 emphasizing role of G_w.

$G_{w(t)}$ as a time increasing gain at the frequency ω_o and very small gain at other frequencies, a mechanism for instability in the error system of Figure 5-27 will be exposed.

Assume the forward loop, $\frac{g^*q^{-d_p}B^*}{k_r^*A^*}$, of the error system of Figure 5-27 has enough phase shift at the frequency ω_o so that, when added to whatever phase shift may occur in the operator $G_{w(t)}$ at the frequency ω_o, the phase shift of the entire loop at ω_o is $\pm 180°$. The combination of this $\pm 180°$ phase shift with the sign reversal of the feedback law will produce positive feedback in the error system loop, thereby reinforcing the sinusoid at the input of $G_{w(t)}$. The sinusoid will then increase in amplitude linearly with time, as the gain of $G_{w(t)}$ grows, until the combined gain of $G_{w(t)}$ and $\frac{g^*B^*q^{-d_p}}{k_r^*A^*}$ exceeds unity at the frequency ω_o. At this point the loop itself will become unstable and all signals will grow without bound very quickly.

Due to the presence of the inevitable unmodeled dynamics in the plant, the phase of the forward path of the error loop, $\frac{g^*q^{-d}B^*}{k_r^*A^*}$, will take on each value between -180° and +180° at some

frequency. Since the infinite gain of $G_{\underline{w}(t)}$ can be achieved at any frequency ω_o, the adaptive system is susceptible to unstable behavior via the mechanism described in this subsection, if subjected to sinusoidal reference inputs and/or disturbances in the frequency range where the error loop produced $\pm 180°$ phase shift.

5.2.3.2 Instability Due to the Gain of the Operator $H_{\underline{w}}$ of Equation (5-55)

In this subsection we examine a mechanism of instability due to a persistent, but not growing, sinusoid in the plant output and the error signals of discrete-time adaptive control system. Such persistent sinusoidal signals could arise from a sinusoidal reference input and/or from a sinusoidal disturbance as explained for continuous-time systems in Section 4.3.3. A signal of the same frequency will also be present in the signal $\underline{w}(t)$ due to the dependence of $\underline{w}(t)$ on the plant output as in, for example, eqn. (2-95).

The correlation of e(t) and signals derived from $\underline{w}(t)$ within the operator $H_{\underline{w}(t)}$ will cause a constant signal at the input to the accumulator of $H_{\underline{w}(t)}$ in eqn. (5-55). The infinite gain of $H_{\underline{w}(t)}$ will then be realized as the output of the accumulator will contain a ramp.

Since the output of the accumulator of eqn. (5-55) is the parameter errors, $\tilde{\underline{k}}(t)$, the parameters of the controller,

$$\underline{k}(t) = \underline{k}^* + \tilde{\underline{k}}(t) \qquad (2\text{-}84)$$

will increase without bound.

If there are any unmodeled dynamics at all, increasing the size of the nominal feedback controller parameters without bound will cause the adaptive system to become unstable. Indeed, since it is the gains of the nominal feedback loop that are unbounded, the system will become unstable for a large class of plants, including all these whose relative degree is three or more, even if no unmodeled dynamics are present.

5.2.4 Analysis of Discrete-Time Adaptive Systems with Sinusoidal Reference Inputs

That the mechanisms of Section 5.2.3 do indeed occur and produce unstable adaptive systems in the presence of unmodeled dynamics with certain sinusoidal reference inputs is verified by digital simulation in this subsection.

All the simulations displayed in this and the next subsection were generated with the example that has been used throughout this thesis, complete with unmodeled dynamics and sampled at the relatively fast rate of T=.04. The plant is represented as

$$y(t) = \frac{(0.00361)(1+.196q^{-1})(1+2.763q^{-1})q^{-1}}{(1-.961q^{-1})(1-(.547+j.044)q^{-1}(1-(.547-j.044)q^{-1}} \; [u(t)] \tag{5-11}$$

The model is represented as

$$y_M(t) = \frac{(.12)q^{-1}}{1-.88q^{-1}} \; [r(t)] \tag{5-12}$$

All simulations were generated with reasonable adaptive gains set well within the region which produces stable linearized systems. All parameters were started with values which match the model closely in some sense. All other states were started at zero. The initial condition are not particularly important to the results obtained.

5.2.4.1 Instability Due the Mechanism Described in Section 5.2.3.1

Figure 5-28 shows the plant output and parameters of DA2 with the discrete-time input

$$r(t) = 1.0 + 4.5 \sin \frac{13.5t}{.04} . \tag{5-73}$$

Figure 5-29 shows the plant output and parameters of DA3 with the discrete-time input

$$r(t) = 1.0 + 2.5 \sin \frac{13.5t}{.04} \tag{5-74}$$

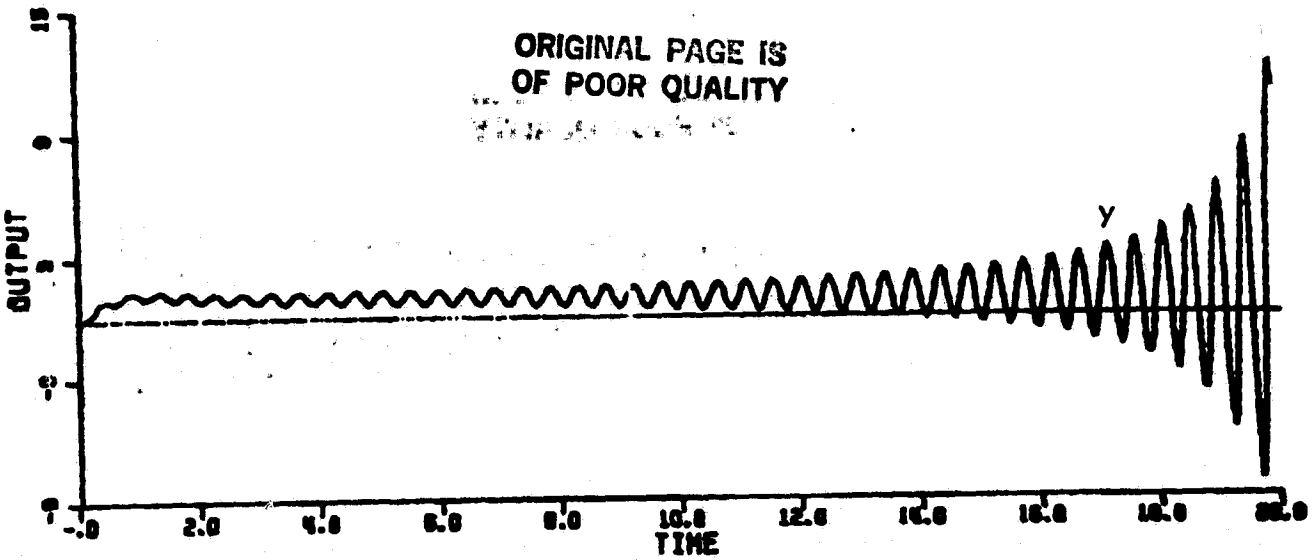

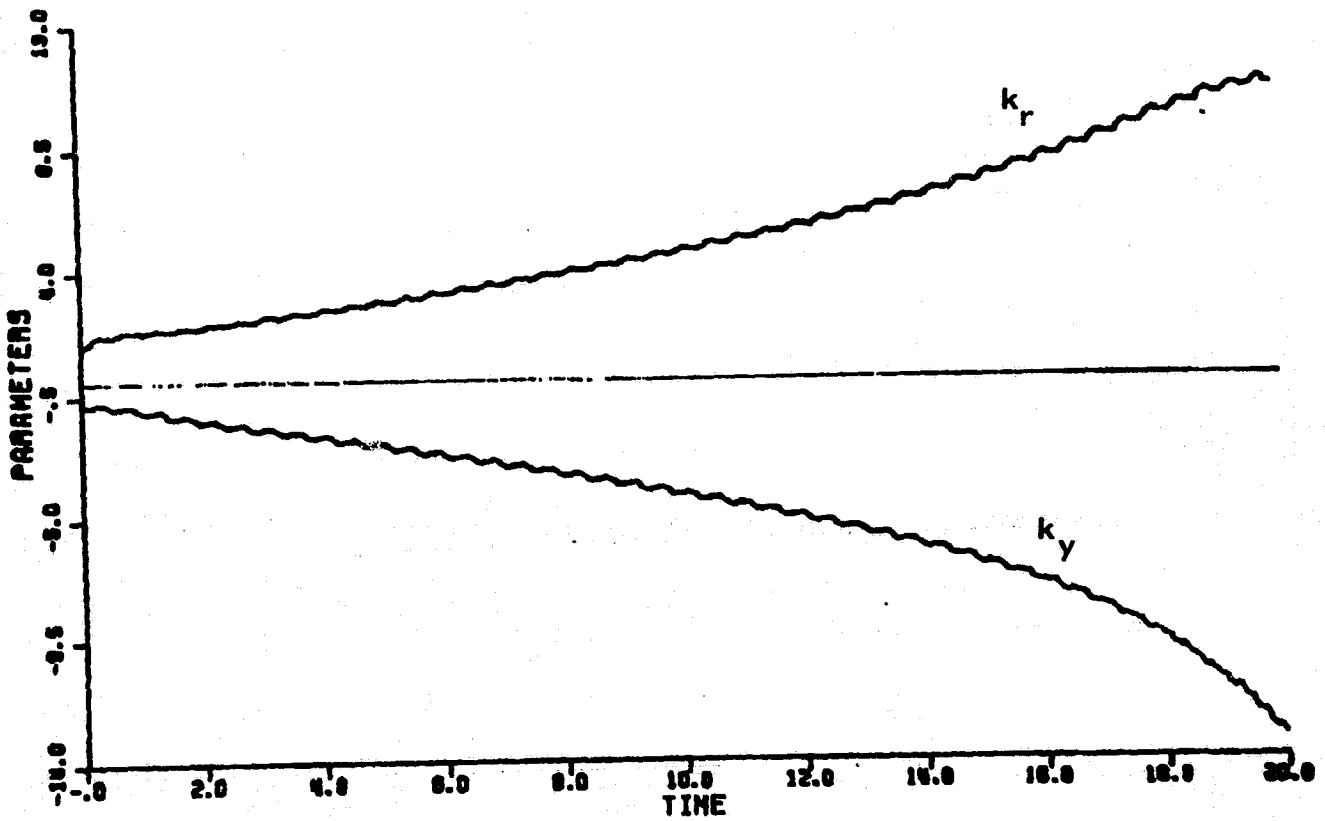

Figure 5-28. Simulation of DA2 with unmodeled dynamics and $r(t)=1.0 + 4.5\sin\frac{13.5}{0.04}t$ (System eventually becomes unstable.)

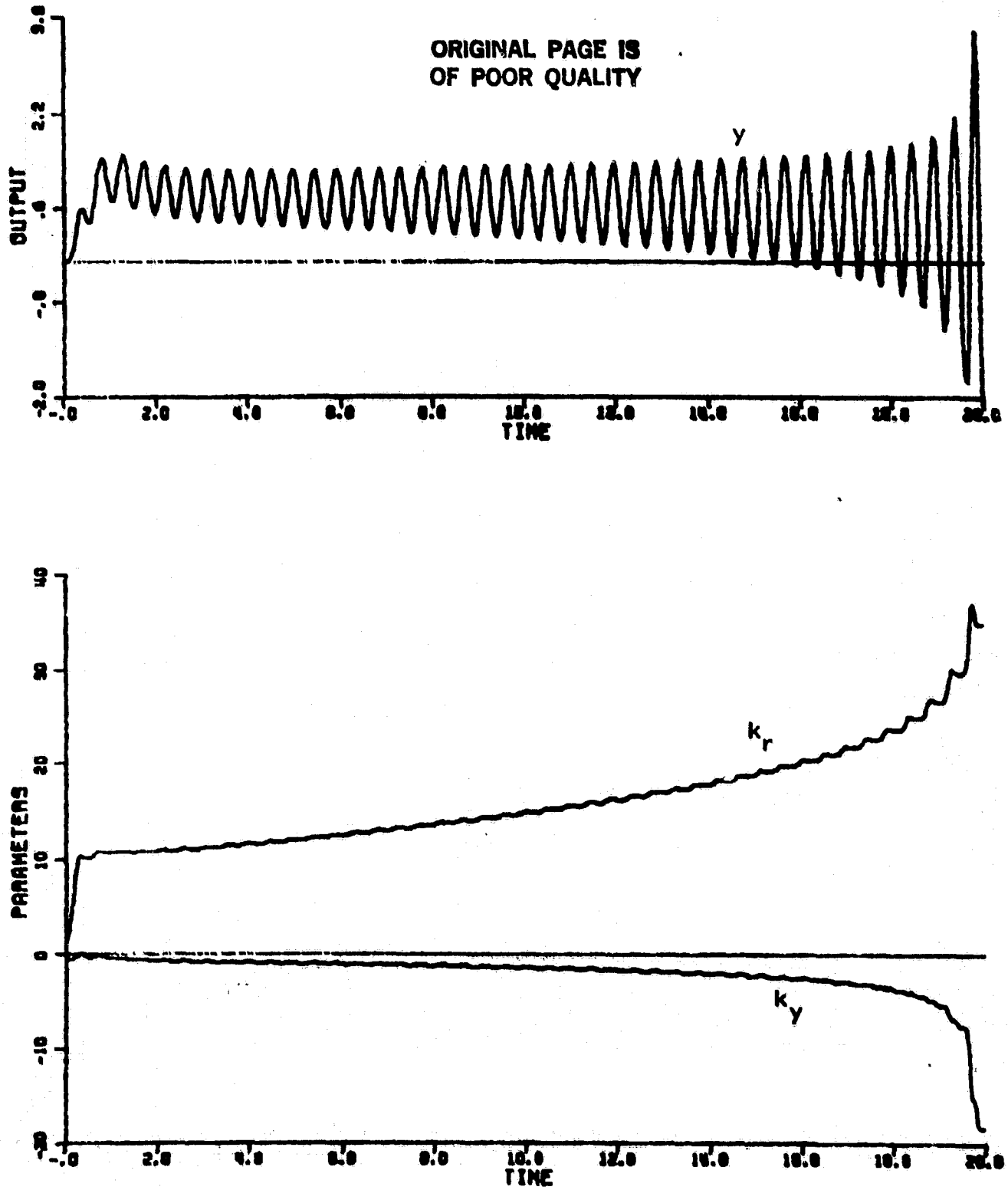

Figure 5-29. Simulation of DA3 with unmodeled dynamics and $r(t)=1.0+2.5\sin\frac{13.5}{0.04}t$.
(System eventually becomes unstable.)

Figure 5-30 shows the auxiliary error ϵ and the parameters of DA1 with the discrete-time input

$$r(t) = 1.0 + 5.0 \sin \frac{13.5t}{.04} \tag{5-75}$$

The frequency $\omega = \frac{13.5}{.04}$ is the frequency at which the discrete-time plant of eqn. (5-11) with unmodeled dynamics has 180° phase shift and at which the positive feedback system discussed in Section 5.2.3.1 is likely to be produced in all the algorithms.

All three algorithms, DA1 to DA3, do exhibit instability in the manner predicted by the mechanism of Section 5.2.3.1. The simulations all show a sinusoidal error linearly increasing in magnitude until a dramatic instability occurs. Only the onset of such an instability is shown in order to maintain reasonable scale in the graphs.

If a sinusoid is introduced at a frequency at which the error system of, for example, Figure 5-27, has little total phase shift, the system may remain stable due to phase considerations even with the infinite gain operator in effect. This is seen in Figure 5-31 and 5-32. Figure 5-31 shows the output error and the parameters of DA3 with a discrete-time input of

$$r(t) = 0.1 + 1.0 \sin \frac{2t}{.04} . \tag{5-76}$$

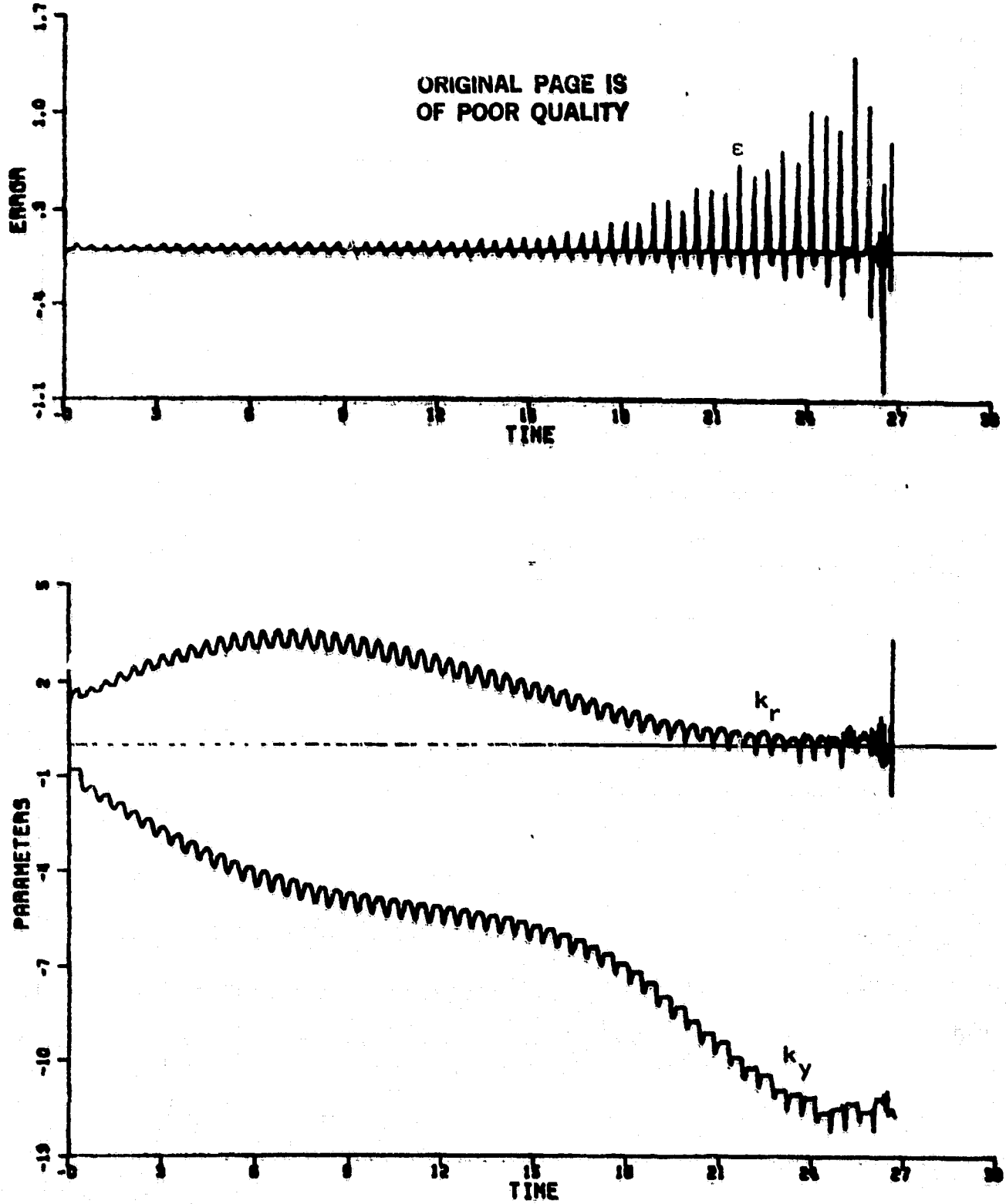

Figure 5-30. Simulation of DA1 with unmodeled dynamics and $r(t)=1.0 + 5.0\sin\frac{13.5}{0.04}t$.
(System eventually becomes unstable.)

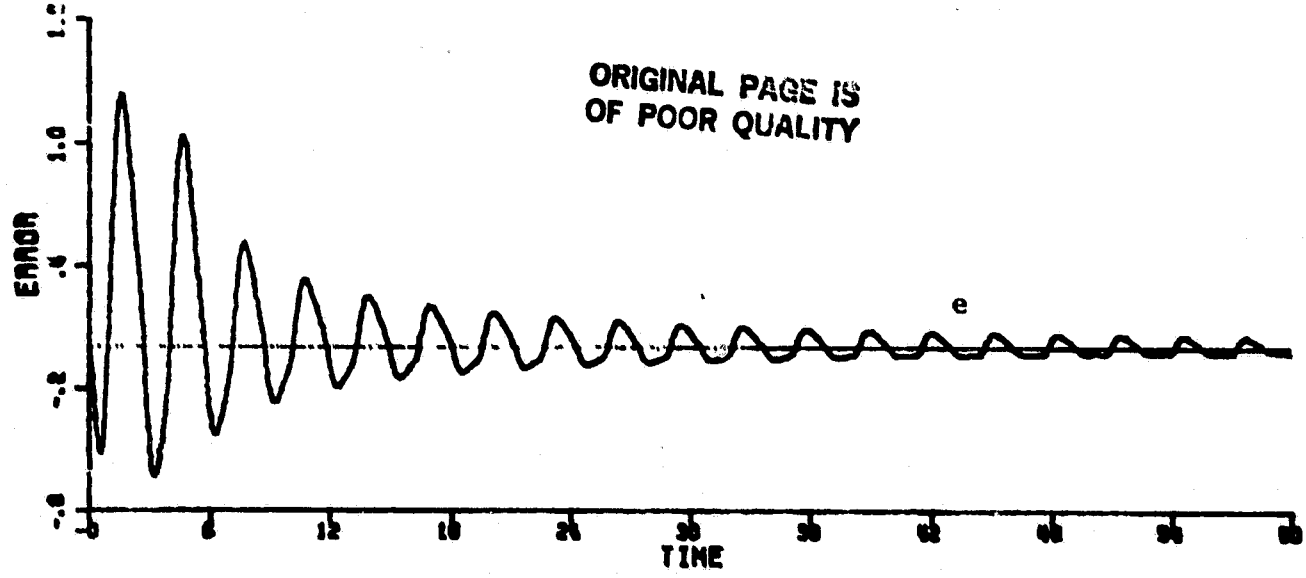

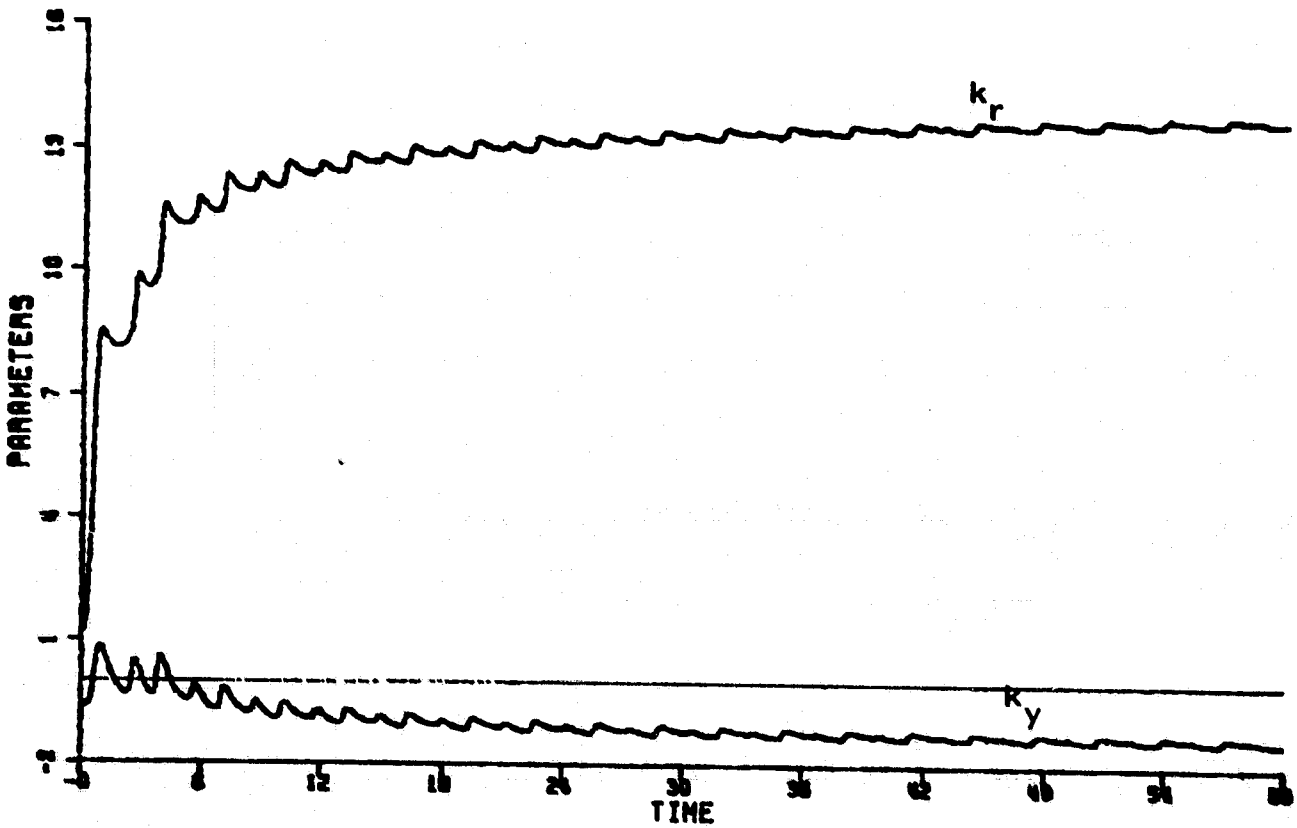

Figure 5-31 Simulation of DA3 with unmodeled dynamics and $r(t)=0.1 + 1.0\sin\frac{2.0}{0.04}t$.
(No instability occurs.)

Figure 5-32 shows the auxiliary error and the parameters of DA1 with the same input of eqn. (5-76).

Figures 5-31 and 5-32 show the algorithms converging nicely to a point where both the dc and low frequency characteristics of the model can be matched.

Figure 5-33 shows the output error and the parameters of DA3 with the input

$$r(t) = 0.1 + 1.0 \sin \frac{7t}{.04} \qquad (5\text{-}77)$$

This demonstrates that the growing sinusoid effect can occur at frequencies other than the exact frequency for which the plant display 180° phase lag. The positive feedback may be caused by phase shift introduced by lags in the infinite gain system or by the shifting of the parameters themselves changing the characteristics of the controlled plant. Similar results were obtained for all the algorithms in both continuous and discrete-time as there may be phase shifts for the infinite gain operator, G, in every algorithm.

5.2.4.2 Instability Due to the Mechanism Described in Section 5.2.3.2

The simulation of DA2 with the input of eqn. (5-59)

$$r(t) = 0.1 + 1.0 \sin \frac{2t}{.04}$$

shows a different behavior than that of DA3 or DA1 from Figures

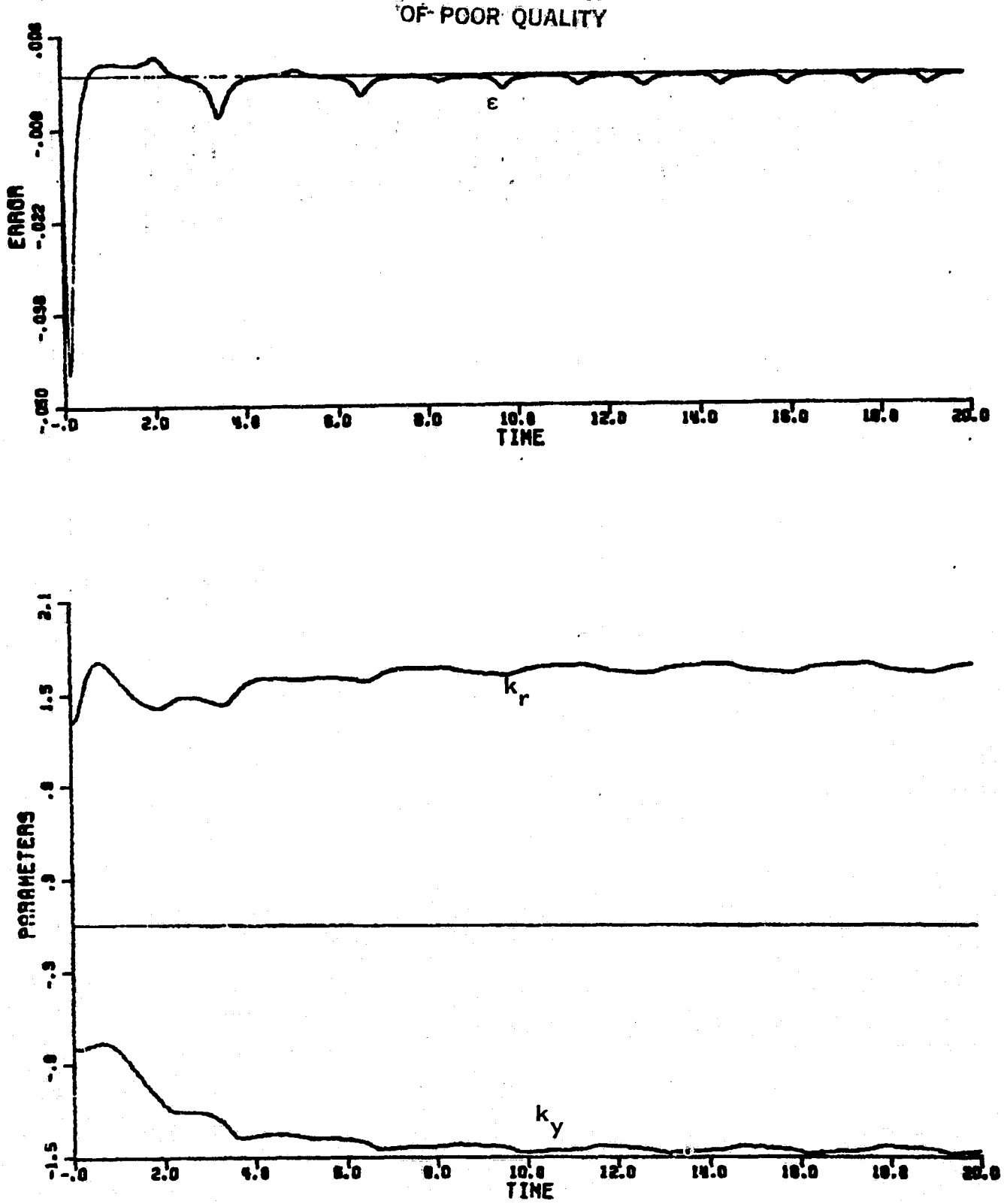

Figure 5-32. Simulation of DA1 with unmodeled dynamics and $r(t)=0.1 + 1.0\sin\frac{2.0}{0.04}t$ (No instability occurs.)

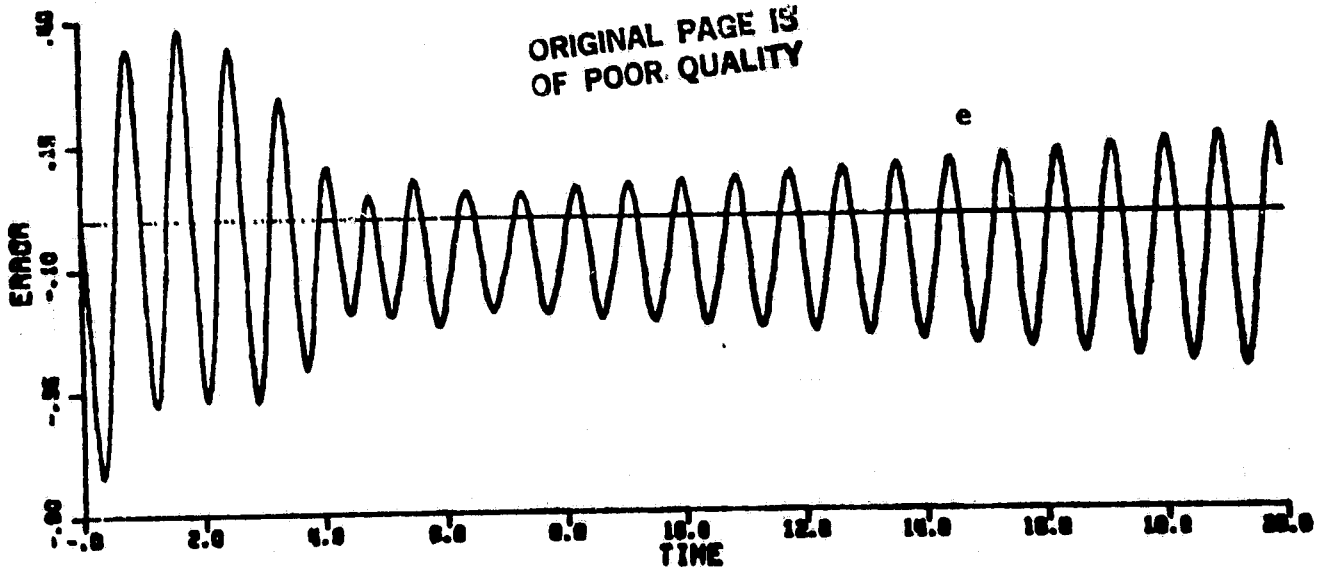

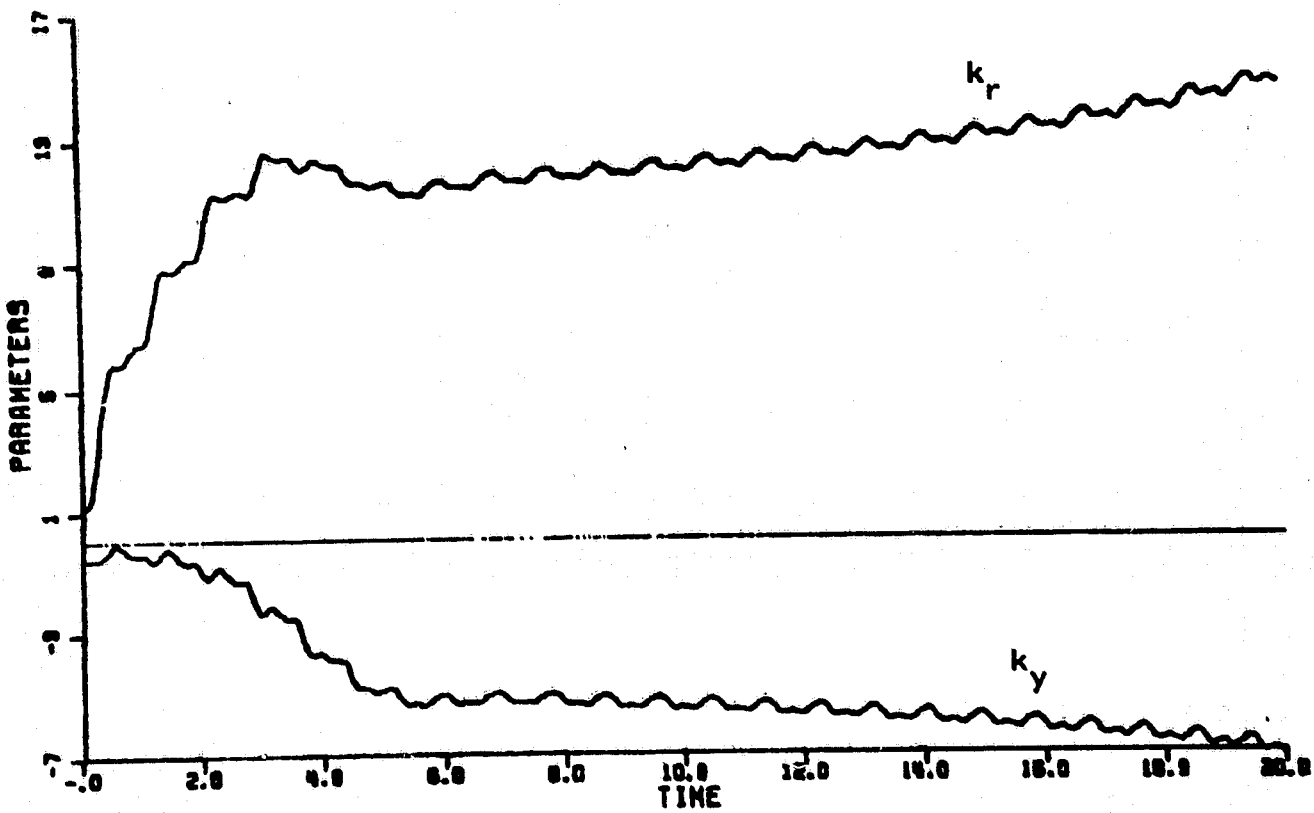

Figure 5-33. Simulation of DA3 with unmodeled dynamics and $r(t)=0.1 + 1.0\sin\frac{7.0}{0.04}t$.
(System eventually becomes unstable.)

5-31 and 5-32. Figure 5-34 shows the output error and the parameters of this simulation.

First of all the error does not grow since the positive feedback is not present. However, because of the deadbeat setup of DA2 discussed in Section 5.1.1, the system cannot match the model in the presence of unmodeled dynamics. This causes the error to converge to a steady state sinusoid. The adaptive system is then driven to instability by the mechanism described in Section 5.2.3.2. The parameters drift away as seen in Figure 5-33. This slow drift will continue until the parameters move to the point where the linearized system is unstable and then the system will become unstable. This is exactly what happened when the simulation was allowed to continue. All the algorithms studied, both in continuous and discrete-time, showed a similar behavior when confronted with a set of input frequencies that could not be well matched.

5.2.4.3 Conclusions

The digital simulations of this section verify the analysis of Section 5.2.3 which showed that, in the presence of unmodeled dynamics, the discrete-time adaptive control algorithms DA1-DA3 can become unstable with sinusoidal reference inputs.

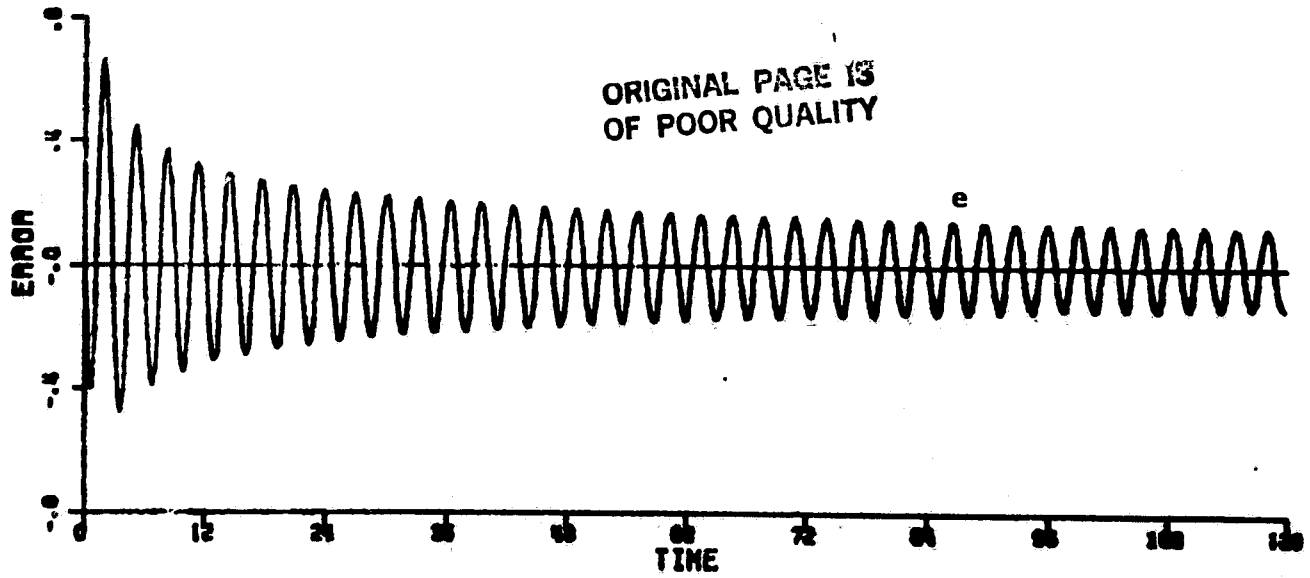

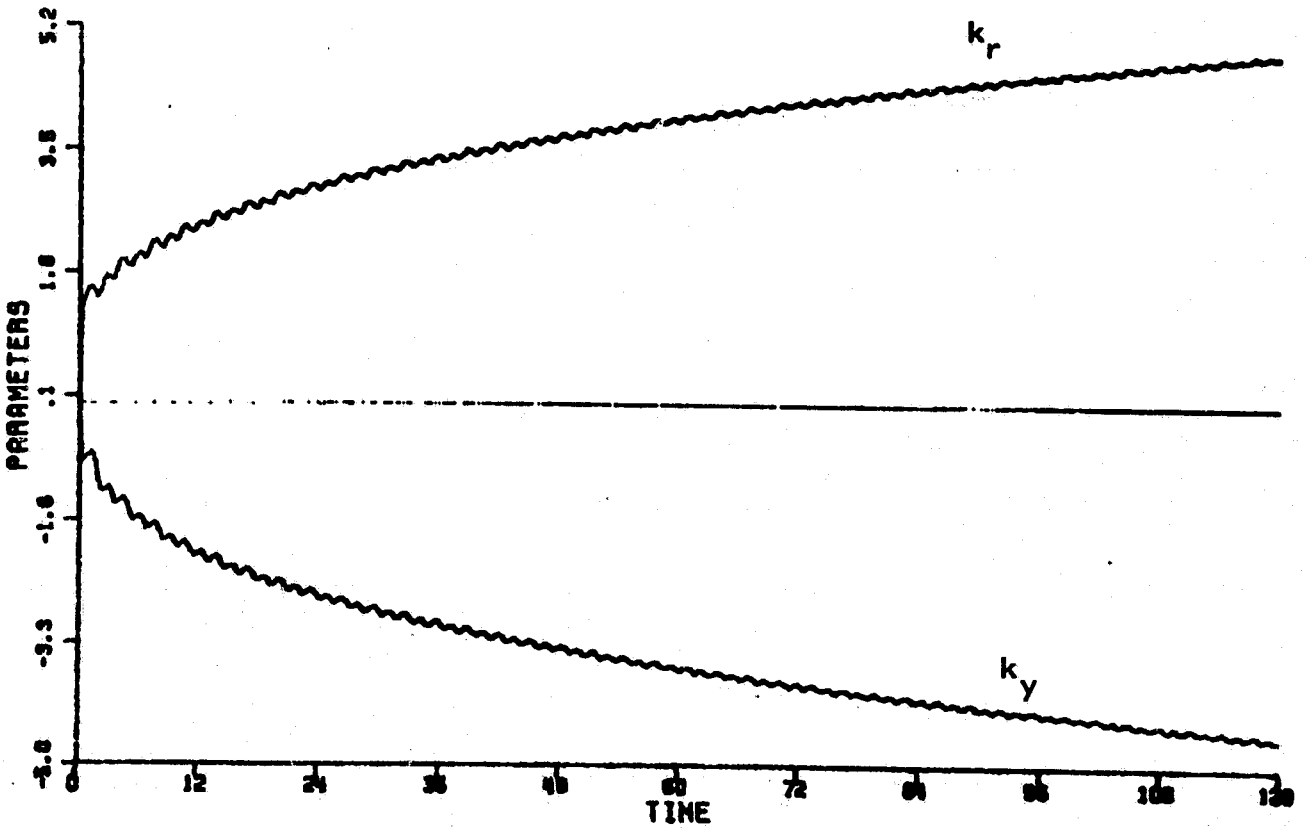

Figure 5-34. Simulation of DA2 with unmodeled dynamics and $r(t)=0.1 + 1.0\sin\frac{2.0}{0.04}t$.
(System eventually becomes unstable.)

In Section 5.2.4.1 it was found that the instability mechanism of Section 5.2.3.1 does indeed occur if the reference input is a sinusoid within a certain range of frequencies. The frequencies required to cause instability are always in the high frequency range but the exact frequencies can only be determined by a detailed analysis of the phase properties of the error system involved.

In Section 5.2.4.2 it was found that instability arose via the mechanism of Section 5.2.3.2, when the reference input consisted of a set of sinusoids for which the controlled plant could not match the response of the reference model due to unmodeled dynamics in the plant.

5.2.5 Response to Additive Output Sinusoidal Disturbances

The discrete-time adaptive control algorithms have the same unstable behavior in the presence of additive output sinusoidal disturbances as their continuous-time counterparts. The instabilities caused by sinusoidal disturbances can come about by the two mechanisms described in Section 5.2.3.

5.2.5.1 Instability Due the Mechanism Described in Section 5.2.3.1

The first mechanism is that a sinusoidal disturbance at the wrong frequency, one at a frequency where the nominally controlled plant with unmodeled dynamics has 180° phase shift, can excite the positive high gain feedback loop described in Section 5.2.3.1. The mechanism is the same as in Section 5.2.4.1 where the sinusoid was due to a reference input. We note, however, that while a designer may be able to control what reference inputs are used in a system, he has no control over what disturbances the system faces.

The sinusoidal disturbance will grow in amplitude, as the infinite gain operator does, until instability occurs. This phenomenon is displayed in Figures 5-35 to 5-37. All simulations in this subsection were generated under the conditions described at the beginning of Section 5.2.4, except that a constant reference input was used and a sinusoidal disturbance, d(t), was added to the output.

Figure 5-35 displays the output and parameters of DA2 under the stimulus

$$r = 0.1;\ d(t) = 0.1 \sin \frac{13.5t}{.04} . \qquad (5\text{-}78)$$

Figure 5-36 displays the output and parameters of DA3 under the stimulus

$$r = 0.1;\ d(t) = 0.015 \sin \frac{13.5t}{.04} . \qquad (5\text{-}79)$$

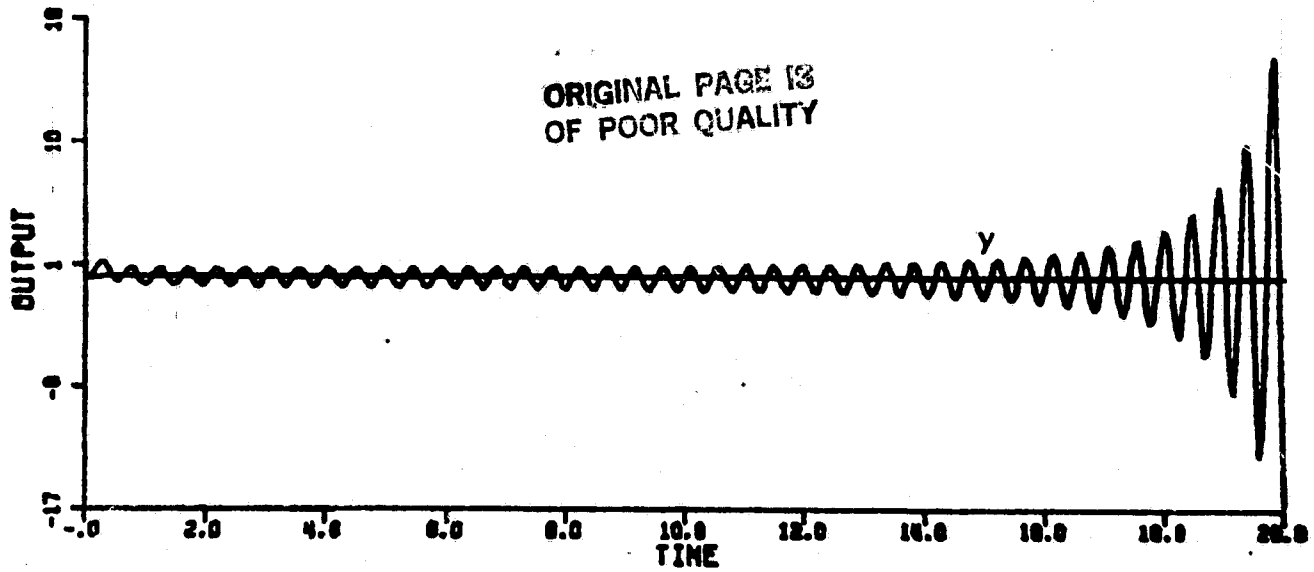

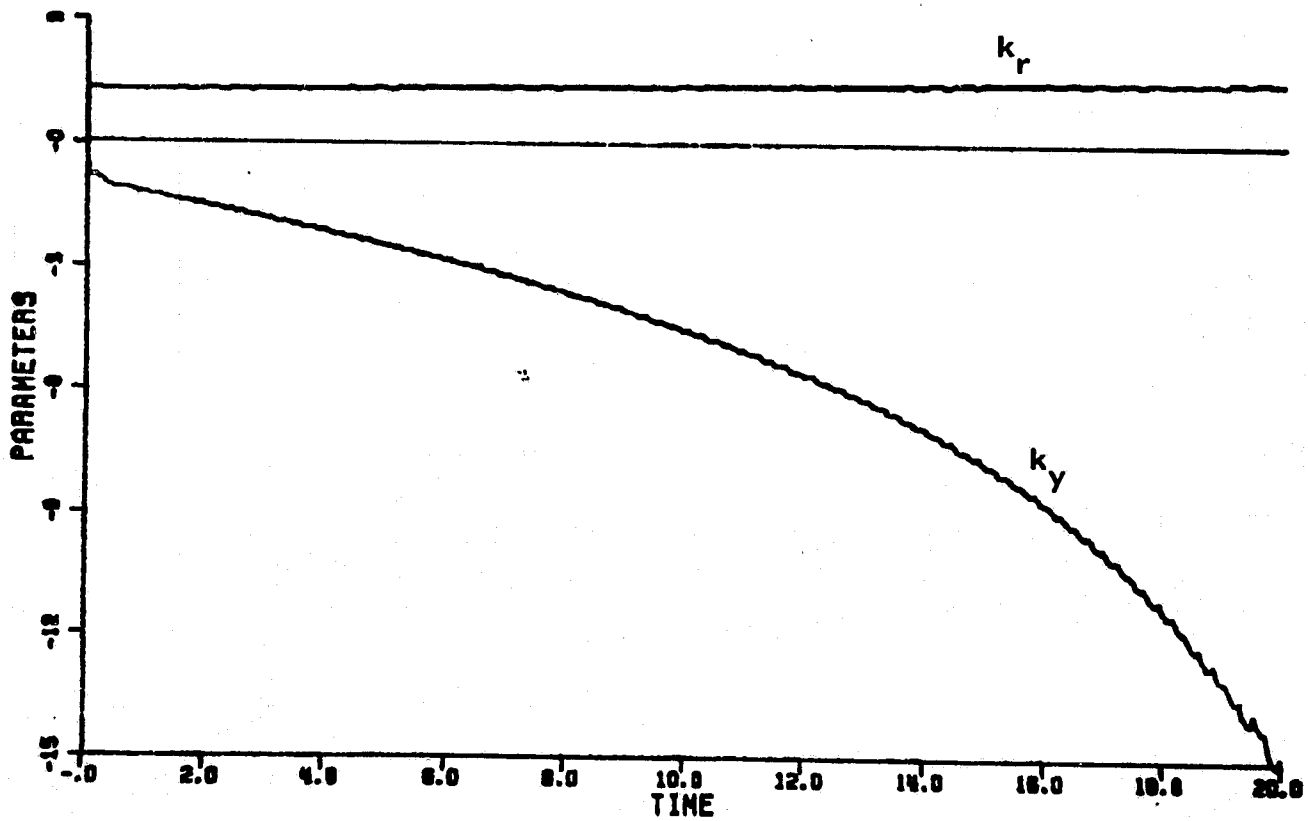

Figure 5-35. Simulation of DA2 with unmodeled dynamics, $r=0.1$, and $d(t)=0.1\sin\frac{13.5}{0.04}t$. (System eventually becomes unstable.)

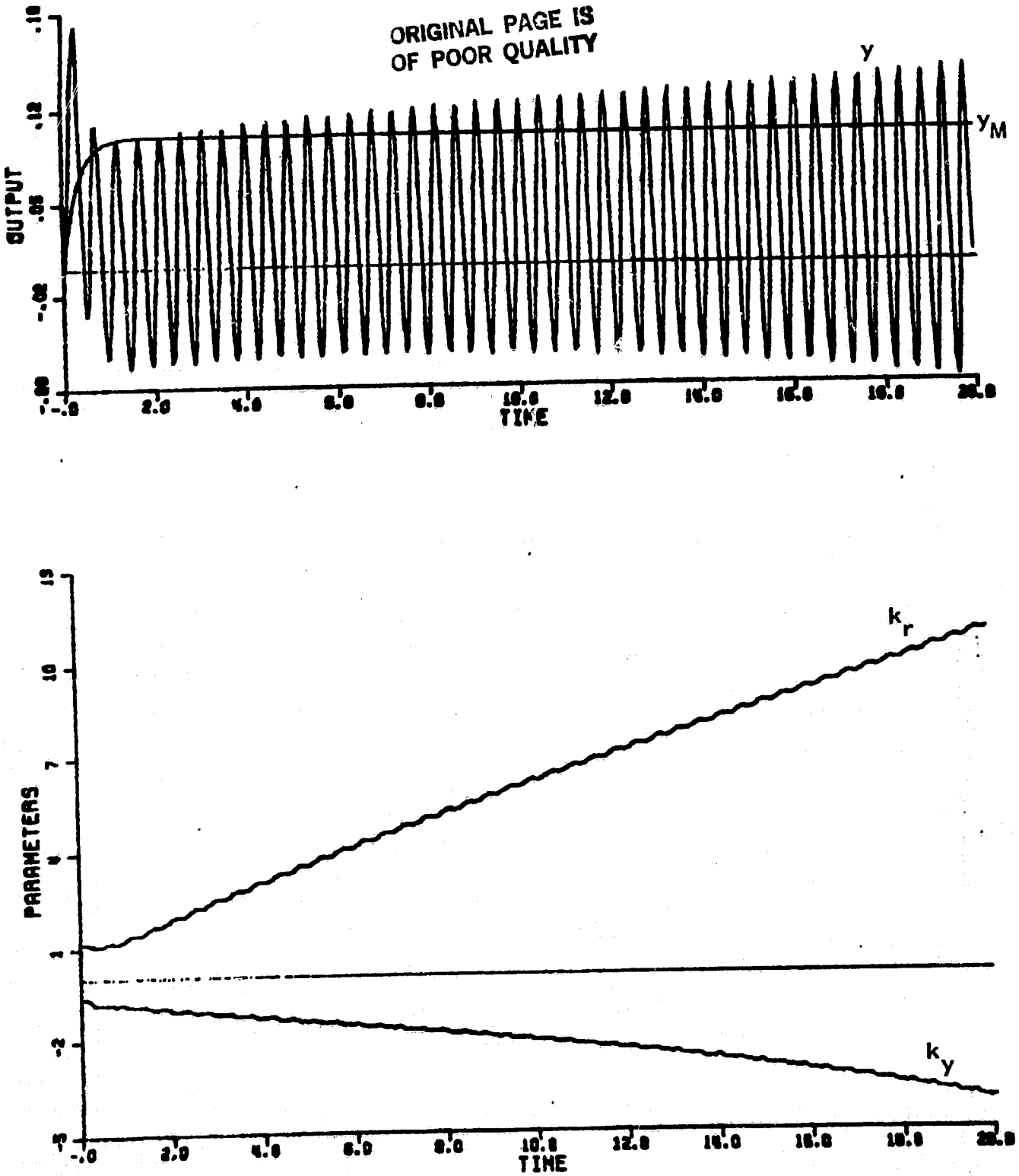

Figure 5-36. Simulation of DA3 with unmodeled dynamics, $r=0.1$, and $d(t)=0.015\sin\frac{13.5}{0.04}t$.
(System eventually becomes unstable.)

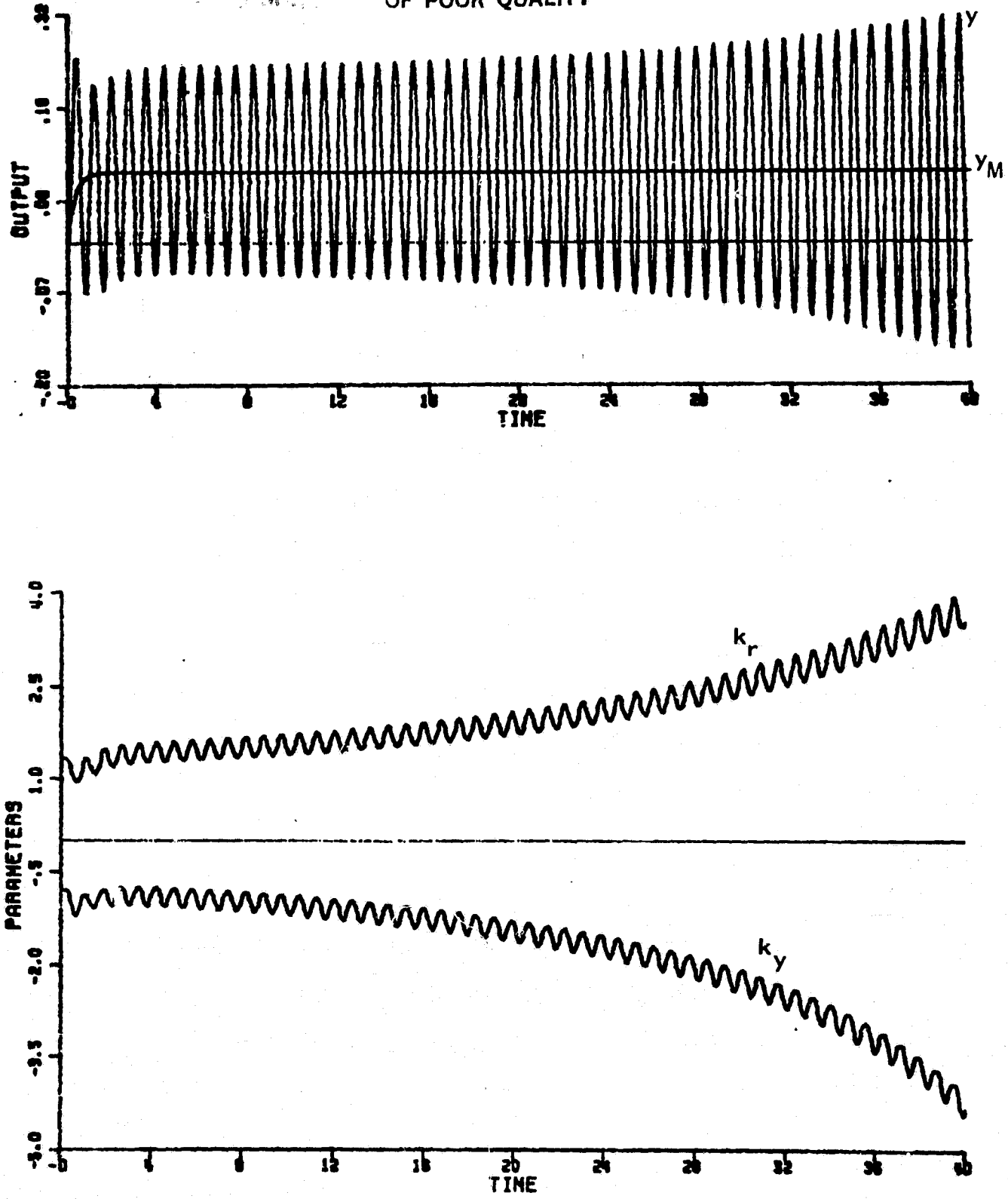

Figure 5-37. Simulation of DA1 with unmodeled dynamics, $r=0.1$, and $d(t)=0.01\sin\frac{8.0}{0.04}t$. (System eventually becomes unstable.)

Figure 5-37 displays the output and parameters of DA1 under the stimulus

$$r = 0.1; d(t) = 0.01 \sin \frac{8t}{.04} \qquad (5\text{-}80)$$

All three systems show the increasing amplitude sinusoid in the error and the steady parameter movement. All three became grossly unstable when the simulation was continued.

In all three simulation there is no semblance of disturbance rejection. Indeed, all three simulations show immediate disturbance amplification from which point the amplification increases until instability occurs.

The amplitude of the disturbance was chosen in the simulation so that the instability would occur within a reasonably short simulation time. Smaller amplitude sinusoids will also cause disturbance amplification and instability but the system will take a longer time to become grossly unstable.

5.2.5.2 Instability Due to the Mechanism of Section 5.2.3.2

The instability caused by the mechanism of Section 5.2.3.2 is again more disconcerting than that caused by the mechanism of Section 5.2.3.1, because the former can happen at any frequency. A sinusoidal disturbance at a frequency where the controlled plant

does not have too much phase shift will not have the positive feedback growing effect. The error will converge for a while. It will not, however, converge to zero since the disturbance does not enter into the model. A steady state error will correlate with the disturbance on the output, creating a constant driving term to the parameter adjustment mechanism. The parameters drift away creating an ever increasing gain in the nominal control system. In the presence of unmodeled dynamics, this will cause instability.

Indeed, any persistent error, which produces a constant correlation with the plant output, will cause instability via the mechanism of Section 5.2.3.2.

Figure 5-38 displays the output and parameters of DA2 with the stimulus.

$$r = 0.1; d(t) = 0.1 \sin \frac{7t}{.04} . \qquad (5\text{-}81)$$

Figure 5-39 displays the output and parameters of DA3 with the stimulus

$$r = 0.1; d(t) = 0.01 \sin \frac{2t}{.04} . \qquad (5\text{-}82)$$

Figure 5-40 shows the output and parameters of DA1 with the stimulus

$$r = 0.1; d(t) = 0.007 \sin \frac{4.5t}{.04} . \qquad (5\text{-}82)$$

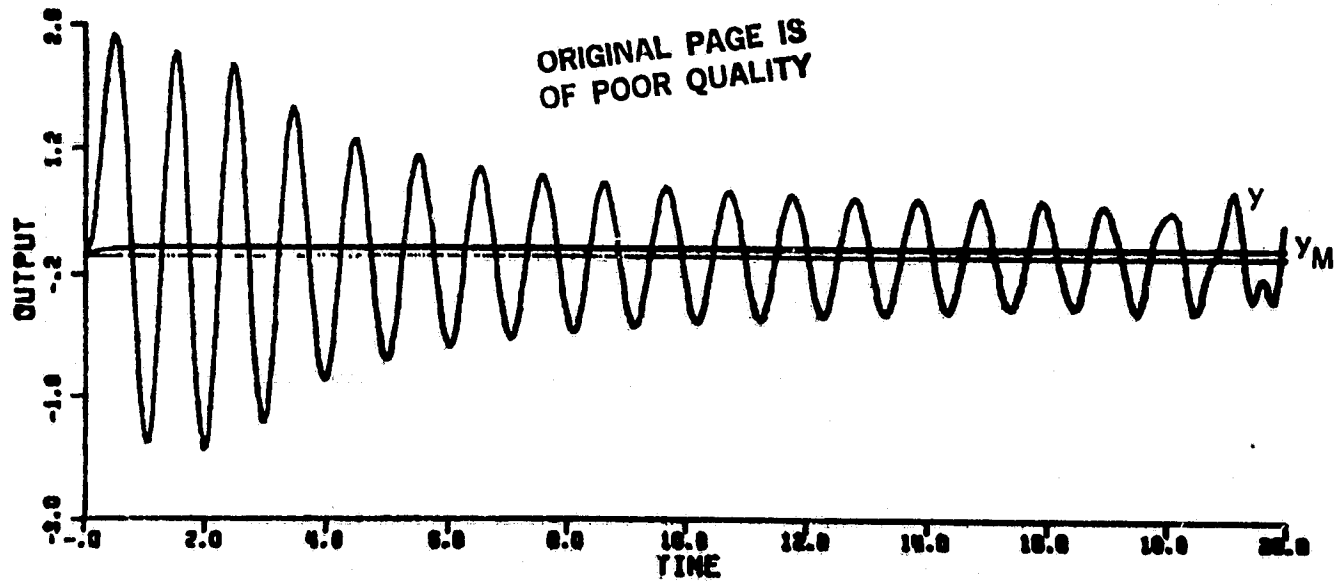

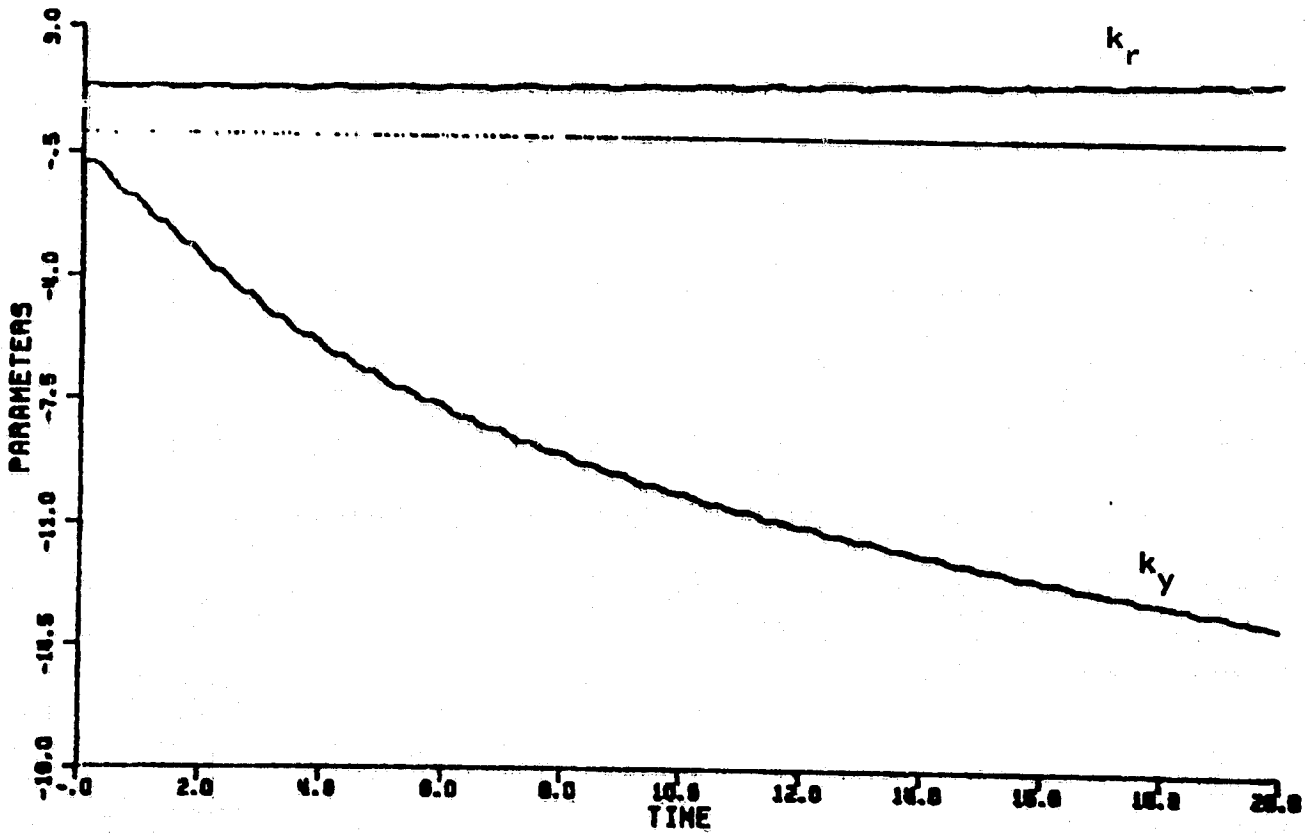

Figure 5-38. Simulation of DA2 with unmodeled dynamics, $r=0.1$, and $d(t)=0.1\sin\frac{7.0}{0.04}t$.
(System eventually becomes unstable.)

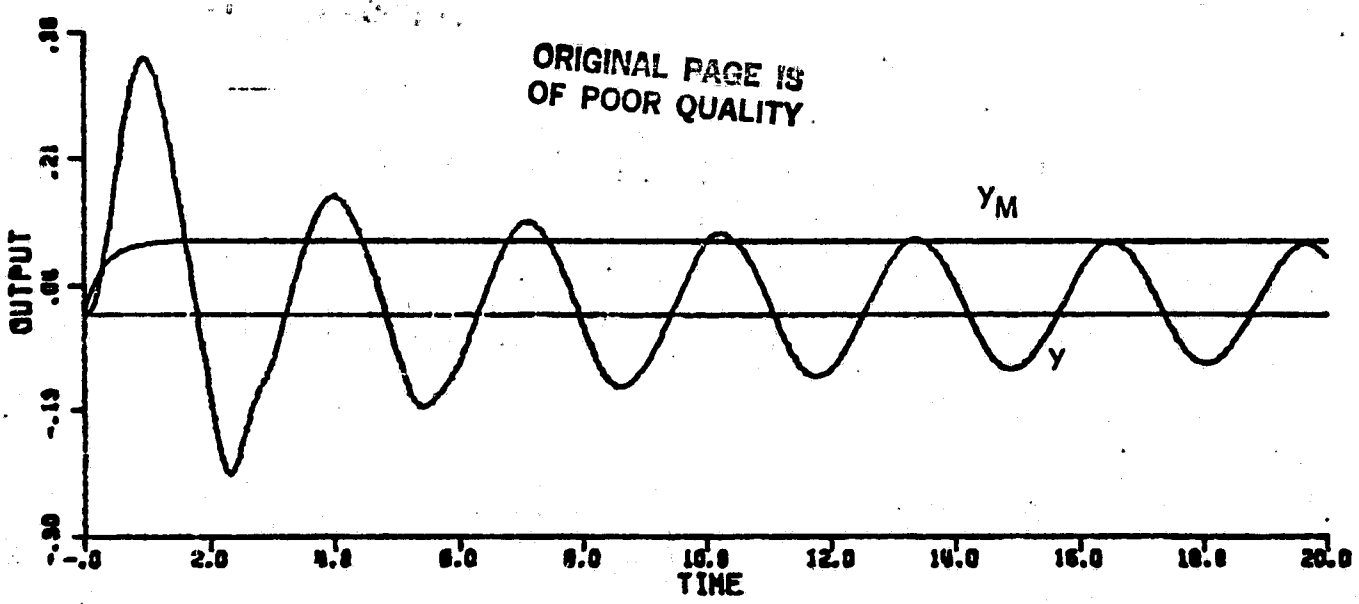

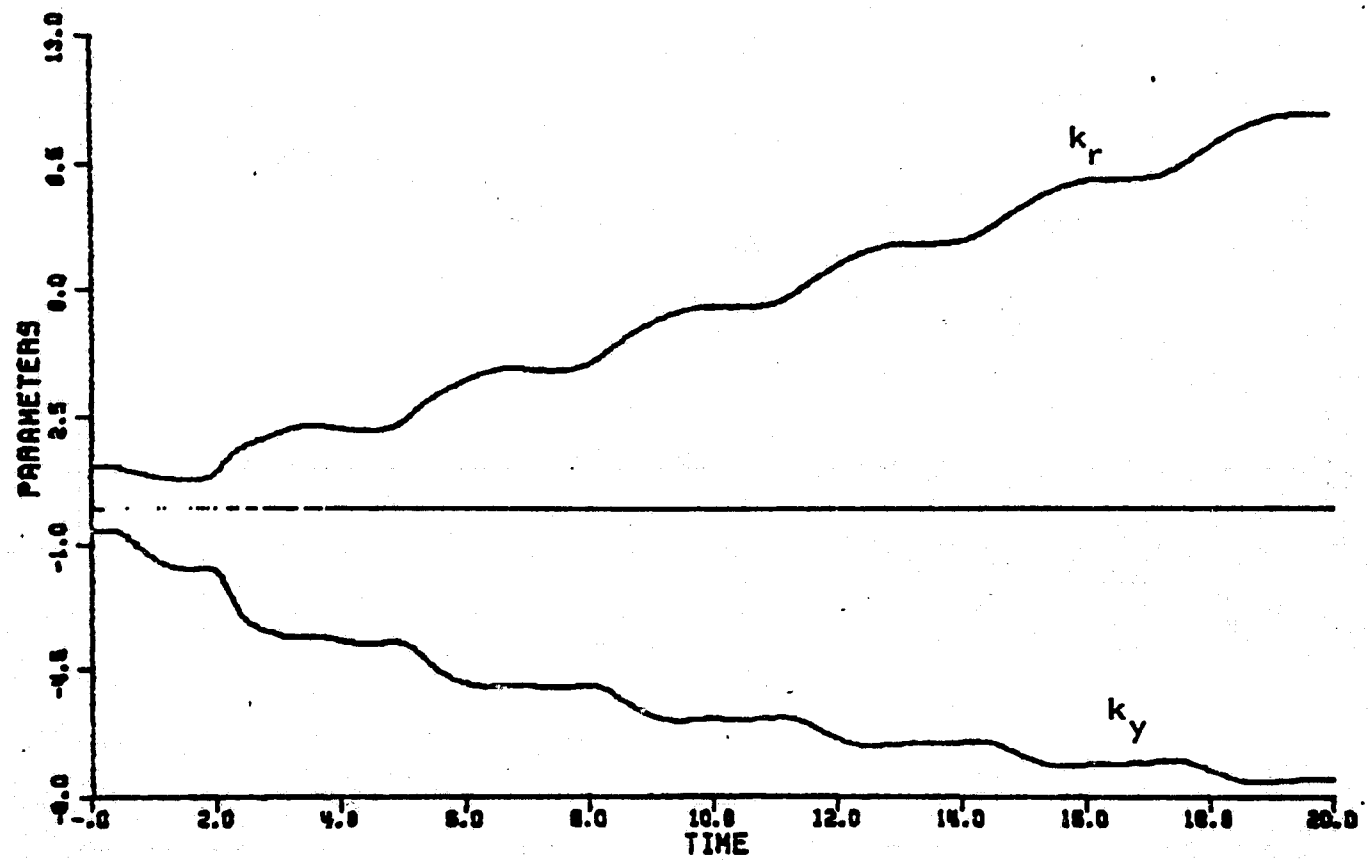

Figure 5-39. Simulation of DA3 with unmodeled dynamics, $r=0.1$, and $d(t)=0.01\sin\frac{2.0}{0.04}t$.
(System eventually becomes unstable.)

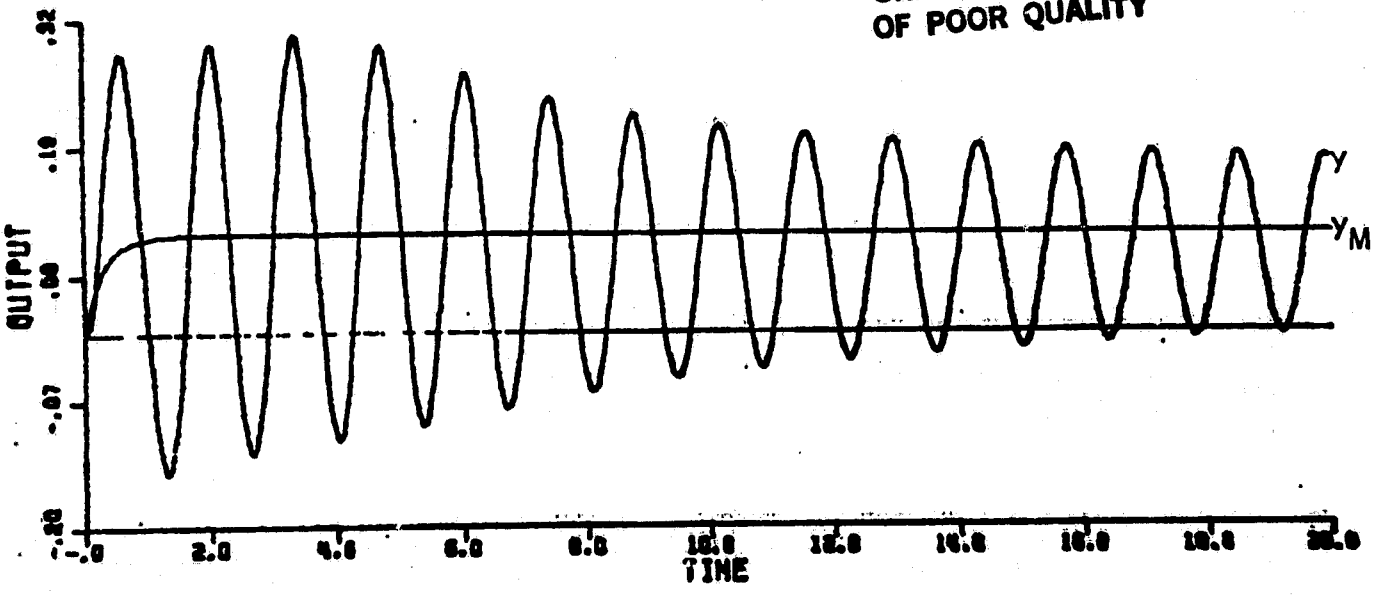

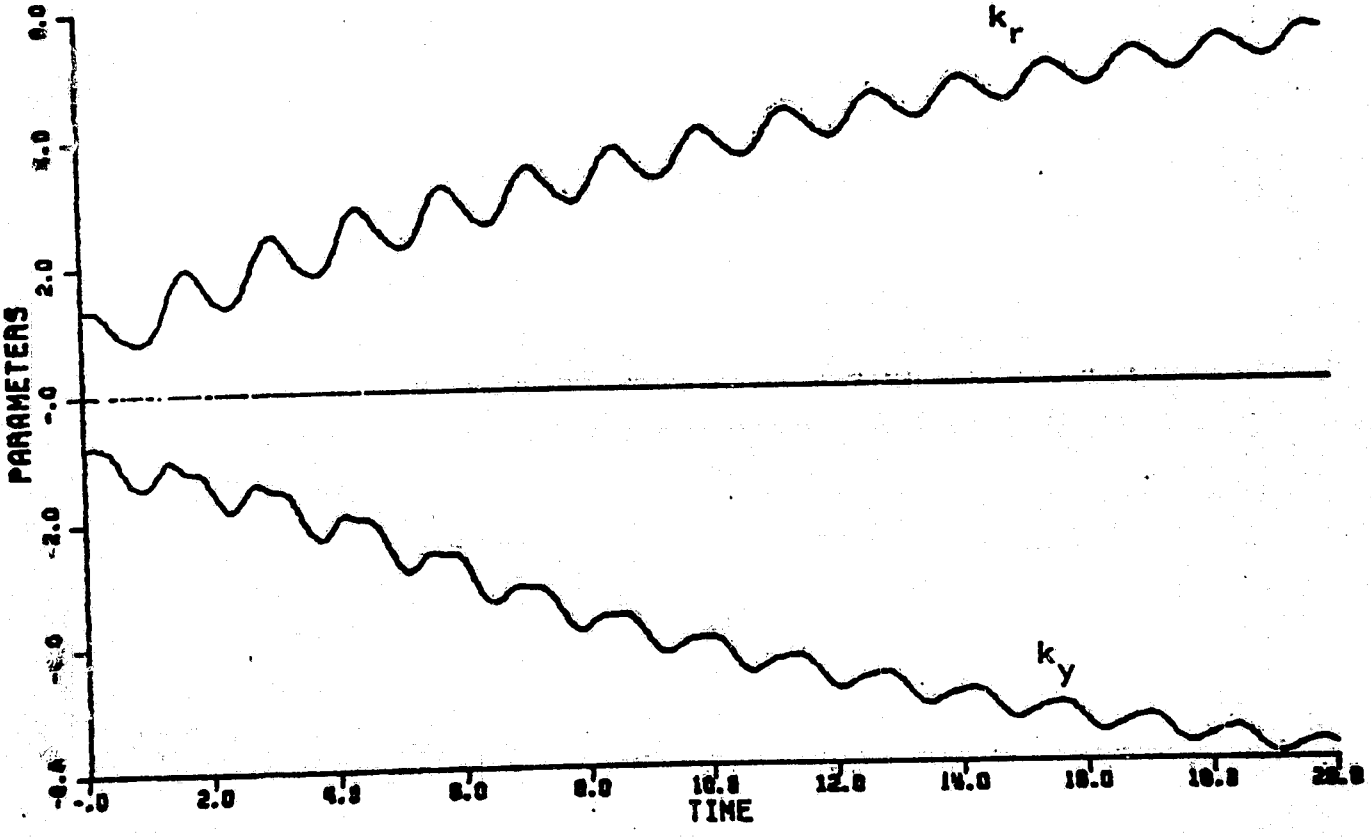

Figure 5-40. Simulation of DA1 with unmodeled dynamics, $r=0.1$, and $d(t)=0.007\sin\frac{4.5}{0.04}t$.
(System eventually becomes unstable.)

All the figures show the characteristic parameter drift and seemingly controlled error. All simulations did indeed become unstable when allowed to continue.

All the simulations also show that right from the beginning the adaptive systems show disturbance amplification rather than disturbance rejection.

5.2.5.3 The Effect of Sinusoidal Disturbance Upon the Self-Tuning Controller of DA3

As was mentioned in Section 2.3.3 the algorithm DA3 has a form which is designed to handle some disturbances. This is a type of self-tuning controller and it was also tested with sinusoidal disturbance. The self-tuning controller was designed so that the system is designed to handle output disturbances of the type

$$d(t) = \frac{1+c_1 q^{-1}+c_2 q^{-2}}{A(q^{-1})} [v(t)] \qquad (5\text{-}84)$$

where $v(t)$ is white noise. It is not too surprising that such a system can not handle the highly correlated output sinusoid disturbance that it was tested with. When the plant output is corrupted with a sinusoid the correlation between $\underline{w}_d(t)$ and $e(t)$ in the operator of Figure 5-26 will produce a constant driving term

to accumulate in the operator no matter how the system adjusts. When the disturbance is of the form of eqn. (5-84) the system can adjust to remove the correlation between $w_d(t)$ and $e(t)$.

Indeed, the self-tuning controller performed just like the other adaptive systems. Figure 5-41 shows the output and main parameters, k_o, k_y, when the simulation was generated with the stimulus

$$r = .1;\ d(t) = .016 \sin \frac{13.5t}{.04}. \tag{5-85}$$

The output shows the characteristic growing sinusoid of the positive feedback high gain system and the parameters show the familiar, by now, drift.

Figure 5-42 shows the output and main parameters under the stimulation

$$r = 0.1;\ d(t) = 0.1 \sin \frac{2t}{.04}. \tag{5-86}$$

The response is again as expected with the output error at least holding its own but with the parameters drifting away. Both simulations became unstable when allowed to continue.

Both simulation show that the systems amplify rather than reject disturbances.

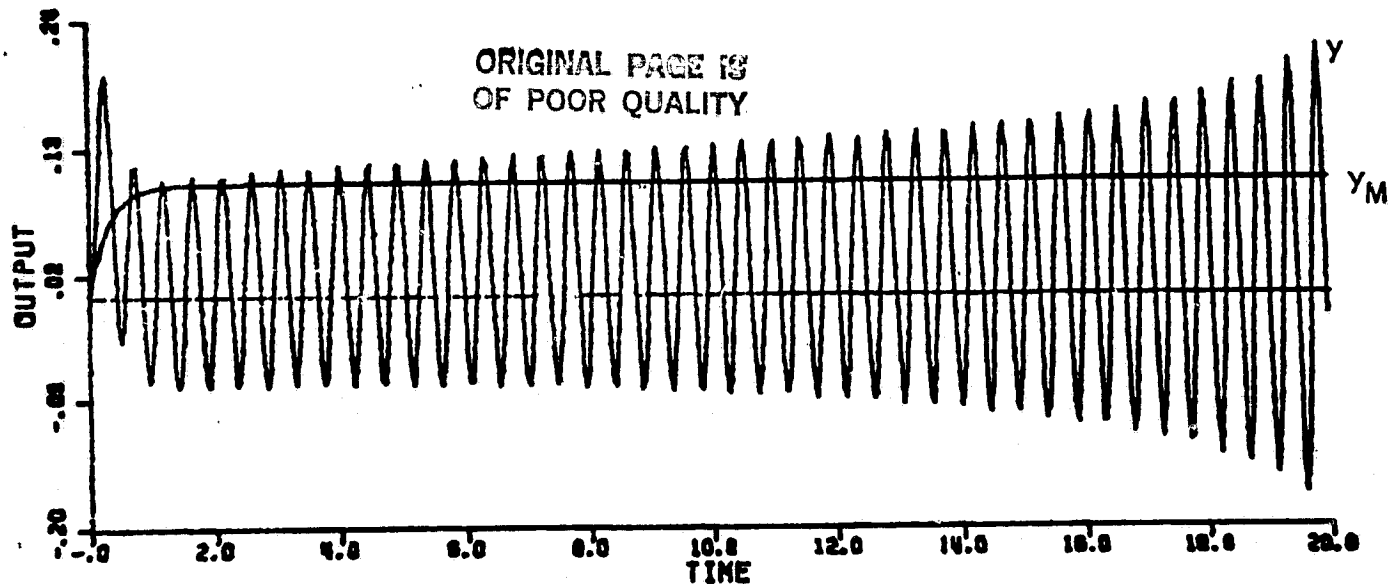

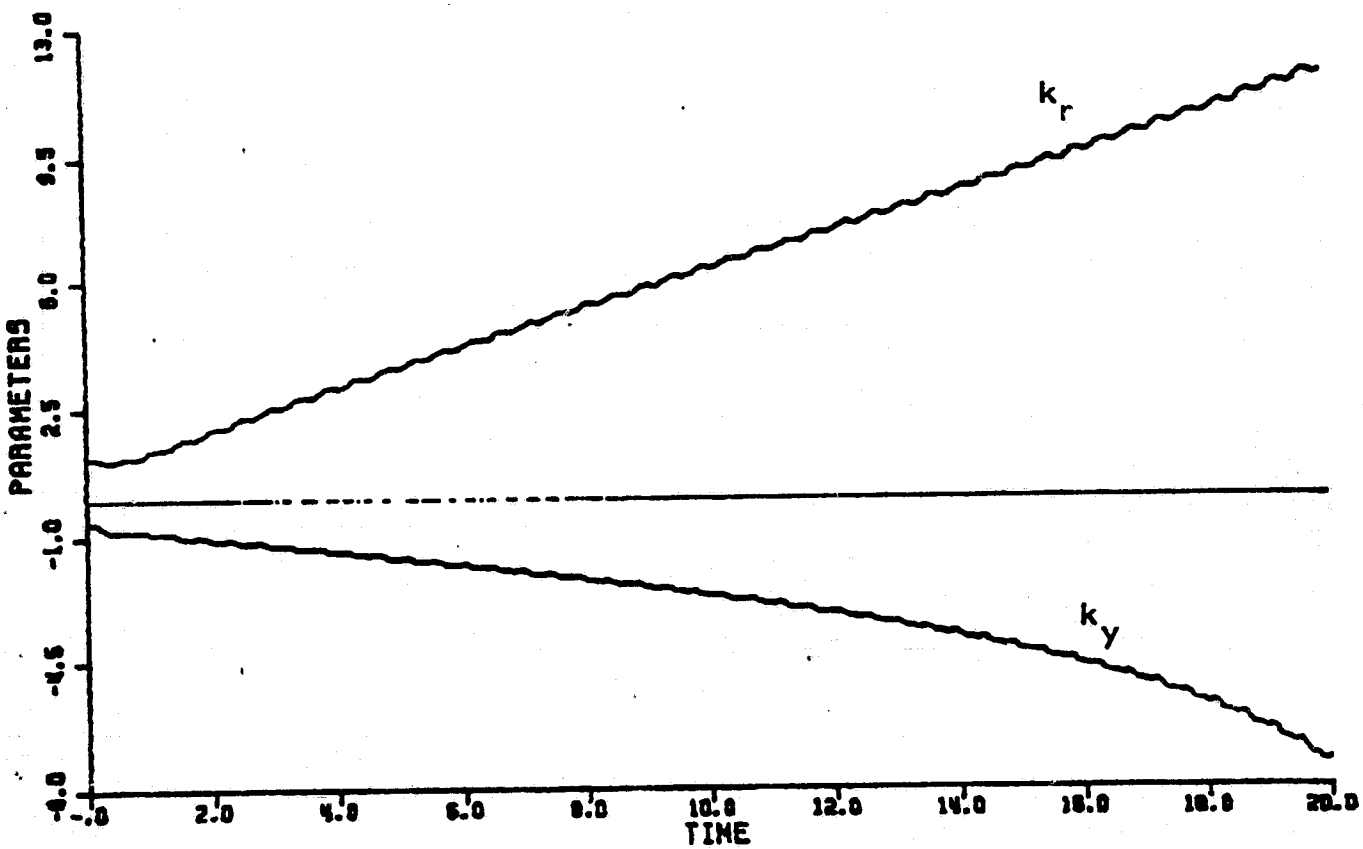

Figure 5-41. Simulation of the Self-Tuning Controller with unmodeled dynamics, $r=0.1$, and $d(t)=0.016\sin\frac{13.5}{0.04}t$.
(System eventually becomes unstable.)

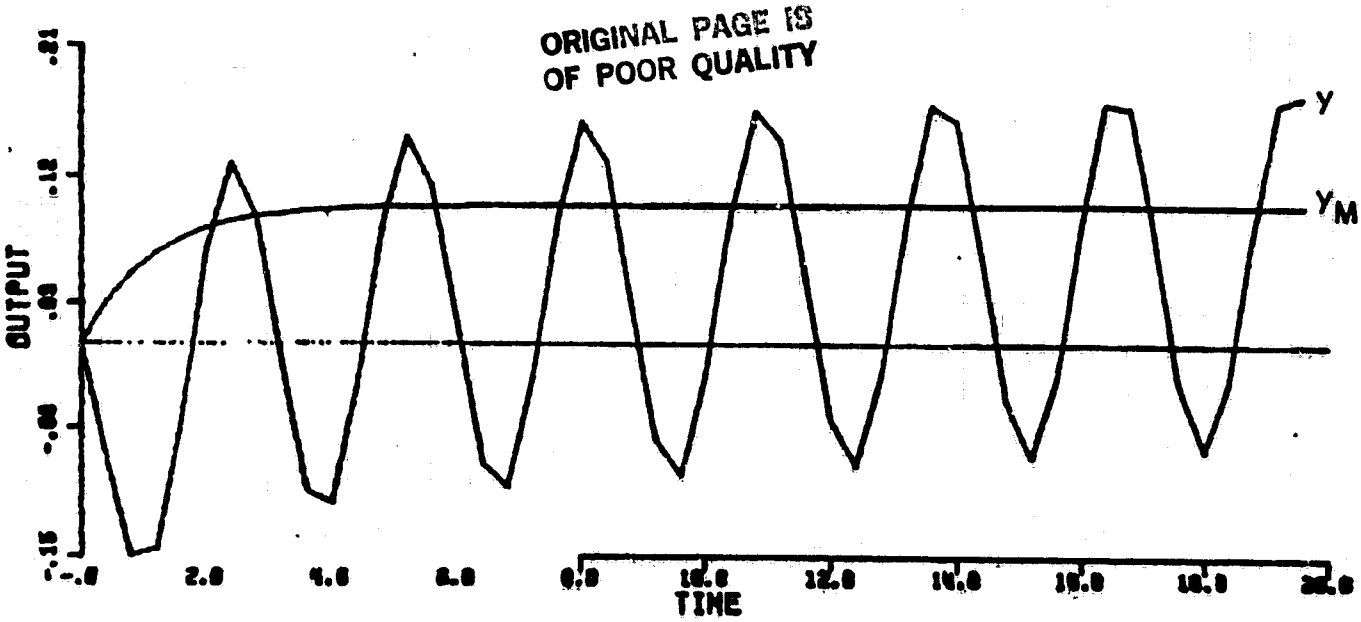

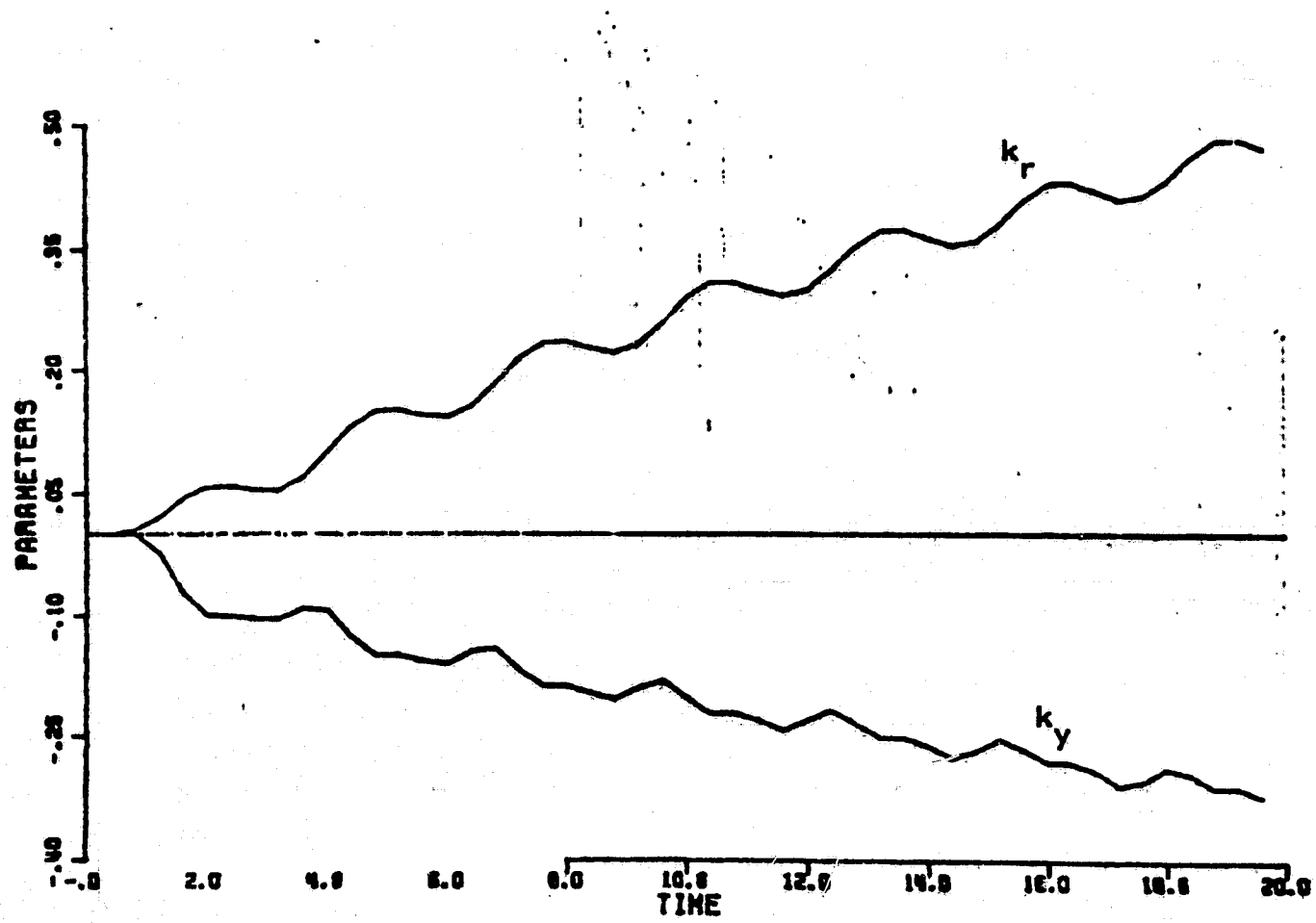

Figure 5-42. Simulation of the Self-Tuning Controller with unmodeled dynamics, $r=0.1$, and $d(t)=0.1\sin\frac{2.0}{0.04}t$.
(System eventually becomes unstable.)

Thus, even the self-tuning controller designed to handle some types of disturbances performs atrociously when faced with a sinusoidal disturbance. We reiterate the disturbance that caused instability is not one that the system is designed to handle. The performance shown, however, still constitutes a major obstacle for the practical implementation of such adaptive controllers.

One is reminded of the paper of Dumont and Belanger, [70] who in describing a "successful" application of a self-tuning regulator, stated

> "The long-term operation of the self-tuning regulator can give rise to some problems. After several weeks of satisfactory operation, the self-tuning regulator can create system oscillations... Another phenomena, ..., is a blow-up of the parameter estimates when working with a forgetting factor less than one."*

5.2.6 Conclusions

It has been shown in Section 5.2 that, through two mechanisms, if any of the discrete-time adaptive control systems studied is operated in the presence of unmodeled dynamics with a high frequency reference input and/or a sinusoidal disturbance at any frequency, the adaptive system will become unstable.

The response to disturbances is especially disconcerting since the disturbance can occur at any frequency and still exhibit the

---

*In our terminology a forgetting factor less than one corresponds to an adaptation gain that does not become arbitrarily small with time.

behavior of disturbance amplification and instability seen in the simulations of Section 5.2. While a designer may be able to select his reference inputs he has no control over the disturbances a system encounters and sinusoidal disturbances are very common.

It is clear that the problems exposed in this section must be successfully resolved for adaptive control systems to become generally useful control systems.

5.3 The Effects of the Sampling Rate on Discrete-Time Adaptive Control Systems

It was seen in Section 5.1.1 that if the sampling rate chosen for discrete-time adaptive control systems with constant reference inputs is slow enough, many of the problems associated with unmodeled dynamics in these systems are greatly alleviated.

This phenomenon is easily understood by looking at the pole-zero locations of a system sampled at different rates. Figure 5-43 shows the pole-zero locations of the plant used as an example throughout this thesis sampled at two different rates. The sampling periods are T=.04 and T=.4.

From this Figure 5-43, one can see that if the system is sampled rapidly the unmodeled poles and zeroes separate so that the poles produce substantial phase lag at intermediate frequencies,

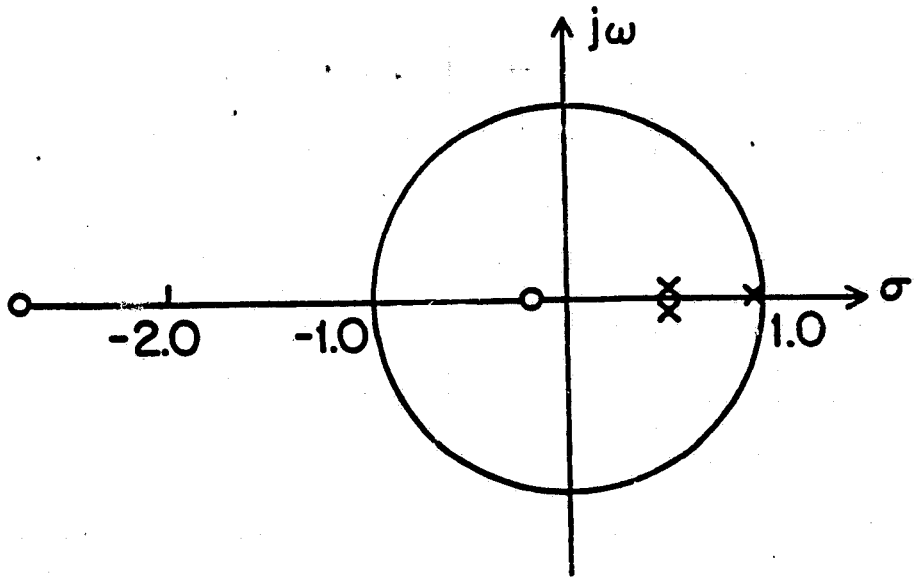

Figure 5-43a. The system (3-27) sampled at T=0.04 secs.

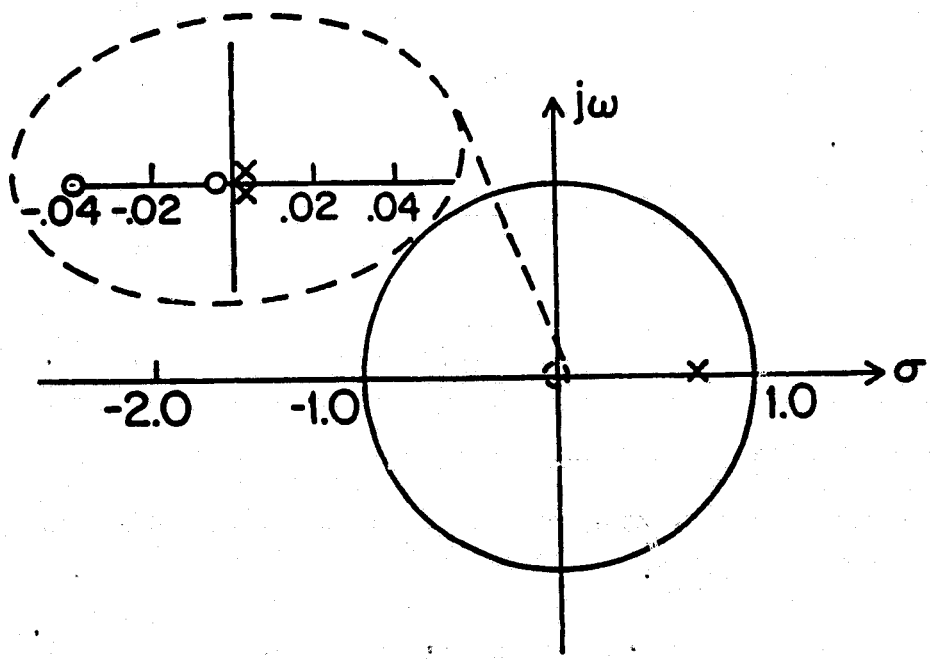

Figure 5-43b. The system (3-27) sampled at T=0.4 secs.

Figure 5-43. Pole-zero plots of the system (3-27) with different sampling intervals.

while zeroes contribute a small amount of phase lead until higher frequencies. Indeed the zero at z=-2.76 has very little effect on the system at any frequency.

When the system is sampled slowly, however, the unmodeled poles and zeroes coincide to all intents and purposes. Thus, they have little effect at all and the system behaves as if there were no unmodeled dynamics.

The previous two sections discussed the response of adaptive control systems to sinusoidal inputs and disturbances when the system is sampled at T=.04 sec. The response of the systems, when sampled more slowly at T=.4 sec., is now studied. Only the responses of the algorithm DA3 are shown in this section. The other algorithms reacted similarly.

Figure 5-44 shows the output error and the parameters of the system under the stimulus

$$r(t) = 1.0 + 1.0 \sin \frac{7.85t}{.04} \qquad (5\text{-}87)$$

and no disturbance. The frequency $\omega_o = \frac{7.85}{.04}$ was chosen as the frequency at which the plant provides 180° phase shift.

In Fig. 5-44 the output error starts out with the, by now, expected growing sinusoid. Since the unmodeled dynamics have little

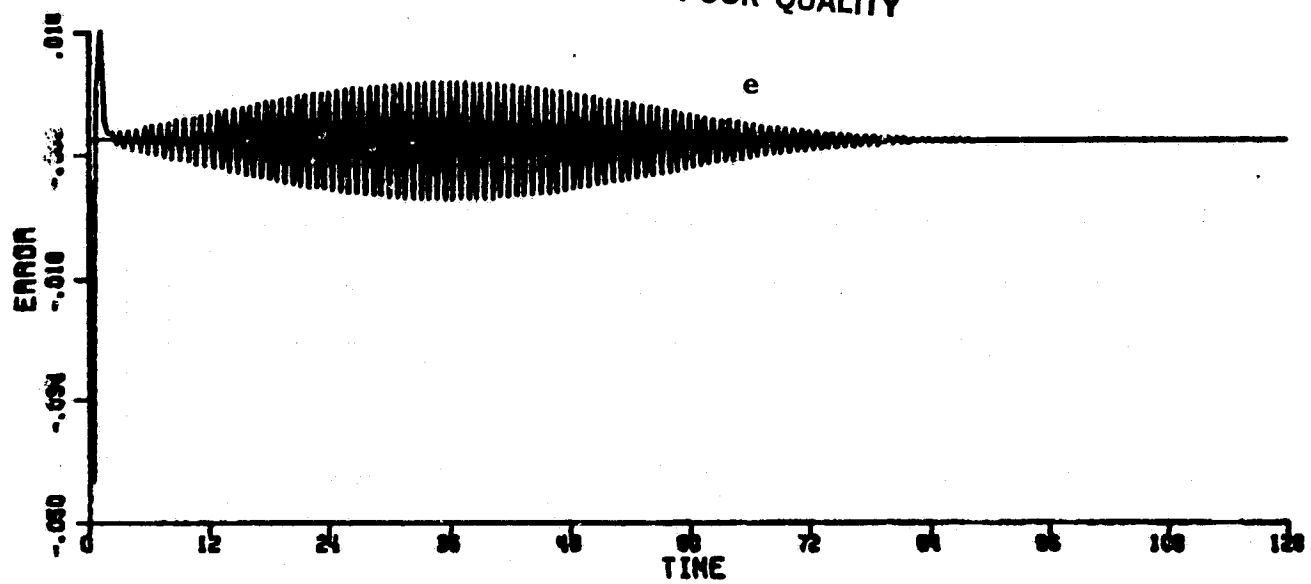

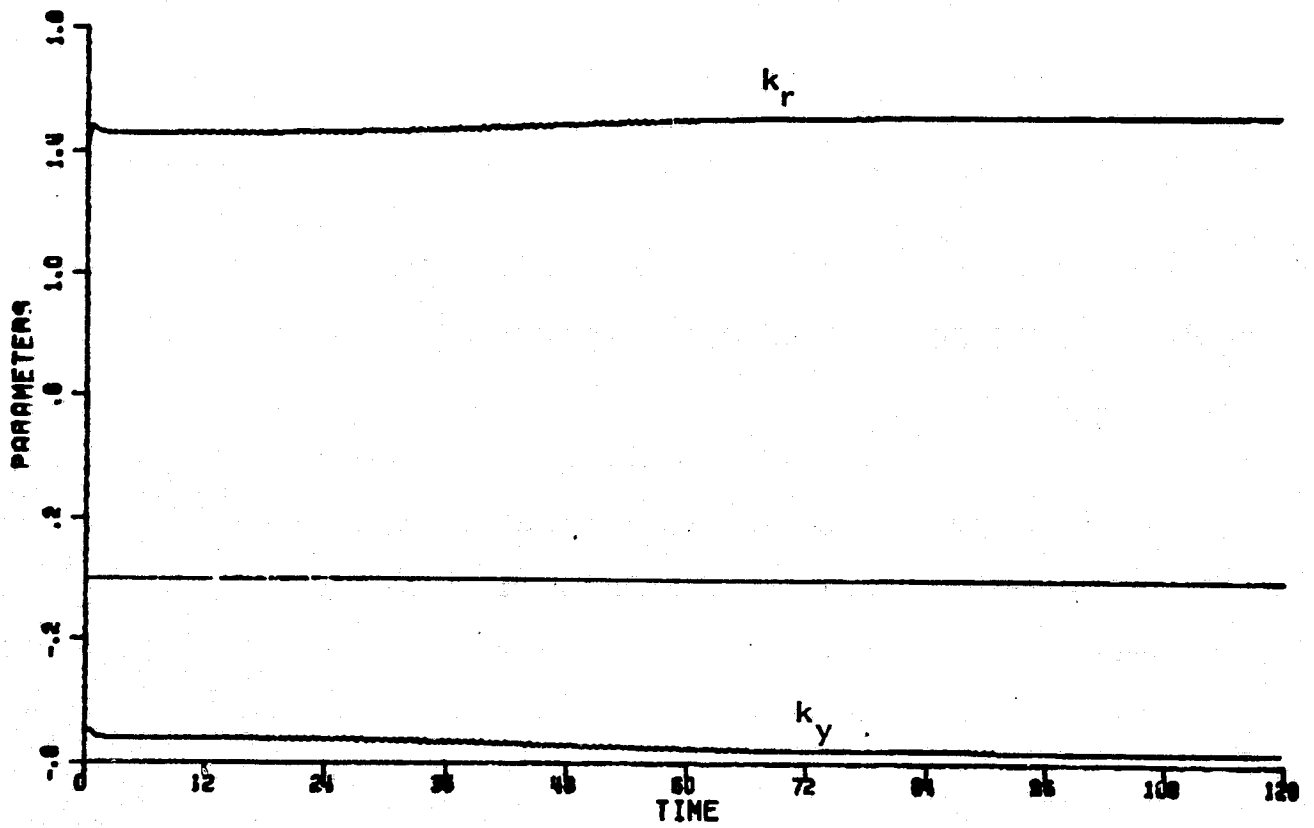

Figure 5-44. Simulation of DA3 with unmodeled dynamics, slow sampling, and $r(t)=1.0+1.0\sin\frac{7.85}{0.4}t$.
(No instability occurs.)

C-5

effect at this slow sampling rate the system can adjust parameters to match the plant at both d.c. and this high frequency at the same time and no persistent error signal develops. The error goes to zero and the parameters converge. Again, it is seen that, if the system is sampled slowly enough, the effects of high frequency unmodeled dynamics are minimized.

Next, the effects of a slow sampling rate on the response to sinusoidal disturbances was investigated still using the algorithm DA3.

Figure 5-45 shows the response to

$$r = 0.1; d(t) = 1.0 \sin \frac{7.85t}{.04} \quad . \tag{5.88}$$

Figure 5-46 shows the response to

$$r = 0.1; d(t) = 0.1 \sin \frac{3.5t}{.04} . \tag{5-89}$$

The system reacts qualitatively the same as it did when the sampling rate was much faster, with the characteristic parameter drift.

The reason why slowing the sampling rate did not improve the reaction of the system to the sinusoidal disturbance is because the debilitating parameter drift is not fundamentally a problem of unmodeled dynamics. It is a problem of the correlation in the algorithm. Unmodeled dynamics serve only to accentuate this problem

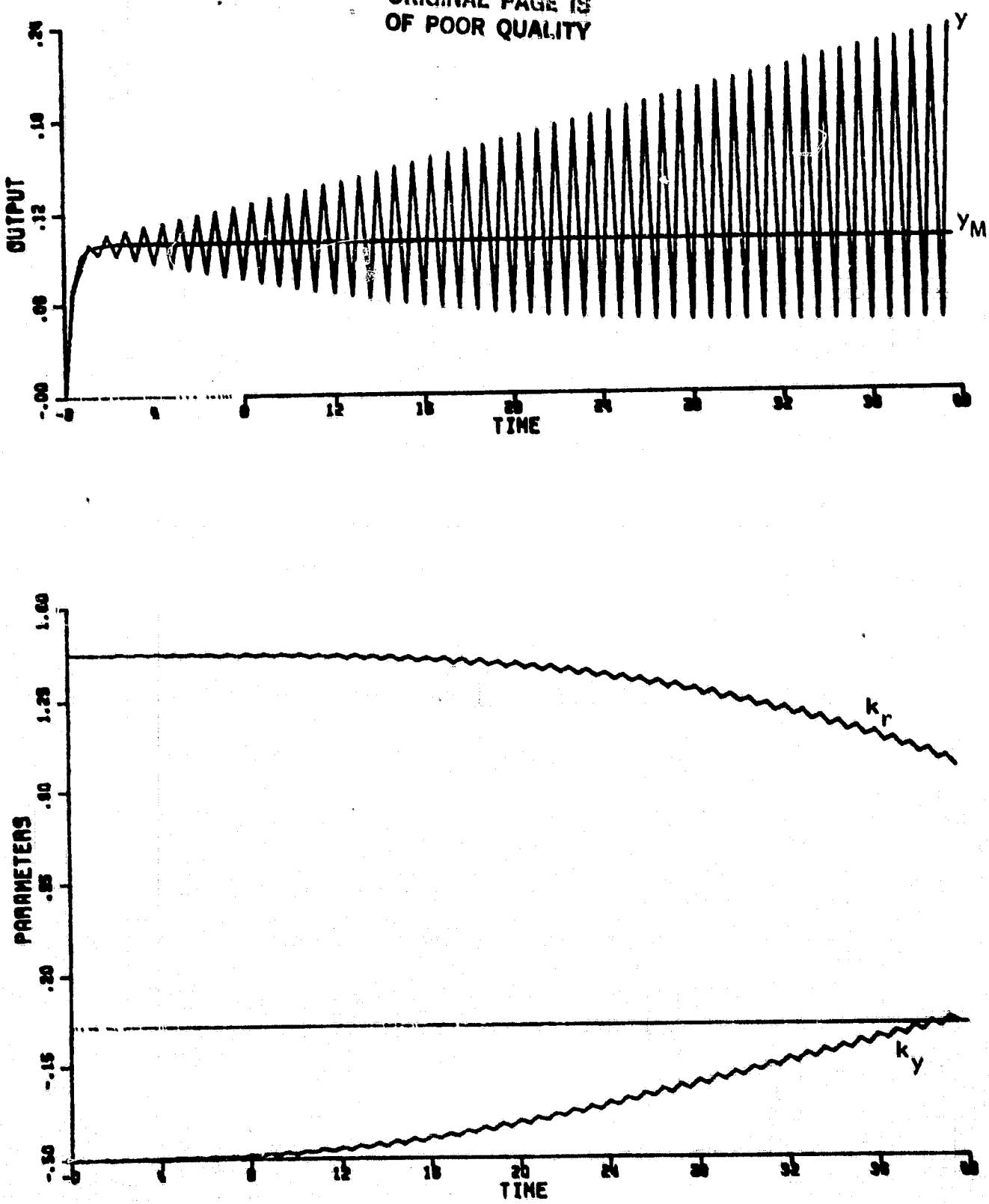

Figure 5-45. Simulation of DA3 with unmodeled dynamics, slow sampling, $r=0.1$, and $d(t)=1.0\sin\frac{7.85}{0.04}t$.
(System eventually becomes unstable.)

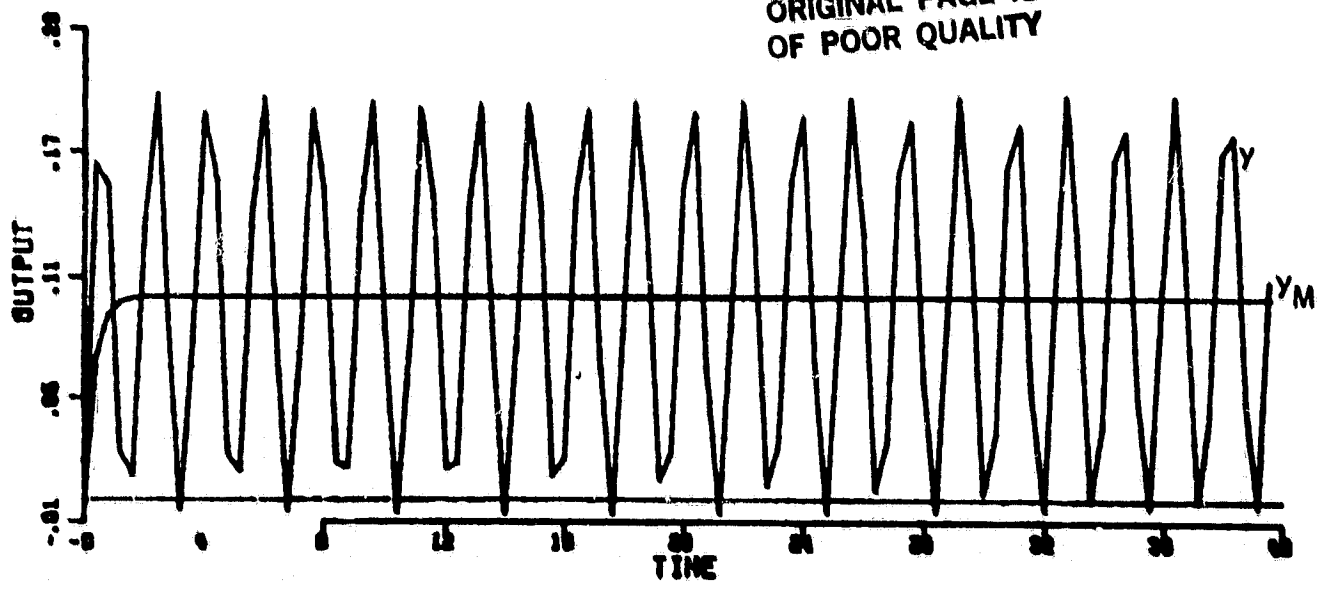

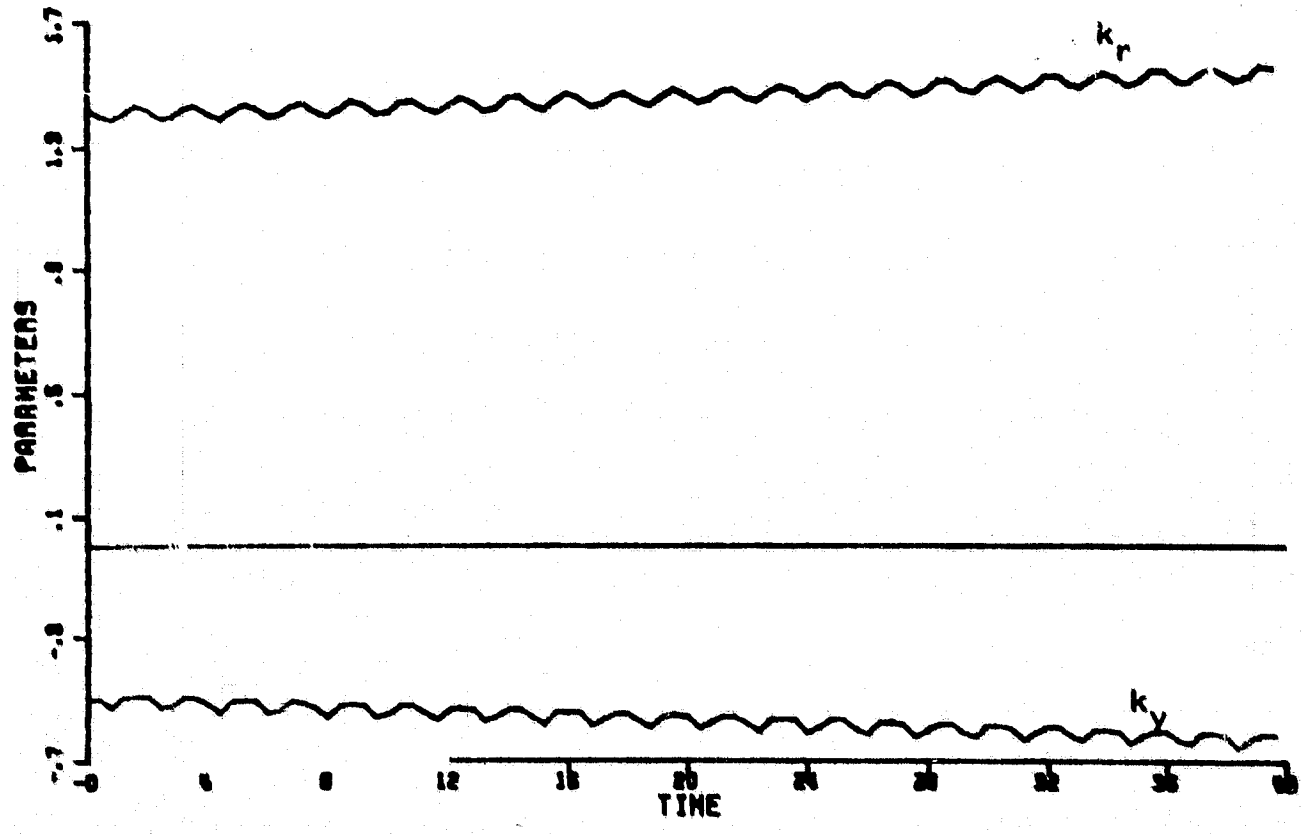

Figure 5-46. Simulation of DAS with unmodeled dynamics, slow sampling, $r=0.1$, and $d(t)=0.1\sin\frac{3.5}{0.04}t$.
(System eventually becomes unstable.)

by, first, creating extra phase lag at smaller frequencies, thus adding to the possibility of the positive feedback effect, and, second, by shrinking the space out of which the parameters must drift to cause instability.

Thus, it has been seen that the detrimental effects of unmodeled dynamics in a disturbance-free environment for discrete-time adaptive control algorithms can be essentially eliminated by sampling the system slowly enough. However, all the problems associated with sinusoidal disturbances remain.

A rule of thumb for choosing a sampling rate may be to have the sampling frequency be the same as the lowest frequency of the unmodeled dynamics. However, such a slow sampling scheme is a luxury seldom, if ever, available. The problems of sampling systems too slowly are well known (see [68], Chapter 10). In order to provide smooth enough and fast enough tracking of inputs and reasonable disturbance rejection in the nominal system, discrete-time systems have to be sampled up to 20 times as fast as their bandwidths. Since one of the goals of adaptive control is to push the bandwidth of systems up to the limit dictated by the unmodeled dynamics, the slow sampling rates required to remove those unmodeled dynamics cannot be used. Some other way to deal with them is required. In addition, even if one has the luxury of a slow sampling rate, the problems of sinusoidal disturbances must still be addressed.

5.4 Conclusions

The following conclusions are obtained from the analysis and digital simulation presented in this chapter:

- All the discrete-time adaptive control systems studied will have their control parameters increase without bound, if they are operated under the influence of a persistent sinusoidal disturbance at any frequency. Such unbounded parameters will surely cause instability in the presence of unmodeled dynamics and are likely to cause instability even when no unmodeled dynamics are present. Also, all the algorithms studied display disturbance amplification rather than disturbance rejection.
- All the algorithms studied will become unstable in the presence of unmodeled dynamics, if a high frequency sinusoidal reference input is used.
- All the algorithms may become unstable in the presence of unmodeled dynamics and constant reference inputs, if the design parameters of the system are not chosen carefully. The analysis of Section 5.1 provides a

design tool which aids in choosing the design parameters to alleviate the stability problems only for constant reference inputs.

- The stability problems associated with constant or sinusoidal reference inputs can be greatly alleviated by choosing a slow enough sampling rate in creating the discrete-time system. The problems associated with disturbances are not helped by the slower sampling.

Clearly, until the aforementioned problems are solved the applications of the adaptive control algorithms studied must be extremely limited. The problems associated with disturbances are extremely troublesome since the designer has no control over what disturbances enter the system. Thus, one of the fundamental advantages of feedback control, i.e., the ability to minimize the effects of external disturbances, becomes the major downfall in the adaptive control algorithms.

CHAPTER 6

CONCLUSIONS AND DIRECTIONS FOR FUTURE RESEARCH

6.1 Conclusions

This thesis contains an exhaustive analytical and numerical investigation of the stability and robustness properties of a wide class of adaptive control algorithms in the presence of unmodeled dynamics and output disturbances, for both continuous-time and discrete-time systems. The class of algorithms considered, those which are commonly referred to as model reference adaptive control algorithms, self-tuning controllers, and deadbeat adaptive controllers, have all been designed using a "black box" model for the plant.

For each of the algorithms the assumption is made that the plant is a "black box", about which nothing is known except for the relative degree and an upper bound for the order of the plant. In addition, the primary performance criterion used for the design of the adaptive systems investigated in past work is related to good command following. Using the "black box" assumption discussed above, each of the algorithms have been proven to be globally asymptotically stable.

However, the "black box" assumption does not reflect adequately the knowledge a control system designer usually has about the plant. On one hand, the assumption on the order and relative degree of the plant is too restrictive from an engineering point of view. Real

plants always contain unmodeled high frequency dynamics and small delays and, hence, no upper bound on the number of the plant poles and zeroes exists. Also, real plants are always subject to unmeasurable additive output disturbances, although these may be small. On the other hand, the "black box" assumption may discard a great deal of knowledge that is available about the plant, e.g., the approximate location of the dominant poles of the system vis-a-vis the nature and range of frequencies of unmodeled dynamics.

A unified analytical approach has been developed in this thesis, that can be employed to examine the stability and performance properties of this class of existing adaptive control algorithms in the presence of unmodeled dynamics and output disturbances. In Sections 4.2 and 5.2.2, it was discovered that all existing algorithms contain an infinite-gain operator in the dynamic system that defines command reference errors and parameter errors; it is argued in Section 4.2.4 that such an infinite-gain operator appears to be generic to all adaptive algorithms, whether they perform explicit or implicit parameter identification. The following practical engineering consequences of the infinite-gain operator are disastrous:

- Analytical results of Section 4.3.2 and Section 5.2.3.1 and simulation studies of Section 4.4.2 and Section 5.2.4 demonstrate that, in the presence of unmodeled dynamics, sinusoidal

reference inputs at specific frequencies cause sinusoidal components in the plant output to grow without bound and the adaptive system to become unstable.

- Analytical results of Section 4.3.3 and Section 5.2.3.2 and simulation results of Section 4.4.3 and 5.2.5 demonstrate that a sinusoidal output disturbance at any frequency, including constant disturbances, will cause the loop-gain of the adaptive control system to increase without bound, thereby exciting the (unmodeled) plant dynamics and yielding an unstable adaptive control system.

Hence, it is concluded that none of the adaptive control algorithms considered can be used with confidence in most practical control system designs, because instability will set in with a high probability.

In addition, results were obtained for the behavior of adaptive systems implemented in the presence of unmodeled dynamics but with constant reference inputs and no disturbances. The main results are:

- By choosing the design parameters of the adaptive system as indicated by the analysis technique of Chapter 3 and Section 5.1, the existing adaptive

control algorithms can be made to remain stable and to follow infrequent changes in constant reference inputs well in the presence of a certain class of unmodeled dynamics, if there are no external disturbances.

- In Section 5.1.2.3 and Section 5.3 it is shown that the instabilities caused by sinusoidal or constant reference inputs in the presence of unmodeled dynamics can be eliminated in systems which use discrete-time algorithms to control continuous-time plants by sampling the continuous-time process slowly enough. However, instabilities caused by output disturbances will still occur regardless of the sampling rate.

Thus, although the analysis techniques developed in this thesis can aid in some aspects of the designs of adaptive controllers using existing algorithms, the adaptive control system will still be vulnerable to instability attributable to the presence of the inevitable output disturbances and unmodeled dynamics.

6.2 Directions for Future Research

It is clear from the preceding conclusions that the "black box" approach to the design of adaptive control systems must be abandoned. While "black box" approaches may lead to elegant theoretical results under idealized assumptions, the results of this thesis indicate that great difficulties arise in more practical settings. Adaptive controllers should be designed based upon the actual knowledge available about the plant. Modeling of the plant itself should include the following three ingredients, each pertaining to a different type of uncertainty [67].

1. The Known Part - The known part usually characterizes the dominant modes of the plant which remain unchanged through various operating conditions.
2. The Structured Uncertainty Part - The structured uncertainty part is characterized by a known structure but with parameters that vary with time as operating conditions do.
3. The Unstructured Uncertainty Part - The unstructured uncertainty part encompasses the inevitable high frequency effects of unmodeled dynamics. It can be characterized as an additive or multiplicative perturbation to the plant transfer function. Only an upper bound to the magnitude of the perturbation at different frequencies is assumed known.

The adaptive controller should then be designed in light of the new modeling information to perform all the functions of feedback control. Thus, in addition to meeting a reference input response criterion, the adaptive controller should perform disturbance and sensor noise rejection, while maintaining stability for the entire class of unmodeled dynamics considered to be part of the real process.

The following suggestions are offered as possible avenues of pursuing the adaptive control problem using the plant model and performance criterion indicated above:

1. By further analyzing existing algorithms under more realistic assumptions, one may develop the insights needed to make modifications to existing algorithms so that the algorithms are better able to handle disturbances and unmodeled dynamics. Moreover, one must realize that in abandoning the idealistic assumptions of the "black box" approach, the possibility of such mathematical niceties as global stability proofs may be severely compromised. On the other hand, one may emerge with an algorithm that performs satisfactorily in practical situations.

2. New parameterizations of the nominal control loop should be investigated. The three part plant model discussed above may lead to parameterization of the control mechanism which are better suited for practical results.
3. It is possible that progress can be made only by abandoning the existing algorithms and addressing the problem from the beginning, this time with a problem formulation which takes unmodeled dynamics and disturbances explicitly into account from the beginning. Possibly, insights can be gained into more practical solutions for adaptive control by solving detailed problem formulations of simple first-order problems under practical assumptions.

Whether or not results can actually be obtained by these or other approaches to the adaptive control problem, it is clear that for adaptive control to take its place as a viable design alternative to other control strategies, design procedures must be developed which are able to produce adaptive control systems that perform acceptably in the presence of unmodeled dynamics and external disturbances.

REFERENCES

[1] C. Rohrs, L. Valavani and M. Athans, "Convergence Studies of Adaptive Control Algorithms, Part I: Analysis," Proc. IEEE CDC Conf., Albuquerque, New Mexico, 1980, pp. 1138-1141.

[2] C. Rohrs, L. Valavani, M. Athans and G. Stein, "Analytical Verification of Undesirable Properties of Direct Model Reference Adaptive Control Algorithms," LIDS-P-1122, M.I.T., August 1981; also Proc. 20th IEEE, Conference on Decision and Control, San Diego, CA, December 1981.

[3] K.S. Narendra and L.S. Valavani, "Stable Adaptive Controller Design-Direct Control, IEEE Trans. Automat. Contr., Vol. AC-23, pp. 570-583, August 1978.

[4] A. Feuer and A.S. Morse, "Adaptive Control of Single-Input Single-Output Linear Systems," IEEE Trans. Automat. Contr., Vol. AC-23, pp. 557-570, August 1978.

[5] K.S. Narendra, Y.H. Lin and L.S. Valavani, "Stable Adaptive Controller Design, Part II: Proof of Stability," IEEE Trans. Automat. Contr., Vol. AC-25, pp. 440-448, June 1980.

[6] A.S. Morse, "Global Stability of Parameter Adaptive Control Systems," IEEE Trans. Automat. Contr., Vol. AC-25, pp. 433-440, June 1980.

[7] K.S. Narendra and Y.H. Lin, "Stable Discrete Adaptive Control," IEEE Trans. Automat. Contr., Vol. AC-25, pp. 456-461, June 1980.

[8] I.D. Landau and H.M. Silveira, "A Stability Theorem with Applications to Adaptive Control," IEEE Trans. Automat. Contr., Vol. AC-24, pp. 305-312, April 1979.

[9] I.D. Landau, "An Extension of A Stability Theorem Applicable to Adaptive Control," IEEE Trans. Automat. Contr., Vol. AC-25, pp. 814-817, August 1980.

[10] G.C. Goodwin, P.J. Ramadge, and P.E. Caines, "Discrete-Time Multivariable Adaptive Control," IEEE Trans. Automat. Contr., Vol. AC-25, pp. 449-456, June 1980.

[11] B. Egardt, "Stability Analysis of Continuous-Time Adaptive Control Systems," SIAM J. of Control and Optimization, Vol. 18, No. 5, pp. 540-557, September 1980.

[12] B. Egardt, "Stability Analysis of Discrete-Time Adaptive Control Scheme," IEEE Trans. Automat. Contr., Vol. AC-25, No. 4, pp. 710-716, August 1980.

[13] B. Egardt, "Unification of Some Continuous-Time Adaptive Control Schemes," IEEE Trans. Automat. Contr., Vol. AC-24, No. 4, pp. 588-592, August 1979.

[14] B. Egardt, "Unification of Some Discrete-Time Adaptive Control Schemes," IEEE Trans. Automat. Contr., Vol. AC-25, No. 4, pp. 693-697, August 1980.

[15] R.L. Carroll and D.P. Lindorff, "An Adaptive Observer for Single-Input Single-Output Linear Systems," IEEE Trans. Automat. Contr., Vol. AC-18, pp. 428-435, October 1973.

[16] G. Lüders and K.S. Narendra, "An Adaptive Observer and Identifier for a Linear System," IEEE Trans. Automat. Contr., Vol. AC-18, pp. 496-499, October 1973.

[17] G. Luders and K.S. Narendra, "A New Canonical Form for an Adaptive Observer," IEEE Trans. Automat. Contr., AC-19, pp. 117-119, April 1974.

[18] K.S. Narendra and P. Kudva, "Stable Adaptive Schemes for System Identification and Control-Parts I and II," IEEE Trans. Systems, Man, and Cybernetics, Vol. SMC-4, November 1974.

[19] G. Kreisselmeier, "Adaptive Observers with Exponential Rate of Convergence," IEEE Trans. Automat. Contr., Vol. AC-22, pp. 2-8, February 1977.

[20] B.D.O. Anderson, "Multivariable Adaptive Identification," Technical Report, University of Newcastle, New South Wales, Australia, June 1974.

[21] A.S. Morse, "Representation and Parameter Identification of Multi-Output Systems," Proceedings of the 1974 IEEE Conference on Decision and Control.

[22] K.S. Narendra, and L.S. Valavani, "Stable Adaptive Observers and Controllers," IEEE Proceedings, pp. 1198-1208, August 1976.

[23] B.D.O. Anderson, "Exponential Stability of Linear Equations Arising in Adaptive Identification," Technical Report, University of Newcastle, New South Wales, Australia, September 1975.

[24] A.P. Morgan and K.S. Narendra, "On the Stability of Nonautonomous Differential Equations $\dot{x}=[A+B(t)]x$, with Skew-Symmetric Matrix $B(t)$," SIAM Journal of Control and Optimization, Vol. 15, pp. 5-24, January 1977.

[25] J.S.C. Yuan and W.M. Wonham, "Probing Signals for Model Reference Identification," IEEE Trans. Automat. Contr., Vol. AC-22, pp. 530-538, August 1977.

[26] R.V. Monopoli, "Model Reference Adaptive Control with an Augmented Error Signal, IEEE Trans. Automat. Contr., Vol. AC-19, pp. 474-484, October 1974.

[27] H. Elliott, "Hybrid Adaptive Control of Continuous-Time Systems," Colorado State University Technical Report No. JL80-DELENG-1, July 1980. (To appear in IEEE Trans. Automat. Contr.,).

[28] K.J. Astrom and B. Wittenmark, "On Self-Tuning Regulator," Automatica, No. 8, pp. 185-199, 1973

[29] L. Ljung and B. Wittenmark, "Asymptotic Properties of Self-Tuning Regulators," Report 7404, Department of Automatic Control, Lund Institute of Technology, Lund, Sweden, February 1974.

[30] K.J. Astrom, U. Borisson, L. Ljung, and B. Wittenmark, "Theory and Applications of Self-Tuning Regulators," Automatica, Vol. 13, pp. 457-476, 1977.

[31] K.S. Astrom, B. Westerberg, B. Wittenmark, "Self-Tuning Controllers Based on Pole-Placement Design," CODEN: LUTFD2/(TFRT-3148)/1-52/ Department of Automatic Control, Lund Institute of Technology, Lund, Sweden, 1978.

[32] G. Kreisselmeier, "Adaptive Control via Adaptive Observation and Asymptotic Feedback Matrix Synthesis," IEEE Trans. Automat. Contr., Vol. AC-25, pp. 717-722, August 1980.

[33] G. Kreisselmeier, "On Adaptive State Regulation," IEEE Trans. Automat. Contr., Vol. AC-27, No. 1, pp. 3-16, February 1982.

[34] H. Elliott and W.A. Wolovich, "Parameter Adaptive Identification and Control," IEEE Trans. Automat. Contr., Vol. AC-24, pp. 592-599, August 1979.

[35] M. Athans, and P. Varaiya, "A Survey of Adaptive Stochastic Control Methods," in ERDA Report Conf. 750867, Systems Engineering for Power, Status and Prospects, L.H. Fink and K. Carlsen, eds., pp. 356-366, October 1975.

[36] J.B. Cruz, ed., 'Workshop on Adaptive Control: Final Report," R-79-1, University Inn, Champaign, IL, May 1979, sponsored by AFOSR and Dynamic Systems, Inc.

[37] M. Aoki and R.M. Staley, "On Input Signal Synthesis in Parameter Identification," Automatica, Vol. 6, p. 431, 1970.

[38] G.C. Goodwin, J.C. Murdoch and R.L Payne, "Optimal Test-Signal Design for Linear Single-Input Single-Output System Identification," Int. J. Contr., Vol. 17, pp. 45-55, 1973.

[39] D.B. Reid, "Optimal Inputs for System Identification," Stanford University, Stanford, CA, SUDAAR 440, May 1972.

[40] N.E. Nahi, and G.A. Napjus, "Design of Optimal Probing Signals for Vector Parameter Estimation," Preprints, IEEE Decision and Control Conference, Miami, FL, December 1971.

[41] L. Kovicsky and C.S. Banyasz, "On Input Signal Synthesis for Linear Discrete Time Systems," 3rd IFAC Symp. on Identification, The Hayne/Delft, The Netherlands, June 1973.

[42] A.A. Lopez-Toledo, "On the Design of Optimal Input Signals for System Identification, Ph.D. Dissertation, M.I.T., Cambridge, MA, 1974.

[43] R.J.N. Chen, "Input Design for Parameter Identification-Part I," presented at the JACC, Austin, Texas, June 1974.

[44] R.K. Mehra, "Optimal Input Signals for Parameter Estimation in Dynamic Systems - Survey and New Results," IEEE Trans. Automat. Contr., Vol. AC-19, pp. 753-768, December 1974.

[45] I.D. Landau, "Unbiased Recursive Identification Using Model Reference Adaptive Techniques," IEEE Trans. Automat. Contr., Vol. AC-21, pp. 194-202, April 1976.

[46] L. Ljung, "On Positive Real Transfer Functions and the Convergence of Some Recursive Schemes," IEEE Trans. Automat. Contr., Vol. AC-22, pp. 539-551, August 1977.

[47] L. Ljung, "Analysis of Recursive Stochastic Algorithms," IEEE Trans. Automat. Contr., Vol. AC-22, pp. 551-575, August 1977.

[48] G.C. Goodwin, P.J. Ramadge, and P.E. Caines, "Discrete-Time Stochastic Adaptive Control," Proceedings IEEE CDC, Ft. Lauderdale, FL, December 1979.

[49] G.C. Goodwin, K.S. Sin, K.K. Saluja, "Stochastic Adaptive Control and Prediction - The General Delay - Colored Noise Case," IEEE Trans. Automat. Contr., Vol. AC-25, pp. 946-950, October 1980.

[50] K.S. Narendra and R.V. Monopoli, eds; Applications of Adaptive Control, Academic Press, New York, 1980.

[51] P.A. Ioannou and P.V. Kokotovic, "An Asymptotic Error Analysis of Identifiers and Adaptive Observers in the Presence of Parasities," IEEE Trans. Automat. Contr., Vol. AC-27, pp. 921-927, August 1982.

[52] P. Ioannou, Robustness of Model Reference Adaptive Schemes with Respect to Modeling Errors, Ph.D. Thesis, Dept. of Electrical Engineering, University of Illinois at Urbana-Champaign, Report DC-53, August 1982.

[53] P. Ioannou and P. Kokotovic, "Singular Perturbations on Robust Redesign of Adaptive Control," presented at IFAC Workshop on Singular Perturbations and Robustness of Control Systems, Lake Ohrid, Yugoslavia, July 1982.

[54] B.D.O. Anderson and C.R. Johnson, Jr., "Exponential Convergence of Adaptive Identification and Control Algorithm," to appear in Automatica, 1981.

[55] B.D.O. Anderson and C.R. Johnson, Jr., "On Reduced Order-Adaptive Output Error Identification and Adaptive IIR Filtering," Technical Report, Virginia Polytechnic Institute and State University, Blacksburg, VA, May 1980.

[56] B.D.O. Anderson and R.M. Johnstone, "Robust Lyapunov Stability Results and Adaptive Systems," Proceedings of IEEE CDC, San Diego, CA, December 1981.

[57] K.S. Narendra and B.B. Peterson, "Bounded Error Adaptive Control," Proceedings IEEE CDC, Albuquerque, NM, December 1980.

[58] G. Kreisselmeier, and K.S. Narendra, "Stable Model Reference Adaptive Control in the Presence of Bounded Disturbance," submitted to IEEE Trans. Automat. Contr.

[59] E.A. Guillemin, The Mathematics of Circuit Analysis, John Wiley, New York, 1961.

[60] V.M. Popov, Hyperstability of Control Systems, Springer Verlag, New York, 1973.

[61] K.S. Narendra and J.H. Taylor, Frequency Domain Criteria for Absolute Stability, Academic Press, New York, 1973.

[62] Y.H. Lin and K.S. Narendra, "A New Error Model for Adaptive Systems," IEEE Trans. Automatic. Contr., Vol. AC-25, No. 3, pp. 585-587, June 1980.

[63] P.C. Parks, "Lyapunov Redesign of Model Reference Adaptive Control Systems," IEEE Trans. Automat. Contr., Vol. AC-11, No. 3, pp. 362-367, July 1966.

[64] I.M. Horowitz, Synthesis of Feedback Systems, Academic Press, New York and London, 1963.

[65] K.J. Åström and P. Eykhoff, "System Identification - A Survey," Automatica, Vol.7, pp. 123-162, 1971.

[66] C.H. Desoer and M. Vidyasagar, Feedback Systems: Input-Output Properties, Academic Press, New York, 1975.

[67] C.R. Johnson, Jr., A.S. Foss, G.F. Franklin, R.V. Monopoli, and G. Stein, "Toward Development of a Practical Benchmark Example for Adaptive Control," IEEE Control Systems Magazine, Vol. 1, No. 4, pp. 25-29, December1981.

[68] G.F. Franklin and J.D. Powell, Digital Control of Dynamic Systems, Addison-Wesley, Reading, 1980.

[69] K.J. Åström, P. Hagander and J. Sternby, "Zeroes of Sampled Systems," Proc. 19th IEEE CDC, Albuquerque, New Mexico, 1980.

[70] G.A. Dumont and P.R. Bélanger, "Successful Industrial Application of Advanced Control Theory to a Chemical Process," IEEE Control Systems Magazine, Vol. 1, No. 1, March 1980.